Pharmacological and Structure-Function Studies of M_1 Muscarinic Acetylcholine Receptor Allosteric Modulation

Alaa Abdul-Ridha

B. Pharm. Sci. (Hons)

Submitted in total fulfilment of the requirements of the degree of Doctor of Philosophy

February 2015

Drug Discovery Biology

Monash University

MONASH University

COPYRIGHT NOTICE

TABLE OF CONTENTS

ABSTRACT

The M_1 muscarinic acetylcholine receptor (mAChR) is predominantly expressed in the brain where it plays a major role in mediating cognitive processes such as learning and memory. As a result, it has been implicated in diseases where such processes are impaired, such as Alzheimer's disease and schizophrenia. Drug discovery efforts aimed at developing selective ligands for this receptor, both as therapeutics and as experimental tools, have largely failed as they focused on targeting the acetylcholine (ACh) binding site, which is identical in all five mAChR subtypes. The discovery of benzyl quinolone carboxylic acid (BQCA), the first positive allosteric modulator (PAM) with high selectivity for the M_1 mAChR, has lead to a renaissance in selective targeting of this receptor family.

In chapter 2 we exploit the unique "two-state" pharmacology of BQCA to investigate allosteric modulation at a chemogenetically modified M_1 mAChR, developed as an alternative means to achieve selective receptor targeting *in vivo.* This study demonstrates that such an approach may not be valid, as chemogenetic modification of the M_1 mAChR leads to changes in the allosteric behaviour of BQCA that are not reminiscent of its behaviour at the native receptor. As a consequence, caution must be exercised when interpreting studies of allosteric modulation using chemogenetically modified receptors *in vivo*.

Despite the unique pharmacology of BQCA, the molecular mechanisms of its binding and function and the structural basis of its M_1 mAChR selectivity remain poorly defined. Such knowledge would enable the design of novel M_1 mAChR PAMs with improved pharmacological profiles. Chapters 3 and 4 comprise studies focussed on identifying the amino acid residues that form the allosteric binding pocket at the M_1 mAChR and/or play a role, either directly or indirectly, in the transmission of cooperativity with the orthosteric (ACh) binding site. Deeper mechanistic insights

into allosteric modulation at the M_1 mAChR are further afforded by the use of benzoquinazolinone 12, a high affinity structural derivative of BQCA. The experimental findings are contextualised using molecular models, and collectively, the results suggest that many of the key residues that form the allosteric binding pocket at the M_1 mAChR are structurally conserved in other mAChR subtypes. The findings in this thesis challenge the common assumption that allosteric ligands achieve subtype selectivity through binding to allosteric sites that are less conserved between subtypes and propose that the selectivity of BQCA and benzoquinazolinone 12 arises from selective cooperativity with ACh at the M_1 mAChR. The information herein may guide the rational design of M_1 mAChR positive and/or negative allosteric ligands with increased therapeutic potential.

DECLARATION

In accordance with Monash University Doctorate Regulation 17.2 Doctor of Philosophy and Research Master's regulations the following declarations are made:

I hereby declare that this thesis contains no material which has been accepted for the award of any other degree or diploma at any university or equivalent institution and that, to the best of my knowledge and belief, this thesis contains no material previously published or written by another person, except where due reference is made in the text of the thesis.

This thesis includes three original papers and one review article published in peer reviewed journals. The core theme of the thesis is "Pharmacological and Structure-Function Studies of M_1 Muscarinic Acetylcholine Receptor Allosteric Modulation". The ideas, development and writing up of all the papers in the thesis were the principal responsibility of myself, the candidate, working within the Drug Discovery Biology Laboratory under the supervision of Dr. Meritxell Canals and Prof. Arthur Christopoulos.

The inclusion of co-authors reflects the fact that the work came from active collaboration between researchers and acknowledges input into team-based research.

In the case of Chapters 2-4 and Appendix I my contribution to the work involved the following:

Thesis chapter	Publication title	Publication status	Nature and extent of candidate's contribution
2	Allosteric Modulation of a Chemogenetically Modified G Protein-Coupled Receptor.	Published	Development of ideas, participation in research design, conduction of experiments, data analysis, writing and editing of the manuscript. (80%)
3	Molecular Determinants of Allosteric Modulation at theM_1 Muscarinic Acetylcholine Receptor.	Published	Development of ideas, participation in research design, conduction of experiments, data analysis, writing and editing of the manuscript. (80%)
4	Mechanistic Insights into Allosteric Structure-Function Relationships at the M_1 Muscarinic Acetylcholine Receptor.	Published	Development of ideas, participation in research design, conduction of experiments, data analysis, writing and editing of the manuscript. (70%)
Appendix I	Regulation of G Protein-Coupled Receptors by Allosteric Ligands.	Published	Development of ideas and writing parts of the article. (25%).

Signed: ……. Date: ……

ACKNOWLEDGEMENTS

First and foremost, I would like to thank God, the creator of the universe, for giving me the health and the strength to gain an understanding of His creation. I thank you God for giving me the ability to gain knowledge, which has and continues to increase my faith in you.

I would like to extend my sincere appreciation to my supervisors Dr. Meritxell Canals and Prof. Arthur Christopoulos for their support and guidance. Thank you for giving me a PhD project, for encouraging me throughout the last four years and for teaching me so many things. Thank you also for sacrificing your time to meet with me regularly and for your patience in reviewing multiple drafts of my work. This thesis, and who I am today as a scientist, would not have come to fruition without your support.

A huge thank you also to Dr. Robert Lane for sharing your infinite knowledge, for your brilliant ideas and valuable contributions to the manuscripts.

Many thanks also to Dr. Laura López for generating the molecular models and for continuing to support my work even after leaving Monash University and to Dr. Shailesh Mistry for sharing your valuable medicinal chemistry expertise and for your contributions to my project.

I would also like to extend my gratitude to Prof. Peter Scammells and Dr. Richard Loiacono for being part of the assessment panel and providing helpful advice for my project.

To Dr. Ann Stewart, Peter Keov, Briana Davie and Thomas Coudrat, thank you for your kindness and willingness to help me every time I asked you for help. The little things you helped me with really mean a lot to me.

To all members of the Drug Discovery Biology laboratory, thank you for your friendship, advice and suggestions through this journey, and thank you for making my time in the lab enjoyable.

To my respected parents, I cannot thank you enough for your endless support and encouragement. Thank you for enduring the stress with me and believing in me and thank you for filling our home with your love and care. I'm forever grateful to you.

To my beautiful sisters Ashraf, Zina, Ghadir and Abrar, thank you for the joy and happiness you have and still bring to my life. I feel blessed to have sisters like you.

Finally, to my wonderful husband Ghyath. Thank you for coming into my life half way through this PhD and changing it in the most beautiful way. Thank you for your love and support and for encouraging me to chase my dreams.

PUBLICATIONS AND COMMUNICATIONS

Peer-reviewed articles

Alaa Abdul-Ridha, J. Robert Lane, Shailesh N. Mistry, Laura López , Patrick M. Sexton, Peter J. Scammells, Arthur Christopoulos and Meritxell Canals. "Mechanistic Insights into Allosteric Structure-Function Relationships at the M_1 Muscarinic Acetylcholine Receptor". ***J. Biol. Chem,*** 289 (48): 33701-33711, 2014.

Alaa Abdul-Ridha, Laura López, Peter Keov, David M. Thal, Shailesh N. Mistry, Patrick M. Sexton, J. Robert Lane, Meritxell Canals & Arthur Christopoulos. "Molecular Determinants of Allosteric Modulation at the M_1 Muscarinic Acetylcholine Receptor". ***J. Biol. Chem***, 289 (9): 6067-6079, 2014.

Alaa Abdul-Ridha, J. Robert Lane, Patrick M. Sexton, Meritxell Canals & Arthur Christopoulos. "Allosteric Modulation of a Chemogenetically Modified G Protein-Coupled Receptors". ***Mol Pharmocol.*** 83:521-530, 2013.

J. Robert Lane, **Alaa Abdul-Ridha** & Meritxell Canals. "Regulation of G Protein-Coupled Receptors by Allosteric Ligands". ***ACS Chem. Neuroscience***, 4:527-534, 2013.

Alaa Abdul-Ridha, Meritxell Canals and J. Robert Lane. "Allosteric Modulation of G Protein-Coupled Receptor Pharmacology". **In preparation**.

Published Abstracts

Alaa Abdul-Ridha, J. Robert Lane, Shailesh N. Mistry, Laura López, Arthur Christopoulos and Meritxell Canals. "Mechanistic Insights into Allosteric Structure-Function Relationships at the M_1 Muscarinic Acetylcholine Receptor". Poster Presentation. ASCEPT-MPGPCR Joint Scientific Meeting. December 2014. Melbourne, Australia.

Alaa Abdul-Ridha, Meritxell Canals & Arthur Christopoulos. "Molecular Determinants of Allosteric Modulation at the M_1 Muscarinic Acetylcholine Receptor". Oral presentation. The Australasian Society of Clinical and Experimental Pharmacologists and Toxicologists (ASCEPT). December 2013. Melbourne, Australia.

Alaa Abdul-Ridha, Laura López, Patrick M. Sexton, J. Robert Lane, Meritxell Canals & Arthur Christopoulos. "Molecular Determinants of Allosteric Modulation at the M_1 Muscarinic Acetylcholine Receptor". Poster presentation. The Australasian Society of Clinical and Experimental Pharmacologists and Toxicologists (ASCEPT). December 2013. Melbourne, Australia.

Meritxell Canals, J. Robert Lane, **Alaa Abdul-Ridha**, Patrick M. Sexton and Arthur Christopoulos. "On the mode of action of BQCA: Assessing the Monod-Wyman-Changeux mechanism in the actions of a G protein-coupled receptor allosteric modulator". Poster presentation. Molecular Pharmacology Gordon Research Conference. April 2013. Lucca, Italy.

Alaa Abdul-Ridha, J. Robert Lane, Meritxell Canals & Arthur Christopoulos. "Allosteric Modulation of a Chemogenetically Modified G Protein-Coupled Receptors". Poster presentation. Melbourne protein group (MPG) student symposium. July 2013, Melbourne, Australia.

Alaa Abdul-Ridha, J. Robert Lane, Meritxell Canals & Arthur Christopoulos. "Allosteric Modulation of a Chemogenetically Modified G Protein-Coupled Receptors". Poster presentation. The Australasian Society of Clinical and Experimental Pharmacologists and Toxicologists (ASCEPT). December 2012, Sydney, Australia.

Alaa Abdul-Ridha, J. Robert Lane, Meritxell Canals & Arthur Christopoulos. "Allosteric Modulation of a Chemogenetically Modified G Protein-Coupled Receptors". Poster presentation. The 7th International Meeting on the Molecular Pharmacology of G Protein-Coupled Receptors (MPGPCR). December 2012. Melbourne, Australia.

ABBREVATIONS

[^{3}H]NMS- tritiated N-methylscopolomine
[^{3}H]QNB- tritiated quinuclidinyl benzilate
77-LH-28-1- (1-[3-(4-butyl-1-piperidinyl)propyl]-3,4-dihydro-2(1*H*)-quinolinone)
AC- adenylyl cyclase
AC-42- (4-n-butyl-1-[4-(2-methylphenyl)-4-oxo-1-butyl]-piperidine hydrogen chloride)
ACh- acetylcholine
AChEI- acetylcholinesterase inhibitors
ADAM17- α secretase producing enzyme 17
AF267B- (2S)-2-Ethyl-8-methyl-1-thia-4,8-diazaspiro[4.5]decan-3-one
Ala- alanine
ANGII- angiotensin II
AP-2- adaptor protein 2
APP- amyloid precursor protein
Arg- arginine
Asn- asparagine
Asp- aspartate
ATCM- allosteric ternary complex model
ATIR- angiotensin 1 receptor
ATP- adenosine triphosphate
ATSM- allosteric two state model
BACE-1- β-secretase converting enzyme
Benzoquinazolinone 12- 3-((1*S*,2*S*)-2-hydroxycyclohexyl)-6-((6-(1-methyl-1*H*-pyrazol-4-yl)pyridin-3 yl)methyl)benzo[*h*]quinazolin-4(3*H*)-one
BMK1- big mitogen-activated protein kinase
BQCA- benzyl quinolone carboxylic acid
C_7/3-phth- heptane-1,7-bis-(dimethyl-39-phthalimidopropyl) ammonium bromide
Ca^{2+}- calcium
cADPR- cyclic ADP-ribose
cAMP- cyclic adenosine monophosphate
CaSR- calcium sensing receptor
CCR-5- chemokine receptor type 5
CCR-7- chemokine receptor type 7
CFC- contextual fear conditioning
CK1α- casein kinase 1α
CNO- clozapine-N-oxide
COPD- chronic obstructive pulmonary disease
CRF- corticotrophin-releasing factor
CRF-1- corticotrophin-releasing factor-1 receptor
CSF- cerebrospinal fluid
c-Src- proto-oncogene tyrosine kinase SRC
Cys- cysteine
DAG- diacylglycerol
DREADD- Designer Receptor Exclusively Activated by Designer Drug
ECL- extracellular loop
EGFR- epidermal growth factor receptor
ER- endoplasmic reticulum
ERK1/2- extracellular regulated kinase 1/2

GABA- γ-aminobutyric acid
GAPS- GTPase accelerating proteins
GDP- guanosine diphosphate
GIP- gastric inhibitory peptide
GIRK- G protein inward rectifier K^+ channel
GLP- glucagon-like peptide
Glu- glutamate
Gly-glycine
GPCR- G protein-coupled receptor
GRAFS- Glutamate, Rhodopsin, Adhesion, Frizzled/Taste2 and Secretin receptors
GRKs- G protein-coupled receptor kinases
GSK1034702 -2H-Benzimidazol-2-one, 4-fluoro-1,3-dihydro-6-(methyl-11C)-1-(1 (tetrahydro-2H-pyran-4-yl)-4-piperidinyl)-
GTP- guanine triphosphate
HIV- human immunodeficiency virus
IBS- Irritable bowel syndrome
ICL- intracellular loop
IP_3- inositol-1,4,5- triphosphate
Iperoxo- 4-[(4,5-Dihydro-3-isoxazolyl)oxy]-N,N,N-trimethyl-2-butyn-1-aminium iodide
JNK- c-Jun N-terminal kinase
Leu- leucine
LY2033298- 3-amino-5-chloro-6-methoxy-4-methylthieno[2,3-b]pyridine-2-carboxylic acid cyclopropylamide
LY2119620- (3-amino-5-chloro-N-cyclopropyl-4-methyl-6-[2-(4-methylpiperazin-1-yl)-2
mAChR- muscarinic acetylcholine receptor
MAPK- mitogen activated protein kinase
mGluR- metabotropic glutamate receptor
mPFC- medial prefrontal cortex
mRNA- messenger ribonucleic acid
MWC- Monod-Wyman-Changeux
NAL- neutral allosteric modulator
NAM- negative allosteric modulator
NC-IUPHAR- International Union of Pharmacology Committee on Receptor Nomenclature and Classification
NDMC-n-desmethyl clozapine
NF-κB- nuclear factor κ-B
NMDA- N-methyl-D-aspartate
NO- nitric oxide
p38- p38 protein kinase
PAM- positive allosteric modulator
Phe- phenylalanine
PI3K- phosphotidylinositol 3' kinase
PIP_2- phosphoinositol-1,4,5-biphosphate
PKA- protein kinase A
PKC- protein kinase C
PLA_2- phospholipase A_2
PLC- phospholipase C
PLD- phospholipase D
PTH- parathyroid hormone
PYK2- protein tyrosine kinase 2

RASSL- Receptor Activated Solely by Synthetic Ligand
RGS- regulators of G protein signaling
ROCK- Rho-associated kinase
RTPα- receptor tyrosine phosphatase α
SB269652- trans-1*H*-indole-2-carboxylic acid {4-[2-(cyano-3,4-dihydro-1*H*-isoquinolin-2 yl)-ethyl]-cyclohexyl}-amide
sEPSP- spontaneous excitatory postsynaptic currents
Ser- serine
TBPB- (1-[1'-(2-methylbenzyl)-1,4'-bipiperidin-4-yl]-1,3-dihydro-2H-benzimidazol-2-one)
Thr- threonine
TM- transmembrane domain
Tyr- tyrosine
VIP- vasoactive intestinal peptide
Xanomeline- 3-[4-(Hexyloxy)-1,2,5-thiadiazol-3-yl]-1,2,5,6-tetrahydro-1-methylpyridine oxalate

CHAPTER 1

General Introduction

1.1 G Protein-Coupled Receptors (GPCRs)

1.1.1 General introduction

Guanine nucleotide (G protein)-coupled receptors (GPCRs) are 7 transmembrane-spanning proteins that comprise the largest family of cell-surface receptors. Accounting for ~1-3% of the human genome, they play crucial roles in virtually all biological processes and mediate signals for a wide range of molecules including neurotransmitters, peptides, ions, photons, pheromones and odorants (Katritch et al., 2013; Pierce et al., 2002). As a result, they are implicated in a multitude of physiological processes and are the target of a large proportion (~30%) of currently marketed drugs (Overington et al., 2006). Despite this clinical success, the extreme diversity of GPCRs with respect to their tissue distribution, endogenous and exogenous ligands and their cellular functions, have resulted in high attrition of drug discovery programs due to lack of efficacy or development of off-target effects. Current drug discovery efforts aim to improve therapies for more than 50 established GPCR targets and expand the list of targeted GPCRs (Katritch et al., 2013). In addition to activating GPCR signals with agonists and inhibiting them with antagonists, the pursuit for improved and selective therapies has driven pharmacological research towards the discovery of allosteric and/or functionally selective modulators (Valant et al., 2012b) that bias downstream signaling toward specific G protein-activated or β-arrestin-activated pathways (Stallaert et al., 2011).

1.1.2 Structural characteristics

Despite their diversity and complexity, all GPCRs share a common basic architecture (Venkatakrishnan et al., 2013). GPCRs are integral membrane proteins with a common three-dimensional structure of seven alpha (α)-helical hydrophobic transmembrane (TM 1-7) domains, connected by 3 intracellular (ICL 1-3) and 3 extracellular (ECL 1-3) loops and flanked by an

extracellular N-terminus and an intracellular C-terminus. Evidence for this seven TM architecture was first observed in the crystal structure of bovine Rhodopsin (Palczewski et al., 2000), and subsequently confirmed in a plethora of GPCR crystal structures (Venkatakrishnan et al., 2013) (Figure 1.1). A distinctive feature of the extracellular region is the presence of disulphide bridges that contribute to receptor stability. The most highly conserved disulphide bridge in most GPCR structures is found connecting a crucial cysteine residue at the top of TM3 with a cysteine in ECL2. This TM3-ECL2 disulphide bridge influences receptor stability and integrity and limits receptor conformational changes (Venkatakrishnan et al., 2013). GPCRs are dynamic proteins that undergo substantial conformational changes upon activation by ligands. The unique conformations they adopt can dictate their intracellular signaling via G protein-dependent and –independent mechanisms.

Although GPCRs can function as single monomeric entities to activate signaling, they can also from homomers, heteromers or higher-order oligomers in intact cells (Bouvier, 2001; Ferré et al., 2014; Milligan, 2013). This is best known for family C GPCRs, which form constitutive homo- or heteromers (Kniazeff et al., 2011), however the phenomenon has also been observed for family A (Gavalas et al., 2013; Han et al., 2009; Hern et al., 2010; Hill et al., 2014; Hu et al., 2013; Nenasheva et al., 2013; Pou et al., 2012; Siddiquee et al., 2013) and family B GPCRs (Harikumar et al., 2010; Harikumar et al., 2012; Pioszak et al., 2010; Schelshorn et al., 2012).

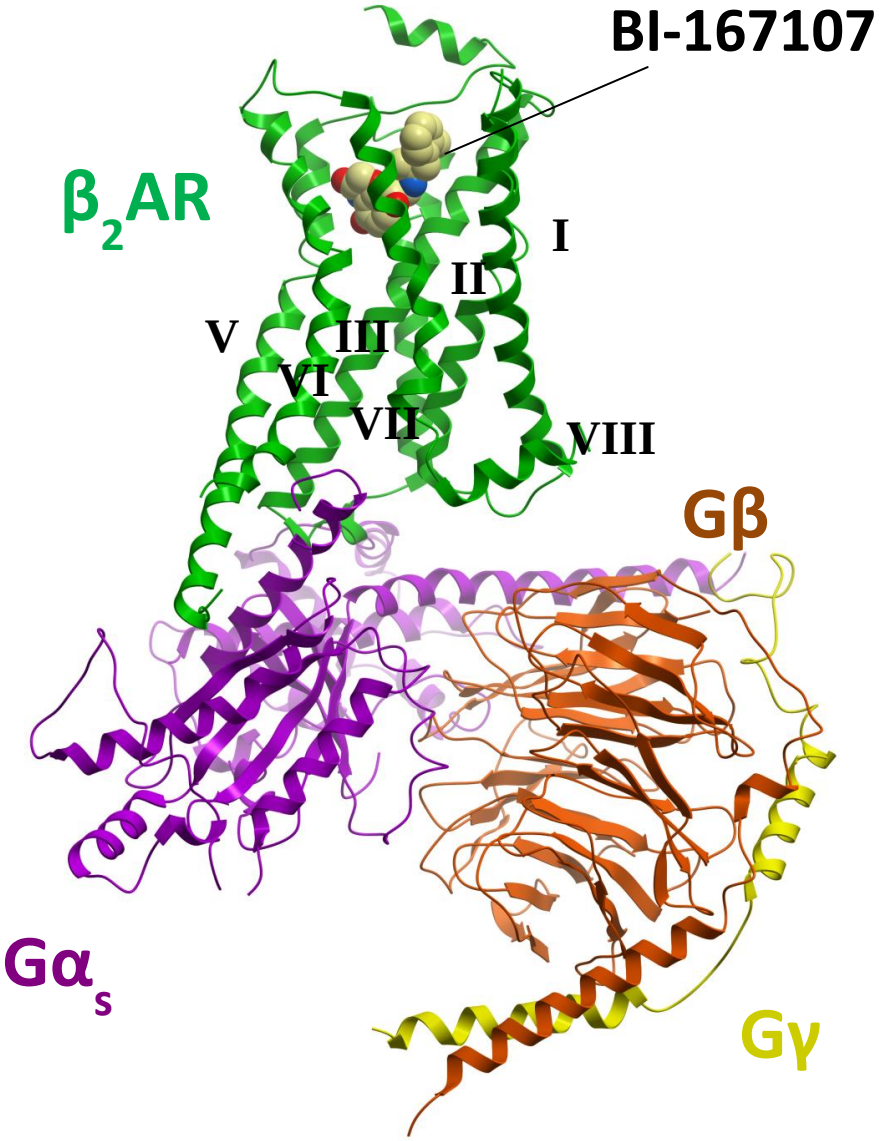

Figure 1.1 Structure of the β_2-adrenergic receptor (β_2AR) in complex with agonist and the G protein heterotrimer (Protein Data Bank code 3SN6). The common three-dimensional GPCR structure of seven TM domains, connected by ICLs 1-3 and ECLs 1-3 and flanked by the extracellular N-terminus and the intracellular C-terminus. The receptor and G protein are shown by coloured ribbons, whereas the agonist is illustrated by spheres with carbon atoms coloured yellow. Adapted from Katritch et al., 2013a

1.1.3 Classification of GPCRs

According to the International Union of Pharmacology Committee on Receptor Nomenclature and Classification (NC-IUPHAR), GPCRs are classified into subfamilies based on phylogenetic criteria (Foord et al., 2005; Kolakowski, 1994). This classification system divides GPCRs into 5 subfamilies known as A, B, C, Frizzled and Other receptors (Lagerstrom and Schioth, 2008a). All the receptor proteins, except some members of the Frizzled family and all the members of the Other family, are proven to bind G proteins. GPCRs for which the endogenous ligand is still unknown are termed "orphan" receptors (Davenport et al., 2013; Kolakowski, 1994). While this is the most widely used GPCR classification system, Fredriksson and colleagues (Fredriksson et al., 2003) developed an alternative classification system which illustrated that most of the human GPCRs can be divided in five main families, termed Glutamate, Rhodopsin, Adhesion, Frizzled/Taste2 and Secretin (GRAFS). The main difference between the two classification systems is that the latter further subdivides the Rhodopsin family into the four groups α, β, γ, δ and the further division of family B into the Secretin family and the Adhesion family (Fredriksson et al., 2003).

1.1.3.1 Family A/Rhodopsin GPCRs

Family A/Rhodopsin is the largest and best-characterised family of GPCRs and contains ~700 receptor proteins, which include olfactory and light activated receptors (Katritch et al., 2013; Lagerstrom and Schioth, 2008a). As mentioned earlier, this family can be further divided into four groups (α, β, γ and δ) based on the vast variety of endogenous ligands they are activated by. GPCRs in the α-group include those that are activated by amines such as histamine, dopamine, serotonin, muscarinic and adrenergic receptors, while those in the β-group of Family A GPCRs include mainly peptide binding receptors such as endothelin and oxytocin receptors. The opioid, angiotensin and somatostatin receptors are important drug targets within the γ-group, which includes receptors for

both peptides and lipid-like compounds, while the δ-group mostly contains receptors for purines and proteases and the olfactory receptors (Lagerstrom and Schioth, 2008a).

In the past 13 years, more than 40 crystal structures of different class A GPCRs have been solved in complex with ligands of varied pharmacology, peptides, antibodies and a G protein (Haga et al., 2012; Hanson et al., 2012; Hollenstein et al., 2013; Kruse et al., 2012a; Rasmussen et al., 2011b; Srivastava et al., 2014; Tan et al., 2013; Wu et al., 2014). These structures have provided unprecedented insights into the structural and functional diversity of this protein family. Despite the ability of family A GPCRs to bind ligands of diverse shapes, sizes and chemical properties, all ligands have been observed to bind in a pocket in the extracellular side of the TM bundle. Systematic comparison of the residues that contact the ligands revealed vast similarities in the ligand binding pocket, and most of these ligand-contacting residues are present in the TM helices. In almost all receptors, key positions in TM3, TM6 and TM7 form a consensus scaffold of the ligand-binding pocket, and variations in the amino acids at these positions contribute to ligand specificity in different receptors (Hulme, 2013; Katritch et al., 2013; Venkatakrishnan et al., 2013). In addition, several conserved amino acid motifs are observed in most Family A GPCRs, such as the D(E)-R-Y(F) motif at the bottom TM3, in which the arginine (R) forms an 'ionic lock' with a conserved residue in ICL2, and the NPxxY motif in TM7 in addition to several conserved proline residues in the middle of TM 5, 6 and 7 (Gether and Kobilka, 1998; Hulme, 2013; Lagerstrom and Schioth, 2008a).

1.1.3.2 Family B/Adhesion and Secretin GPCRs

The second largest GPCR family in humans is the Family B, which comprises 33 Adhesion and 15 Secretin-like receptors. The Secretin-like receptors all have an extracellular hormone-binding domain and bind peptide hormones. They include receptors for calcitonin, corticotrophin-releasing

factor (CRF), glucagon, glucagon-like peptide (GLP), gastric inhibitory polypeptides (GIP), vasoactive intestinal peptide (VIP) and secretin. They also contain conserved cysteine residues in the N-terminus, which have been shown to be crucial for ligand interactions along with the extracellular loops and TM6. Adhesion receptors differ from Secretin-like receptors in their N-terminal architecture, which contains several domains that play an important role in the specificity of receptor ligand binding interactions (Bjarnadottir et al., 2004; Lagerstrom and Schioth, 2008a; Lin et al., 2001) and contain GPCR photolytic (GPS) domains, which the Secretin-like receptors lack (Krasnoperov et al., 1997). In addition, Adhesion receptors bind extracellular matrix molecules rather than peptide hormones (Lagerstrom and Schioth, 2008a).

Recently, the first crystal structures of Family B GPCRs were solved for the glucagon and the CRF-1 receptors, both of which are Secretin-like receptors (Hollenstein et al., 2013; Siu et al., 2013). The relative positions of the TM helices at the intracellular face of the proteins were found to overlap with those in class A GPCRs, however there was substantial deviation between the two families of GPCRs at the extracellular face (Sexton and Wootten, 2013). In addition, the conserved amino acid motifs described above for family A GPCRs (DRY and NPxxY) were not present in the two Family B receptors, which contained distinct patterns of conserved motifs specific to this family (Hollenstein et al., 2013; Siu et al., 2013).

1.1.3.3 Family C/Glutamate Receptors

Family C/ Glutamate GPCRs consists of 22 human proteins that include the metabotropic glutamate receptors (mGluRs), the γ-aminobutyric acid receptor B ($GABA_B$) and the calcium-sensing receptor (CaSR). Most Family C GPCRs bind their respective endogenous orthosteric ligand within the N-terminal region of the receptor in which two lobes of the region form a ligand encasing cavity described as a ‘Venus fly trap’ (Fredriksson et al., 2003). This class of receptors is distinct from the

other receptor families as they exist constitutively as homo- or heterodimers, which is required for their structural integrity, trafficking to the cell surface and signaling (Comps-Agrar et al., 2011; Kniazeff et al., 2011; Rondard et al., 2011). Two Family C GPCRs have been crystallised to date, namely the $mGlu_1R$ and $mGlu_5R$, both crystallised with allosteric modulators (Dore et al., 2014; Wu et al., 2014).

1.1.3.4 Frizzled/ Taste2 GPCRs

The Frizzled family of receptors consists of 10 frizzled receptors and the smoothened receptor (Fredriksson et al., 2003). The frizzled receptors bind the family of Wnt glycoproteins (Bhanot et al., 1996), whereas the smoothened receptor binds small organic compounds and has been reported to function in a ligand-independent manner as the signaling unit in the patched, sonic hedgehog and smoothened complex (Lagerstrom and Schioth, 2008b; Murone et al., 1999). This subfamily also contains the Taste2 receptors, which mediate the bitter taste (Chandrashekar et al., 2000). The frizzled and smoothened receptors both contain an extracellular cysteine-rich domain. This domain is the site of binding of the Wnt glycoproteins in frizzled receptors, but its function is not clear in the smoothened receptor (Wang et al., 2013b). Recently, several crystal structures of the human smoothened receptor were reported in complex with either the small molecule antagonists LY2940680 (Wang et al., 2013b), SANT1 and Anta XV or with the agonist SAG1.5 (Wang et al., 2014), providing detailed insights into the structural basis of molecular recognition and modulation of smoothened receptors by small molecules.

1.1.4 Functional characteristics

1.1.4.1 G protein-dependent signaling

G proteins are intracellular heterotrimeric proteins composed of three subunits; alpha (α), beta (β) and gamma (γ) (Gilman, 1987). Upon activation of a GPCR by an agonist, or constitutive receptor activity in absence of agonist, the receptor undergoes conformational changes that lead to rearrangements of the TM helices, exposing intracellular binding sites for many effector proteins, including G proteins (Pierce et al., 2002; Rasmussen et al., 2011b). The activated receptor serves as a guanine exchange factor for the G protein to promote the catalytic exchange of guanosine diphosphate (GDP) for guanosine-5'-triphosphate (GTP) at the α subunit. The activated G protein dissociates into the α-GTP-bound subunit and the βγ complex, each of which have an independent capacity to regulate separate effectors and initiate intracellular signaling pathways (Gilman, 1987; Milligan and Kostenis, 2006). The heterotrimer reassembles following hydrolysis of GTP to GDP in the α subunit. While this is the most widely accepted mechanism of G protein-dependent signaling, there are a few exceptions. These include examples of inactive state receptor-G protein pre-assembly (Challiss and Wess, 2011; Qin et al., 2011) and cell signaling in the absence of heterotrimeric G protein dissociation (Frank et al., 2005).

G proteins are generally classified according to their α subunit. The principal G protein families are $G\alpha_s$, $G\alpha_{q/11}$, $G\alpha_{i/o}$ and $G\alpha_{12/13}$, each of which are responsible for activating specific intracellular signaling pathways (Figure 1.2) (Gilman, 1987; Neer, 1995; Wess, 1998). Signaling by $G\alpha_s$ involves the activation of the enzymatic function of membrane bound adenylyl cyclases (ACs) for the catalytic conversion of adenosine-triphosphate (ATP) to cyclic adenosine monophosphate (cAMP), which in turn activates protein kinase A (PKA) and downstream effectors. In contrast, $G\alpha_{i/o}$ G proteins inhibit the activation of ACs and the cAMP pathways. $G\alpha_{q/11}$ G proteins stimulate phospholipase C (PLC), which causes hydrolysis of phosphoinositol-1,4,5-biphosphate (PIP_2) into two second messengers, namely inositol-1,4,5- triphosphate (IP_3) and diacylglycerol (DAG) which

leads to a subsequent rise in intracellular Ca^{2+} levels and activation of protein kinase C (PKC) (Felder, 1995). $G\alpha_{12/13}$ G proteins couple to the activation of Rho, leading to a variety of effects that include regulation of the Na^{+}-H^{+} exchanger and cytoskeletal rearrangements (Milligan and Kostenis, 2006; Neer, 1995; Neves et al., 2002; Wess, 1998). In addition to the role of α-subunits, the βγ complex also contributes to cellular signaling (Bondar and Lazar, 2014; Khan et al., 2013b; Mahajan et al., 2013; O'Neill et al., 2012) including activation of G protein-gated inward rectifier K^{+} (GIRK) channels (Whorton and MacKinnon, 2013b), phosphorylation of extracellular signal-related kinase 1 and 2 (pERK1/2) and activation of PLC and phosphotidylinositol 3' kinase (PI3K) (Gutkind, 2000). In addition, a number of receptors demonstrate promiscuous coupling to multiple G proteins to elicit a wide range of signals, however this often occurs in a cell-type-specific, agonist-specific and even a dose-dependent manner (Daaka et al., 1997; Defea, 2008; Marinissen et al., 2003; Vanhauwe et al., 2002).

The alterations in cellular behaviour and functions that result from G protein activation are manifested in many critical physiological functions, including embryonic development, locomotion, learning, memory and metabolism (Neves et al., 2002).

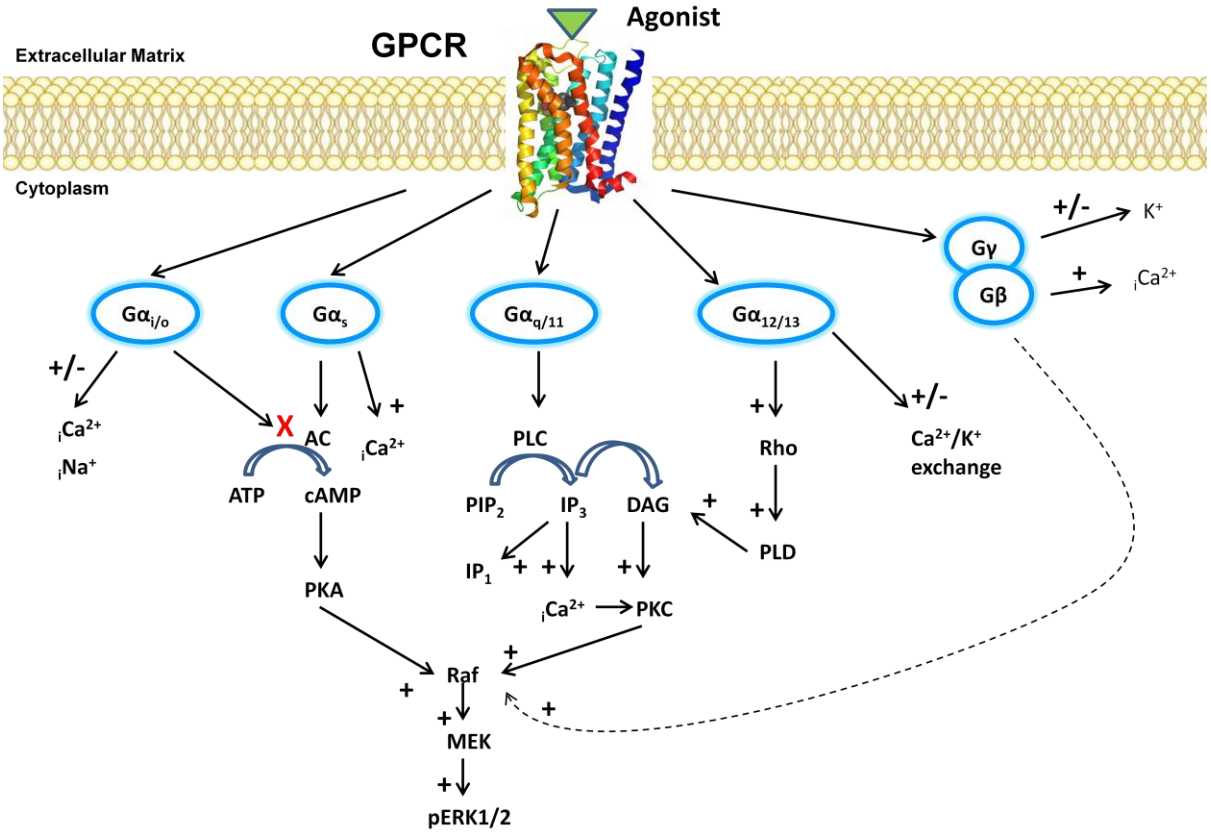

Figure 1.2 Major G protein-mediated signaling pathways. Upon binding of an agonist to a GPCR, the α subunit of the G protein complex exchanges GDP for GTP and dissociates away from the βγ complex. The α-subunit and βγ complex can in turn activate, suppress and regulate various signaling cascades, the major of which are detailed here. AC -adenylyl cyclase; cAMP - cyclic adenosine monophosphate; DAG - diacyl glycerol; ERK1/2 - extracellular signal regulated kinase 1/2 ; IP_3 - inositol 1,4,5 trisphosphate; K^+- potassium; MEK1/2 - MAPK/ERK kinase 1/2; PIP_2 - phosphotidylinositol 4,5 -bisphosphate; PKA- protein kinase A; PKC- protein kinase C; PLC - phospholipase C; PLD- phospholipase D; Raf - a serine/threonine kinase.

1.1.4.2 G protein-independent signaling

In addition to G protein-mediated signaling, some GPCRs can signal independently of G proteins via interaction with tyrosine kinases and adaptor proteins (Pyne and Pyne, 2011; Pyne et al., 2003; Ritter and Hall, 2009). The most extensively studied G protein-independent signaling pathways are those mediated by β-arrestins and G protein-coupled receptor kinases (GRKs) (Pierce et al., 2002; Pitcher et al., 1998; Shukla et al., 2013; Shukla et al., 2014; Zheng et al., 2012). Classically, upon persistent GPCR activation, plasma membrane signaling is terminated by phosphorylation of the cytoplasmic loops and C-tail of the receptor by GRKs. This results in the recruitment and binding of β-arrestins and subsequent desensitization followed by internalization into clathrin-coated pits (Rajagopal et al., 2010). However, β-arrestins act not only as regulators of GPCR desensitisation, but also as multifunctional adaptor proteins that can signal through multiple mediators (Defea, 2008). For example, β-arrestin can function as an adaptor protein to recruit the proto-oncogene tyrosine kinase SRC (c-Src) to the activated receptor and facilitate activation of downstream ERK1/2 (Luttrell et al., 1999). In addition, β-arrestins can scaffold mitogen-activated protein kinases (MAPKs) (Luttrell et al., 2001), p38 (Sun et al., 2002), c-Jun N-terminal kinases (JNKs) (McDonald et al., 2000), nuclear factor κB (NF-κB) (Cianfrocca et al.) and PI3K (Lin and DeFea, 2013).

1.1.4.3 Biased signaling

Classically, agonists were thought to encompass the entire signal repertoire of a receptor such that they were either ‘on’ or ‘off’ as depicted in the classic two-state model of receptor function (Leff, 1995; Samama et al., 1993). In this model it was envisioned that binding of inverse agonists preferentially stabilise the inactive state, whereas full and partial agonists stabilise the active state and neutral antagonists do not discriminate between the two conformations and this would block both agonist and inverse agonist activities (Stallaert et al., 2011). However, over several decades,

numerous examples of drug action were found that did not fit this paradigm, thus giving rise to the conceptualisation of the phenomenon of biased signaling (Violin et al., 2014). Biased signaling, also known as biased agonism, stimulus bias, ligand-directed signaling, collateral efficacy or functional selectively, refers to the ability of ligands for a single receptor to elicit differential efficiency for different signaling responses (Lefkowitz, 2013). This phenomenon results from the fact that GPCRs are able to pleotropically couple to, and signal through, multiple G protein-dependent and –independent mechanisms upon receptor activation (Kenakin, 2007). Biased signaling entails the existence of distinct conformations of the receptor, stabilized by different ligands, which lead to the activation of distinct signaling pathways (Kenakin, 1995a; Kenakin, 1995b). Signaling bias is exemplified by the angiotensin II (AngII) type 1 receptor (AT1R) ligand Sar^1 IIe^4 IIe^4-angiotensin (SII), which induces AT1R-dependent MAPK activation but not PI3K turnover through preferential recruitment of β-arrestins over $G\alpha_q$ (Wei et al., 2003) G protein activation. Another example of ligand bias comes from the parathyroid hormone (PTH) 1 receptor, whereby PTH(1-34) activates both PKA and PKC, PTH(1-31) activates only cAMP, and PTH(3-38) activates only PKC (Luttrell and Kenakin, 2011; Mohan et al., 2000; Takasu et al., 1999). The endogenous chemokine ligands CCL21 and CCL19 demonstrate bias at the chemokine receptor type 7 (CCR7), where the former is G protein biased and the latter is unbiased (Kohout et al., 2004).

Quantitative measures of ligand bias necessitate determination of the overall activity of an agonist in multiple cellular pathways in comparison to a reference ligand (usually the endogenous agonist). This can be achieved by use of an operational model of agonism (Black and Leff, 1983) to qualify ligand functional affinity, K_A, and operational efficacy, τ, the latter incorporates both receptor coupling efficiency to a particular signaling pathway, K_E, and receptor density, R_T. Both K_A and τ contribute to agonist potency, while only τ contributes to ligand efficacy. Calculation of τ/K_A ratios of agonists from multiple pathways allows determination if the bias profile of ligands as

demonstrated recently in a number of studies (Evans et al., 2011; Kenakin and Christopoulos, 2013; Shonberg et al., 2013; Stallaert et al., 2011).

1.2 Allosteric Modulation of GPCRs

1.2.1 General introduction

The term ‘allosteric’ was first coined by Monod and colleagues in their studies of enzymes (Monod et al., 1963; Monod and Jacob, 1961; Monod et al., 1965) where they highlighted the ability of these proteins to undergo global conformational changes that yield binding pockets with different affinities for ligands. They described that enzymes possess two or more non-overlapping binding sites for which enzymatic substrates could bind to engender “allosteric transition” that leads to change in the biological activity of the protein (Monod et al., 1963; Monod et al., 1965). Their observations followed earlier studies on haemoglobin that revealed one of the first examples of allosterism, in which the protein could simultaneously bind more than one molecule of oxygen (Bohr C, 1904). Today, IUPHAR defines the term ‘allosteric’ in relation to any binding site on a receptor protein that is topographically distinct to that of the endogenous ‘orthosteric’ binding site. The ‘effectors’ that bind to these sites are termed ‘allosteric ligands’ (Christopoulos et al., 2014; Christopoulos and Kenakin, 2002; Neubig et al., 2003). In addition to the ability of allosteric ligands to promote conformational changes in the receptor that manifest as an alteration in the properties (change in the affinity and/or efficacy) of a ligand bound to the orthosteric site, they have the potential for direct activation or inhibition of receptor signaling via the allosteric site. Positive allosteric modulators (PAMs) enhance orthosteric ligand activity, negative allosteric modulators (NAMs) inhibit it, and agents that occupy an allosteric site but do not change the activity of orthosteric ligands are said to have neutral ‘cooperativity’ and are referred to as neutral allosteric ligands (NALs). Allosteric compounds that directly activate the receptors are called allosteric agonists (Christopoulos, 2014; Christopoulos et al., 2014; Keov et al., 2011; Kruse et al., 2014b). Allosteric modulators have been identified for all receptor super families including GPCRs, nuclear hormone receptors, receptor tyrosine kinases, and ligand- and voltage-gated ion channels (Christopoulos et al., 2014).

The binding of G proteins to intracellular binding sites that are topographically distinct from the orthosteric binding site makes these proteins the best-known and prototypical allosteric modulators of GPCRs (Christopoulos and Kenakin, 2002; Ehlert, 1985; May et al., 2007b). Moreover, the interaction of GPCRs with regulatory proteins, such as β-arrestins and GRKs, suggests that the activity of GPCRs is largely allosteric (Kenakin, 2010). This idea is also supported by the presence of several endogenous peptides, lipids and cholesterol that have been reported to allosterically regulate GPCR activity (Gimpl et al., 1997; Massot et al., 1996; Thomas et al., 1997; Verma et al., 2005).

The binding of ions, such as Na^+, Ca^{2+} and Zn^{2+} has also been shown to play a role in allosterically modulating the activity of orthosteric ligands at several GPCRs (Galvez et al., 2000; Schetz et al., 1999; Swaminath et al., 2003). In particular, Na^+ has been shown to bind to an evolutionary conserved binding site in most family A GPCRs. The central cluster that harbours the Na^+ ion is predicted to play a key functional role in the modulation of conformational transitions upon receptor activation and the observed activation-related collapse of the sodium pocket implicates a role for Na^+ in signal transduction, where the ion translocates towards or into the cytoplasm (Katritch et al., 2014; Liu et al., 2012).

Structural complexes that have provided molecular insights into allosteric mechanisms at GPCRs include studies on sodium ion binding (Liu et al., 2012) (discussed above) as well as the GPCR structures bound to small molecules with allosteric pharmacology such as the Class A chemokine CCR5 receptor bound to maraviroc (Tan et al., 2013), the free fatty acid receptor-1 bound to TAK-875 (Srivastava et al., 2014), the M_2 mAChR bound to LY2119620 and the orthosteric agonist iperoxo (Kruse et al., 2013), the Class B CRF1 receptor bound to CP-376395 (Hollenstein et al., 2013), the Class C mGluR1 bound to FITM (Wu et al., 2014) and mGluR5 bound to magvoglurant (Dore et al., 2014).

Emerging evidence also suggests that allosteric modulation may occur across GPCR dimers (Lane et al., 2014; Smith and Milligan, 2010). It is possible for a ligand binding to the orthosteric binding site of one protomer of a dimer to allosterically modulate the binding and/or function of the orthosteric ligand in the other protomer. Examples in the literature also provide evidence that GPCR oligomerisation influences the affinity and specificity of ligand binding and receptor signaling and internalisation (El-Asmar et al., 2005; Ellis et al., 2006; Harikumar et al., 2012; Rocheville et al., 2000; Wootten et al., 2013).

The therapeutic potential of allosteric modulators has been demonstrated by the clinical use of the PAM of the CaSR, cinacalcet, to treat secondary hyperparathyroidism, a disorder characterised by increased levels of PTH (Kebig and Mohr, 2008), and the NAM, maraviroc, at CCR5, to prevent cellular entry of human immunodeficiency virus (HIV) (Dorr et al., 2005; Fatkenheuer et al., 2005; Watson et al., 2005).

1.2.2 Advantages of allosteric modulators

GPCR allosteric modulators offer several advantages over ligands that target the orthosteric sites (Christopoulos, 2002) (Figure 1.3). First, allosteric modulators that lack intrinsic efficacy will only exert their effects in the presence of a released endogenous agonist, thus maintaining the temporal and spatial specificity of physiological signaling. Second, the effects of the allosteric modulator on the function of the orthosteric ligand is saturable, such that no further allosteric effects are observed upon complete occupancy of the allosteric sites. This 'ceiling' to the effects of allosteric modulators protects against potential overdosing of a drug. A clinical example of this property of allosteric ligands relates to allosteric modulation of the $GABA_A$ ligand-gated ion channel by the benzodiazepine PAMs. These molecules produce their effects by a subtle potentiation the actions of GABA. The potentiation is limited by a small degree of positive cooperativity between the two ligands, making the benzodiazepines relatively safe in overdose situations (Christopoulos, 2014; Ehlert et al., 1982). Third, allosteric modulators have the potential to achieve greater selectivity

among receptor subtypes via binding to less evolutionary conserved binding sites compared to the orthosteric site or by subtype-selective cooperativity with orthosteric ligands (Christopoulos, 2002; Keov et al., 2011; May et al., 2007b; Wootten et al., 2013).

1.2.3 Probe dependence

A fundamental pharmacological property displayed by allosteric ligands is the phenomenon of 'probe dependence' (Figure 1.3); so named as to highlight the fact that the extent and direction of an allosteric interaction can vary with the nature of the orthosteric ligand used as a probe of receptor function (Kenakin, 2005; Keov et al., 2011; Valant et al., 2012a). For example, LY2033298 (Figure 1.10), is a PAM of the binding affinity of the M_4 muscarinic acetylcholine receptor (mAChR) orthosteric agonist acetylcholine (ACh) (Figure 1.5), but had neutral cooperativity with the orthosteric antagonists [^{3}H]N-methylscopolamine ([^{3}H]NMS) or [^{3}H]quinuclidinyl benzilate ([^{3}H]QNB) (Figure 1.6), at the same receptor and in the same assay (Leach et al., 2011). When tested at the M_2 mAChR with the orthosteric agonists oxotremorine-M and xanomeline, LY2033298 acted as a PAM and a NAM of the two ligands, respectively (Valant et al., 2012a). In addition, probe dependence is relevant for receptors that respond to multiple endogenous ligands. For example, the chemokine receptor type 5 (CCR5) allosteric modulator aplaviroc, produced very little effect on the binding of the chemokine ligand CCL5 to the receptor, but completely blocked the binding of the chemokine ligand CCL3 (Watson et al., 2005). The phenomenon of probe dependence highlights the importance of choosing the right orthosteric ligands to assess the effects of allosteric modulators (Kenakin, 2008; Leach et al., 2007).

1.2.4 Bitopic ligands

Although allosteric ligands could provide greater subtype selectivity for a given GPCR target, they often have low affinity compared to orthosteric ligands. Recent studies have exploited the

properties of orthosteric and allosteric compounds to develop a new class of ligands termed 'bitopic', 'dualsteric' or 'multivalent' (Lane et al., 2013b; Mohr et al., 2010; Valant et al., 2009). These hybrid molecules are rationally designed to simultaneously bridge orthosteric and allosteric sites within a single receptor. This approach attempts to target the allosteric site to achieve selectivity and the orthosteric site to provide high affinity as has been demonstrated in several studies ((Daval et al., 2013; Keov et al., 2013; Valant et al., 2008; Valant et al., 2014). Bitopic ligands are further discussed in section 1.4.5.2.

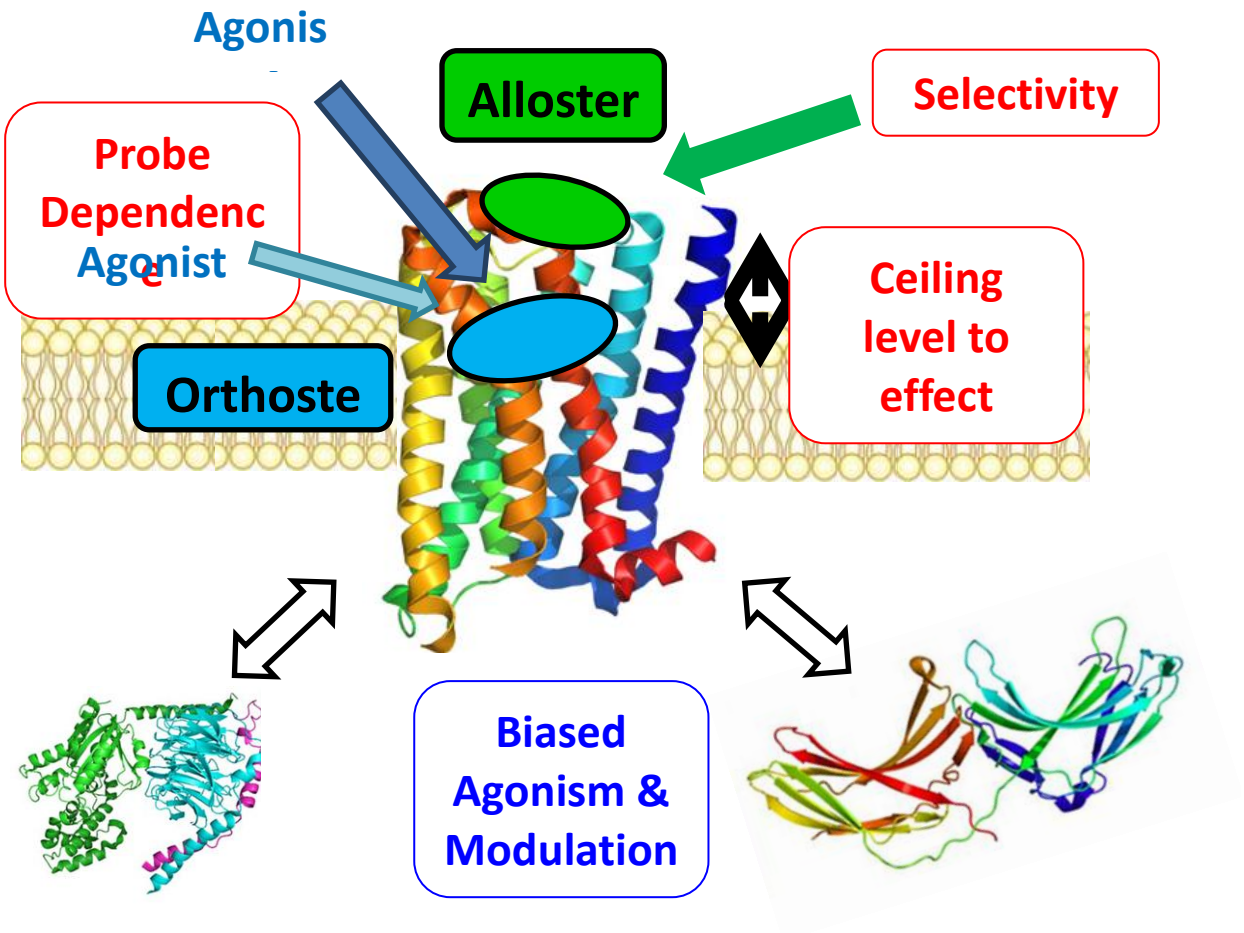

Figure 1.3 Pharmacological Characteristics of GPCR allostery. Adapted from Christopoulos. A, 2014.

1.2.5 Quantifying allosteric effects

1.2.5.1 *The allosteric ternary complex model*

Various analytical approaches can be used to analyse and quantify the complex interactions between allosteric ligands and GPCRs (Christopoulos and Kenakin, 2002; Leach et al., 2007; May et al., 2007b). The allosteric ternary complex model (ATCM) is the simplest mass-action scheme that can be applied to experimental data of allosteric interactions (Figure 1.4) (Ehlert, 1988). This model describes the allosteric interactions in terms of the equilibrium dissociation constants for orthosteric (K_A) and allosteric (K_B) ligands, and the allosteric effect, governed by the cooperativity factor (α), that each ligand exerts on the affinity of the other. Values of α greater than 1 denote positive cooperativity, values of α less than 1 but more than 0 denote negative cooperativity, and α values equal to 1 denote neutral cooperativity. However, despite the utility of the ATCM in directly quantifying experimental data where an allosteric ligand modifies orthosteric ligand affinity, the model is limited as it does not take into account the isomerisation of a GPCR between active and inactive states and does not consider allosteric modulators that change orthosteric ligand efficacy in addition to, or instead of, effects on binding affinity (Keov et al., 2011; Leach et al., 2007).

1.2.5.2 The allosteric two state model

To accommodate the effects of modulators that alter orthosteric ligand efficacy, and the isomerisation of receptors between active (R^*) and inactive (R) states, the ATCM has been extended into the allosteric two-state model (ATSM) (Figure 1.4) (Hall, 2000). This model describes the allosteric ligand effects on affinity, efficacy and the ability to modulate orthosteric ligands across active and inactive receptor states. The isomerisation of receptors between states is denoted by the parameter L, while α is the binding cooperativity factor. The parameters β and γ denote the intrinsic efficacy of orthosteric and allosteric ligands, respectively (ability to stabilise

active receptor state), while δ denotes the activation cooperativity between both ligands to form the active state of the ternary complex (Hall, 2000). As such, the ATSM holds an additional feature in that it can account for allosteric agonism at a receptor that is not occupied by an orthosteric ligand (*R*B*) (Keov et al., 2011).

Although this model describes both binding and efficacy parameters, it includes multiple parameters that are difficult to measure experimentally. An alternative 'operational approach' had been proposed to overcome the limitations of the ATSM (Keov et al., 2011; Leach et al., 2007).

1.2.5.3 The operational model of allosterism

The ATCM has been extended to incorporate the classic operational model of agonism postulated by Black and Leff (Black and Leff, 1983) to derive the operational model of allosteric modulation and agonism (Ehlert, 2005; Kenakin, 2005; Leach et al., 2007; Price et al., 2005) (Figure 1.4). In this model, the binding cooperativity between orthosteric (*A*) and allosteric (*B*) ligands is governed by the factor α, but in contrast to the ATSM, the operational model defines allosteric modulation of orthosteric ligand efficacy by the parameter β, and does not differentiate between active and inactive receptor states. The magnitude and direction of β should not change for a given set of ligands at a given receptor across different assay systems; however, allosteric modulator-mediated stimulus-bias will manifest as a pathway-dependent change in the β parameter (Keov et al., 2011). Moreover, the parameters τ_A and τ_B denote the capacity of orthosteric and allosteric ligands, respectively, to exhibit agonism, and incorporate the intrinsic efficacy of each ligand, the total density of receptors and the efficiency of stimulus-response coupling. In a system with low stimulus–response coupling efficiency or very low receptor density, the efficacy of the allosteric ligand might not be apparent. Conversely, under conditions of high coupling efficiency and/or high receptor expression levels, allosteric ligand efficacy is detected as changes in the basal responsiveness of the system (Leach et al., 2007). The remaining parameters, E_m and n denote the

maximal possible system response and the slope factor of the transducer function that links occupancy to response, respectively (Keov et al., 2011; Leach et al., 2007).

The operational model of agonism can be applied to functional data where concentration-response curves for the orthosteric ligands are performed in the presence of increasing concentrations of allosteric ligands to obtain values for the above mentioned parameters, as demonstrated in Chapters 2-4.

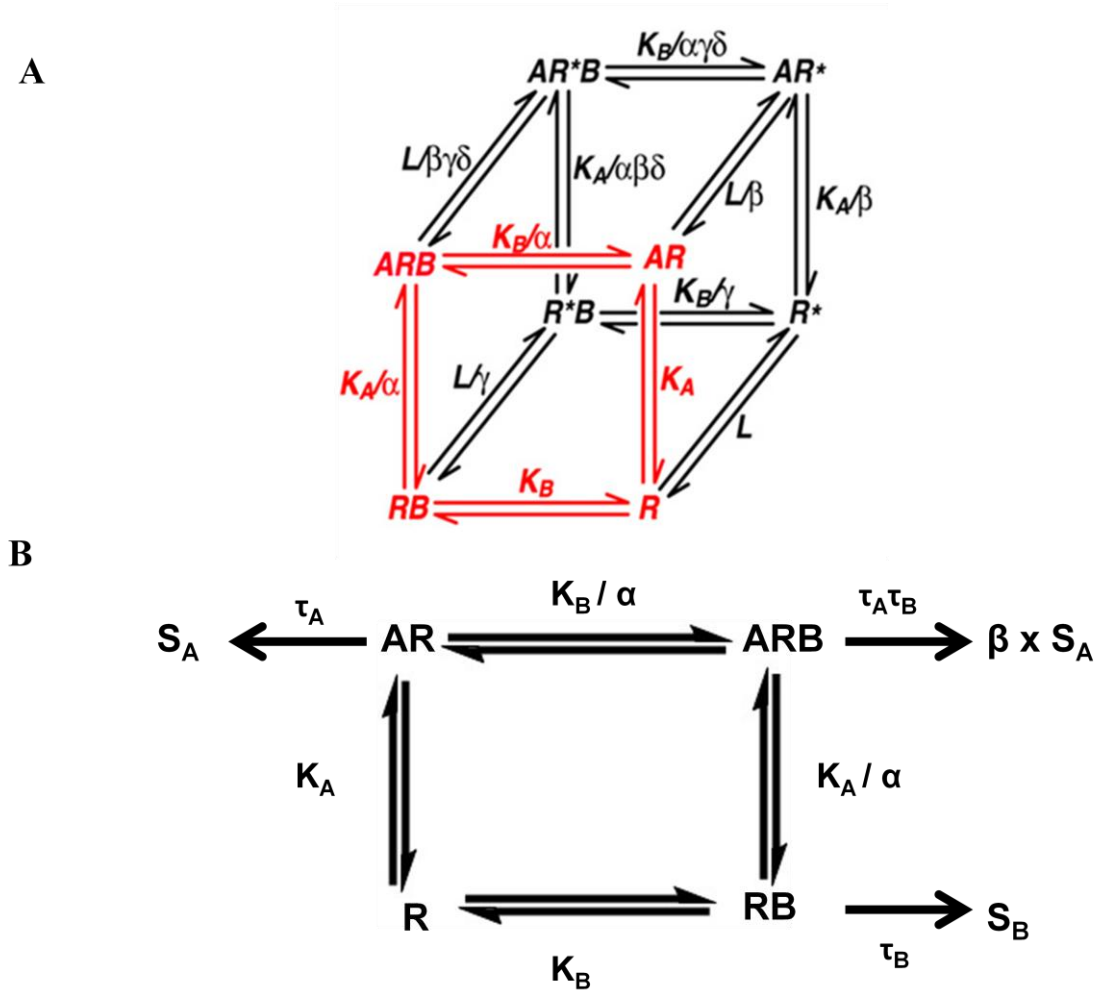

Figure 1.4 Models of allosteric interactions

(A) The allosteric ternary complex model (ATCM) (red) and the allosteric two-state model (ATSM; cubic scheme). (B) The operational model of allosterism. In all models, K_A and K_B denote the equilibrium dissociation constants of orthosteric, *A*, and allosteric, *B*, ligands, respectively. *L* denotes the isomerisation constant governing the transition between active and inactive receptor states. The parameter, α, denotes the binding cooperativity factor for interaction at the ground state of the receptor, the parameters β and γ denote the intrinsic efficacies of orthosteric and allosteric ligands, respectively (ability to stabilize active receptor state), and the parameter, δ, denotes the activation cooperativity factor for the ternary complex (Hall, 2000; Keov et al., 2011). Stimulus in any given system is governed by SA and SB for the orthosteric and allosteric ligand, respectively, the parameters τ_A and τ_B denote the capacity of orthosteric and allosteric ligands, respectively, to

exhibit agonism, and incorporate the intrinsic efficacy of each ligand, the total density of receptors and the efficiency of stimulus-response coupling (Leach et al., 2007).

1.3 Muscarinic Acetylcholine Receptors

1.3.1 General introduction

Muscarinic acetylcholine receptors (mAChRs) are family A GPCRs that mediate the majority of the actions of the biogenic amine neurotransmitter ACh. They consist of five molecularly distinct subtypes, denoted as M_1, M_2, M_3, M_4 and M_5 mAChRs, encoded by five distinct genes (CHRM1, CHRM2, CHRM3, CHRM4, and CHRM5) (Bonner et al., 1987; Caulfield and Birdsall, 1998; Hammer et al., 1980). Although mAChRs share evolutionarily conserved amino acid sequences and a high degree of sequence homology, they show pronounced differences in G protein coupling preferences and the physiological roles they mediate (Hulme et al., 1990; Wess, 1996).

1.3.2 Localisation and function

Each of the mAChR subtypes has a unique distribution throughout the central nervous system, where they are expressed both pre- and post-synaptically and in peripheral tissues (Felder, 1995). Centrally expressed mAChRs mediate cognitive, sensory and motor processes, while some of the roles of peripherally expressed receptors include stimulation of smooth muscle contraction, slowing of the heart rate and glandular secretions (Eglen, 2005; Wess et al., 2007).

The M_1 mAChR is predominantly expressed in the CNS, particularly in the forebrain areas including the cerebral cortex, hippocampus and the striatum (Eglen, 2006). It is therefore implicated in learning and memory processes and represents an important therapeutic target for diseases in which these processes are impaired, such as Alzheimer's disease and schizophrenia (Conn et al., 2009; Langmead et al., 2008b). The M_1 mAChR is further discussed in section 1.4.

The M_2 mAChRs are widely expressed both centrally and peripherally (Levey, 1993). Their blockade leads to increased cholinergic outflow as a result of reduced autoreceptor function in both

the brain and the periphery. Studies with M_2 mAChR deficient mice suggest a role for these receptors in mediating cognitive processes and bipolar depressive disorders due to their involvement in hippocampal cholinergic neurotransmission (Cannon et al., 2011; Eglen, 2012). In the periphery, the M_2 mAChR is expressed predominantly in the myocardium, where it mediates the negative chronotropic and inotropic effects of ACh. Genetic deletion of this receptor shows abolished bradycardic effects in response to ACh (Eglen, 2012; Gomeza et al., 1999a).

The M_3 mAChR is widely distributed in the CNS with the highest levels of expression in the hypothalamus (Levey, 1993). While little is known about the role of these receptors in the CNS, M_3 mAChR-deficient mice are hypophagic and lean, suggesting a role for this subtype in regulating food intake (Gautam et al., 2008). These studies also suggest a role for these receptors in promoting growth and regulating bone mass (Gautam et al., 2008; Wess et al., 2007). Both the M_2 and M_3 mAChRs mediate contractile responses in smooth muscle cells, and have been targeted therapeutically for hyperactive smooth muscle disorders such as irritable bowel syndrome (IBS) and chronic obstructive pulmonary disease (COPD) (Eglen, 2012; Peretto et al., 2009).

The M_4 mAChR is expressed centrally in the corpus striatum, mostly co-localised with dopamine receptors on striatal neurons. In the periphery, this receptor subtype is present on prejunctional nerve endings where it plays a role in inhibiting sympathetic and parasympathetic transmission (Eglen, 2012; Levey, 1993; Trendelenburg et al., 2003). Studies with the M_1/M_4 mAChR agonist xanomeline suggest a role for this receptor subtype in psychosis (see below) and this evidence is supported by the finding that M_4 mAChR-deficient mice display an increased sensitivity to compounds that disrupt prepulse inhibition (a preclinical model of psychosis) (Bodick et al., 1997a; Chan et al., 2008; Shekhar et al., 2008; Tzavara et al., 2003). Studies with M_4 mAChR-deficient mice also show increased locomotor activity and an enhancement of dopamine D_1 receptor-mediated effects (Gomeza et al., 1999b). As such, this receptor subtype has been targeted

therapeutically for the treatment of schizophrenia and Parkinson's disease (Jones et al., 2012; Langmead et al., 2008b).

The M_5 mAChR is expressed in the dopaminergic neurons of the substantia nigra, which provide the principal dopaminergic transmission to the striatum (Felder et al., 2000). The activation of this receptor subtype, along with the M_4 mAChR, facilitates striatal dopamine release in the brain (Vilaro et al., 1990). The M_5 mAChR is also the predominant subtype expressed in the ventral tegmental area, a tissue that provides major dopaminergic innervations to the nucleus accumbens and other limbic areas (Eglen, 2012; Eglen and Nahorski, 2000). These brain areas play a major role in the rewarding effects of drugs of abuse, as evidenced by studies with M_5 mAChR knockout mice, which show reduced sensitivity to the actions of addictive drugs such as morphine and cocaine (Fink-Jensen et al., 2003). Therefore, M_5 mAChR antagonism may be an important approach as novel therapeutics for compound addiction (Eglen, 2012; Kruse et al., 2014b).

1.3.3 Structural characteristics

The structural and functional features of mAChRs have been extensively explored by site-directed mutagenesis, covalent-labelling and molecular modelling studies (Hulme, 2013; Leach et al., 2012). Recently, the first crystal structures of mAChRs were solved, revealing the molecular organisation of the M_2 and M_3 mAChR subtypes in inactive (inverse agonist-bound) conformations (Haga et al., 2012; Kruse et al., 2012b), and an active agonist-bound structure of the M_2 mAChR with and without the presence of a PAM. Moreover, structural and computational studies have identified the mechanisms by which drug-like allosteric modulators bind to the M_2 mAChR (Dror et al., 2013; Kruse et al., 2013).

The structures of the inactive M_2 and M_3 mAChR revealed that, like other biogenic amine receptors, members of the mAChR family share the seven transmembrane topology and overall GPCR fold

(Dror et al., 2013; Kruse et al., 2014b; Kruse et al., 2013). Structural conservation includes ICLs 1 and 2 and ECLs 1-3, which share highly similar overall folds despite low sequence conservation (Kruse et al., 2014a). Both, M_2 and M_3 mAChRs exhibit features unique to the mAChR group, including a large extracellular vestibule as part of an extended hydrophilic channel containing the orthosteric binding site. This channel is separated from the cytoplasmic surface by a hydrophobic layer formed by three amino acids: $Leu^{2.46}$, $Leu^{4.43}$ and $Ile^{6.40}$, which are absolutely conserved among all five muscarinic subtypes (Haga et al., 2012) [Numbering in superscript corresponds to the Ballesteros–Weinstein system (Ballesteros and Weinstein, 1995)]. Both M_2 and M_3 mAChRs also feature a unique outward bend at the extracellular end of TM4 that is not seen in other GPCR crystal structures. This bend is stabilised by a hydrogen bond between the $Gln^{4.64}$ side chain and the $Leu^{4.61}$ backbone peptide carbonyl (Kruse et al., 2012a). This bend is part of a polar interaction network involving four residues absolutely conserved within the mAChR family, suggesting that this unusual feature is important to mAChRs in general. Mutagenesis of $Gln^{4.64}$ in the M_3 mAChR impaired both ligand binding and receptor activation (Scarselli et al., 2007).

The extracellular domains of mAChRs contribute to the structural stability of the receptors. In particular, the ECL2 is stabilised by a conserved disulphide with $Cys^{3.25}$ at the N terminus of TM3 and a Cys in the middle of ECL2. The ECL2 defines a boundary of the orthosteric binding site that forms a lid-like structure over the orthosteric binding pocket and limits the extent of the conformational changes of this region upon receptor activation (Hulme, 2013; Hulme et al., 2003b; Kruse et al., 2014b). Restriction of flexibility of this region in the M_2 mAChR (via engineering of an additional disulphide bond) substantially hinders access of orthosteric ligands (Avlani et al., 2007). The ECL3 contains an additional intra-loop disulphide bridge between $Cys^{6.61}$ and $Cys^{7.29}$ that also contributes to receptor stability. In addition, other conserved amino acid residues have also been found that are essential for maintaining the overall helical structure, stability and folding of mAChRs $Asp^{2.50}$, $Leu^{3.43}$, $Asp^{3.49}$, $Tyr^{3.51}$, $Trp^{4.50}$, and $Pro^{7.50}$ such that mutation of such residues

leads to reduction in cell surface expression (Hulme et al., 2001; Hulme et al., 2003b; Lu and Hulme, 1999a; Lu et al., 2001a; Lu et al., 1997).

Unlike other GPCRs, the mAChR (and opioid) crystal structures show that there is no interaction involving $Arg^{3.50}$ in the conserved DRY sequence in TM3 and $Glu^{6.30}$ in TM6 (the so-called "ionic lock"), instead a conserved Arg in ICL2 forms a salt bridge with $Asp^{3.49}$ of the DRY motif in TM3, thereby tethering ICL2 with the TM core (Haga et al., 2012; Kruse et al., 2012b).

1.3.4 Signaling

Muscarinic receptors are classified according to their G protein coupling preferences (Caulfield and Birdsall, 1998). Generally, upon activation by agonists, the M_2 and M_4 mAChRs preferentially couple to $G\alpha_{i/o}$ G proteins, resulting in the inhibition of AC, reduction in cAMP levels and prolongation in the opening of potassium, non-selective cation, and transient receptor potential channels (Felder, 1995; Migeon et al., 1995; Whorton and MacKinnon, 2013a). The M_1, M_3 and M_5 mAChRs couple preferentially to $G\alpha_{q/11}$ G proteins and activate PLCβ which leads to the generation of IP_3 and DAG and a subsequent rise in intracellular Ca^{2+} levels (Lanzafame et al., 2003; Peralta et al., 1988) (Figure 1.2 and 1.11). These three subtypes also activate other cellular messengers such as nitric oxide (NO) or phospholipase A_2 (PLA_2) (Eglen, 2005; Felder, 1995). Both $G\alpha_{i/o}$- and $G\alpha_{q/11}$ -coupled receptors also activate small GTPase proteins such as Rho, leading to cytoskeletal effects (Eglen, 2006). They also signal through a variety of effector molecules such as PI3Ks and MAPKs, such as ERK1/2, to effect cell growth and proliferation (Eglen, 2006). In some cases the βγ subunits also play a role in cellular signaling and provide a mechanism by which the M_2 mAChRs activate PLCβ (Katz et al., 1992; Stehno-Bittel et al., 1995). Muscarinic receptors have also been shown to promiscuously couple to more than one G protein and multiple effector pathways (Akam et al., 2001; Lee et al., 1998a; Michal et al., 2007; Migeon et al., 1995; Thomas et

al., 2008), suggesting the capacity for biased signaling (Kenakin, 2007). However, activation of these different signaling pathways occurs in a cell-type-specific and agonist-specific manner.

1.3.5 Regulation and trafficking

In addition to cellular mechanisms that control receptor activation and signaling, GPCRs are highly regulated (van Koppen and Kaiser, 2003). Generally, regulatory processes can be divided into three distinct events based on their timing and mechanism. First, desensitisation takes place upon receptor activation, which results in receptor uncoupling from G proteins (seconds to minutes). Second, receptors are sequestered and internalised away from the cell surface (minutes), and third, down-regulation of receptors results in a decrease in the total number of cellular receptors (hours) (Eglen, 2012).

The prototypic internalisation process that occurs after agonist activation of the receptor begins by phosphorylation of serine and threonine residues on ICL3 of the receptor by an array of protein kinases including members of the GRK family, PKC and casein kinase 1α (CK1α) (van Koppen and Kaiser, 2003). This is followed by binding of β-arrestins, which promotes receptor desensitisation by blocking interaction of the receptor with the G protein. In addition, β-arrestins can also bind the adaptor protein AP2 and recruit the receptor into clathrin-coated pits in a dynamin-dependent manner to cause receptor internalisation (Bouvier et al., 1988; Eglen, 2012; Ferguson et al., 1996; Lohse et al., 1989). Among the muscarinic receptors, the M_1, M_3 and M_4 mAChR subtypes follow this prototypical pathway more closely than the M_2 subtype. These three subtypes are internalised through the dynamin-dependent, clathrin-mediated pathway (Claing et al., 2000; Lee et al., 1998b; van Koppen, 2001; Vogler et al., 1998; Vogler et al., 1999a; Vogler et al., 1999b; Yeatman et al., 2014). However, it has been shown that the M_2 mAChR internalises in a β-

arrestin and clathrin-independent manner, suggesting potential alternative pathways for mAChR internalisation (Eglen, 2012; van Koppen and Kaiser, 2003).

Following internalisation, receptors are either recycled back to the cell surface or targeted to the lysosome, leading to down regulation or permanent loss of the receptors from the cell. The M_1, M_3 and M_4 but not the M_2 mAChRs recycle back to the cell surface upon their short exposure to the orthosteric agonist carbachol and a recovery period (van Koppen, 2001; Yeatman et al., 2014).

1.3.6 Ligand binding

In addition to the endogenous agonist ACh, mAChRs bind a large number of ligands with varying structural and pharmacological properties. Some of the non-selective mAChR orthosteric agonists include carbachol, pilocarpine, oxotremorine-M and arecoline (Figure 1.5), while inverse agonists include atropine, tiotropium, NMS and QNB (Figure 1.6) (Langmead and Christopoulos, 2006). Numerous allosteric modulators also exist, some of which are selective for specific mAChR subtypes (Conn et al., 2009; De Amici et al., 2010). Both orthosteric and allosteric binding sites have been mapped out in recent mAChR crystal structures and computational studies (Haga et al., 2012; Kruse et al., 2012b; Kruse et al., 2013).

1.3.6.1 Inverse agonist binding

The M_2 and M_3 mAChRs were crystallised in complex with the non-selective muscarinic inverse agonists QNB and tiotropium, respectively (Figure 1.6). The two ligands have a similar chemical structure and bind in similar poses (Haga et al., 2012; Kruse et al., 2012b). The orthosteric binding pocket occupied by these ligands is deeply buried within the membrane and is placed similarly to the orthosteric binding sites of the biogenic amine receptors such as histamine (Shimamura et al.,

2011), dopamine (Chien et al., 2010), adrenaline (Cherezov et al., 2007; Rasmussen et al., 2007; Warne et al., 2008) and serotonin (Wacker et al., 2013) receptors. The binding pocket is defined by side chains of TM3, 4, 5, 6 and 7 and is covered by a lid comprising four conserved tyrosines- $Tyr^{3.33}$, $Tyr^{6.51}$, $Tyr^{7.39}$ and $Tyr^{7.43}$- that completely occlude the ligand from solvent to facilitate hydrophobic contacts with the receptor. The amino acids that form the binding pocket are identical in all five muscarinic receptor subtypes, with the exception of Phe181 in the M_2 mAChR, which extends downward from the ECL2 and interacts with one of the phenyl rings of QNB.

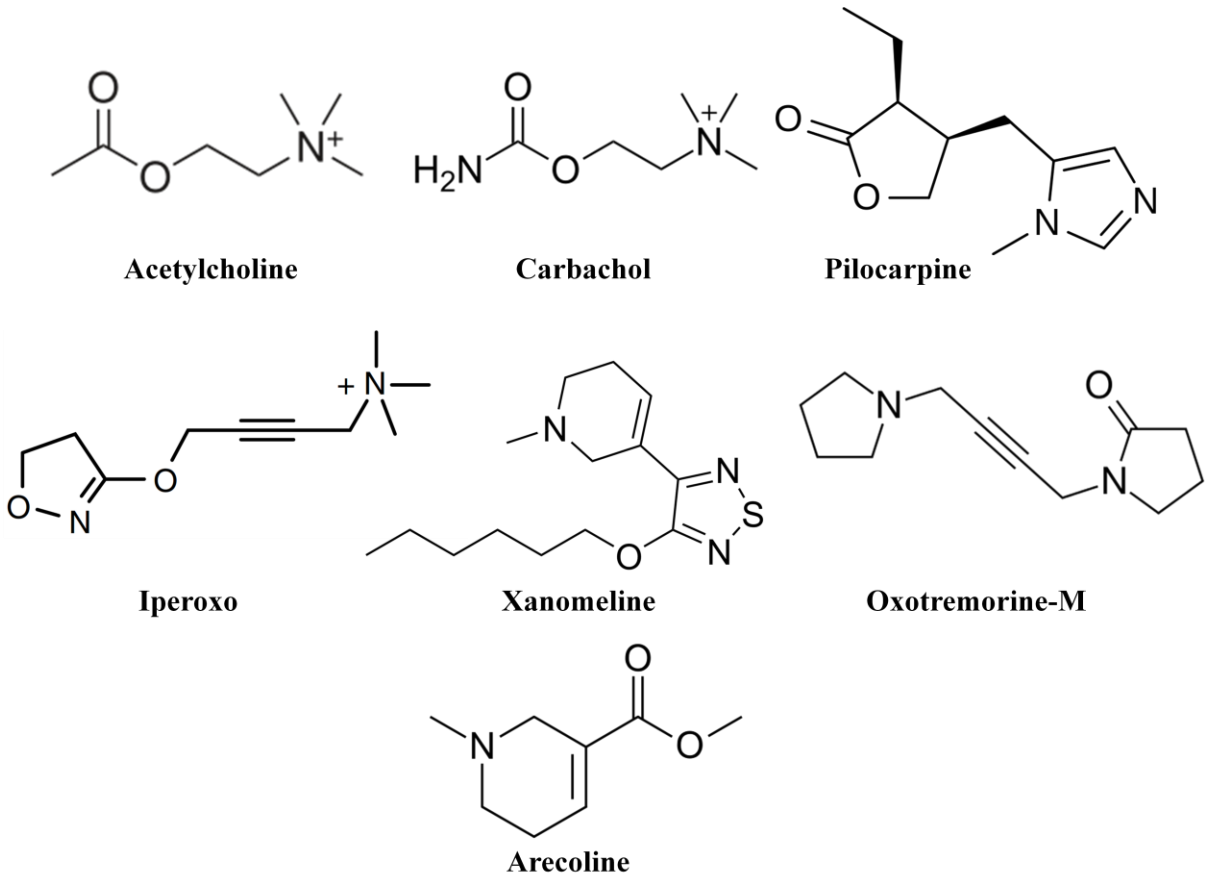

Figure 1.5 Structure of non-selective orthosteric mAChR agonists.

All other mAChR subtypes have a leucine in the homologous position (Haga et al., 2012; Hulme, 2013; Kruse et al., 2012b). Substitutions of $Tyr^{3.33}$, $Tyr^{6.51}$, $Tyr^{7.39}$ and $Tyr^{7.43}$ for the aromatic

amino acid Phe, causes minimal effects on binding of the muscarinic inverse-agonist NMS (Lu et al., 2001b; Ward et al., 1999; Wess et al., 1991; Wess et al., 1992a). However alanine substitution of these residues, in addition to residues at position 4.57, 5.39 and 5.42, reduces the binding affinity of both NMS and QNB, with the exception of $Tyr^{6.51,}$ which is able to discriminate between different mAChR antagonists by showing loss of binding to NMS but unaltered affinity for QNB (Avlani et al., 2010; Heitz et al., 1999; Lu and Hulme, 1999a; Lu et al., 2001b; Matsui et al., 1995; Ward et al., 1999) (Figure 1.7). Collectively, this evidence indicates that aromaticity at these positions is essential for the interaction of these ligands with the receptor.

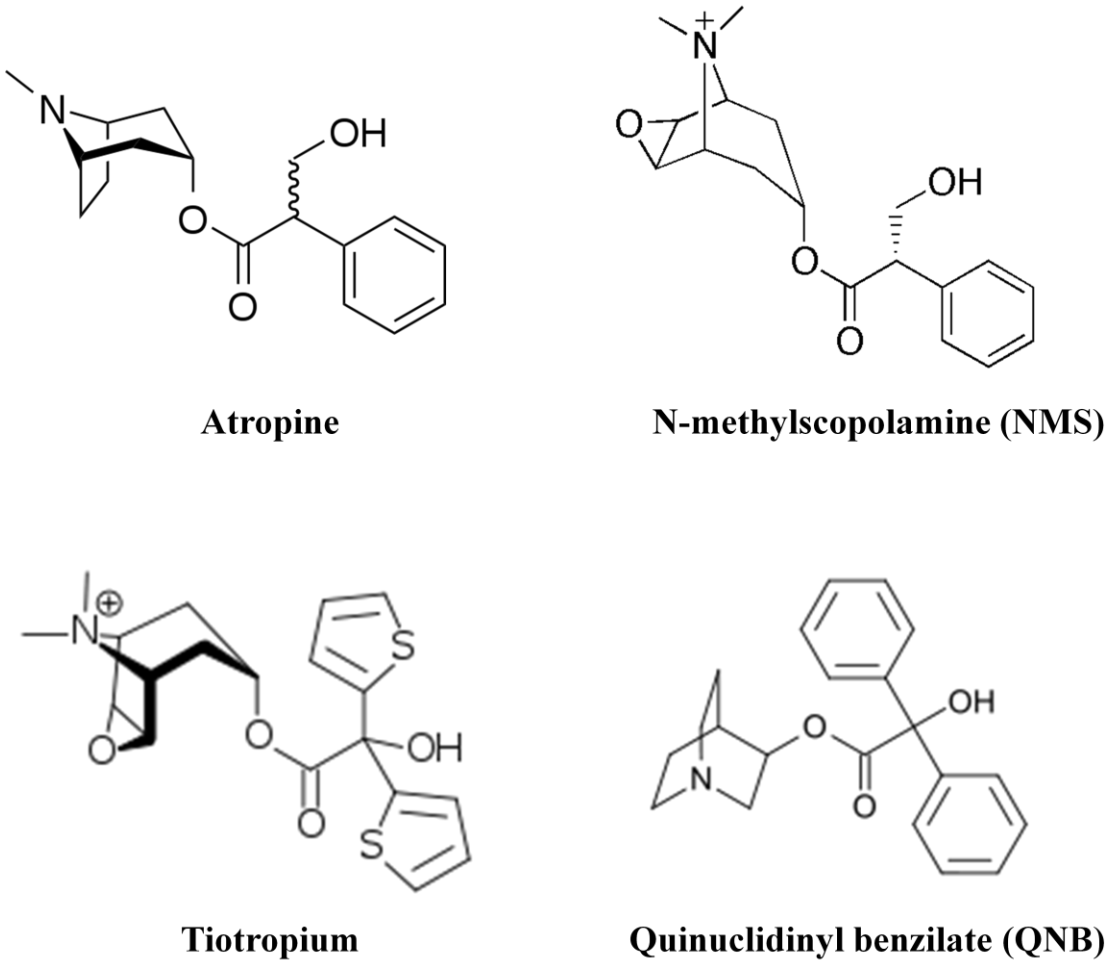

Figure 1.6 Structure of non-selective orthosteric mAChR antagonists/inverse agonists.

The cationic amine moieties of NMS, QNB and tiotropium form a charge-charge interaction with $Asp^{3.32}$. The importance of $Asp^{3.32}$ for both agonist and antagonist binding has been demonstrated in mutagenesis, covalent-labelling, and modelling studies (Goodwin et al., 2007; Heitz et al., 1999; Hulme et al., 2003a). This interaction is also observed in all biogenic amine receptor structures solved to date and has been shown to make a major energetic contribution to ligand binding (Kooistra et al., 2013; Venkatakrishnan et al., 2013). In the M_2 and M_3 mAChR crystal structures, $Asn^{6.52}$ forms a paired hydrogen bond with the hydroxyl and ketone groups of QNB and tiotropium (Haga et al., 2012; Kruse et al., 2012b; Kruse et al., 2013). Mutagenesis studies on $Asn^{6.52}$ have shown the importance of this residue for the binding of atropine and NMS and QNB to a lower extent (Bluml et al., 1994a; Hulme et al., 2003a; Ward et al., 1999). The paired hydrogen bonding between the ligand and $Asn^{6.52}$ is a unique feature of the mAChR family and has been proposed to be an important factor in slow ligand dissociation from mAChRs (Kruse et al., 2014b; Tautermann et al., 2013).

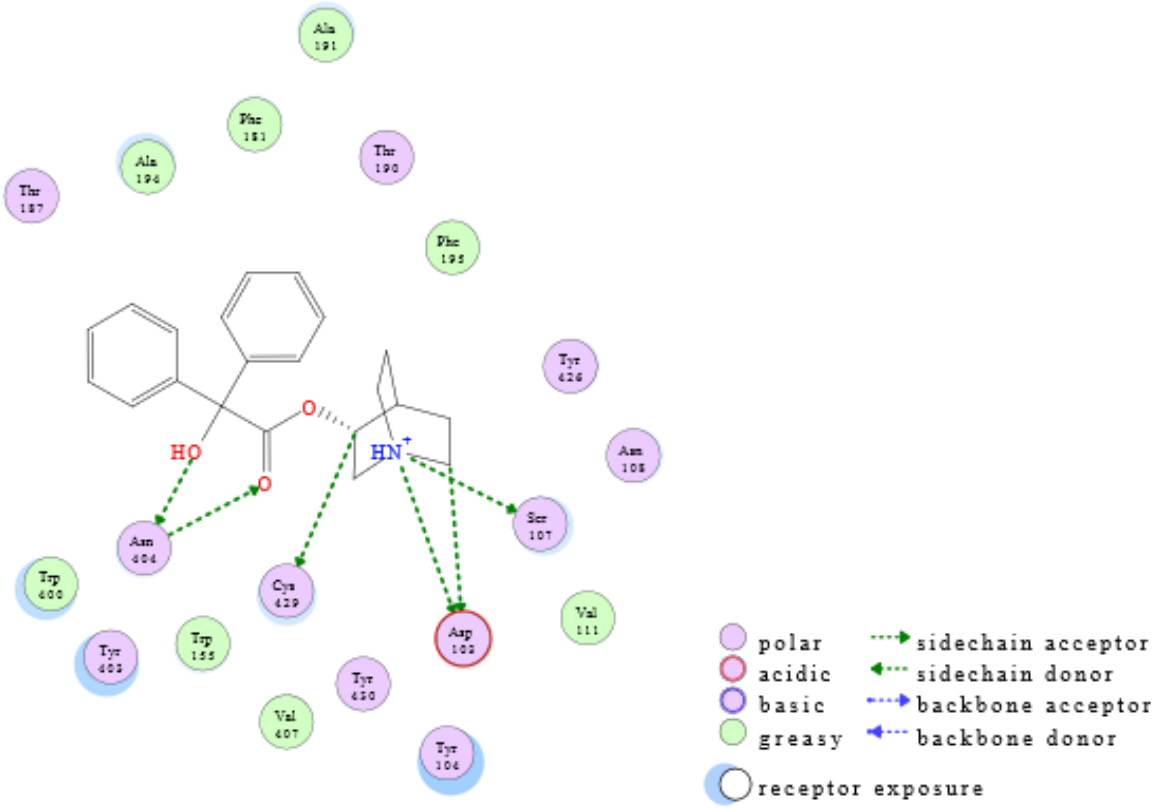

Figure 1.7 Binding interactions between the M_2 mAChR and QNB. A schematic representation of QNB binding interactions in the orthosteric pocket. Polar interactions are indicated by green dashed lines. Adapted from Haga et al,. 2012 (Protein Data Bank code 3UON).

1.3.6.2 Agonist binding and receptor activation

The crystal structure of an agonist (iperoxo)-bound, active state of the human M_2 mAChR stabilised by a G protein-mimetic antibody fragment, was recently solved (Kruse et al., 2013). In addition to mapping the orthosteric agonist binding site, this study highlights the receptor conformational changes that occur upon receptor activation (Haga et al., 2012) (Figure 1.8).

Iperoxo is an orthosteric agonist that displays high affinity and potency at all mAChRs and was used rather than ACh as the latter has lower affinity and is prone to hydrolysis (Schrage et al., 2013) (Figure 1.5). Iperoxo binding to the M_2 mAChR leads to contraction of the orthosteric binding site,

which completely occludes the agonist ligand from solvent and creates a cavity that is smaller than that observed for QNB. TM5, TM6, and TM7 move inward towards iperoxo and TM3 undergoes a slight rotation around its axis (Kruse et al., 2014a; Kruse et al., 2014b; Kruse et al., 2013). Despite these activation-related structural changes, polar contacts between the agonist and the receptor resemble those of QNB-bound to the inactive M_2 mAChR structure. $Asp^{3.32}$ serves as a counter-ion to the ligand amine and the side chain of $Asn^{6.52}$ form a hydrogen bond with the isoxazoline ring of iperoxo. However, the smaller size of iperoxo relative to QNB causes an inward motion of TM6 and results in more limited hydrophobic contacts particularly with residues in TM5. The inward motion of the exofacial portion of TM6 leads to the formation of a hydrogen bond network between $Tyr^{6.51}$, $Tyr^{3.33}$, and $Tyr^{7.39}$, resulting in the closure of the tyrosine lid above the ligand (Kruse et al., 2014a; Kruse et al., 2014b; Kruse et al., 2013) (Figure 1.8).

Although the M_2 mAChR was crystallised with iperoxo rather than ACh, docking of ACh to the inactive M_2 mAChR conformation shows that both ligands contact identical residues (Haga et al., 2012). Moreover, the results with iperoxo are in agreement with the results from a plethora of site-directed mutagenesis and covalent-labelling studies that identified amino acids that are critical for the binding of ACh to the mAChRs (Hulme, 2013; Lu et al., 2001b; Ward et al., 1999; Wess et al., 1991), many of which are also essential for the binding of inverse agonists such as NMS and QNB. For example, similar to the inverse agonists QNB, NMS and tiotropium, the negative charge on $Asp^{3.32}$ was found to form a salt bridge with the quaternary nitrogen of ACh. Conservative substitution of this residue for a Glu or Asn reduces the affinity of ACh, although the effect is less pronounced with Glu, highlighting the importance of the negative charge for the binding of ACh (Abdul-Ridha et al., 2014b; Curtis et al., 1989; Leach et al., 2011; Lu and Hulme, 1999a; Page et al., 1995; Spalding et al., 1994). In addition, hydrogen bonding of the Tyr lid was shown to be important for agonist binding and activation in muscarinic receptors. Mutation of any of the three

Tyr to Ala, or more conservatively, to Phe leads to impaired ACh binding (Gregory et al., 2010; Lu and Hulme, 1999a; Lu et al., 2001b; Ward et al., 1999; Wess et al., 1991; Wess et al., 1992b).

Additional features of the active conformation of the M_2 mAChR relative to the inactive conformation are a significant outward displacement of the cytoplasmic end of TM6, together with a smaller outward movement of the C-terminal portion of TM5 and a rearrangement of the highly conserved $^{3.49}$DRY$^{3.51}$ and $^{7.49}$NPxxY$^{7.53}$ motifs (Kruse et al., 2014a; Kruse et al., 2014b; Kruse et al., 2013). Similar conformational changes have been reported for the active-state conformations of rhodopsin (Choe et al., 2011a; Scheerer et al., 2008) and the β_2-adrenergic receptor (Rasmussen et al., 2011a; Rasmussen et al., 2011b).

In this structure, Asp$^{3.49}$ of the $^{3.49}$DRY$^{3.51}$ motif is stabilised by a hydrogen bond with Asn$^{2.39}$. Asp$^{3.49}$ and Tyr$^{3.51}$ are essential for the function of the majority of Family A GPCRs (Lu et al., 1997). In the mAChRs, Ala mutation of Asp$^{3.49}$ and Tyr$^{3.51}$ causes significant decrease in ligand efficacy and reduces receptor expression while Ala mutation of Asn$^{2.39}$ results in normal ligand-binding properties, but impaired ability to activate G proteins (Jones et al., 1995; Kruse et al., 2013; Leach et al., 2011; Lu et al., 1997). Thus, Asn$^{2.39}$ either directly stabilises the active conformation, or engages in direct interactions with the G protein while Asp$^{3.49}$ and Tyr$^{3.51}$ are critical for maintaining a receptor conformation able to bind ligand.

The rearrangements of the $^{7.49}$NPxxY$^{7.53}$ region upon receptor activation include a partial 'unwinding' of TM7 around Tyr$^{7.53}$, which places this residue in close proximity to the highly conserved Tyr$^{5.58}$, allowing the formation of a water mediated hydrogen bond that is also seen in the active-state conformations of rhodopsin (Choe et al., 2011a; Scheerer et al., 2008) and the β_2-adrenergic receptor (Rasmussen et al., 2011a; Rasmussen et al., 2011b) indicating that this feature represents a hallmark of GPCR activation (Kruse et al., 2013; Miao and McCammon, 2013). Mutation of Tyr$^{5.58}$ to Phe, which is predicted to disrupt the water-mediated hydrogen bond, causes significant decrease is agonist affinity and abolished response to ACh. However, it has no effect on

antagonist binding, indicating that the interaction between these tyrosine residues stabilises the active conformation of the receptor in a manner reminiscent of the 'ionic lock' interaction, which stabilizes the inactive conformation of family A GPCRs (Kruse et al., 2013).

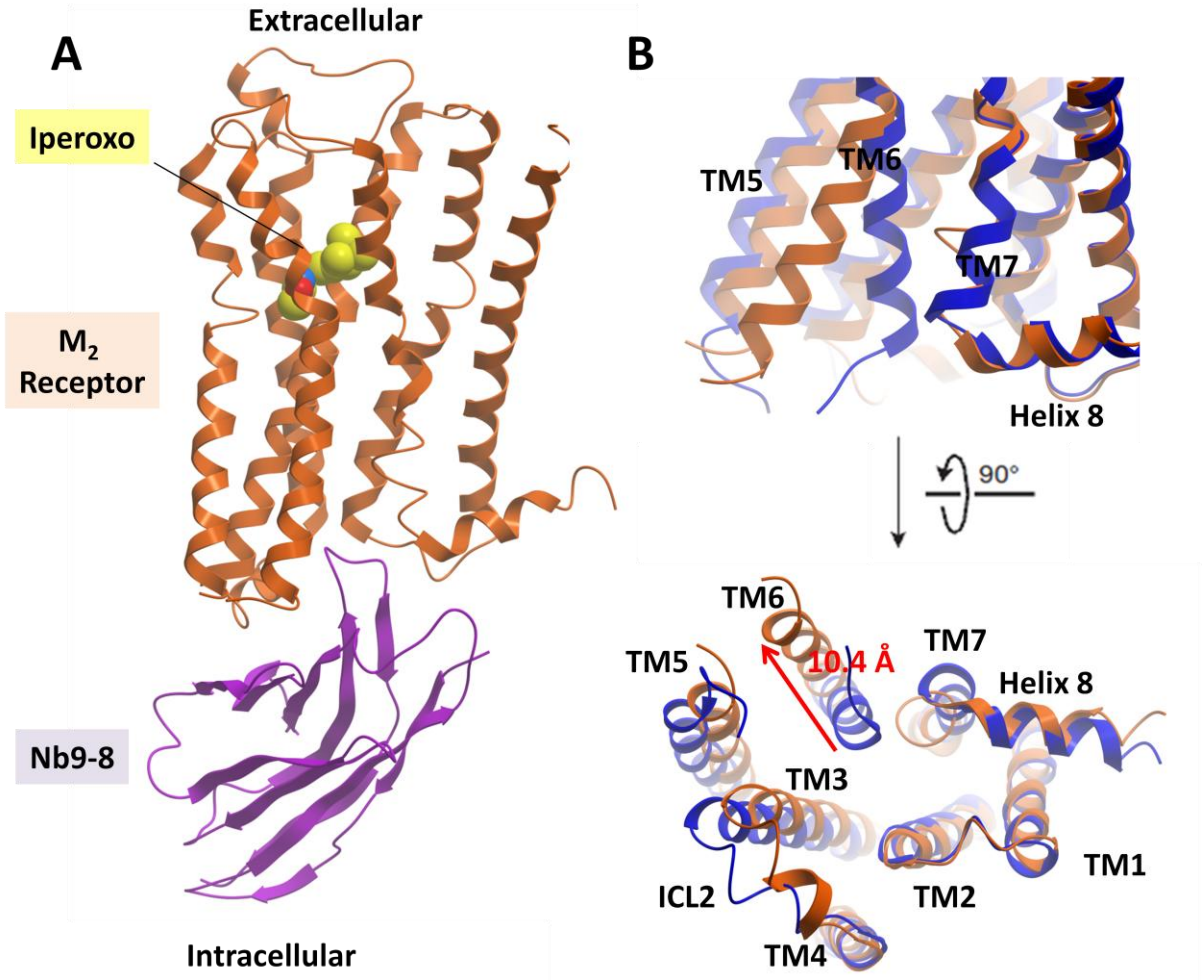

Figure 1.8 Intracellular changes on activation of the M_2 mAChR receptor. (A) The overall structure of the active-state M_2 mAChR (orange) in complex with the orthosteric agonist iperoxo and the active-state stabilizing nanobody Nb9-8. (B) Compared to the inactive structure of the M_2 mAChR (blue), TM6 is substantially displaced outward, and TM7 has moved inward. Together, these motions lead to the formation of the G-protein-binding site. Adapted from Kruse et al., 2013 (Protein Data Bank code 4MQS).

1.3.6.3 G protein-coupling

The structure of the β_2 adrenergic receptor-Gα_s complex reveals that the G protein only contacts residues in TM3, 5, 6 and ICL2 of the receptor and does not interact with residues in TM7 and helix 8 (Figure 1.1) (Rasmussen et al., 2011b). The outward displacement of the cytoplasmic ends of the TM domains that occur upon agonist binding allows the initial insertion of the Gα_s C-terminal α5-helix into the transiently accessible G protein coupling site between helices on the intracellular side of the receptor. However, the structure of rhodopsin crystallised with a peptide that resembles the C-terminus of Gα_s, indicates that ICL2 and 3, the cytoplasmic ends of TM3, 5 and 6 and the N-terminal segment of helix 8 are all involved in G protein binding (Scheerer et al., 2008). Nonetheless, both receptors show the specific interaction between the conserved $^{3.49}$DRY$^{3.51}$ motif residue, Arg$^{3.50}$, and the Gα_s α5-helix confirming the importance of Arg$^{3.50}$ in receptor signaling and underlining its importance in stabilizing an active receptor state (Choe et al., 2011b).

In agreement with these results, mutagenic studies suggest an interaction between Gα_q and ICL3, TM5 and 6 and helix 8 of the M_3 mAChR, with four residues at the cytoplasmic end of TM6 (positions 6.33, 6.34, 6.37 and 6.38) identified as critical in determining G-protein coupling selectivity (Blin et al., 1995; Bluml et al., 1994c; Kostenis et al., 1997; Liu et al., 1995). Similar observations have been made in the M_5 mAChR (Burstein et al., 1996; Burstein et al., 1998a; Burstein et al., 1998b; Hill-Eubanks et al., 1996) and in the β_2 adrenergic receptor-Gα_s complex (Rasmussen et al., 2011b) two of the four corresponding residues make contact with C-terminal α5-helix of Gα_s.

In addition, a cysteine cross-linking study additionally identified Leu173 and Arg176 in ICL2 and Thr549, Thr552, and Thr556 in the N-terminal segment of helix 8 of the M_3 mAChR as residues that directly interact with the C-terminal α5-helix of Gα_q (Hu et al., 2010).

The differences in the cytoplasmic ends of TM5 and ICL2 of the M_2 and M_3 mAChRs may underlie the G protein-coupling specificity of the two receptors (Kruse et al., 2012b). The highly conserved

$Tyr^{5.58}$ residue shows a deviation between the two receptors, pointing towards the core of the protein in M_2 mAChR, and away from the receptor towards the surrounding lipid bilayer in M_3 mAChR (Haga et al., 2012; Kruse et al., 2012b). $Tyr^{5.62}$ at the bottom of TM5 in the M_3 mAChR has also been shown to play a role in activation of $G\alpha_q$ (Bluml et al., 1994b). In the M_2 mAChR, the corresponding residue, $Ser^{5.62,}$ is displaced by approximately 4Å relative to the same residue in the M_3 mAChR (Haga et al., 2012; Kruse et al., 2012b). Comparison of the position of TM5 in the M_2 and M_3 receptors to that in other GPCR structures found that it is M_2 mAChR-like in all $G\alpha_{i/o}$-coupled receptors, whereas the two mammalian $G\alpha_q$-coupled receptors solved to date (Histamine H_1 and squid rhodopsin) (Murakami and Kouyama, 2008; Shimamura et al., 2011) exhibit a different conformation (Katritch et al., 2013; Venkatakrishnan et al., 2013).

1.3.7 Chemogenetic strategies for studying GPCR physiology

1.3.7.1 Development of DREADDs

In order to gain insight into their physiological role *in vivo*, different families of GPCRs have been engineered to allow control over their cell type- or tissue-specific expression or to provide targeted and selective activation (Nichols and Roth, 2009; Wess et al., 2013).

Early attempts to produce such engineered receptors resulted in the generation of Receptors Activated Solely by Synthetic Ligands (RASSLs) (Nichols and Roth, 2009). RASSLs have a significantly reduced ability to interact with their endogenous ligands but are able to interact with exogenously administered synthetic ligands. A large number of studies have demonstrated the utility of these receptors as tools to study complex biological behaviours (Bruysters et al., 2005; Coward et al., 1998). An example of such modified GPCRs is Ro1, a $G\alpha_{i/o}$-coupled kappa-opioid receptor with drastically reduced affinity for the natural peptide ligand, but very high affinity for the small synthetic ligand spiradoline (Coward et al., 1998). This receptor was expressed in transgenic mice to study cardiac function after its selective activation (Redfern et al., 1999).

Although they have been shown to be valuable tools, RASSLs have some significant limitations. Often, the synthetic ligands used to activate these receptors exhibit high affinities for the native receptors as well as other off-target actions, limiting their use *in vivo*. In addition, many RASSLs have high basal signalling and display constitutive activity *in vivo* which could obscure any ligand-induced phenotypes (Pei et al., 2008).

To overcome the imitations associated with RASSLs, a second generation of engineered GPCRs was generated for the mAChR family, named Designer Receptors Exclusively Activated by Designer Drugs (DREADDs) (Armbruster, 2007). DREADDs contain mutations at two strictly conserved amino acid residues, namely $Tyr^{3.33}Cys$ and $Ala^{5.46}Gly$. As a result of these mutations, these receptors are activated by Clozapine-N-Oxide (CNO) with high potency and efficacy (Figure 1.9), but show little response to the native ligand ACh. CNO is a pharmacologically inert metabolite of clozapine, an antipsychotic drug. However, DREADDs still show the same G protein coupling preference as their parent receptors (M_1, M_3, and M_5 for $G\alpha_{q/11}$; M_2 and M_4 for $G\alpha_{i/o}$) (Armbruster et al., 2007). Unlike RASSLs, expression of DREADDs *in vivo* in mice or rats does not result in constitutive signaling in the absence of CNO (Armbruster, 2007; Wess et al., 2013).

To validate DREADDs, Alvarez-Curto et al., 2011 investigated whether the action of the synthetic ligand (CNO) at DREADDs can cause signaling outcomes that are equivalent to those caused by the native mAChRs when activated by ACh. The effects of CNO at the M_3 DREADD were found to be similar to WT at the varying endpoints measured, including equivalent conformational changes of ICL3, activation of ERK1/2 phosphorylation, phosphorylation of intracellular Ser residues, interaction with β-arrestin 2 and internalisation from the cell surface in response to the corresponding ligand. Such results provided confidence that, at least for the M_3 mAChR, the results obtained after transgenic expression of M_3 DREADD are likely to mirror the actions of ACh at the WT receptor (Alvarez-Curto et al., 2011).

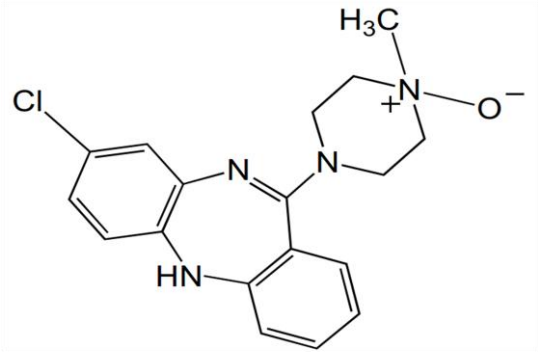

Clozapine-N-oxide (CNO)

Figure 1.9 The structure of clozapine-N-oxide (CNO)

1.3.7.2 Molecular basis of CNO-DREADD interactions

CNO binds to the mAChRs with a 1000-fold lower affinity compared to its parent molecule clozapine (Abdul-Ridha et al., 2013; Johnson et al., 2005). Structurally, CNO differs from clozapine by the presence of the N-oxide group. It is proposed that the negative charge on this group may interfere, via electrostatic repulsion, with formation of a salt bridge between the positively charged nitrogen of CNO and the negative charge of $Asp^{3.32}$ (Wess et al., 2013).

Mutagenesis studies at the M_1 and M_3 mAChRs involving the $Tyr^{3.33}$, show that mutation of this residue to either Ala or Cys caused a significant reduction in the affinity of orthosteric antagonists QNB and NMS and reduction in affinity, potency and efficacy of agonists (ACh or carbachol) (Han et al., 2005; Lu and Hulme, 1999b). Mutation of $Ala^{5.46}Gly$ at the M_1 mAChR caused a similar decrease in ACh affinity, potency and signaling efficacy as well as a decreased affinity for QNB (Allman et al., 2000). These results explain why DREADDs containing both the $Tyr^{3.33}Cys$ and $Ala^{5.46}Gly$ point mutations show minimal ACh binding affinity and efficacy.

Docking of CNO into the M_3 mAChR crystal structure shows that it adopts a pose similar to that of tiotropium and, like tiotropium, makes contact with both the $Tyr^{3.33}$ and $Ala^{5.46}$ residues. It is unclear why CNO shows high affinity and efficacy at the DREADD but not at the WT mAChRs, though it has been suggested that the $Tyr^{3.33}Cys$ mutation causes minor conformational rearrangements of the aromatic Tyr lid that lead to changes in the kinetics of CNO binding, resulting in an increase in CNO binding affinity. The $Ala^{5.46}Gly$ mutation has been suggested to increases the conformational flexibility of TM5, thus facilitating a CNO dependent inward movement of TM5 (Wess et al., 2013).

1.3.7.3 Expression in vivo

The cell-type or tissue-specific expression of DREADDs *in vivo* has been achieved using several experimental strategies. For example, the generation of transgenic mice in which DREADD expression can be temporally and spatially controlled by the use of Tet-off technology and tissue-specific promoters (Alexander et al., 2009; Garner et al., 2012). A knock-in mouse model has also been used in which the expression of M_4 DREADD is dependent on Cre-mediated removal of a floxed stop sequence preceding the M_4 DREADD coding sequence (Ray et al., 2011; Ray et al., 2013). Using these approaches, DREADDs have been successfully employed to study GPCR signaling pathways and to investigate biological processes and behaviours. In particular, DREADD technology has been used by neuroscientists to map neuronal circuits underlying CNS functions such as memory formation, regulation of food intake, wakefulness, motor control and drug seeking behaviour (Farrell et al., 2013; Ferguson et al., 2011; Garner et al., 2012; Guettier et al., 2009; Karunarathne et al., 2013; Krashes et al., 2011; Mahler et al., 2014; Michaelides et al., 2013; Ray et al., 2011; Sasaki et al., 2011; Zhu and Roth, 2014).

Transgenic mouse lines expressing the hM_3 DREADD or $M_3G\alpha s$ DREADD (M_3 DREADD receptors modified to couple to Gαs) in pancreatic β-cells have been reported and show that stimulation of either receptor has significant effects on β-cells function including glucose tolerance and insulin release (Guettier et al., 2009; Jain et al., 2013). Another study demonstrated remote control of neuronal activity in mice also expressing the hM_3 DREADD receptor in the hippocampus. Administration of CNO to these transgenic mice lead to increases in hippocampal neural activity as well as behavioural modifications in a dose dependent manner (Alexander et al., 2009). Additional studies have also used M_3 DREADD transgenic mice to study the consequences of activating Agouti-Related Protein neurons on mice feeding behaviour and found that activation of these neurons induces feeding, reduces energy expenditure and leads to increases in fat storage (Krashes et al., 2011). Ferguson *et al*. further demonstrated the utility of this approach for deconstructing neuronal pathway contributions to behaviour in relation to development of drug addiction upon repeated drug intake (Ferguson et al., 2011). Finally, a recent study expressed DREADD receptors in Drosophila as an approach to control behaviour, neuronal signaling and physiology in the fly (Becnel et al., 2013). A list of all studies that used DREADD technology is found in the review by Wess et al., (2013).

1.3.7.4 Allosteric modulation of DREADDs

Although DREADD technology has been most often used for *in vivo* studies, it has also been useful in understanding mechanisms of allosteric modulation in cultured cell lines (Abdul-Ridha et al., 2013; Nawaratne et al., 2008). The M_4 mAChR allosteric modulator, LY2033298 (Figure 1.10) (Chan et al., 2008) has been shown to act cooperatively with the orthosteric binding site to remarkably restore the functionality of ACh at the M_4 DREADD receptor (Nawaratne et al., 2008). This study provides evidence for the retention of a functional allosteric site on the M_4 DREADD

and highlights the roles of the mutated residues in transmission of cooperativity across binding sites. Furthermore, these modified receptors can be used as model 'inactive' receptors to study the two-state behaviour of GPCRs as allosteric proteins and allosteric ligands that have been shown to display 'state-dependence', such as the M_1 mAChR allosteric modulator benzyl quinolone carboxylic acid (BQCA) (Figure 1.15) (Canals et al., 2012). Abdul-Ridha et al., (2013) used BQCA to investigate whether the allosteric modulation of CNO-bound M_1 DREADD is equivalent to the modulation of the ACh-bound WT receptor as detailed in Chapter 2.

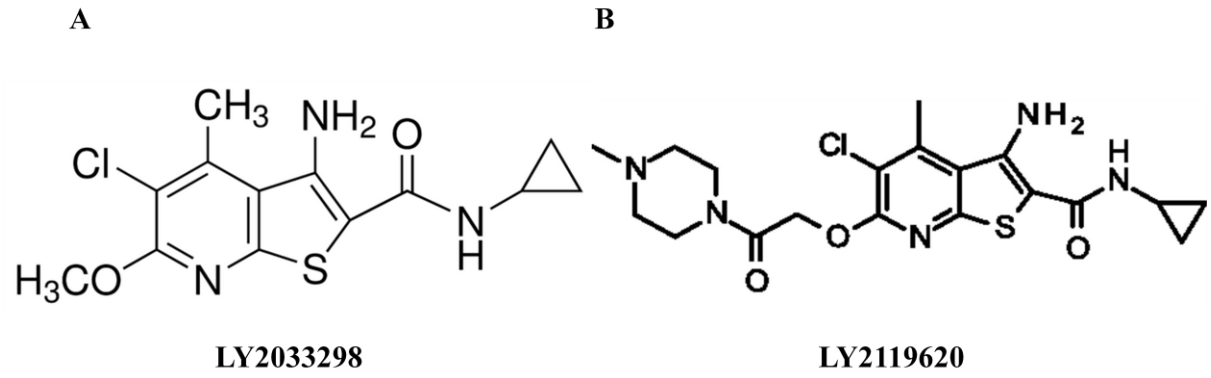

Figure 1.10 (A) Structure the M_4 mAChR and (B) the M_2 mAChR PAMs.

1.3.7.5 Arrestin biased DREADD

A β-arrestin-biased DREADD has been generated as a tool for studying the physiological relevance of arrestin-dependent signaling pathways (Nakajima and Wess, 2012). The M_3 β-arrestin-biased DREADD contains an additional $Arg^{3.50}Lys$ point mutation and is unable to activate G protein signaling pathways such as cAMP accumulation/inhibition and calcium mobilisation. However, it is able to recruit arrestins and promote ERK1/2 phosphorylation in a CNO- and arrestin- dependent fashion. CNO treatment of MIN6 mouse insulinoma cells expressing the M_3 arrestin-biased

DREADD resulted in insulin release, and this effect is reduced was genetic deletion of β-arrestin 1 and 2, supporting previous studies that arrestins play a role in insulin release (Kong et al., 2010). It is anticipated that further studies that express the β-arrestin-biased DREADD *in vivo* may provide novel information about the physiological and pathophysiological roles of β-arrestin signaling pathways (Nakajima and Wess, 2012; Wess et al., 2013).

1.4 The M_1 Muscarinic Acetylcholine Receptor

1.4.1 Localisation and function

The hM_1 mAChR, encoded by the gene located in the long arm of chromosome 11 (q12-13), is the predominant mAChR subtype in the CNS. It is located in major forebrain areas including the cortex, hippocampus, striatum, and thalamus and to a lower extent in the amygdala (Caulfield and Birdsall, 1998; Langmead et al., 2008b). Immunoprecipitation studies indicate that approximately 40% of total mAChRs in the rodent cortex represent the M_1 mAChR subtype, and in the human brain, it is the primary receptor in the frontal, temporal, parietal and occipital cortical areas, accounting for 35-60% of total mAChRs (Flynn et al., 1995; Levey et al., 1991; Volpicelli and Levey, 2004). Cortical M_1 mAChRs localise post-synaptically in all layers of cortical pyramidal cells with enriched expression in layers II, III and VI. In the striatum, the M_1 mAChR is confined to the caudate-putamen where it is expressed both pre- and post-synaptically on cell bodies, dendrites and spines of medium spiny neurons. The hippocampus has the highest density of M_1 mAChR expression where the receptors localise to pyramidal cell bodies and apical and basal dendrites of the striatum and stratum oriens (Flynn et al., 1995; Hersch et al., 1994; Hersch and Levey, 1995; Kamsler et al., 2010; Levey et al., 1991). Peripherally, the M_1 mAChR localises to salivary glands, where it mediates salivary secretion (Gautam et al., 2004; Lin et al., 2008), to lymphocytes, where it causes the activation of the inflammatory cytokine interleukin 2 and plays a role in regulating the immune response (Levey, 1993; Nomura et al., 2003), and to colonic epithelial cells, where it is predicted to regulate epithelial chloride secretion and may play a role in inflammatory gut dysfunction (Khan et al., 2013a).

Given the widespread distribution of M_1 mAChRs in the brain, they are implicated in a multitude of neurologic and psychiatric disorders such as Alzheimer's disease and schizophrenia (Langmead et al., 2008b).

At a cellular level, activation of the M_1 mAChR potentiated N-methyl-D-aspartate (NMDA) receptor currents in hippocampal pyramidal and cortical cells (Ishibashi et al., 2014; Marino and Conn, 2002; Marino et al., 1998). NMDA receptors play a critical role in regulating synaptic plasticity, and disrupted NMDA-receptor neurotransmission is thought to underlie the cognitive deficits observed in numerous psychiatric diseases (Foster et al., 2014). The MAPK-signaling pathway is also considered to play an important role in synaptic plasticity and many cognitive functions (Adams and Sweatt, 2002). Activation of the MAPK pathway by muscarinic agonists was abolished in primary cortical cultures or hippocampal pyramidal neurons in M_1 mAChR knockout mice (Berkeley et al., 2001; Hamilton and Nathanson, 2001), supporting the concept that M_1 mAChR activation plays a role in cognition. In addition, M_1 mAChR knockout mice showed deficits in neuronal plasticity in different regions of the forebrain (Caruana et al., 2011; Origlia et al., 2006; Shinoe et al., 2005; Zhang et al., 2006) and demonstrated an age-dependent cognitive decline in tasks that they performed normally at a younger age (Medeiros et al., 2011). Mice lacking the M_1 mAChR gene also showed performance deficits in the eight-arm radial maze and fear conditioning studies, both of which involve learning and memory tasks, and a profound increase in locomotor activity in all behavioural tests (Hamilton et al., 1997; Kamsler et al., 2010; Miyakawa et al., 2001). It is thought that the behavioural pattern displayed by the M_1 mAChR knockout mice is reminiscent of human attention-deficit/hyperactivity disorder in which hyperactivity is often accompanied by cognitive deficits (Paule et al., 2000; Wess et al., 2007). Furthermore, M_1 mAChR knockout mice showed normal or improved memory in tests that involved matching-to-sample tasks, but showed significant impairments in non-matching-to-sample working memory and consolidation (Anagnostaras et al., 2003; Wess et al., 2007), indicating that M_1 mAChRs receptors are not essential for memory formation or for the initial stability of memory in the hippocampus. Rather, they are likely to be involved in cortical memory function and processes requiring interactions between the cortex and hippocampus (Anagnostaras et al., 2003; Wess et al., 2007).

Recently, the M_1 mAChR selective agonist GSK1034702 (Figure 1.11) showed efficacy in improving episodic memory in humans in a nicotine abstinence model of cognitive dysfunction, including significant improvements in immediate recall (but not delayed recall) following abstinence-induced impairment (Nathan et al., 2013).

1.4.2 Activation and signaling

The M_1 mAChR preferentially couples to pertussis toxin-insensitive $G\alpha_{q/11}$ to initiate the activation of PLC which causes hydrolysis PIP_2 into two second messengers, IP_3 and DAG. IP_3 binds to receptors located on the endoplasmic reticulum (ER) and causes the release of intracellular Ca^{2+} which then activates Ca^{2+}-calmodulin. (Berstein et al., 1992; Felder, 1995; Odagaki et al., 2013; van Koppen and Kaiser, 2003) (Figure 1.2). DAG is involved in the activation of PKC isoenzymes that can initiate a number of signaling events (Felder, 1995; Nelson et al., 2007; Xu et al., 1990). PKC mediated events include activation of the transcription factor Nrf2 that regulates the expression of genes containing antioxidant response elements in hippocampal and cerebellar neurons (Espada et al., 2009), mediating M_1 mAChR-activated NMDA currents in the striatum (Calabresi et al., 1998) and activation of MAPKs (Werry et al., 2006). M_1 mAChR signaling via PLC is complex due to the presence of multiple PLC enzymes. Thirteen PLC enzymes have been identified consisting on PLCβ1-4, PLCγ1-2, PLCδ1, 3, 4, PLCε, PLCζ and PLCη. However, the M_1 mAChR is most commonly associated with activation of the PLCβ subfamily (Suh et al., 2008; Taylor et al., 1991; Young and Thomas, 2014). Kinetic studies have shown that binding of PLC to $G\alpha_{q/11}$ upon M_1 mAChR activation accelerates nucleotide exchange and GTPase activity, and that PLC is maintained in the active state by cycles of rapid GTP hydrolysis and nucleotide exchange on $G\alpha_{q/11}$ subunits bound to PLC (Falkenburger et al., 2010).

The ability of the M_1 mAChR to influence additional downstream effector pathways via activation of other G protein subtypes has also been reported (Nathanson, 2000). The M_1 mAChRs is able to activate $G\alpha_{i/o}$ (Akam et al., 2001; Offermanns et al., 1994) and increase AC activity via a $G\alpha_s$ protein-dependent (Burford and Nahorski, 1996; Gurwitz et al., 1994; Hao et al., 2005; Migeon and Nathanson, 1994; Olianas et al., 2013) or -independent mechanisms based on increased intracellular Ca^{2+}, calmodulin and PKC activity (Baumgold, 1992; Baumgold et al., 1992; Felder et al., 1989; Jansson et al., 1991). The M_1 mAChR is able to affect cell cytoskeleton and induce membrane ruffling by coupling to $G\alpha_{12/13}$ G proteins (Canals et al., 2012). G protein coupling preferences can also be ligand-dependent. For example, Thomas et al, 2008 showed that the orthosteric agonists oxotremorine-M, arecoline, and pilocarpine and the allosteric agonists AC-42 and 77-LH-21-1 both stabilise receptor conformations associated with $G\alpha_{q/11}$- and $G\alpha_s$-dependent signaling. However, AC-42 and 77-LH-28-1, unlike the orthosteric agonists do not promote M_1 mAChR $G\alpha_{i1/2}$ coupling, suggesting that these ligands have the potential to activate distinct subsets of downstream effectors (Thomas et al., 2008).

The M_1 mAChR has been shown to activate MAPK pathways which are involved in a diverse array of functions including cell survival, proliferation, apoptosis and gene transcription (Werry et al., 2005). MAPKs are serine/threonine kinases that are divided into subfamilies including JNK1-3, ERK1/2, p38 protein kinase (p38) and big-mitogen-activated protein kinase 1 (BMK1) (Werry et al., 2005). The M_1 mAChR can activate the MAPK pathways by multiple mechanisms including activation of protein tyrosine kinase 2 (PYK2) via calmodulin-dependent protein kinases and PKC-mediated mechanisms; PYK2 can activate c-Src to cause activation of the ERK1/2 pathway (Felsch et al., 1998; Gudermann et al., 2000; Gutkind, 1998). Activation of ERK1/2 in response to M_1 mAChR activation has been reported in numerous cell lines including hippocampal dendrites and somata pyramidal neurons (Berkeley et al., 2001), cerebral cortical neurons (Hamilton and Nathanson, 2001), human salivary cell lines (Lin et al., 2008), CHO cells (Abdul-Ridha et al., 2013)

and in PC12 cells (Berkeley and Levey, 2000; Haring et al., 1998). Activation of the M_1 mAChR induced neuronal differentiation in pyramidal hippocampal neurons through induction of Ca^{2+} mobilisation, activation of PKC and most importantly of ERK1/2 (VanDeMark et al., 2009). The M_1 mAChR can also increased JNK activity in Cos-7, PC12 and NIH-3T3 cells (Coso et al., 1995; Coso et al., 1996; Mangelus et al., 2001) and activated p38 in PC12 and DT40 lymphoma cells (Bence et al., 1997; Mangelus et al., 2001). The M_1 mAChR was also able to activate MAPK pathways via transactivation of epidermal growth factor receptors (EGFR). For example, activation of the M_1 mAChR caused PKC-mediated activation of a metalloprotease that released an epidermal growth factor-like ligand that can activated the EGFR to initiate signaling (Prenzel et al., 1999). Activation of the M_1 mAChR lead to direct stimulation of Bruton's tyrosine kinase through direct interaction with $G\alpha_{q/11}$ (Bence et al., 1997) and caused Ras activation through a $G\beta\gamma$-mediated phosphorylation and activation of a guanine nucleotide exchange factor (Mattingly and Macara, 1996). The M_1 mAChR has also been reported to activate PLA_2 to release arachidonic acid (Felder et al., 1991) and to regulate phospholipase D (PLD) activity to yield phosphatidic acid that is involved in a number of cellular responses including Ca^{2+} mobilisation, cytoskeletal rearrangements and vesicle trafficking (Felder, 1995; Sandmann et al., 1991). The M_1 mAChR is also known to interact with the cytoskeletal protein spectrin by forming a $G\alpha_{q/11}$-associated protein complex that controls cytoskeletal modelling in CHO cells, a process mediated by PLC, PKC and Rho-associated kinase (ROCK) (Street et al., 2006). Cyclic ADP-ribose (cADPR) has also been shown to play a role in signaling downstream of the M_1 mAChR in rat superior cervical ganglion (Zhang et al., 2005). In the cerebral cortex, activation of the M_1 mAChR caused an increase in the levels of the neural and inducible isoforms of nitric oxide synthase (nNOS and iNOS), which are associated with increased levels of NO via a signaling cascade involving PLC, calcium/calmodulin and PKC (Sterin-Borda et al., 2003).

The M_1 mAChR plays an important role in the regulation of the function of numerous ion channels either by direct coupling to the channels or indirectly via transactivation of receptor tyrosine kinases or channel phosphorylation mediated by kinases such as PKA and PKC (Cantrell et al., 1996; Huang et al., 1993; Nathanson, 2000; Thiele, 2013). M_1 mAChR affected neuronal activity by closing voltage-gated K^+ channels which are usually held open by binding to PIP_2 (Brown, 2010; McCormick and Prince, 1986; McCormick and Williamson, 1989; Selyanko et al., 2000; Womble and Moises, 1992). However, M_1 mAChR-induced hydrolysis of PIP_2 leads to channel closure (Gamper and Shapiro, 2007; Kobrinsky et al., 2000; Suh and Hille, 2005). The M_1 mAChR has been shown to modulate the activity of voltage gated K^+ channels via transactivation of EGFRs in a PKC- and receptor tyrosine phosphatase α (RTPα)-dependent manner (Daub et al., 1997; Tsai et al., 1999; Tsai et al., 1997). M_1 mAChR signaling also leads to closure of inward rectifying K^+ type 1, 2 and 4 channels (Carr and Surmeier, 2007; Hill and Peralta, 2001; Huang et al., 1993; Jones, 1996), closure of slow after hyperpolarisation K^+ channels (Ghamari-Langroudi and Bourque, 2004; McCormick et al., 1993), closure of leaky K^+ channels (Womble and Moises, 1992), and opening (Gulledge et al., 2007; Gulledge and Stuart, 2005) but also closing (Giessel and Sabatini, 2010) of SK-type calcium-activated K^+ channels. The release of Ca^{2+} from intracellular stores after M_1 mAChR activation is thought to cause the opening of SK-type calcium-activated K^+ channels (Gulledge et al. 2007). However, M_1 mAChR activation reduced the sensitivity of calcium-activated K^+ channels to Ca^{2+} through a PKC pathway (Buchanan et al., 2010) or casein kinase-2 pathway (Giessel and Sabatini, 2010) thus also resulting in reduced calcium-activated K^+ channels opening.

Voltage gated Ca^{2+} channels are also regulated by the M_1 mAChR via slow (soluble second-messenger) and fast (membrane-delimited) mechanisms (Hille, 1994; Wickman and Clapham, 1995). P/Q-, N-, and L-type Ca^{2+} channels are part of the high voltage-activated class of Ca^{2+} channels. M_1 mAChR activation contributed to Ca^{2+} channel inhibition by PLC/Ca^{2+}- dependent PKC pathways (Salgado et al., 2007). Specifically, L- and N-currents are inhibited via DAG lipase

in cervical ganglion neurons (Liu et al., 2008). Low voltage-activated T-type Ca^{2+} channels are also blocked upon M_1 mAChR activation (Hildebrand et al., 2007). M_1 mAChR activation caused opening of Ca^{2+}- dependent (Haj-Dahmane and Andrade, 1998; Yan et al., 2009) and -independent (Egorov et al., 2003) nonspecific cation channels.

Finally, M_1 mAChR-mediated activation of $G\alpha_{q/11}$ proteins is regulated by RGS2 (regulators of G protein signaling 2) and RGS4 (Bernstein et al., 2004; Lin et al., 2002). RGS proteins are GAPs (GTPase accelerating proteins) that increase the GTPase activity of G proteins to reduce G protein-mediated cell signaling.

1.4.3 Regulation and trafficking

In response to agonist stimulation, the M_1 mAChR receptor signaling is terminated by receptor desensitisation and internalisation. This regulation is dependent on receptor phosphorylation by protein kinases such as GRKs, PKC and CK1α, which promotes the interaction of the receptor with scaffolding proteins such as β-arrestins (Butcher et al., 2012; Pitcher et al., 1998; van Koppen and Kaiser, 2003; Waugh et al., 1999).

The desensitisation of the M_1 mAChR upon agonist stimulation involves phosphorylation of specific serine and threonine amino acid residues on the ICL3 and the C-terminus of the receptor (Haga et al., 1996). PKC has been shown to phosphorylate the M_1 mAChR both *in vivo* and *in vitro* in an agonist-independent manner (Haga et al., 1996; Richardson and Hosey, 1990; Uchiyama et al., 1990). Phosphorylation sites for PKC include Thr354, Ser356 and Ser451, Thr455, Ser457 (Haga et al., 1996). M_1 mAChR-independent PKC activation can lead to heterologous desensitisation of the M_1 mAChR in numerous cell lines including rat cerebral cortical astrocytes (Pearce et al., 1988) and N1E-115 neuroblastoma cells (Kanba et al., 1990; Kanba et al., 1986).

Phosphorylation of agonist-occupied M_1 mAChR by GRKs is mediated by GRK2 in Sf9 insect cells (Debburman et al., 1995; Haga et al., 1996), CHO and human embryonic kidney 293 (HEK293)

cells (Yeatman et al., 2014) and hippocampal neurons (Willets et al., 2005; Willets et al., 2007). GRK phosphorylation sites on the M_1 mAChR are located in the 284SerMetGIuSerLeuThrSerSerGlu292 sequence in ICL3 (Haga et al., 1996; Lameh et al., 1992; Moro et al., 1993). There is also weak evidence that the M_1 mAChR may be a substrate for GRK5 and GRK6, however further studies are required to confirm this (van Koppen and Kaiser, 2003). CK1α has also been shown to mediate agonist induced M_1 mAChR phosphorylation in CHO cells (Waugh et al., 1999).

Phosphorylation of the M_1 mAChR facilitates receptor internalisation. Ala substitution of phosphorylation sites in ICL3 of the M_1 mAChR impairs receptor internalisation (Moro et al., 1993). Phosphorylation of the M_1 mAChR leads to internalisation in clathrin- and β-arrestin-dependent manner (Santini et al., 2000; Tolbert and Lameh, 1996; Yeatman et al., 2014). One study also reported that the M_1 mAChR can internalise in a clathrin- but not β-arrestin-dependent manner (Lee et al., 1998b). Internalised M_1 mAChRs colocalise with β-arrestin and clathrin in HEK293 and RBL-2H3 cells (Mundell and Benovic, 2000; Santini et al., 2000; Tolbert and Lameh, 1996). The use of a dominant-negative β-arrestin that is able to bind to phosphorylated M_1 mAChR but not to clathrin, inhibits its internalisation (Claing et al., 2000). Similarly, the use of a dominant-negative clathrin mutant also inhibited M_1 mAChR internalisation (Vogler et al., 1999b). Clathrin-coated pits are cleaved from the membrane by the actions of dynamin GTPase, a dominant-negative dynamin mutant is able to inhibit internalisation of the M_1 mAChR (Claing et al., 2000; Vogler et al., 1999b). The M_1 mAChR internalisation process requires phosphorylation of dynamin by c-Src. A mutant and catalytically-deficient c-Src is able to suppress M_1 mAChR internalisation (Werbonat et al., 2000). In polarized epithelial kidney cells, caveolin was shown to be involved in regulating M_1 mAChR trafficking by means of attenuating of the M_1 mAChR movement to and from the plasma membrane (Shmuel et al., 2007). Once internalised, M_1 mAChRs can be either degraded or recycled back to the cell surface.

The continued exposure of the M_1 mAChR to agonists leads to a loss of total number of receptors in a process known as down-regulation that results from degradation of receptors (van Koppen and Kaiser, 2003). Several studies suggest that down-regulation of mAChR involves a decrease in receptor mRNA levels. For example, M_1 mAChR activation in CHO, IMR-32 and SH-SY5Y neuroblastoma cells leads to a decrease in total receptor number accompanied by a decrease in the level of M_1 mAChR mRNA transcript (Koman et al., 1993; Lee et al., 1994). However, down-regulation of M_1 mAChR expression is not always accompanied by a decrease in mRNA levels. Decreased M_1 mAChR expression in primary rat cortico-striatal cells is accompanied by an increase in the mRNA transcript over the first 2-6 hours of agonist treatment (Brusa et al., 1995). Four mutations in the M_1 mAChR located in ICL2 or in the N- and C- terminal regions of ICL3 impair M_1 mAChR down-regulation in CHO cells (Shockley et al., 1997).

Receptor trafficking through the endocytic machinery and the fate of internalised receptors is dependent on the agonist (Lane et al., 2013a). Allosteric modulators may potentially induce receptor desensitization/internalization or conversely increase cell surface expression or prevent the internalization induced by the endogenous/orthosteric ligand. Examples of such scenarios are summarised in Table 1 Appendix 1.

1.4.4 Therapeutic potential of M_1 mAChRs in CNS

1.4.4.1 Alzheimer's disease

Alzheimer's disease is the most common form of dementia, currently affecting 35 million individuals worldwide and considered a public health crisis (Ballard et al., 2011; Foster et al., 2014). It is a disease that commonly affects the elderly, resulting in cognitive dysfunction and severe memory loss (Melancon et al., 2013b). The hallmarks of Alzheimer's disease pathology are the accumulation of amyloid-beta (Aβ) peptide aggregates (Aβ plaques) and hyperphosphorylated

tau protein (neurofibrillary tangles) (Foster et al., 2014). Aβ is derived from proteolytic cleavage of the membrane bound amyloid precursor protein (APP), which is known to undergo proteolytic cleavage via two competing routes, nonamyloidogenic and amyloidogenic. In the amyloidogenic pathway APP is sequentially cleaved by β- and γ-secretases to release Aβ peptides. However, in the nonamyloidogenic route, APP is cleaved by α-secretase to yield soluble APP and preventing Aβ peptide generation (Huang and Mucke, 2012; Langmead et al., 2008b). The build-up of Aβ plaques leads to neuronal inflammation, dysfunction, and cell death. The two brain regions most critically affected by this degeneration are the cortex and hippocampus (Foster et al., 2014). Alzheimer's disease is also associated with reduced cholinergic innervations of these brain regions (Auld et al., 2002). The cognitive and behavioural deficits observed in Alzheimer's disease patients highlight the importance of the cholinergic system in mediating these processes. A large body of evidence indicates that the M_1 mAChR mediates the cognitive-enhancing effects of ACh (Hasselmo, 2006; Wess et al., 2007). For example, the use of mAChR antagonists, as well as cholinergic lesions in the forebrain of rats, leads to cognitive impairment (Hagan et al., 1987; Hagan et al., 1988; Smith et al., 1988), while M_1 mAChR deficiency increases amyloidogenic processing of APP and exacerbate cognitive processes and other Alzheimer's disease-related pathological features in mice (Davis et al., 2010). The M_1 mAChR interacts with β-site APP-cleaving enzyme 1 (BACE1), the β-secretase enzyme responsible for formation of Aβ, to regulate its proteosomal degradation (Fisher, 2007). Furthermore, M_1 mAChR activation lowers Aβ levels and increases soluble APP formation *in vitro* thereby preventing the formation of Aβ via MAPK- and PKC- dependent pathways (Jiang et al., 2012; Lahmy et al., 2013). In addition, M_1 mAChR activation decreases tau phosphorylation; thereby affecting both pathological hallmarks of Alzheimer's disease (Tarr et al., 2012). Transgenic Tg2576 mice, which overexpress a familial Alzheimer's disease mutant form of the APP, are impaired on compound discrimination reversal learning (Zhuo et al., 2008; Zhuo et al., 2007). Treatment of these mice with the M_1 mAChR selective agonist, AF267B (Figure 1.11), showed

increased cerebrospinal fluid (CSF) levels of α-secretase producing enzyme, ADAM17, and a decrease in β-secretase formation (Fisher et al., 2000; Giessel and Sabatini, 2010).

The current primary treatments for Alzheimer's disease symptoms are acetylcholinesterase inhibitors (AChEIs) such as galantamine, donepezil, tacrine and rivastigmine, which potentiate cholinergic signaling by reducing enzymatic degradation of ACh (Munoz-Torrero, 2008). Although these treatments provide improvements in cognitive and psychiatric symptoms associated with Alzheimer's disease, cardiovascular and gastrointestinal side effects are often observed, thought to be mediated by peripherally located ACh receptors (Foster et al., 2014).

Phase III clinical studies with the M_1/M_4 mAChR-preferring agonist xanomeline (Figure 1.5) showed efficacy in ameliorating cognitive and psychotic deficits observed in Alzheimer's disease patients. These included significant improvements in verbal learning and short-term memory, reductions in hallucinations, delusions, vocal outbursts, and other behavioural disturbances. (Bodick et al., 1997a; Bodick et al., 1997b). However, due to dose limitations and severe gastrointestinal side effects, the use of xanomeline was discontinued. Nonetheless, the results from the xanomeline studies provide strong clinical validation of M_1 mAChRs as a target for the treatment of both psychotic and cognitive disturbances in Alzheimer's disease. Further validation of the critical role of the M_1 mAChR in modulating these processes was obtained from treatment of Alzheimer's disease patients with a selective M_1 mAChR agonist, talsaclidine, which led to an observed reduction in Aβ plaque levels in their CSF (Hock et al., 2003).

Furthermore, several studies have shown that M_1 mAChR-selective agonists or PAMs have cognition-enhancing activity in rodents and are able to improve impaired cognition in mouse models of Alzheimer's disease (Caccamo et al., 2009; Caccamo et al., 2006; Davie et al., 2013; Melancon et al., 2013b; Shirey et al., 2009). As a result, a large number of ligands aimed at selectively targeting the M_1 mAChR have been developed in the last decade (discussed in section 1.4.5.2).

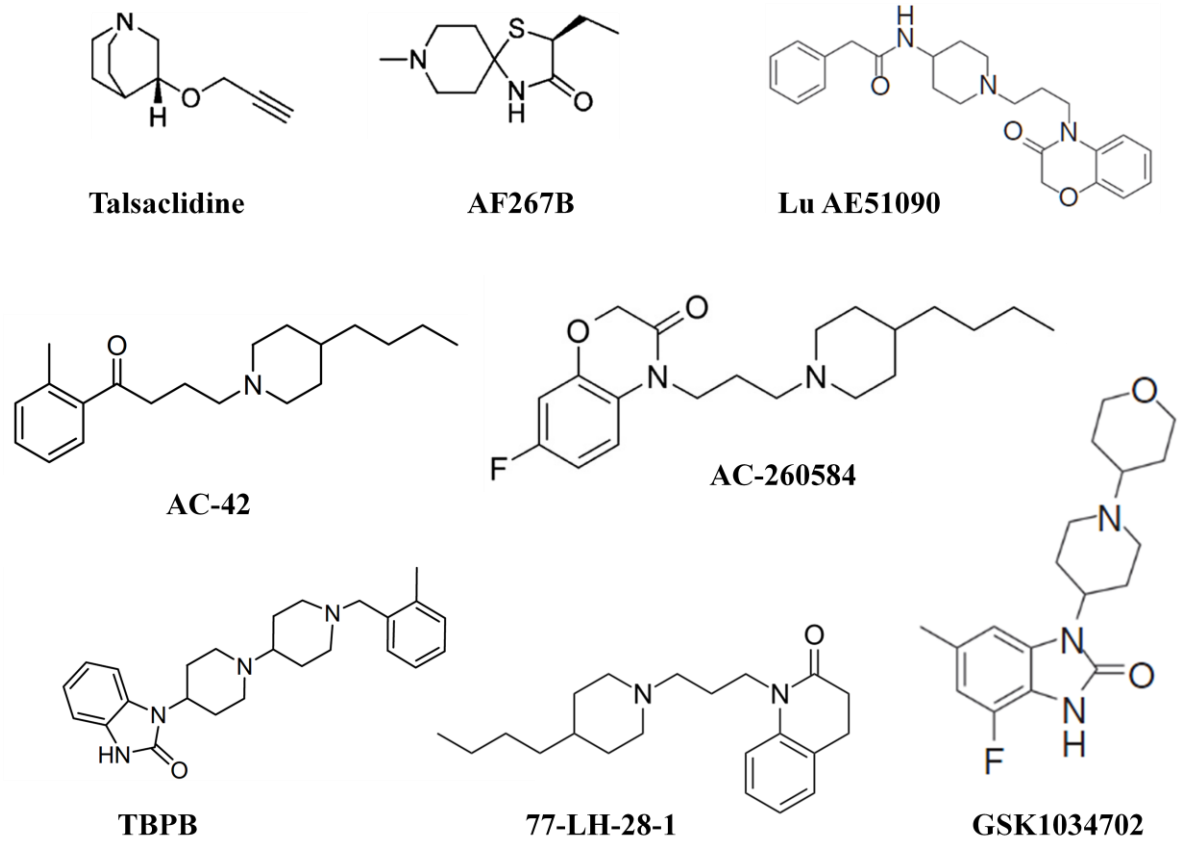

Figure 1.11 Structures of M_1 mAChR selective agonists.

1.4.4.2 Schizophrenia

Schizophrenia is a chronic brain disorder that affects ~1% of the general population and is characterised by three classical symptom clusters: positive symptoms, negative symptoms and cognitive impairments. Cognitive symptoms include deficits in attention, memory and executive function; negative symptoms include social withdrawal, anhedonia and apathy, while positive symptoms include delusions, hallucinations and thought disorders. The negative and cognitive symptoms are not effectively treated by current antipsychotic drugs, and represent a lifelong disability for patients with schizophrenia (Melancon et al., 2013b; van Os and Kapur, 2009).

A key feature associated with schizophrenia is increased dopaminergic signaling in subcortical areas of the brain such as the nucleus accumbens (Melancon et al., 2013b). However, behavioural, anatomical, neurochemical and neuroimaging studies suggest that muscarinic cholinergic transmission contributes to the pathophysiology of schizophrenia (Wess et al., 2007). Non-selective muscarinic antagonists induce symptoms associated with schizophrenia in healthy humans and exacerbate existing symptoms in schizophrenia patients (Melancon et al., 2013b; Scarr et al., 2013). Specifically, the M_1 mAChR is postulated to play a role in schizophrenia (Kruse et al., 2014b; Scarr et al., 2013; Wess et al., 2007). Receptor protein and mRNA levels of M_1 mAChR are decreased in frontal cortex of schizophrenic patients (Scarr et al., 2007) and genetic polymorphisms of the M_1 mAChR are also associated with schizophrenia (Liao et al., 2003). Elevated levels of autoantibodies targeting the M_1 mAChR has also been observed in patients with schizophrenia (Jones et al., 2014). M_1 mAChR-knockout mice have indicated that the lack of central M_1 mAChR leads to a 'dopamine hypersensitivity phenotype', further supporting the idea which suggests that agents that act through the M_1 mAChR may be capable of antipsychotic activity (Gerber et al., 2001; Kruse et al., 2014b). NMDA receptors have an important role in the regulation of circuits that are needed for normal cognitive and executive functions that are disrupted in schizophrenic patients. A prominent effect of M_1 mAChR activation is in the hippocampus and other forebrain areas is the potentiation of NMDA receptor currents (Marino et al., 1998). Therefore, it is postulated that M_1 mAChR-induced potentiation of NMDA receptor function may be important for the therapeutic efficacy of mAChR activation in psychotic disorders (Marino et al., 1998). This is supported by the finding that N-desmethylclozapine (NDMC) which is an M_1 allosteric agonist, potentiated NMDA receptor currents in hippocampal CA1 pyramidal cells (Sur et al., 2003). More importantly, xanomeline produced improvements in psychotic symptoms in a pilot study involving schizophrenic patients (Shekhar et al., 2008). However, as with the clinical trials in Alzheimer's disease patients and despite the encouraging results, the use of xanomeline was discontinued. Taken together, these

findings have been the driving force behind the generation of a large number of novel M_1 mAChR ligands.

1.4.4.3 Parkinson's disease

Parkinson's disease represents another CNS disorder in which the M_1 mAChR may be implicated (Gerber et al., 2001; Langmead et al., 2008b). The pathological hallmark of Parkinson's disease is a loss of dopaminergic neurons in the substantia nigra that provide dopaminergic innervations to the striatum (Langmead et al., 2008b; Wess et al., 2007). Imbalance between striatal dopaminergic and muscarinic cholinergic neurotransmission leads to impairments in coordinated locomotor activity such as tremor and bradykinesia (Di Chiara et al., 1994; Xiang et al., 2012). Muscarinic antagonists are used clinically to relieve the movement disorder associated with Parkinson's disease, but their use is limited due to central and peripheral adverse effects mediated my mAChR subtypes not involved in regulation of basal ganglia motor function (Wess et al., 2007). *In vivo* and *in vitro* studies suggest that pharmacological blockade of central M_1 mAChRs may be beneficial in the treatment of Parkinson's disease. M_1 mAChRs knockout mice exhibit a pronounced increase in extracellular dopamine levels in the striatum (Gerber et al., 2001), while the selective M_1 mAChR antagonist VU0255035 has recently been shown to regulate basal ganglia functions and produce antiparkinsonian effects (Xiang et al., 2012).

Although the majority of studies focus on the therapeutic aspect of targeting M_1 mAChRs in the CNS, it should be noted that on-target side-effects may limit the utility of selective M_1 mAChR ligands. For example, activation of M_1 mAChRs in the salivary glands may lead to excessive salivation (Gautam et al., 2004; Lin et al., 2008) while activation of M_1 mAChR in lymphocytes may cause an altered immune response as a result of the increased activity of the inflammatory cytokine interleukin 2 (Levey, 1993; Nomura et al., 2003). Moreover, colonic epithelial cells also

express the M_1 mAChR and its activation is predicted to regulate epithelial chloride secretion and may play a role in inflammatory gut dysfunction (Khan et al., 2013a). Indeed, excessive salivation and seizures have been recorded in mice treated with the M_1 mAChR PAM, benzoquinazolinone 12 (unpublished observations).

1.4.5 Allosteric modulation of mAChRs

1.4.5.1 General introduction

Among family A GPCRs, the mAChRs have long served as a model system for understanding GPCR allostery and much of what we know in this field today comes from studies of allosteric modulation at mAChRs (Christopoulos, 2014). All five mAChR subtypes are known to possess at least one allosteric site, in addition to the highly conserved orthosteric site (Christopoulos et al., 1998). As with the other mAChRs, the M_1 mAChR is activated by prototypical orthosteric agonists such as ACh, oxotremorine-M, arecoline, pilocarpine and carbachol (Figure 1.5) and inhibited by inverse agonists such as NMS, QNB and atropine (Figure 1.6) (Langmead and Christopoulos, 2006). Biochemical, covalent labelling, mutagenic and crystallographic studies have revealed that the amino acids forming the ACh binding pocket are identical across the five mAChR subtypes and other ACh binding proteins in humans and other species (Haga et al., 2012; Hulme, 2013). Despite the significant clinical potential for selectively targeting different mAChR subtypes in disorders such as Alzheimer's disease and schizophrenia, conservation in the orthosteric pocket has hindered the clinical progression of orthosteric mAChR ligands due to insufficient subtype selectivity (Christopoulos, 2014). Fortunately, the last few years witnessed an increasing number subtype of selective ligands that that bind to topographically distinct allosteric sites on mAChRs (Conn et al., 2009; Foster et al., 2014; Kruse et al., 2014b; Melancon et al., 2013b). Allosteric ligands may attain subtype selectivity by two means. First, allosteric sites show greater divergence in their amino acid sequences between subtypes and, unlike orthosteric sites they did not evolve to accommodate an

endogenous ligand such as ACh (Christopoulos, 2014; Conn et al., 2009). Second, even if the allosteric site is shared between subtypes, selectivity may be achieved via selective cooperativity with the orthosteric ligand (Lazareno et al., 2004; Lazareno et al., 1998). This phenomenon is exemplified in mAChRs as they possess an extracellular vestibule that contains a "common" allosteric site (Dror et al., 2013; Ellis and Seidenberg, 1992; Matsui et al., 1995; Trankle et al., 1998), however, selectivity is still achieved in this region due to a combination of variability in amino acid sequence and prominent differences in the magnitude of cooperativity between the allosteric and orthosteric sites across subtypes.

1.4.5.2 Prototypical allosteric modulators

The earliest demonstration of allosteric modulation at a mAChR was shown in a seminal study by Clark and Mitchelson (1976) that described and quantified the mechanism of action of gallamine (Figure 1.12) as a negative allosteric modulator of the M_2 mAChR in isolated rat atria (Clark and Mitchelson, 1976). These findings were later confirmed in radioligand binding studies that demonstrated that gallamine is unable to completely inhibit specific [^{3}H]NMS binding at the M_2 mAChR but is able to delay the rate of dissociation of [^{3}H]NMS and [^{3}H]QNB, indicating that it exerts its effect through a site distinct to the orthosteric binding site (Dunlap and Brown, 1983; Stockton et al., 1983). Gallamine was later reported to act allosterically at all five mAChRs, suggesting the presence of at least one common allosteric site present on each receptor subtype (Ellis et al., 1991; Lee and el-Fakahany, 1991a; Lee and el-Fakahany, 1991b). Early "prototypical" allosteric modulators discovered also include curare-like alkaloids (alcuronium, strychnine and brucine) and alkane bis-ammonium compounds (W84, C_7/3-phth) which bind to the same (or overlapping) allosteric site and modulate orthosteric ligand function with minimal activity on their own (Figure 1.12) (Christopoulos et al., 1998; Dror et al., 2013; Ellis and Seidenberg, 1992; Lanzafame et al., 1997). Gallamine and C_7/3-phth both display negative binding cooperativity with

[^{3}H]NMS and [^{3}H]QNB and show the highest affinity for the M_2 over other mAChR subtypes (Christopoulos et al., 1999; Ellis et al., 1991; Gnagey et al., 1999; Leach et al., 2011; Michel et al., 1990; Prilla et al., 2006). Curare-like alkaloids (alcuronium, strychnine, and brucine) also bind to all mAChRs and slow the dissociation rate of [^{3}H]NMS and [^{3}H]QNB (Jakubik et al., 1995; Lazareno and Birdsall, 1995; Lazareno et al., 1998). These compounds have been useful in demonstrating the phenomenon of 'probe-dependence'. For example, alcuronium and strychnine display positive cooperativity with [^{3}H]NMS at both the M_2 and M_4 mAChRs, while alcuronium shows negative cooperativity with [^{3}H]NMS at the M_1, M_3 and M_5 (Jakubik et al., 1995; Lazareno and Birdsall, 1995). Brucine demonstrated positive modulation of ACh function at the M_1 mAChR, providing the first validation for selective allosteric modulation of M_1 mAChR activity (Jakubik et al., 1995; Lazareno and Birdsall, 1995; Lazareno et al., 1998). Modification of brucine to N-chloromethylbrucine results in positive cooperativity with ACh at the M_2 and M_3 mAChRs while neutral cooperativity is maintained at the M_4 mAChR (Birdsall et al., 1999).

A second allosteric binding site has been proposed to exist on mAChRs and is recognised by indolocarbazole and benzimidazole compounds (Lazareno et al., 2000). Indolocarbazoles, such as staurosporine and its analogue KT5720 (Figure 1.13) have been reported to act allosterically at the M_1-M_4 mAChRs with varying degrees of cooperativity with ACh and NMS depending on the particular subtype (Lazareno et al., 2000). Unlike the prototypical allosteric modulators, indolocarbazoles display the highest affinity for the M_1 rather than M_2 mAChR subtype and have limited effects on the dissociation rate of [^{3}H]NMS (Lazareno et al., 2000). Equilibrium binding interaction studies between gallamine and KT5720 at the M_1 mAChR showed that the latter compound was unable to antagonise gallamine-induced inhibition of [^{3}H]NMS, thus displaying neutral cooperativity instead of a competitive interaction which indicates that both ligands can bind to the [^{3}H]NMS-occupied receptor at the same time (Lazareno et al., 2000). Similar findings were

observed for interaction studies between brucine and KT5720, providing additional evidence for the existence of a second allosteric site (Lazareno et al., 2000).

Further evidence for a second allosteric site comes from studies that investigated the actions of benzimidazole compounds such as WIN 51,708 and WIN 62,577 (Figure 1.13) which were initially characterised as neurokinin receptor antagonists (Lazareno et al., 2002). WIN 62,577 positively modulates the action of ACh at the M_3 and M_4 mAChRs but displays negative cooperativity with the prototypical allosteric modulators C_7/3-phth, alcuronium and brucine, indicating that WIN 62,577 binds to a second allosteric site (Lanzafame et al., 2006). Furthermore, the interaction between staurosporine and KT5720 was found to be competitive, indicating that both types of allosteric modulators may be binding to the same site (Lazareno et al., 2002).

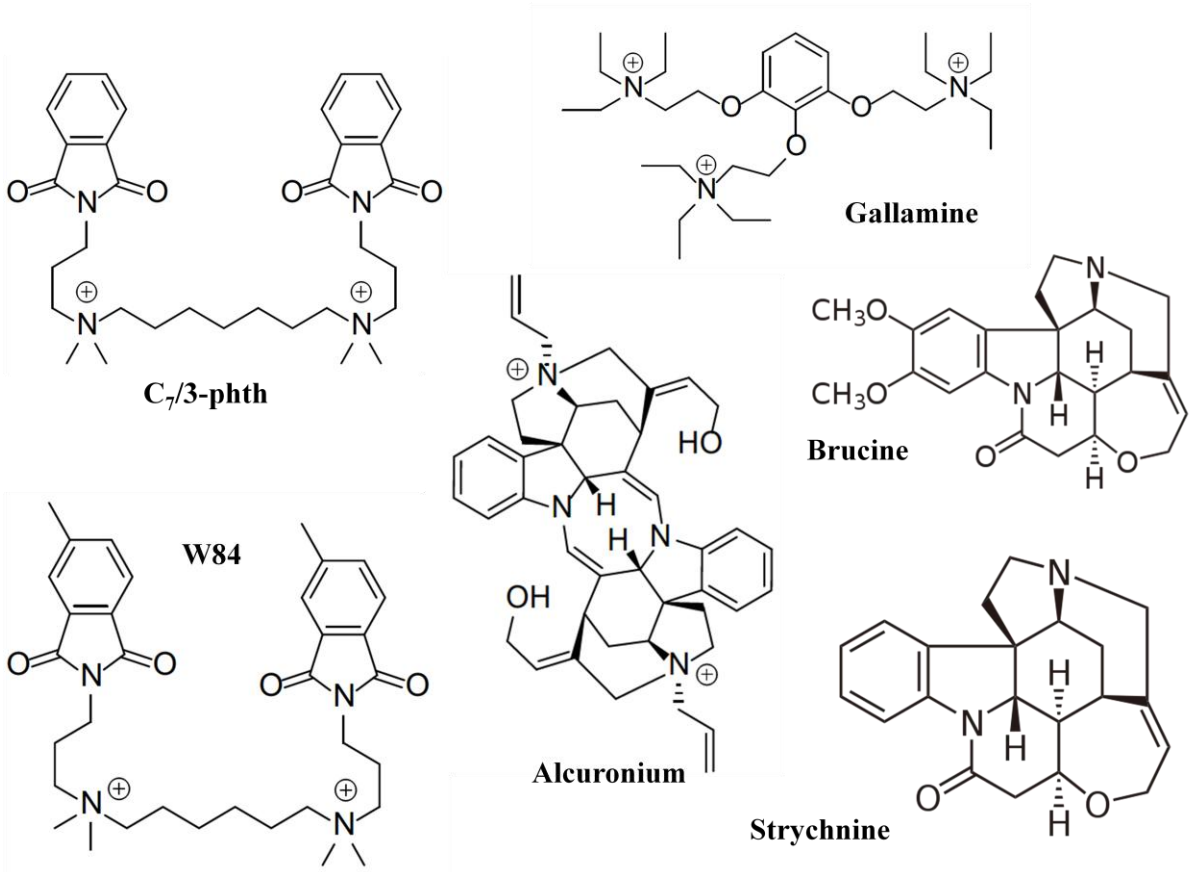

Figure 1.12 Structure of prototypical allosteric modulators.

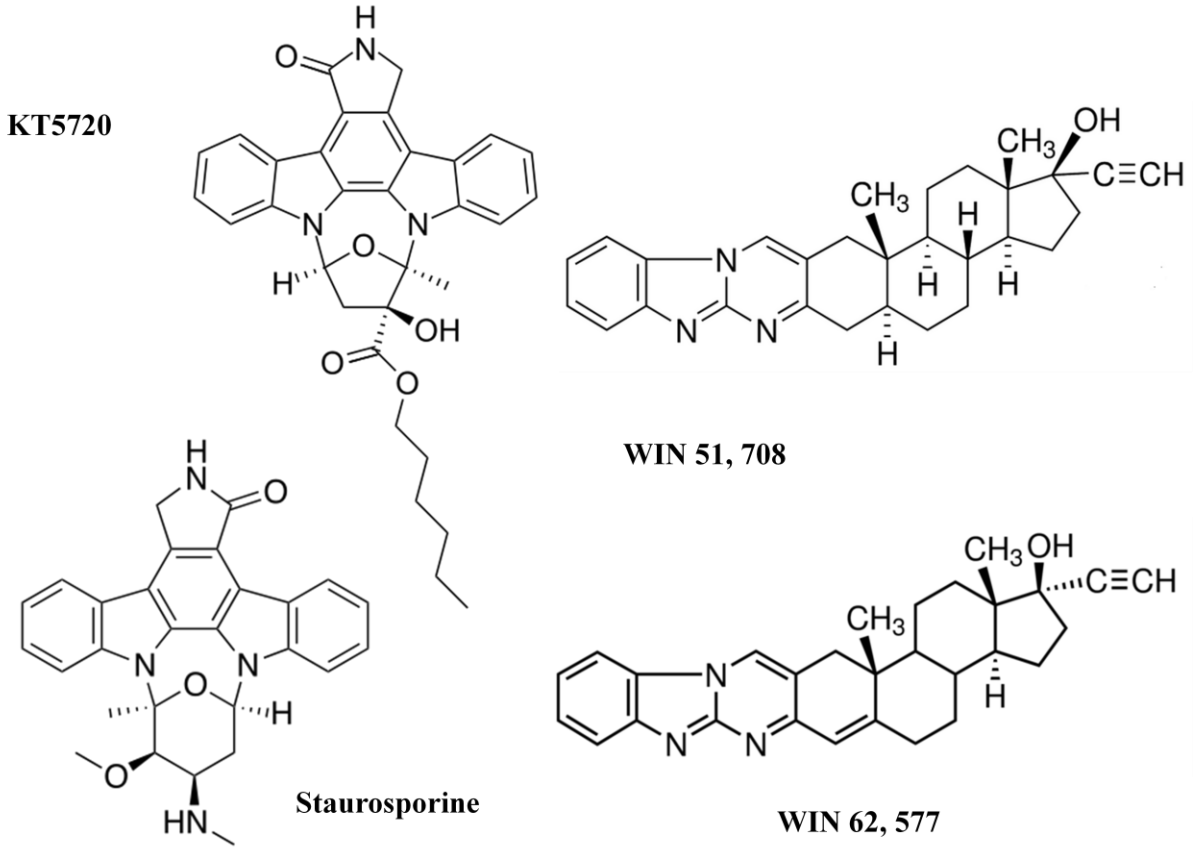

Figure 1.13 Structure of the 'second allosteric site' ligands.

1.4.5.3 Bitopic ligands

Recent studies have exploited the properties of orthosteric and allosteric compounds to develop a new class of ligands termed 'bitopic', 'dualsteric' or 'multivalent', which are rationally designed, hybrid molecules that are composed of two pharmacophores, each known to independently interact with an orthosteric and allosteric site (Antony et al., 2009; Bock and Mohr, 2013; Christopoulos, 2014; Disingrini et al., 2006; Lane et al., 2013b; Mohr et al., 2010; Steinfeld et al., 2007; Valant et al., 2014). Advantages of bitopic ligands include the potential for greater receptor selectivity by means of targeting an allosteric site and greater affinity due to simultaneous engagement with the orthosteric site (Christopoulos, 2014). In addition, the concomitant binding to two different sites may promote unique receptor conformations that engender biased agonism (Kebig et al., 2009; Keov et al., 2014; Valant et al., 2014). The first study to demonstrate a bitopic mechanism of action for a mAChR ligand was achieved using the nonselective mAChR agonist, McN-A-343 (Figure 1.14) (Valant et al., 2008). McN-A-34 was reverse engineered into two distinct pharmacophores: tetramethylammonium (a high efficacy orthosteric agonist) and 3-chlorophenylcarbamate (a negative allosteric modulator). Combination of the two pharmacophores recapitulates the pharmacology of the parent molecule, resulting in a partial biased agonist (Valant et al., 2008).

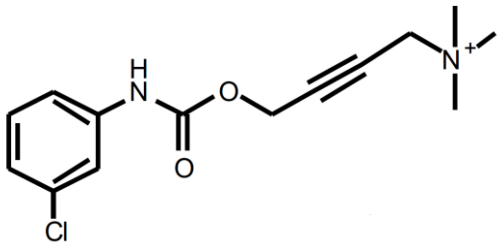

McN-A-343

Figure 1.14 Structure of the bitopic mAChR ligand McN-A-343.

As a consequence of this finding, other mAChR ligands such as AC-42, TBPB, and 77-LH-28-1 (Figure 1.11) have been re-examined as they have been previously classified as "allosteric" but it is

still uncertain whether they covey their actions solely via an allosteric site or via interaction with the orthosteric site (Digby et al., 2012b; Jacobson et al., 2010; Keov et al., 2014; Keov et al., 2013; Langmead et al., 2008a; Langmead and Christopoulos, 2006; Sheffler et al., 2013; Spalding et al., 2002). This highlights the importance to distinguish between classes of ligands at the preclinical stage of discovery in order to improve the likelihood of clinical translation of such molecules. The recently identified M_1 mAChR–selective agonist TBPB, displays high functional selectivity for the M_1 mAChR, potentiates NMDA receptor currents in rat hippocampal neurons, promotes nonamyloidogenic APP processing in PC12 cells and elicits antipsychotic-like behaviour in rodent models of schizophrenia (Jones et al., 2008). However, evidence to support an allosteric mode of action for TBPB remained unclear for some time. For example, TBPB displays a non-competitive interaction with the atropine in a calcium mobilization assay, functional insensitivity to mutation of the orthosteric residue $Y381^{6.51}A$ (Ward et al., 1999), and retards the dissociation of NMS from the M_1 mAChR (Jacobson et al., 2010), suggesting an allosteric binding mode of action. However, the non-competitive interaction with atropine may also reflect a hemiequilibrium state rather than allostery (Charlton and Vauquelin, 2010; Jones et al., 2008) and TBPB may be binding to the orthosteric pocket but adopting a different pose, such that it does not interact with $Y381^{6.51}$. Moreover, the dissociation binding assay reflects interaction of a test ligand with a receptor that has been pre-equilibrated with an orthosteric antagonist and thus does not guarantee that TBPB will adopt an allosteric mode of binding if the orthosteric site is unoccupied (Avlani et al., 2010; Keov et al., 2013). Moreover, the positive allosteric modulator, VU0029767 potentiated the action of TBPB at the M_1 mAChR to the same extent as its potentiation of ACh. While this observation may indicate positive cooperativity between two ligands binding to two distinct allosteric sites on the M_1 mAChR, it also suggests a potential orthosteric site-interaction of TBPB (Marlo et al., 2009). Keov at al., (2013) used a reverse engineering approach and showed that removal of an allosteric pharmacophore from TBPB results in the generation of an agonist fragment that lost M_1 mAChR

selectivity. This study also conclusively demonstrated that TBPB interacts concomitantly with orthosteric and allosteric sites in a bitopic mode of action (Keov et al., 2013). Similar to TBPB, pharmacological studies also report that AC-42 and 77-LH-28-1 exhibit characteristics suggestive of both orthosteric and allosteric modes of action (Avlani et al., 2010; Jacobson et al., 2010; Keov et al., 2014; Langmead et al., 2006; Spalding et al., 2006; Spalding et al., 2002). Despite not engaging with some amino acid residues required by prototypical agonists, AC-42 and 77-LH-28-1 have been shown to occupy the orthosteric domain of the M_1 mAChR in addition to, or simultaneously with, the allosteric site via a bitopic mechanism (Avlani et al., 2010; Gregory et al., 2010; May et al., 2007a). Recently, Keov et al., (2014) used a mutagenesis, molecular modelling and a fragment based approach to investigate the molecular mechanisms of bitopic engagement of TBPB and 77-LH-28-1 with the M_1 mAChR and identified regions on the receptor that have distinct roles and differential effects on the affinity and efficacy of bitopic ligands compared to orthosteric ligands (Keov et al., 2014).

Numerous M_1 mAChR agonists such as NDMC (Sur et al., 2003; Thomas et al., 2010), LU AE51090 (Figure 1.11) (Sams et al., 2010), the Vanderbilt University compounds VU0184670, VU0357017 (Digby et al., 2012a; Digby et al., 2012b; Lebois et al., 2010) and VU0364572 (Lebois et al., 2011), and several GlaxoSmithKline compounds (Budzik et al., 2010a; Budzik et al., 2010b; Budzik et al., 2010c; Johnson et al., 2010) including the clinically efficacious GSK1034702 (Figure 1.11) (Nathan et al., 2013) have also been suggested to engage with the M_1 mAChR via a bitopic manner (Davie et al., 2013). However, further studies are needed to confirm the mode of action of these ligands.

While most studies of bitopic ligands to date have assumed that such ligands bind to monomeric GPCRs, recent studies have considered the behaviour of bitopic ligands in the context of GPCR dimers or oligomers (Ferré et al., 2014; Lane et al., 2014; Smith and Milligan, 2010). A recent study at the dopamine D2 receptor was the first to demonstrate that the allosteric modulator, SB269652

(Silvano et al., 2010) appears to mediate its action by binding to one D2 receptor protomer to allosterically modulate the binding of dopamine at an another (Lane et al., 2014). SB269652 engages both the orthosteric site and a secondary pocket on the D2 receptor to transmit its allosteric effect to the second associated protomer (Lane et al., 2014). However, such a mechanism has yet to be demonstrated at a mAChR.

1.4.5.4 M_1 mAChR positive allosteric modulators

Since the first demonstration of selective allosteric modulation of M_1 mAChR activity by brucine in 1998 (Lazareno et al., 1998), a large number of structurally diverse M_1 mAChR-selective positive allosteric modulators have been identified and characterized (Davie et al., 2013; Foster et al., 2014; Kuduk and Beshore, 2012; Melancon et al., 2013b; Nickols and Conn, 2014).

The first subtype-selective M_1 mAChR PAM among those was benzyl quinolone carboxylic acid (BQCA) (Figure 1.15). Discovered by scientists at Merck Laboratories, BQCA exhibits high selectivity with no activity at M_2-M_4 mAChR subtypes and induces a 300-fold increase in ACh affinity and 129-fold leftward shift in ACh potency in addition to displaying allosteric agonism on its own at the M_1 mAChR (Abdul-Ridha et al., 2013; Canals et al., 2012; Ma et al., 2009; Shirey et al., 2009). In mice, BQCA reversed scopolamine-induced memory loss by potentiating endogenous ACh activity, displayed efficacy in a contextual fear conditioning (CFC) mouse model of cognitive dysfunction (Chambon et al., 2012; Ma et al., 2009), and prevented natural forgetting in rats (Chambon et al., 2011). BQCA was also efficacious in reversing amphetamine-induced hyperlocomotion in mice (Ma et al., 2009). Both *in vivo* and *in vitro*, BQCA potentiated carbachol-induced spontaneous excitatory postsynaptic currents (sEPSCs) in medial prefrontal cortex pyramidal (mPFC) cells, an area critical for higher cognitive, learning, and memory functions (Miller and Cohen, 2001). These effects were absent in brain slices from M_1 mAChR knockout mice (Shirey et al., 2009). BQCA also restored discrimination reversal learning in a transgenic mouse

model of Alzheimer's disease and was found to regulate non-amyloidogenic APP processing *in vitro*, suggesting that M_1 mAChR PAMs have the potential to provide both symptomatic and disease modifying effects in Alzheimer's disease patients (Shirey et al., 2009).

BQCA is the first allosteric GPCR ligand proven to behave according to a strict two-state Monod-Wyman-Changeux (MWC) model of receptor activation at the M_1 mAChR (Canals et al., 2012; Canals et al., 2011). According to this model, the degree of allosteric modulation depends on both the intrinsic efficacy of the cobound orthosteric ligand and the coupling efficiency of the receptor for a given intracellular signaling pathway, the later element also dictates the magnitude of the modulators' allosteric agonism. As such, BQCA displays probe dependence by engendering high positive cooperativity with high efficacy orthosteric agonists and lower positive cooperativity with low efficacy ones. In addition, it displays negative cooperativity when co-bound with orthosteric antagonists (Canals et al., 2012). The activity of BQCA was abolished at an inactive mutant but significantly increased at a constitutively active M_1 mAChR. These findings revealed the unique nature of BQCAs' behaviour and provided a framework that can be applied to the study and classification of allosteric modulators across different GPCR families (Canals et al., 2012).

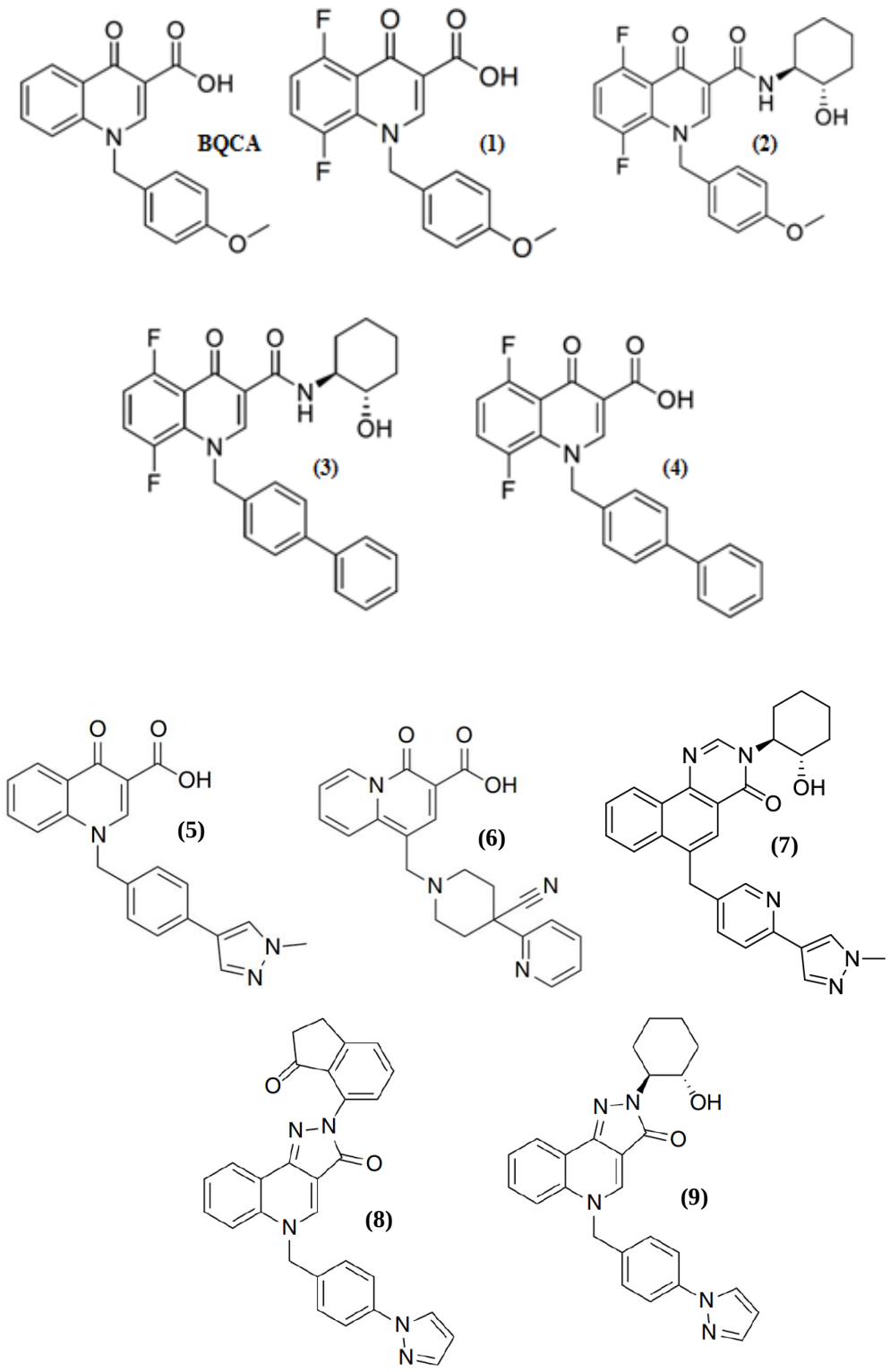

Figure 1.15 Structures of M_1 mAChR selective positive allosteric modulators based on the BQCA scaffold.

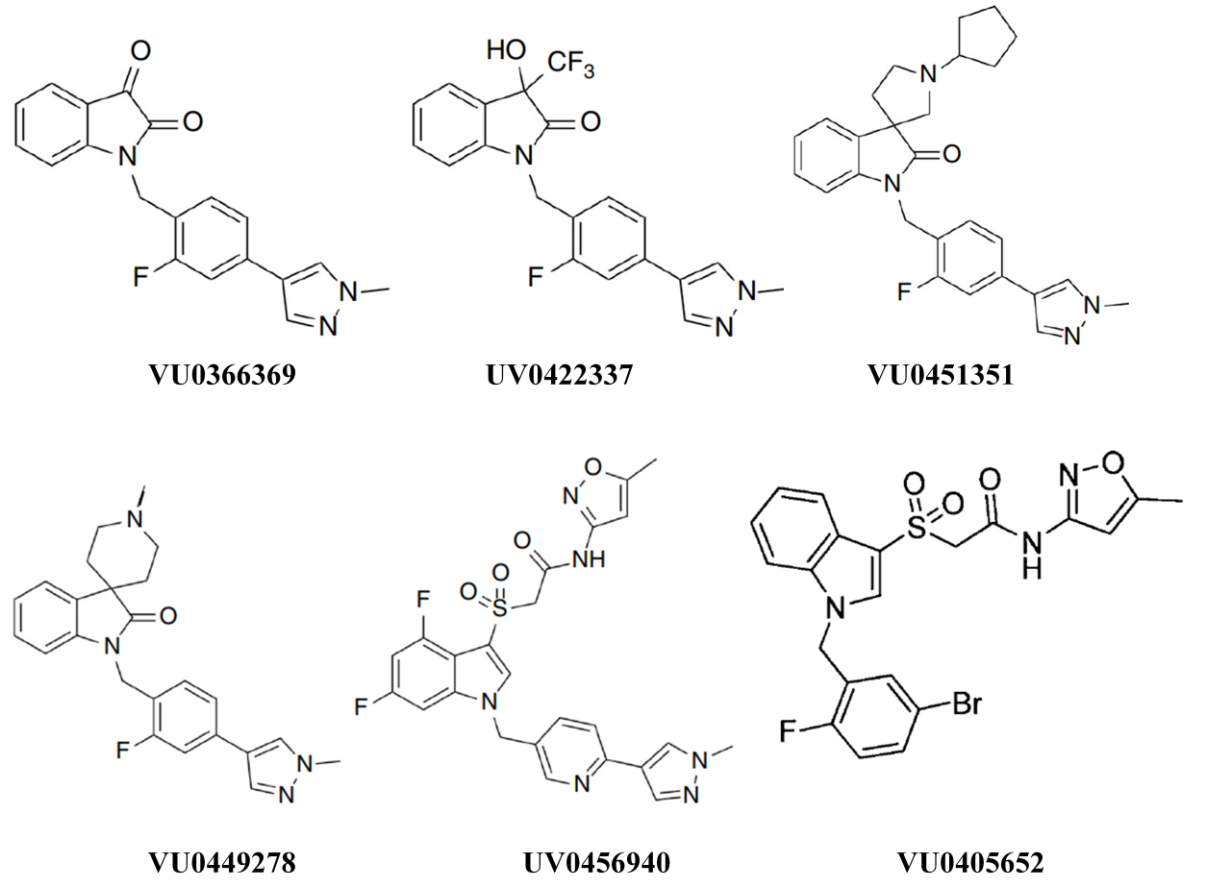

Figure 1.16 Structures of M_1 mAChR selective positive allosteric modulators from Vanderbilt University.

Despite the numerous favourable features of BQCA, this compound is also characterised by low affinity for the M_1 mAChR (~100µM) which greatly limits its *in vivo* and potentially, therapeutic utility. The low affinity also restricts the prospect of gaining mechanistic insights of modulator activity from structure-function studies (Abdul-Ridha et al., 2014b). As a result, recent drug discovery efforts have yielded an increasing number of novel M_1 mAChR-selective PAMs (Foster et al., 2014; Melancon et al., 2013b; Nickols and Conn, 2014). Merck and others exploited the multiple points of diversification on the BQCA scaffold to generate a plethora of analogues (Kuduk and Beshore, 2012; Kuduk et al., 2010b; Kuduk et al., 2011; Kuduk et al., 2012; Kuduk et al., 2014;

Mistry et al., 2013; Uslaner et al., 2013). Amongst such BQCA analogues (Figure 1.15), some display substantial improvement on the characteristics of the parent compound, as exemplified by benzoquinazolinone 12 (Compound 7 in Figure 1.15) (discussed in Chapter 4) (Davie et al., 2013; Kuduk and Beshore, 2012; Kuduk et al., 2010a).

Vanderbilt University researchers have also reported several M_1 mAChR-selective PAMs based on novel, structurally distinct chemical scaffolds (Marlo et al., 2009; Melancon et al., 2013b). For example, VU0456940 (ML137) and VU0405652 (ML169) (Figure 1.16), both display M_1 mAChR selectivity and potentiate M_1 mAChR-mediated non-amyloidogenic APP processing (Melancon et al., 2013a; Poslusney et al., 2013; Reid et al., 2011; Tarr et al., 2012). However, further development of this series of M_1 mAChR PAMs was discontinued owing to problems with high clearance and moderate CYP450 inhibition. Another structurally distinct series arose from M_1, M_3 and M_5 mAChR PAMs which, through chemical optimisation efforts, generated VU0366369, VU0422337, VU0451351 and VU0449278 all of which are highly M_1 mAChR-selective PAMs (Figure 1.16) (Bridges et al., 2010; Melancon et al., 2013a; Poslusney et al., 2013). The development of novel M_1 PAMs related to these ligands are currently underway.

1.4.5.5 The allosteric binding site

Compelling evidence from pharmacological, molecular dynamic simulations and crystallographic studies indicates that mAChRs have an allosteric binding site located extracellularly to the TM-bound orthosteric pocket (Dror et al., 2013; Kruse et al., 2013; Leach et al., 2012). This site, referred to as the "common" or the "prototypical modulator" site is typically known to bind compounds such as gallamine, C_7/3-phth, brucine and alcuronium (Figure 1.12). The location of the "second" allosteric site, which has been proposed to bind certain indolocarbazoles and the benzimidazole analogues, WIN 51,708 and WIN 62,577 (Figure 1.13) (Lanzafame et al., 2006; Lazareno et al., 2000) is currently unknown, although molecular modelling studies suggest an

intracellular location (Espinoza-Fonseca and Trujillo-Ferrara, 2005; Espinoza-Fonseca and Trujillo-Ferrara, 2006).

An early study at the M_1 mAChR proposed that $Trp^{3.28}$ and $Trp^{7.35}$, which lie at the top of TM3 and TM7, respectively, play a role in the binding of gallamine (Matsui et al., 1995). The higher affinity of gallamine at the M_2 mAChR (as compared to other mAChR subtypes) maybe be attributed to interaction with $Trp^{7.35}$ in addition to a conserved Tyr residue in ECL2 (Tyr177) and to a lesser degree to 172Glu-Asp-Gly-Glu175, as well as residues at the junction of ECL3 and top of TM7, namely $Asn^{7.32}$ and $Thr^{7.36}$ (Huang et al., 2005; May et al., 2007a; Prilla et al., 2006; Valant et al., 2008; Voigtlander et al., 2003). At the M_4 mAChR, $Ser^{7.36}$ has also been implicated in gallamine binding (Buller et al., 2002) whilst $Glu^{7.32}$ is implicated in the transmission of cooperativity between brucine and ACh at the M_3 mAChR (Stewart et al., 2010). A recent study used the inactive-state crystal structure of the M_2 mAChR as a template to perform molecular dynamic simulations in order to identify the mode of binding and function of a number of prototypical allosteric modulators including gallamine, C_7/3-phth, dimethyl-W84, alcuronium and strychnine (Dror et al., 2013). Despite their structural diversity, all the allosteric modulators bound to the same site in the extracellular vestibule, approximately 15Å from the orthosteric site and made similar interactions with the receptor. The study identified two core "centres" that contribute to the "common" allosteric site in the extracellular vestibule. Each centre is defined by a pair of aromatic residues (centre 1, Tyr177 in ECL2 and $Trp^{7.35}$; centre 2, $Tyr^{2.61}$ and $Tyr^{2.64}$) (Dror et al., 2013). Mutagenesis of these residues suggest that centre 1 contributes more strongly than centre 2 to C_7/3-phth and gallamine binding, in agreement with computational and previous mutagenesis findings (Dror et al., 2013; Huang et al., 2005; May et al., 2007a; Prilla et al., 2006). In addition, several residues also contribute to different extents to the binding of ligands at each centre; centre 1 ($Asn^{6.58}$ and $Asn^{7.32}$), centre 2 ($Tyr^{2.60}$, $Tyr^{2.63}$, $Thr^{2.64}$ and $Thr^{7.36}$) (Dror et al., 2013). The binding site for the M_4 mAChR PAM, LY2033298 (Figure 1.10), may also overlap with the common allosteric site as C_7/3-phth has

been shown to interact competitively with LY2033298 (Leach et al., 2010). In addition, alanine substitution of the ECL2 residue Phe186 at the M_4 mAChR (equivalent to Tyr177 at the M_2 and Tyr179 at the M_1 mAChR) attenuates the binding of LY2033298 (Nawaratne et al., 2010). Furthermore, substitution of $Asp^{7.32}$ and $Ser^{7.36}$ in the M_4 mAChR to the corresponding M_2 mAChR residues $Asn^{7.32}$ and $Thr^{7.36}$, respectively, did not alter the binding affinity or interaction of LY2033298 with ACh (Chan et al., 2008; Nawaratne et al., 2010).

The active-state structure of the M_2 mAChR in complex with a nanobody G protein mimetic and the high affinity agonist, iperoxo with and without the PAM, LY2119620 (Figure 1.10), has been recently determined (Kruse et al., 2013). This study provided the first structural view of how an allosteric ligand binds to a GPCR. The M_2 mAChR PAM LY2119620, which displays similar pharmacological properties to its congener, LY2033298, engages the extracellular vestibule directly above the orthosteric site (Kruse et al., 2013). Specifically, the aromatic rings of the modulator are situated directly between Tyr177 and $Trp^{7.35}$, both of which have been largely implicated in the binding of the ligands discussed above (Huang et al., 2005; Matsui et al., 1995; May et al., 2007a; Prilla et al., 2006; Valant et al., 2008; Voigtlander et al., 2003). Additionally, $Tyr^{2.61}$, $Asn^{6.58}$ and Asn419 in ECL3 form hydrogen bonds with the modulator, and Glu172 in ECL2 engages in a charge–charge interaction with the ligand piperidine. LY2119620 binding site is separated from the orthosteric binding site by a tyrosine lid, with $Tyr^{7.39}$ interacting with both LY2119620 and iperoxo (Kruse et al., 2013).

It is noteworthy that most of the residues implicated in the binding of the allosteric ligands discussed above (including $Tyr^{2.61}$, $Glu^{7.32}$, $Trp^{7.35}$, $Glu^{7.36}$ and Tyr179 in addition to $Tyr^{2.64}$) have been identified as key contributors for the binding and function of BQCA and, in some cases benzoquinazolinone 12 (see Chapters 3 and 4). This is consistent with BQCA sharing a common binding site with other mAChR allosteric modulators (Abdul-Ridha et al., 2014b; Ma et al., 2009). Overall, these studies suggest that, as with orthosteric ligands, allosteric ligands can recognize a

common site but, nonetheless, adopt different poses within that site such that they display differential sensitivity to specific mutations. Subtype-selective allosteric ligands that bind to this site may attain their selectivity through this differential sensitivity or via selective cooperativity with orthosteric agonists at the particular subtype they bind.

1.4.5.6 Molecular basis of allosteric modulation

Despite the discovery of a large number of allosteric modulators and identification of a vast repertoire of behaviours for muscarinic allosteric ligands, the molecular mechanisms underlying allosteric modulation and allosteric ligand behaviours are not well understood. Recent structural and computational biology studies have provided some insight into the mechanism of action of negative and positive allosteric modulators (Christopoulos, 2014; Dror et al., 2013; Kruse et al., 2014b; Langmead and Christopoulos, 2014).

Computational molecular dynamics simulations show that binding of cationic allosteric modulators such as gallamine, C_7/3-phth, dimethyl-W84, alcuronium and strychnine at the inactive M_2 mAChR structure is driven largely by interactions between cationic amines on the modulators and aromatic residues on the receptor (Dror et al., 2013). The abundant aromatic residues that comprise the allosteric pocket (described above) form cation-π interactions with the modulator ammonium groups (Dror et al., 2013). Substitution of non-aromatic residues in this pocket to aromatic ones strengthens the cation-π interactions and enhanced the binding affinity, while introduction of cationic residues reduced the binding affinity of the NAMs C7/3-phth and gallamine (Dror et al., 2013). Examination of the mechanisms that contribute to the transmission of cooperativity between orthosteric and allosteric ligands revealed that electrostatic repulsion between a cationic orthosteric ligand such as NMS and a cationic allosteric modulator such as C7/3-phth, weakens the binding of one in the presence of the other, resulting in negative cooperativity. The degree of repulsion varies, such that less cationic NAMs experience less repulsion (Dror et al., 2013). Neutralising the cationic

nitrogen atom with a silicon atom shifted the cooperativity of C_7/3-phth in the positive direction (Daiss et al., 2002; Dror et al., 2013). It is hypothesised that the presence of cationic residues in mAChR allosteric pockets may cause cationic allosteric modulators to have lower affinity for a receptor. For example, the presence of a cationic residue ($Lys^{7.32}$) at the M_3 mAChR may be the reason for the typically lower affinity of modulators at this receptor (Conn et al., 2009; Dror et al., 2013). Despite the presence of a cationic group on alcuronium, the cooperativity between NMS and this modulator is positive, an observation that cannot be explained by electrostatic repulsion (Dror et al., 2013).

Another possible mechanism underlying cooperativity relates to the conformations of the orthosteric and allosteric sites which are conformationally linked such that the presence of a ligand in one site, affects the shape of the other. When NMS is bound, both the allosteric and orthosteric sites of the M_2 mAChR are maintained in a wide-open conformation while both sites assume a narrow conformation in absence of ligands (Dror et al., 2013). Binding of the "bulky" PAM alcuronium to the empty receptor forces both sites into an open conformation which seems to contribute to the positive cooperativity between NMS and alcuronium (Dror et al., 2013). By contrast, the NAM C_7/3-phth favours binding to the narrow conformation formed in the absence of orthosteric ligand. Therefore, small allosteric modulators destabilise antagonist binding in the inactive mAChR state, leading to negative cooperativity between the two ligands, whereas "bulkier" modulators enhance antagonist binding (Christopoulos, 2014). The addition of "bulky" substituents to C_7/3-phth improved the binding affinity at the NMS-occupied M_2 mAChR but reduced the negative cooperativity (Dror et al., 2013), supporting the concept that orthosteric antagonist binding can be enhanced or diminished by a modulator that preferentially stabilizes a particular conformation of the extracellular vestibule (Christopoulos, 2014).

The iperoxo-bound M_2 mAChR crystal structure shows that large extracellular vestibule, which has been shown to bind to allosteric modulators (Bock et al., 2012; Dror et al., 2013; Gregory et al., 2007), undergoes a substantial contraction upon receptor activation due to rotation of TM6 (Kruse et al., 2013). As with other active-state GPCR crystal structures (Rasmussen et al., 2011a; Rasmussen et al., 2011b), the movement of TM6 facilitates structural coupling of the extracellular vestibule, the orthosteric binding pocket, and the intracellular surface of the receptor, allowing allosteric modulators to affect the affinity and efficacy of orthosteric ligands and in some cases activate G proteins as allosteric agonists (Kruse et al., 2013; May et al., 2007a). The iperoxo- and LY2119620-bound M_2 mAChR structure is largely similar to that of receptor and agonist without LY2119620, with slight additional contraction around the allosteric ligand, indicating that the allosteric binding site is mostly pre-formed in the presence of agonist (Kruse et al., 2013). In contrast, the extracellular vestibule is wide open in the inactive M_2 mAChR conformation. $Trp^{7.35}$, which is largely implicated in the binding of numerous allosteric ligands at mAChRs (Dror et al., 2013; Ma et al., 2009; Prilla et al., 2006), adopts a vertical conformation in the presence of LY2119620 and a horizontal conformation with iperoxo alone to allow it to engage in an aromatic stacking interaction with the modulator. Closure of the allosteric pocket in the presence of LY2119620 permits more extensive interactions with the modulator and allows the modulator to potentiate agonist binding affinity by slowing agonist dissociation (Kruse et al., 2013). The inward movement of the top of TM6 upon receptor activation is responsible for the closed conformation of the extracellular vestibule and stabilization of the closed extracellular vestibule. Allosteric modulators may in turn stabilize the open, active conformation of the intracellular side of TM6, facilitating allosteric agonism and transmission of positive cooperativity with orthosteric agonists (Kruse et al., 2013). It remains questionable as to whether a similar mechanism of allosteric modulation occurs at the M_1 mAChR or indeed with another allosteric modulators at the M_2 mAChR. In order to truly understand the atomistic basis of small molecule allosteric modulation at

GPCRs via structural biology, multiple structures are required of the same receptor in active and inactive states.

1.5 Scope of Thesis

The M_1 mAChR is highly expressed in brain regions responsible for learning, cognition and memory and has therefore been implicated in numerous CNS disorders where such processes are impaired (Melancon et al., 2013b). M_1 mAChR knockout mice show cognitive deficits (Anagnostaras et al., 2003; Hamilton et al., 1997; Kamsler et al., 2010; Kruse et al., 2014b), while evidence from clinical trials supports the importance of targeting this receptor for improving memory and reducing cognitive deficits (Bodick et al., 1997a; Bodick et al., 1997b; Nathan et al., 2013). Despite the abundance of studies that support the involvement of this receptor in cognition and memory formation, it is still unclear how M_1 mAChR-activated signaling proteins and pathways are linked to accomplish such processes. While such processes are likely an integration of signaling pathways involving many receptors in the CNS, dissecting the physiological and pathophysiological role of M_1 mAChR signaling and physiology has been hindered by the lack of subtype selective ligands for this receptor (owing to the highly conserved orthosteric site). The lack of subtype selectivity has also been the reason for the high attrition rates of compounds developed as therapies for Alzheimer's disease and schizophrenia.

With the discovery of M_1 mAChR selective allosteric ligands, there is considerable potential to understand the role of this receptor subtype in disease and as therapeutics for the treatment of CNS disorders. Despite the abundance of mutagenesis studies on the M_1 mAChR, they have largely focused on delineating the location of the orthosteric ligand binding site and identifying the role these residues play in receptor function (Hulme, 2013). The inactive-crystal structures of the M_2 and M_3 mAChRs provided additional insight into the location of the orthosteric binding pocket at mAChRs and illustrated the 7TM architecture of this family of receptors (Haga et al., 2012; Kruse et al., 2012b). Despite the recent surge in the number of selective M_1 mAChR allosteric modulators, there have been very little investigations into the molecular determinants of selective allosteric

ligand activity at this receptor and it remains largely unknown how these ligands achieve their receptor subtype selectivity and mediate their allosteric effects on the receptor. Only recently have structural and molecular dynamic simulation studies shed light on the structural basis of allosteric modulation by both NAMs and PAMs and identified possible location of an allosteric site on the M_2 mAChR (Dror et al., 2013; Kruse et al., 2013). While these studies provide a significant milestone in the GPCR allostery, the information they provide is limited to the M_2 mAChR, and represents only a snapshot of the vast repertoire of behaviours displayed by allosteric ligands. The current project therefore aimed to address key knowledge gaps for the M_1 mAChR, including investigating allosteric modulation at a mutant M_1 mAChR designed as a biological tool for understanding *in vivo* GPCR signaling and delineating the molecular basis of binding and function of selective M_1 mAChR PAMs.

In Chapter 2, the activity of BQCA is explored in binding studies and across multiple signaling pathways at the WT M_1 mAChR, confirming its "two-state" behaviour. This distinctive feature of BQCA was exploited to investigate whether allosteric modulation at a chemogenetically modified M_1 DREADD receptor (developed as a tool to study the physiological function of this receptor *in vivo)* is equivalent to the corresponding modulation at the WT receptor. This evaluation is important if DREADD receptors are to be used to investigate allosteric modulation *in vivo* given the potential for these receptors to adopt conformations that may lead to biased downstream signaling or change the behaviour of allosteric ligands (Abdul-Ridha et al., 2013).

Several studies, mostly on the M_2 mAChR, report the involvement of a number of amino acid residues in allosteric ligand binding and formation of the allosteric binding site (Dror et al., 2013; Kruse et al., 2013; Ma et al., 2009; Matsui et al., 1995; May et al., 2007a; Voigtlander et al., 2003). In Chapter 3, numerous residues, including some equivalent to those reported in the above studies, are introduced into the M_1 mAChR in order to determine their contribution to the allosteric binding site at the M_1 mAChR and investigate the role they play in allosteric modulation. The

pharmacology of orthosteric ligands and BQCA is extensively characterised at each mutant receptor in radioligand binding and functional studies and analysed via application of operational allosteric models to the data to quantify the effects of the mutations on the various allosteric parameters. The results are confirmed by molecular modelling studies (Abdul-Ridha et al., 2014b).

The low affinity of BQCA prompted researchers to develop a large number of M_1 mAChR PAMs. Amongst the BQCA analogues generated, some display substantial improvement on the characteristics of BQCA, as exemplified by benzoquinazolinone 12. Chapter 4 reports the optimized synthesis and detailed pharmacological characterization of benzoquinazolinone 12. Site-directed mutagenesis and molecular modeling is utilized to validate the allosteric binding pocket described for BQCA and provide the molecular basis for its improved affinity at the M_1 mAChR. The study highlights how the properties of affinity and cooperativity can be differentially modified on a common structural scaffold, and identifies molecular features that can be exploited to tailor the development of M_1 mAChR-targeting PAMs (Abdul-Ridha et al., 2014a).

Collectively, these studies use mutagenesis, molecular modelling and SAR approaches to provide unprecedented insights into the molecular mechanisms of allosteric modulation at the M_1 mAChR and highlight that BQCA and its derivatives share a common binding site with other prototypical mAChR allosteric modulators. Although these findings provide insight into the location of the binding pocket for mAChR allosteric modulators, they do not explain how subtype selectivity is achieved. However, it is likely that selectivity is achieved via selective cooperativity of the modulators with ACh.

CHAPTER 2

Allosteric Modulation of a Chemogenetically Modified G Protein-Coupled Receptor

Alaa Abdul-Ridha, J. Robert Lane, Patrick M. Sexton, Meritxell Canals, and Arthur Christopoulos

Mol Pharmacol **83**: 521-530, February 2013.

Monash University

Declaration for Thesis Chapter 2

Declaration by candidate

In the case of Chapter 2, the nature and extent of my contribution to the work was the following:

Nature of contribution	**Extent of contribution (%)**
Development of ideas, participated in research design, conducted experiments, performed data analysis, contributed to the writing and editing of the manuscript.	80%

The following co-authors contributed to the work. If co-authors are students at Monash University, the extent of their contribution in percentage terms must be stated:

Name	**Nature of contribution**
J. Robert Lane	Participated in research design, performed data analysis, contributed to manuscript preparation
Patrick M. Sexton	Contributed to manuscript preparation
Meritxell Canals	Development of ideas, participated in research design, performed data analysis, contributed to manuscript preparation
Arthur Christopoulos	Participated in research design, performed data analysis, contributed to manuscript preparation

The undersigned hereby certify that the above declaration correctly reflects the nature and extent of the candidate's and co-authors' contributions to this work.

Candidate's Signature		**Date**
Main Supervisor's Signature		**Date**

Supplemental Material can be found at:
http://molpharm.aspetjournals.org/content/suppl/2012/11/29/mol.112.083006.DC1.html

1521-0111/83/2/521–530$25.00
MOLECULAR PHARMACOLOGY

http://dx.doi.org/10.1124/mol.112.083006
Mol Pharmacol 83:521–530, February 2013

MOL PHARM
MOLECULAR PHARMACOLOGY

Allosteric Modulation of a Chemogenetically Modified G Protein-Coupled Receptor[S]

Alaa Abdul-Ridha, J. Robert Lane, Patrick M. Sexton, Meritxell Canals, and Arthur Christopoulos

Drug Discovery Biology, Monash Institute of Pharmaceutical Sciences and Department of Pharmacology, Monash University, Parkville, Victoria, Australia

Received October 17, 2012; accepted November 29, 2012

ABSTRACT

Designer receptors exclusively activated by designer drugs (DREADDs) are chemogenetically modified muscarinic acetylcholine receptors (mAChRs) that have minimal responsiveness to acetylcholine (ACh) but are potently and efficaciously activated by an otherwise inert synthetic ligand, clozapine-*N*-oxide (CNO). DREADDs have been used as tools for selectively modulating signal transduction pathways in vitro and in vivo. Recent comprehensive studies have validated how the pharmacology of a CNO-bound DREADD mirrors that of an ACh-bound wild-type (WT) mAChR. However, nothing is known about whether this equivalence extends to the allosteric modulation of DREADDs by small molecules. To address this, we investigated the actions at an M_1 DREADD of benzyl quinolone carboxylic acid (BQCA), a positive allosteric modulator of ACh binding and function that is known to behave according to a simple two-state mechanism at the WT receptor. We found that allosteric modulation of the CNO-bound DREADD receptor is not equivalent to the corresponding modulation of the ACh-bound WT receptor. We also found that BQCA engenders stimulus bias at the M_1 DREADD, having differential types of cooperativity depending on the signaling pathway. Furthermore, the modulation of ACh itself by BQCA at the DREADD is not compatible with the two-state model that we previously applied to the M_1 WT receptor.

Introduction

Over the last decade, chemical-genetic strategies have been applied in the generation of tools for investigating G protein-coupled receptor (GPCR) function with increasing degrees of spatial and temporal specificity. Such chemogenetically modified GPCRs include receptors activated solely by synthetic ligands (Pei et al., 2008) and designer receptors exclusively activated by designer drugs (DREADDs) (Armbruster et al., 2007), the latter having been specifically generated using the muscarinic acetylcholine receptor (mAChR) subtypes as the model system (Armbruster et al., 2007). These mAChR DREADDs contain two mutations of conserved orthosteric site residues (Y106C and A196G in the M_1 mAChR) that cause a loss of responsiveness to the cognate agonist acetylcholine (ACh) while engendering the ability to be potently activated by the otherwise biologically inert ligand, clozapine-*N*-oxide (CNO). When these mutant GPCRs are expressed in a particular tissue, the resultant biological effects observed after administration of CNO only reflect the activation of the chosen DREADD in that particular tissue. As such, DREADDs have proven to be valuable biological tools and have been expressed transgenically to investigate specific functions of several mAChRs and the physiologic consequences of their activation in vivo (Alexander et al., 2009; Guettier et al., 2009; Ferguson et al., 2011; Krashes et al., 2011; Ray et al., 2011; Sasaki et al., 2011; Garner et al., 2012).

Recently, it has become apparent that different ligands binding to the same GPCR can stabilize specific receptor conformations that are coupled to distinct functional outcomes; a phenomenon termed "stimulus bias," "biased agonism," or "functional selectivity" (Stallaert et al., 2011). This begs the question as to how much the action of the CNO-bound DREADD truly reflects that of the ACh-bound wild-type (WT) receptor. Fortunately, a recent rigorous investigation of multiple signaling and receptor regulatory pathways at the M_3 DREADD concluded that the results obtained from the transgenic expression of the DREADD when activated by CNO are indeed likely to mirror the actions of ACh at the WT

This work was funded by the National Health and Medical Research Council of Australia (NHMRC) [Program Grant 519461] (A.C., P.M.S), [Project Grant APP1011796] (M.C), and [Project Grant APP1011920] (J.R.L.). A.C is a Senior, and P.M.S a Principal, Research Fellow of the NHMRC. A.A. is a recipient of an Australian Postgraduate Award scholarship.
M.C. and A.C. contributed equally to this work.
dx.doi.org/10.1124/mol.112.083006.
[S] This article has supplemental material available at molpharm.aspetjournals.org.

ABBREVIATIONS: ACh, acetylcholine; BQCA, benzyl quinolone carboxylic acid; CHO, Chinese hamster ovary; CNO, clozapine-*N*-oxide; CNS, central nervous system; DMEM, Dulbecco's modified Eagle's medium; DREADD, designer receptor exclusively activated by designer drug; FBS, fetal bovine serum; GPCR, G protein-coupled receptor; GppNHp, guanosine 5′-[β, γ-imido] triphosphate; IBMX, 3-isobutyl-1-methylxanthine; IP1, inositolphosphate-1; mAChR, muscarinic acetylcholine receptor; McN-A-343, 4-I-[3-chlorophenyl]carbamoyloxy)-2-butynyltrimethylammnonium chloride; MWC, Monod-Wyman-Changeux; NDMC, *n*-desmethyl-clozapine; pERK1/2, phosphorylated extracellular signal-regulated kinase; QNB, quinuclidinyl benzilate; TBPB, 1-[1′-(2-methylbenzyl)-1,4′-bipiperidin-4-yl]-1,3-dihydro-2H-benzimidazol-2-one; WT, wild-type.

receptor (Alvarez-Curto et al., 2011). However, there exist alternative possible utilities of DREADDs for which such vital equivalence with the WT remains undetermined; these possibilities involve the potential combination of DREADDs with small molecule allosteric modulators of GPCRs. As we previously showed using the M_4 DREADD, it is possible to use an allosteric modulator to "reactivate" the DREADD to its cognate agonist, ACh (Nawaratne et al., 2008). A potential advantage of this approach is that the temporal specificity associated with endogenous ACh release and uptake can be retained while activating the DREADD in a spatially controlled fashion. Irrespective, the nature of allosteric modulation of CNO itself at a DREADD remains unknown, although this approach may also be considered as a means to better understand GPCR allostery in a tissue/pathway-targeted manner.

An ideal requirement for addressing these issues would be an allosteric modulator that behaves in a predictable manner and does not promote stimulus bias when tested against ACh at a WT mAChR. We recently characterized the actions of such a ligand, benzyl quinolone carboxylic acid (BQCA), at the M_1 WT mAChR (Canals et al., 2012). Specifically, BQCA displays simple receptor "state dependence," exhibiting positive cooperativity with orthosteric agonists but negative cooperativity with inverse agonists in a manner that correlates with orthosteric ligand efficacy. Importantly, the allosteric modulation of BQCA did not engender stimulus-bias at a variety of M_1 mAChR-linked signaling pathways (Canals et al., 2012). The discovery of such a molecule thus presents an unprecedented opportunity to investigate the nature of allosteric modulation of a DREADD with regards to both the cognate receptor agonist and the synthetic activator CNO. Herein, we provide a comprehensive analysis of the allosteric interaction of BQCA with ACh, CNO, and a diverse range of M_1 mAChR ligands at multiple downstream signaling pathways linked to the M_1 WT and DREADD mAChRs. We reveal that allosteric modulation of the CNO-bound DREADD receptor is not equivalent to the ACh-bound WT receptor and that BQCA engenders stimulus bias at the M_1 DREADD.

Materials and Methods

Materials. Chinese hamster ovary (CHO) FlpIn cells and Dulbecco's modified Eagle's medium (DMEM) were purchased from Invitrogen (Carlsbad, CA). Fetal bovine serum (FBS) was purchased from ThermoTrace (Melbourne, Australia). Hygromycin-B was purchased from Roche (Mannheim, Germany). [^{3}H]quinuclidinyl benzilate ([^{3}H]QNB; specific activity, 50 Ci/mmol), cAMP AlphaScreen beads, AlphaScreen reagents and Ultima gold scintillation liquid were purchased from PerkinElmer Life Sciences (Boston, MA). The *SureFire* cellular extracellular signal-regulated kinase (ERK1/2) assay kits were a generous gift from TGR BioSciences (Adelaide, Australia). IP-One assay kit and reagents were purchased from Cisbio (Codolet, France). Fluo-4-AM was purchased from Molecular Probes (Carlsbad, CA). All other chemicals were purchased from Sigma Aldrich (St. Louis, MO). BQCA was synthesized in house at the Monash Institute of Pharmaceutical Sciences (Parkville, Australia).

Cell Culture and Receptor Mutagenesis. The M_1 DREADD mutations [Y106C/A196G-3.33 and -5.46, respectively, using the Ballesteros-Weinstein numbering system (Ballesteros and Weinstein, 1995)] were generated using the QuickChange site-directed mutagenesis kit (Agilent Technologies, La Jolla, CA), following the manufacturer's instructions. CHO FlpIn cells stably expressing the M_1 WT or DREADD mAChRs were generated and maintained as described previously (Avlani et al., 2010).

Membrane Preparation and Radioligand Binding. Membranes from CHO FlpIn cells stably expressing either M_1 WT or DREADD mAChRs were prepared as described previously (Nawaratne et al., 2008). Radioligand binding assays were performed using 5μg and 20 μg of M_1 WT and DREADD mAChR membrane homogenates, respectively. Membranes were incubated in 1 ml binding buffer (20 mM HEPES, 100 mM NaCl, 10 mM, $MgCl_2$, pH 7.4) containing 100 μM guanosine 5′-[β, γ-imido] triphosphate and increasing concentrations of the competing ligand for 1 hour at 37°C in the presence of a fixed concentration of [^{3}H]QNB. Homologous competition binding assays were initially performed to determine the equilibrium dissociation constant of [^{3}H]QNB and the number of binding sites at both M_1 WT and DREADD mAChRs (K_i and B_{max}, respectively). The concentration of [^{3}H]QNB used in all subsequent heterologous competition binding assays was approximately equal to its equilibrium dissociation constant at the M_1 WT mAChR (0.13 ± 0.03 nM; n = 3). Interaction studies were performed in the absence or presence of increasing concentrations of BQCA. For all experiments, total and nonspecific binding was defined by the absence of competing ligand and the presence of 100 μM atropine, respectively. The termination of the assay and measurements of bound radioactivity were performed as described in Avlani et al. (2010).

Extracellular Signal-Regulated Kinase 1/2 Phosphorylation Assays. Assays to measure M_1 mAChR-mediated stimulation of ERK1/2 phosphorylation were performed using the AlphaScreen-based SureFire kit (TGR Biosciences), following the manufacturer's instructions. Briefly, FlpIn CHO cells stably expressing either the M_1 WT or DREADD mAChRs were seeded into 96-well culture plates at 40,000 cells per well and allowed to adhere. Cells were then rinsed with phosphate-buffered saline and serum starved overnight at 37°C, 5% CO_2. The following day, cells were stimulated with agonist. Initial ERK1/2 phosphorylation (pERK1/2) time course experiments were performed to determine the time of maximal ERK1/2 phosphorylation for each agonist (found to be 5 minutes for all agonists tested). The time of peak agonist response was then used for the establishment of concentration-response curves. For functional interaction studies, cells were incubated at 37°C with varying concentrations of agonist in the absence and presence of varying concentrations of BQCA, which was co-added with the agonist. In all experiments, 10% (v/v) FBS was used as positive control of pERK1/2. The reaction was terminated by removal of media and addition of lysis buffer. Samples were processed according to kit instructions. The fluorescence signal was measured using a Fusion-α plate reader (PerkinElmer Life Sciences). Data were normalized to the maximum response elicited by 10% (v/v) FBS at the same time point.

Intracellular Ca^{2+} Mobilization Assays. FlpIn CHO cells were seeded at 35,000 cells per well into 96-well culture plates and allowed to grow overnight at 37°C, 5% CO_2. Cells were washed twice with Ca^{2+} assay buffer [150 mM NaCl, 2.6 mM KCl, 1.2 mM $MgCl_2$, 10 mM D-glucose, 10 mM HEPES, 2.2 mM $CaCl_2$, 0.5% (w/v) BSA, and 4 mM probenecid, pH 7.4] and incubated in Ca^{2+} assay buffer containing 1 μM Fluo-4-AM for 1 hour in the dark at 37°C 5% CO_2. After two washes with Ca^{2+} assay buffer, fluorescence was measured for 1.5 minutes upon the addition of agonist (or coaddition of agonist and BQCA) in a Flexstation (Molecular Devices, Sunnyvale, CA) using an excitation wavelength of 485 nm and emission wavelength of 520 nm. Data were normalized to the peak response elicited by 2 μM ionomycin.

cAMP Accumulation Assays. FlpIn CHO cells were seeded at 35,000 cells per well into 96-well culture plates and allowed to grow overnight at 37°C, 5% CO_2. Cells were incubated with 90 μl of stimulation buffer [phenol red-free DMEM containing 0.1% (w/v) BSA, 5 mM HEPES, 0.5 mM 3-isobutyl-1-methylxanthine (IBMX), pH 7.4] for 30 minutes at 37°C, 5% CO_2. Cells were stimulated with agonist for 30 minutes, after which the medium was removed and cells were precipitated with 100% ethanol. Ethanol was allowed to

evaporate at room temperature or in a nonhumidified incubator at 37°C. After ethanol evaporation, cells were lysed with lysis buffer [0.3% Tween20, 5 mM HEPES, 0.1% (w/v) BSA]. Lysates were processed according to the AlphaScreen kit manufacturer instructions (PerkinElmer Life Sciences). The fluorescence signal was measured using a Fusion-α plate reader (PerkinElmer Life Sciences). Data were normalized to the maximum response elicited by 100 μM forskolin.

IP-One Accumulation Assays. Inositol phosphate-1 (IP_1) was measured using the IP-One assay kit (Cisbio), following the manufacturer's instructions. Briefly, FlpIn CHO cells were seeded into 384-well proxy-plates at 7500 cells per well and allowed to grow overnight at 37°C, 5% CO_2. The following day cells were stimulated with agonists in IP-One stimulation buffer (in the absence or presence of BQCA) and incubated for 1 hour at 37°C, 5% CO_2. IP_1-d2 and anti-IP_1-cryptate were prepared in IP-One lysis buffer and incubated with the cells for 1 hour at room temperature. Homogeneous time resolved fluorescence resonance energy transfer was measured in an Envision plate reader (PerkinElmer Life Sciences). Values for each sample were extrapolated from the IP_1 standard curve, and data were normalized to the maximum control response.

Data Analysis. All data were analyzed using Prism 5.0 (GraphPad, San Diego, CA). Inhibition binding curves between [^{3}H]QNB and unlabeled ligands were fitted to a one-site binding model (Motulsky, 2004). BQCA binding-interaction studies were fitted to the following allosteric ternary complex model (Ehlert, 1988):

$$Y = \frac{Bmax\ [A]}{[A] + \left(\frac{K_A K_B}{\alpha'[B] + K_B}\right)\left(1 + \frac{[I]}{K_I} + \frac{[B]}{K_B} + \frac{\alpha[I][B]}{K_I K_B}\right)} \quad (1)$$

where Y is percentage (vehicle control) binding; Bmax is the total number of receptors; [A], [B] and [I] are the concentrations of [^{3}H]QNB, BQCA, and the orthosteric ligand, respectively; K_A and K_B and K_I are the equilibrium dissociation constants of [^{3}H]QNB, BQCA, and the orthosteric ligand, respectively. α' and α are the binding cooperativities between BQCA and [^{3}H]QNB, and BQCA the orthosteric ligand, respectively. Values of α (or α') >1 denote positive cooperativity; values <1 (but >0) denote negative cooperativity, and values = 1 denote neutral cooperativity.

Concentration-response curves for the interaction between BQCA and the orthosteric ligand in the various functional signaling assays were globally fitted to the following operational model of allosterism and agonism (Leach et al., 2007):

$$E = \frac{E_m(\tau_A[A](K_B + \alpha\beta[B]) + \tau_B[B]K_A)^n}{([A]K_B + K_A K_B + [B]K_A + \alpha[A][B])^n + (\tau_A[A](K_B + \alpha\beta[B]) + \tau_B[B]K_A)^n} \quad (2)$$

where E_m is the maximum possible cellular response, [A] and [B] are the concentrations of orthosteric and allosteric ligands, respectively, K_A and K_B are the equilibrium dissociation constant of the orthosteric and allosteric ligands, respectively, τ_A and τ_B are operational measures of orthosteric and allosteric ligand efficacy (which incorporate both signal efficiency and receptor density), respectively, α is the binding cooperativity parameter between the orthosteric and allosteric ligand, and β denotes the magnitude of the allosteric effect of the modulator on the efficacy of the orthosteric agonist. In all instances, the equilibrium dissociation constant of each agonist was fixed to that determined from the binding assays. All affinity, potency, and cooperativity values are estimated as logarithms (Christopoulos, 1998), and statistical comparisons between values were by Student's t-test. A value of $P < 0.05$ was considered statistically significant.

Results

Pharmacological Characterization of the M_1 WT and M_1 DREADD mAChR. To characterize the pharmacology of the M_1 DREADD in comparison with that of the M_1 WT mAChR, the binding and activation profiles of a range of ligands were examined (Supplemental Fig. 1). Using [^{3}H]QNB as a prototypical orthosteric antagonist, we performed equilibrium homologous competition binding studies in membrane preparations of CHO FlpIn cells stably expressing the M_1 WT or M_1 DREADD mAChRs. The DREADD displayed a significant reduction in the affinity of [^{3}H]QNB ($pK_A = 8.23 \pm 0.06$; $n = 3$, $P < 0.05$) compared with the WT ($pK_A = 9.88 \pm 0.12$; $n = 3$), consistent with previous findings for DREADDs (Armbruster et al., 2007; Nawaratne et al., 2008). The receptor expression level of the M_1 DREADD was not significantly different from the WT receptor ($B_{max} = 4.90 \pm 0.35$ versus 5.10 ± 0.12 pmol/mg of protein for WT and DREADD receptors, respectively). Subsequent testing of structurally diverse ligands in equilibrium binding studies using 0.13 nM [^{3}H]QNB revealed different effects of the DREADD mutations on ligand binding depending on the nature of the ligand studied (Fig. 1; Supplemental Fig. 2; Table 1). The affinities of the endogenous orthosteric agonist, ACh, and the partial agonist xanomeline were significantly reduced at the M_1 DREADD (Fig. 1: Supplemental Figs. 1 and 2; Table 1). In contrast, the affinities of clozapine, its metabolite *N*-desmethylclozapine (NDMC), and the synthetic analog CNO, were significantly enhanced at the M_1 DREADD. Interestingly, 1-[1′-(2-methylbenzyl)-1,4′-bipiperidin-4-yl]-1,3-dihydro-2H-benzimidazol-2-one (TBPB) and McN-A-343, which may have a "bitopic" (dual allosteric/orthosteric) mode of interaction at the mAChRs (Valant et al., 2012b) and display distinct sensitivities to residues proposed to be involved in orthosteric ligand binding (Valant et al., 2008; Jacobson et al., 2010), showed no significant difference in their binding affinity at the M_1 WT and M_1 DREADD (Supplemental Figs. 1 and 2; Table 1). BQCA itself caused partial inhibition of [^{3}H]QNB binding both at the WT and DREADD M_1 mAChR, consistent with our previous finding of a negative cooperativity with the antagonist and a low affinity for the allosteric site on the free receptor (Canals et al., 2012); estimates of the pK_I value from the current study were 4.15 ± 0.11 and 4.05 ± 0.13 for M_1 WT and DREADD mAChRs, respectively (Fig. 1; Table 1).

We also investigated the ability of the different ligands to activate WT and DREADD receptors using intracellular Ca^{2+} mobilization as a canonical measure of M_1 mAChR activation resulting from preferential coupling to $G\alpha_q$ proteins. Both ACh and xanomeline displayed a significant loss of potency at the M_1 DREADD, whereas clozapine and its derivatives CNO and NDMC gained potency and/or efficacy at the M_1 DREADD (Fig. 1; Supplemental Fig. 3; Table 1). TBPB activated the M_1 DREADD with comparable potency and efficacy to its activity at the WT receptor. However, in contrast to the unaltered binding profile at the M_1 DREADD, McN-A-343 displayed reduced potency and efficacy at this receptor (Supplemental Fig. 3; Table 1). At the M_1 WT mAChR, BQCA also behaved as a potent and efficacious allosteric agonist in its own right. However, the mutations in the M_1 DREADD caused a significant abolishment in BQCA's action, despite having no effect on its affinity (Fig. 1, C and F; Table 1).

Allosteric Modulation of CNO Binding Affinity at the M_1 DREADD is Less than that of ACh at the M_1 WT mAChR. Given the previously determined functional equivalence between CNO at the DREADD and ACh at the WT mAChR (Armbruster et al., 2007; Alvarez-Curto et al., 2011), we investigated whether such equivalence is retained in terms

MOL PHARM
MOLECULAR PHARMACOLOGY
aspet

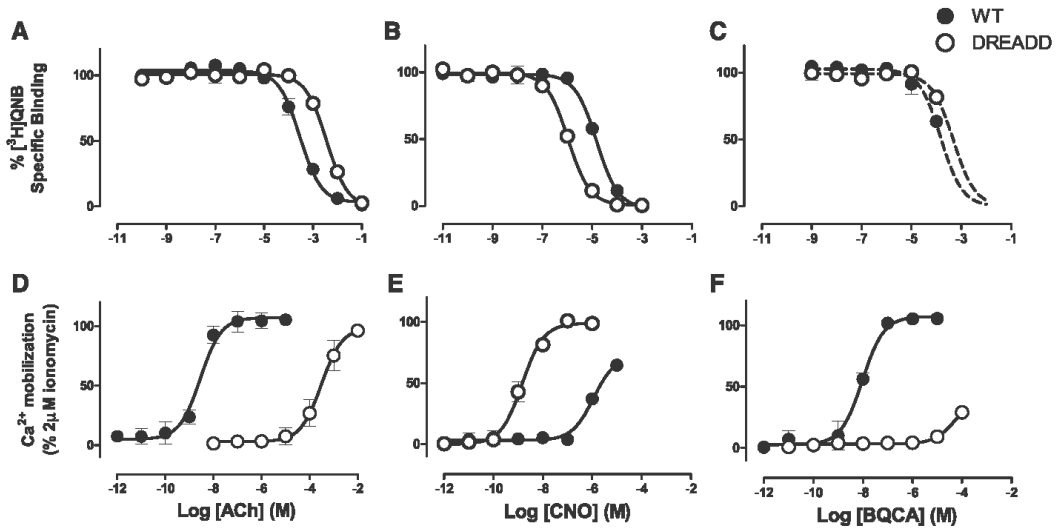

Fig. 1. Ligand binding and activation properties at the M_1 WT and DREADD mAChRs. The equilibrium binding of the antagonist [^{3}H]QNB was inhibited by ACh (A), CNO (B), and BQCA (C) in membranes of FlpIn CHO cells expressing the WT M_1 mAChR (closed circles) and M_1 DREADD (open circles). All assays were performed using 0.13 nM [^{3}H]QNB in the presence of 100 μM guanosine 5′-[β, γ-imido] triphosphate (GppNHp) for 1 hour at 37°C. Concentration-response curves of intracellular Ca^{2+} mobilization assays were constructed for ACh (D), CNO (E), and BQCA (F) in CHO FlpIn cells stably expressing the WT M_1 mAChR (closed circles) and M_1 DREADD (open circles) at 37°C. Data points represent the mean ± S.E. of three independent experiments performed in duplicate. Refer to Table 1 for parameters.

of allosteric modulation. To investigate the effects of BQCA on the affinity of the cobound ligand, interaction studies were performed between ACh or CNO and varying concentrations of BQCA against a fixed concentration of [^{3}H]QNB (Fig. 2). BQCA substantially potentiated ACh-mediated inhibition of equilibrium binding of [^{3}H]QNB at the M_1 WT mAChR (Fig. 2A). A similar pattern of potentiation was observed in the interaction between CNO and BQCA at the M_1 DREADD (Fig. 2D). However, when this potentiation was quantified by application of an allosteric ternary complex model to the data (Eq. 1; Table 2), we found that the positive binding cooperativity between ACh and BQCA at the M_1 WT mAChR (α = 331) was significantly higher than that with CNO at the M_1 DREADD (α = 60). Conversely, BQCA had no effects on the affinity of CNO at the M_1 WT and of ACh at the M_1 DREADD, indicating neutral binding cooperativity (Fig. 2, B and C).

TABLE 1
[^{3}H]QNB inhibition binding (pK_I) and Ca^{2+} mobilization potency (pEC_{50}) parameters for various ligands at the M_1 WT and DREADD mAChRs
Estimated parameter values represent the mean ± S.E. of three experiments performed in duplicate.

	M_1 WT		M_1 DREADD	
Ligand	pK_I[a]	pEC_{50}[b]	pK_I	pEC_{50}
ACh	3.86 ± 0.04	8.54 ± 0.06	2.43 ± 0.07*	3.74 ± 0.12*
Xanomeline	6.84 ± 0.02	8.38 ± 0.06	5.10 ± 0.03*	5.83 ± 0.07*
TBPB	6.76 ± 0.08	7.86 ± 0.10	6.45 ± 0.09	7.30 ± 0.19
McN-A-343	4.71 ± 0.08	7.54 ± 0.05	4.37 ± 0.10	5.39 ± 0.08*
CNO	5.18 ± 0.07	5.95 ± 0.07	5.93 ± 0.04*	8.87 ± 0.07*
Clozapine	6.81 ± 0.07	7.14 ± 0.40	7.93 ± 0.08*	9.30 ± 0.07*
NDMC	6.60 ± 0.05	7.49 ± 0.09	7.40 ± 0.02*	9.33 ± 0.08*
BQCA	4.15 ± 0.11	8.02 ± 0.06	4.05 ± 0.13	4.16 ± 0.16*

[a] Negative logarithm of the equilibrium dissociation constant for each ligand.
[b] Negative logarithm of the EC_{50}.
* Significantly different ($P < 0.05$), two-tailed Students t-test, from the corresponding parameter at the M_1 WT mAChR.

The Allosteric Interaction between ACh and BQCA is Consistent with a Two-state Mechanism at the M_1 WT but Not at the M_1 DREADD. To gain further insight into the functional modulation mediated by BQCA, we performed interaction studies using multiple signaling pathways linked to M_1 mAChR activation, namely; intracellular Ca^{2+} mobilization, ERK1/2 phosphorylation, cAMP and IP_1 accumulation. Figure 3 shows the interaction between ACh and BQCA at both the M_1 WT and DREADD mAChRs in the various signaling pathways. BQCA strongly potentiated the action of ACh at the M_1 WT mAChR, in addition to exhibiting agonism on its own in the two highly amplified and efficiently coupled signaling pathways, i.e., intracellular Ca^{2+} mobilization and ERK1/2 phosphorylation (Fig. 3, A and B). In the cAMP accumulation pathway (where stimulus-response coupling efficiency is weak), BQCA's agonism was less pronounced, but robust potentiation of ACh was still evident (Fig. 3C). These data were globally fitted to an operational model of allosterism (Eq. 2) to yield the parameters shown in Table 3; for this analysis, the binding affinity of BQCA was fixed to the pK_B value determined from the binding studies (Table 1). In agreement with our previous study (Canals et al., 2012), BQCA displayed the highest levels of positive cooperativity (quantified by the operational $\alpha\beta$ parameter) at the pathways where the orthosteric agonist exhibited the highest degrees of signaling efficacy (quantified by the operational model τ_A parameter), as would be expected if the allostery was operative within a simple two-state mechanism. However, when analogous interaction studies between ACh and BQCA were

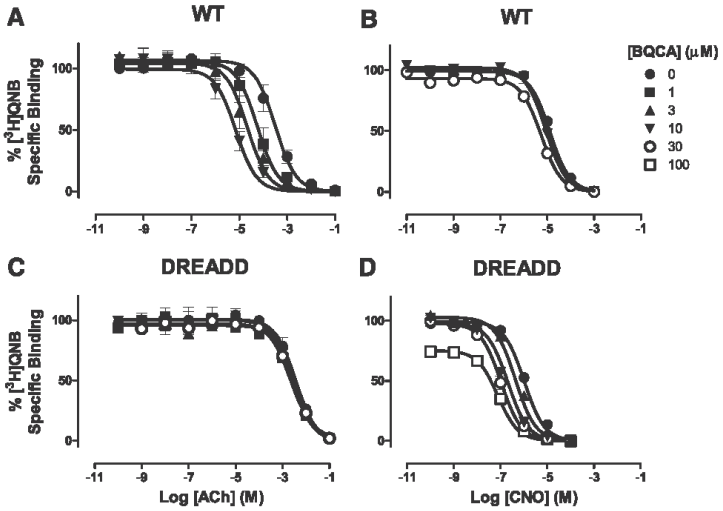

Fig. 2. Allosteric modulation of CNO binding affinity at the M_1 DREADD is less than that of ACh at the M_1 WT mAChR. BQCA potentiated ACh and CNO-mediated inhibition of equilibrium binding of [^{3}H]QNB (A and D) but had no effect on the binding affinity of CNO and ACh (B and C) in membranes of FlpIn CHO cells at the WT M_1 and DREADD mAChRs, respectively. All assays were performed using 0.13 nM [^{3}H]QNB in the presence of 100 μM GppNHp for 1 hour at 37°C. Data points represent the mean ± S.E. of three independent experiments performed in triplicate. Curves drawn through the points in (A and D) represent the best fit of an allosteric ternary complex model (Eq. 1; Table 2).

performed at the M_1 DREADD, we noted that BQCA robustly enhanced the potency of ACh in both the Ca^{2+} mobilization and pERK1/2 pathways (Fig. 3, D and E) despite having no effect on ACh binding affinity. Additionally, in experiments measuring stimulation of intracellular cAMP production, where ACh showed no agonistic activity at the DREADD, BQCA was able to partially rescue its signaling efficacy (Fig. 3F). Although BQCA displayed high positive cooperativity with ACh at the M_1 DREADD, this cooperativity did not track with the degree of agonist efficacy across the pathways, in contrast to what was observed at the M_1 WT mAChR (Table 3; see correlation analysis below), suggesting that the two state behavior of BQCA versus ACh may not be maintained at the M_1 DREADD.

BQCA Engenders Biased Allosteric Modulation of CNO at the M_1 DREADD. Subsequent experiments focused on the functional modulation by BQCA of CNO. In contrast to the large and positive cooperativity seen between ACh and BQCA in the Ca^{2+} mobilization pathway at the M_1 WT mAChR (Fig. 3A; Table 3), BQCA had a minimal effect on the action of CNO at the M_1 DREADD in the same pathway (Fig. 4A). To rule out the possibility that this observation resulted from potential hemi-equilibrium conditions in the Ca^{2+} mobilization assay, we repeated the same experiment in an IP^1 accumulation assay. Again, BQCA did not potentiate the action of CNO in this latter assay (Fig. 4B). Application of the operational model to the data yielded the estimates shown in Table 4. Given that the positive binding cooperativity (α value) between CNO and BQCA was 60, our results suggest that BQCA actually has a *negative* effect on the signaling efficacy of CNO, with estimated values of $\beta = 0.03$ and $\beta = 0.13$ for the Ca^{2+} mobilization and IP_1 assays, respectively. In contrast, BQCA enhanced the action of CNO in the ERK1/2 phosphorylation pathway (Fig. 4C) with a composite cooperativity ($\alpha\beta$) of 41 (Table 4). Given the similar cooperativity estimated from binding studies ($\alpha = 60$), this indicates the presence of essentially neutral modulation at the level of signaling efficacy (β).

Collectively, as summarized in Fig. 5, these findings suggest that BQCA engenders stimulus bias at the M_1 DREADD by demonstrating neutral functional modulation in one pathway (ERK1/2 phosphorylation) and negative functional modulation in another (Ca^{2+} mobilization). Despite the overall large positive cooperativity between BQCA and CNO at the M_1 DREADD in the pERK1/2 pathway, it is still significantly smaller than the cooperativity between ACh and BQCA at both the M_1 WT and DREADD mAChRs in the same signaling pathway. When this interaction was examined in the cAMP pathway, BQCA positively modulated the potency of CNO but had negative effects on its efficacy (Fig. 4D). This broad spectrum of pharmacological behaviors at the M_1 DREADD indicates that the actions of BQCA do not conform to a simple "two-state" model, in contrast to its behavior at the M_1 WT mAChR.

TABLE 2

Binding cooperativity parameters for the interaction between [^{3}H]QNB, BQCA and various mAChR ligands at the M_1 WT and DREADD mAChRs

Estimated parameter values represent the mean ± S.E. of three experiments performed in triplicate and analyzed according to Eq. 1.

	M_1 WT	M_1 DREADD
	Log α (α)[a]	Log α (α)
ACh	2.52 ± 0.03 (331)	ND
Xanomeline	ND	ND
TBPB	ND	ND
McN-A-343	1.06 ± 0.07 (11)	ND
CNO	0.64 ± 0.06 (4.5)	1.78 ± 0.05* (60)
Clozapine	ND	1.10 ± 0.14 (13)
NDMC	1.02 ± 0.06 (10.5)	2.15 ± 0.03* (141)

ND, not determined (no modulation of affinity).
[a] Logarithm of the binding cooperativity factor between BQCA and the interacting ligand as estimated from Eq. 1; antilogarithm shown in parentheses. For this analysis, pK_A was constrained to 9.88 and 8.32, and pK_B was constrained to 4.15 and 4.05 at the M_1 WT and DREADD mAChRs, respectively (Table 1). The cooperativity between BQCA and [^{3}H]QNB was constrained to zero, consistent with high negative cooperativity between the modulator and the radioligand.
* Significantly different ($P < 0.05$), two-tailed Students t-test, from the value of ACh at the M_1 WT.

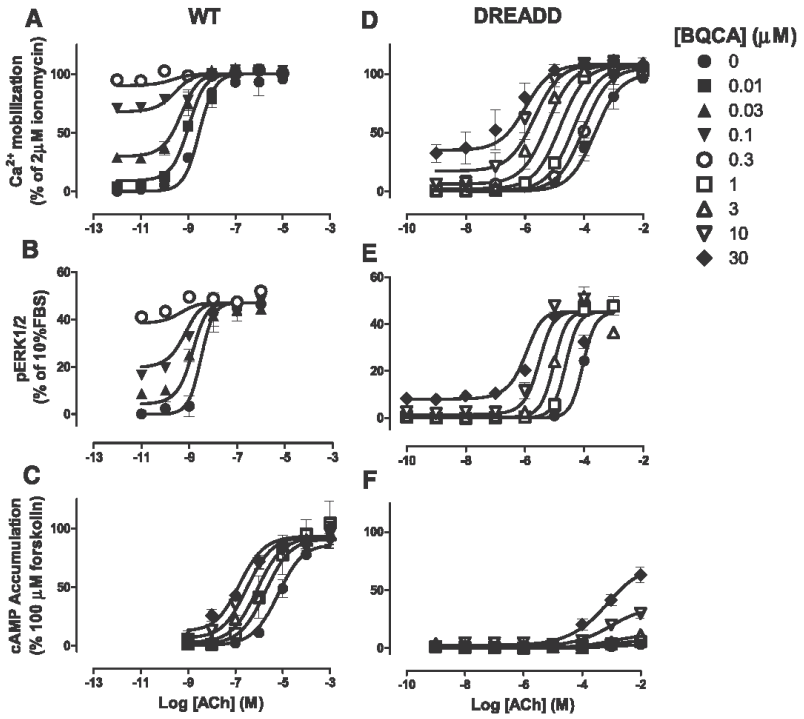

Fig. 3. The allosteric interaction between ACh and BQCA is consistent with a two-state mechanism at the M_1 WT but not at the M_1 DREADD. Interaction between BQCA and ACh in intracellular Ca^{2+} mobilization (A and D), ERK1/2 phosphorylation (B and E), or cAMP accumulation (C and F) in CHO FlpIn cells stably expressing the M_1 WT or M_1 DREADD mAChRs. Data points represent the mean ± S.E. of three independent experiments performed in duplicate. Curves drawn through the points represent the best fit of an operational allosteric model (Eq. 2; Table 3).

BQCA Consistently Conforms to a "Two-state" Allosteric Model in its Interaction with Various Ligands at the M_1 WT mAChR but Not at the M_1 DREADD. To examine if the bias engendered by BQCA at the M_1 DREADD is a result of the receptor conformation stabilized by the co-bound ligand, we explored the interaction of BQCA with various mAChR ligands. We first used NDMC, a clozapine metabolite with a similar binding and activation profile to CNO at the M_1 DREADD (Supplemental Figs. 2E and 3E; Table 1). In the binding interaction studies, BQCA caused a substantial increase in the affinity of NDMC to compete with [^{3}H]QNB. The positive binding cooperativity was estimated to have a value of log α = 2.15±0.03 (α=141) (Supplemental Fig. 4A; Table 2). Furthermore, the stimulus bias of BQCA at the M_1 DREADD was again demonstrated by its interaction with NDMC in the functional signaling pathways, whereby it displayed negative efficacy modulation of NDMC in the Ca^{2+} mobilization pathway, but neutral modulation of NDMC efficacy in the ERK1/2 phosphorylation pathway (Supplemental Fig. 4, B and C; Supplemental Table 1). Similar to the CNO interaction studies, BQCA caused a reduction in the efficacy of NDMC in the cAMP pathway (Supplemental

TABLE 3

Operational model parameters for the functional allosteric interaction between ACh and BQCA at the M_1 mAChR

Estimated parameter values represent the mean ± S.E. of three experiments performed in duplicate and analyzed according to Eq. 2. For this analysis, the pK_B value for BQCA was fixed to that determined from the radioligand binding assays.

	M_1 WT			M_1 DREADD		
	Ca^{2+}	pERK1/2	cAMP	Ca^{2+}	pERK1/2	cAMP
Log τ_A[a]	4.78 ± 0.10	4.71 ± 0.07	1.36 ± 0.16	1.31 ± 0.11	1.53 ± 0.05	ND
Log τ_B[b] (τ_B)	3.19 ± 0.05 (1550)	2.75 ± 0.03 (560)	−0.51 ± 0.30 (0.31)	0.30 ± 0.08 (2)	0.28 ± 0.06 (2)	ND
Log $\alpha\beta$[c] ($\alpha\beta$)	4.10 ± 0.20 (12590)	3.84 ± 0.17 (6918)	2.30 ± 0.14 (200)	2.92 ± 0.14 (831)	2.40 ± 0.07 (251)	ND

ND, not determined.
[a] Logarithm of the operational efficacy parameter of the orthosteric agonist.
[b] Logarithm of the operational efficacy parameter of the allosteric agonist.
[c] Logarithm of the cooperativity between ACh and BQCA. Antilogarithm shown in parentheses.

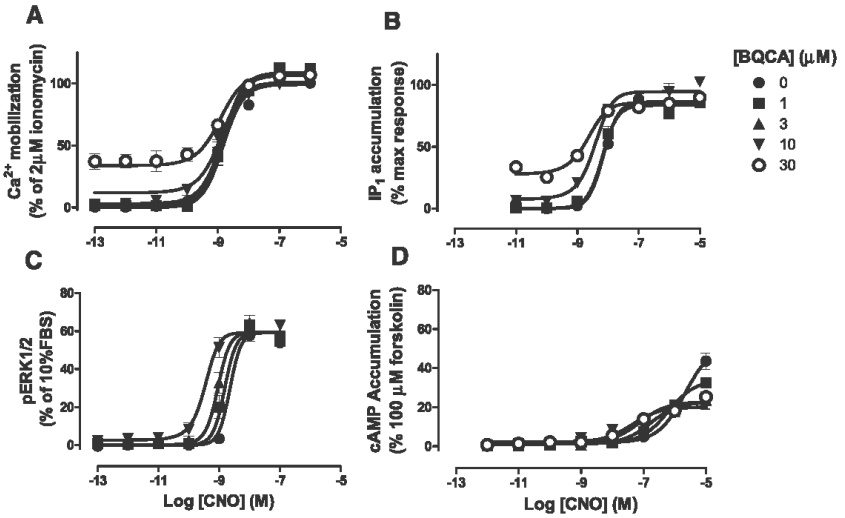

Fig. 4. BQCA engenders biased allosteric modulation of CNO at the M_1 DREADD. Interaction between BQCA and CNO in intracellular Ca^{2+} mobilization (A), IP_1 accumulation (B), ERK1/2 phosphorylation (C), and cAMP accumulation (D) in CHO FlpIn cells stably expressing the M_1 DREADD mAChR. Data points represent the mean ± S.E. of three independent experiments performed in duplicate. Curves drawn through the points in (A–C) represent the best fit of an operational allosteric model (Eq. 2; Table 4).

Fig. 4D). These results demonstrate that the biased allosteric behavior of BQCA at the M_1 DREADD is likely to be resulting from the conformations stabilized by the clozapine derivatives CNO and NDMC at this receptor, because the same pattern of modulatory bias across signaling pathways at the M_1 DREADD was not observed in the interaction of BQCA with ACh (Fig. 3, D–F).

Subsequently, we extended these studies to the other mAChR ligands. The data from each ligand-BQCA interaction experiment were globally fitted to the operational model of allosterism (eq. 2), and the relationship between the parameters log τ_A and log $\alpha\beta$ was examined for each set of ligand interactions (Supplemental Table 2). As shown in Fig. 6, A and B, a significant correlation between the parameters log τ_A and log $\alpha\beta$ can be observed at the M_1 WT mAChR in both the Ca^{2+} mobilization (Pearson's $r^2 = 0.736$; $P = 0.01$) and pERK1/2 pathways (Pearson's $r^2 = 0.625$; $P = 0.03$), providing further evidence for the allosteric two-state behavior of BQCA at this receptor. When the same set of ligand-BQCA interactions studies were performed at the M_1 DREADD and analyzed in the same manner, no significant correlation was observed between the parameters log τ_A and log $\alpha\beta$ in both the Ca^{2+} mobilization (Pearson's $r^2 = 0.004$; $P = 0.89$) and pERK1/2 pathways (Pearson's $r^2 = 0.264$; $P = 0.24$) (Fig. 6, C and D). These results therefore suggest that the two-state model proposed for the mechanism of action of BQCA at the WT mAChR is applicable beyond its interaction with ACh, but is not applicable at the M_1 DREADD.

TABLE 4

Operational model parameters for the functional allosteric interaction between CNO and BQCA at the M_1 DREADD

Estimated parameter values represent the mean ± S.E from three experiments performed in duplicate and analyzed according to Eq. 2. All other details are as for Table 3.

	Ca^{2+}	pERK1/2	IP_1
Log τ_A	2.81 ± 0.04	2.65 ± 0.10	2.12 ± 0.05
Log τ_B (τ_B)	0.38 ± 0.04 (2.4)	0.44 ± 0.17 (2.8)	0.41 ± 0.07 (2.6)
Log $\alpha\beta$ ($\alpha\beta$)	0.30 ± 0.29 (2)*	1.61 ± 0.22 (41)*	0.88 ± 0.21 (7.5)

* Significantly different ($P < 0.05$), two-tailed Students t-test, from the corresponding value at the M_1 WT in Table 3.

Discussion

Recent studies have provided compelling evidence that the CNO-bound DREADD mAChR retains functional equivalence with the ACh-bound WT mAChR, thus validating the chemogenetically modified DREADD as a powerful tool for probing GPCR signaling in a highly specific manner (Alexander et al., 2009; Guettier et al., 2009; Alvarez-Curto et al., 2011; Krashes et al., 2011). In the current study, we extended this question to the phenomenon of small molecule allostery and explored the behavior of BQCA in its interaction with a number of structurally and functionally diverse ligands at the M_1 DREADD. This modulator was chosen because we recently demonstrated that its actions at the M_1 WT mAChR can be reconciled within a two-state receptor model, akin to that applied to many ion channels, thus representing the simplest case of allosteric modulation with clear, predictable properties (Canals et al., 2012). We reveal that allosteric modulation of the CNO-bound DREADD receptor is not equivalent to the corresponding modulation of the ACh-bound WT receptor. In addition, we find that BQCA engenders stimulus bias at the M_1 DREADD, most strikingly by behaving as a neutral allosteric modulator of CNO efficacy in the pERK1/2 pathway while having negative modulation in the Ca^{2+} mobilization and IP_1 pathways. Moreover, the modulation of ACh itself by BQCA at the DREADD is also not compatible with a simple

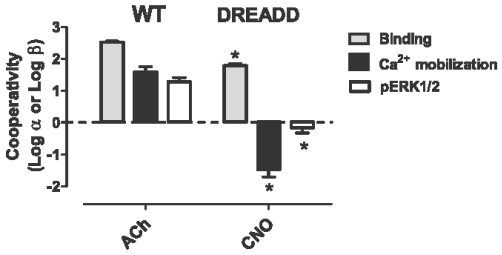

Fig. 5. BQCA displays divergent cooperativity estimates with ACh and CNO at the WT M_1 and DREADD mAChRs. Individual estimates of α and β values calculated by subtraction of the cooperativity factors determined in the radioligand binding studies (Fig. 2, A and D; Table 2) from the composite estimates determined from the functional assays (Fig. 3, A and B; Fig. 4, A and C; Tables 3 and 4). *Significantly different ($P < 0.05$), two-tailed Students t-test, from the corresponding parameter at the WT receptor.

two-state model that we have applied to the M_1 WT. These findings indicate that the behavior of the DREADD with respect to allosteric modulation is a manifestation of multiple, distinct, receptor conformations.

Because mAChR subtypes are characterized by a very high degree of amino acid sequence conservation within the orthosteric (ACh) binding site (Wess et al., 2003), previous attempts to target the M_1 mAChR have failed due to unwanted side effects that result from their lack of subtype selectivity (Conn et al., 2009). An alternative approach to achieve subtype selectivity is to develop ligands that target allosteric sites that are less conserved between subtypes (Christopoulos, 2002). BQCA is one such compound that has high subtype selectivity for the M_1 mAChR. Importantly, the modulator exhibits both in vitro and in vivo efficacy as a potentiator of ACh affinity and signaling (Ma et al., 2009; Shirey et al., 2009; Canals et al., 2012). Allosteric modulators such as BQCA represent not only potential therapeutics, but are also useful tools to study the selective activation of GPCRs both in vitro and in vivo. Another powerful method for generating tools to study receptor activity in a defined spatial and temporal manner is the chemogenetic approach, as exemplified by the generation of DREADDs (Conklin, 2007). Given the potential offered by the combination of these two approaches to interrogate M_1 mAChR function, it is essential to perform a detailed pharmacological characterization of this mutant receptor. Although several studies have transgenically expressed the DREADD receptors in animal models and investigated the physiologic consequence of activating them in vivo (Alexander et al., 2009; Guettier et al., 2009; Krashes et al., 2011; Ferguson et al., 2011; Ray et al., 2011; Sasaki et al., 2011; Garner et al., 2012), no study has thus far studied allosteric or bitopic ligands at these mutant receptors. By using ACh and xanomeline as orthosteric ligands, TBPB and McN-A-343 as ligands that possibly have a bitopic mode of interaction with the mAChRs (Valant et al., 2008; Jacobson et al., 2010), CNO as the orthosteric ligand at the M_1 DREADD and its analogs clozapine and NDMC, we identified different profiles of receptor binding and activation at the M_1 DREADD that suggest multiple modes of receptor engagement (Fig. 1; Supplemental Figs. 1–3; Table 1). As expected from prior studies using DREADDs, the affinity and potency of ACh and xanomeline were reduced, while CNO and its

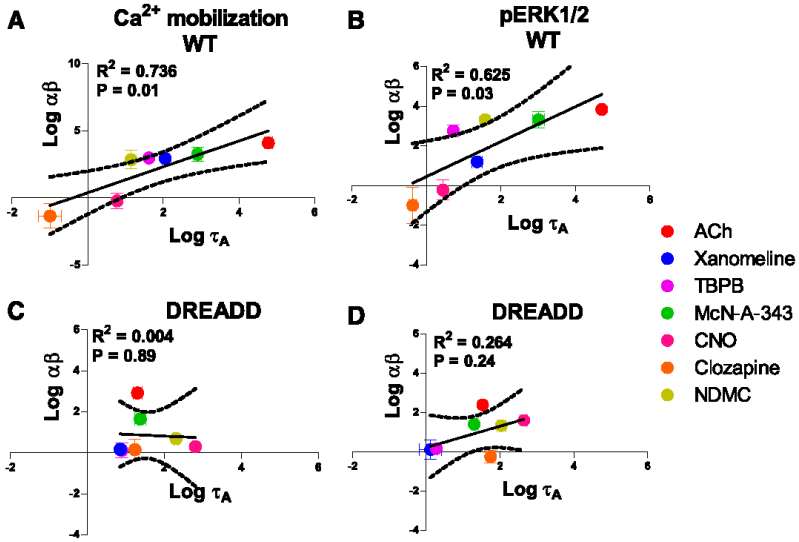

Fig. 6. Correlation plots examining the allosteric behavior of BQCA and its interaction with various ligands at the WT M_1 (A and B) and DREADD (C and D) mAChRs. Significant correlation between log τ_A and log $\alpha\beta$ parameters is observed in BQCA's allosteric interaction with various ligands at the M_1 WT mAChR in both the Ca^{2+} mobilization (A and C) and ERK1/2 phosphorylation (B and D) pathways; dashed lines indicate the 95% confidence intervals. No significant correlation can be observed at the M_1 DREADD in the same signaling pathways. Data points represent the operational model parameters (Supplemental Table 2) for the functional allosteric interactions between BQCA and each of the ligands.

MOL PHARM
MOLECULAR PHARMACOLOGY
aspet

structural analogs, NDMC and clozapine, showed significant gains in these parameters. Interestingly, we reveal for the first time that the affinity and potency of TBPB was unaffected by the M_1 DREADD mutations. Unlike TBPB, however, McN-A-343, a partial M_1 mAChR agonist that has been shown to be bitopic at the M_2 mAChR (Valant et al., 2008), displayed reduced potency and efficacy at the M_1 DREADD that was not due to a loss of binding affinity (Supplemental Figs. 2 and 3; Table 1), indicating that the DREADD mutations had a specific effect on the ability of McN-A-343 to mediate receptor transition into an active state; this appears not to be the case for TBPB.

In addition to providing insights into the nature of putative bitopic ligand interactions on the DREADDs, the key finding of the current study was the consequences of allosteric modulation of both the cognate and synthetic agonists in this system. In agreement with our previous study (Canals et al., 2012), BQCA exhibited key hallmarks of allostery within a two-state system at the WT M_1 mAChR, including positive or negative modulation of orthosteric ligand activity depending on the nature of the orthosteric ligand (i.e., positive or inverse agonist) and different strengths of cooperativity depending on the intrinsic efficacy of the orthosteric ligand and the magnitude of stimulus-response coupling of the studied signal pathway. It can, of course, be questioned as to how an allosteric modulator can behave in a manner consistent with a two-state model at GPCRs given that these receptors adopt a larger spectrum of biologically active states, a prerequisite, in fact, for biased signaling (Vaidehi and Kenakin, 2010; Mary et al., 2012). This can be reconciled within a model whereby the modulator changes the abundance, but not the quality/nature, of different microstates that govern receptor activity; an overall change in abundance of active microstates in one direction relative to "inactive" microstates would still appear, at a macroscopic level, as a "two-state" system. In contrast, a change in the nature or quality of the microstates, in addition to their abundance, would manifest as biased modulation. In this regard, BQCA is a relatively unique, but extremely useful tool compound for probing allosteric principles compared with the more complex behaviors of numerous allosteric modulators at different GPCR families that appear to promote pathway-biased modulation to various extents (Mathiesen et al., 2005; Maillet et al., 2007; Marlo et al., 2009; Stewart et al., 2010; Davey et al., 2012; Valant et al., 2012a)

At first glance, it may also be argued that the functional equivalence between ACh at the WT M_1 mAChR and CNO at the M_1 DREADD is retained with regards to the effects of BQCA in a two-state model. Specifically, the higher degree of positive cooperativity between the modulator and ACh at the WT M_1 mAChR, relative to its effects on CNO at the M_1 DREADD, would be expected, given that ACh displays higher efficacy at the WT than CNO at the DREADD (compare, for instance, the log τ_A values for ACh at the WT M_1 mAChR in Table 3 to the log τ_A values for CNO at the M_1 DREADD in Table 4). However, there were two key lines of evidence arguing against this conformational equivalence with regards to allosteric modulation of the two receptors. First, the degree of cooperativity between various orthosteric agonists and BQCA at the DREADD did not track with the degree of efficacy displayed by the agonists, which is a key expectation of the two-state model and is generally evident at the WT M_1 mAChR (Fig. 6). Second, and more strikingly, the interaction between BQCA and CNO at the DREADD was characterized by positive, neutral, or negative modulation of CNO efficacy, depending on the pathway being monitored. A similar pattern of BQCA allosteric modulation was observed when the functional interaction studies were performed with NDMC instead of CNO (Supplemental Fig. 4; Supplemental Table 1). These results suggest that the pattern of biased modulation is likely to result from a unique receptor conformation stabilized by clozapine derivatives in combination with BQCA at the M_1 DREADD that is distinct from that stabilized by ACh and BQCA at the M_1 WT mAChR. The recent advances in GPCR (and mAChR particularly) structural biology (Haga et al., 2012; Kruse et al., 2012), together with novel biophysical approaches to study receptor conformations, offer an ideal platform to compare the M_1 WT and M_1 DREADD from a structural perspective and therefore to provide mechanistic insight into the differences observed in our studies

Acknowledgments

The authors thank Dr. Michael Crouch (TGR Biosciences) for generously providing the ERK1/2 phosphorylation assay kit and Briana J. Davie for the chemical synthesis of BQCA.

Authorship Contributions

Participated in research design: Abdul-Ridha, Lane, Sexton, Canals, Christopoulos.

Conducted experiments: Abdul-Ridha.

Performed data analysis: Abdul-Ridha, Lane, Canals, Christopoulos.

Wrote or contributed to writing of the manuscript: Abdul-Ridha, Lane, Sexton, Canals, Christopoulos.

References

Alexander GM, Rogan SC, Abbas AI, Armbruster BN, Pei Y, Allen JA, Nonneman RJ, Hartmann J, Moy SS, and Nicolelis MA et al. (2009) Remote control of neuronal activity in transgenic mice expressing evolved G protein-coupled receptors. *Neuron* **63**:27–39.

Alvarez-Curto E, Prihandoko R, Tautermann CS, Zwier JM, Pediani JD, Lohse MJ, Hoffmann C, Tobin AB, and Milligan G (2011) Developing chemical genetic approaches to explore G protein-coupled receptor function: validation of the use of a receptor activated solely by synthetic ligand (RASSL). *Mol Pharmacol* **80**: 1033–1046.

Armbruster BN, Li X, Pausch MH, Herlitze S, and Roth BL (2007) Evolving the lock to fit the key to create a family of G protein-coupled receptors potently activated by an inert ligand. *Proc Natl Acad Sci USA* **104**:5163–5168.

Avlani VA, Langmead CJ, Guida E, Wood MD, Tehan BG, Herdon HJ, Watson JM, Sexton PM, and Christopoulos A (2010) Orthosteric and allosteric modes of interaction of novel selective agonists of the M1 muscarinic acetylcholine receptor. *Mol Pharmacol* **78**:94–104.

Ballesteros JA and Weinstein H (1995) Integrated methods for the construction of three-dimensional models and computational probing of structure-function relations in G protein-coupled receptors, in *Methods in Neurosciences* (Stuart CS, ed) pp 366–428, Academic Press, San Diego. [19].

Canals M, Lane JR, Wen A, Scammells PJ, Sexton PM, and Christopoulos A (2012) A Monod-Wyman-Changeux mechanism can explain G protein-coupled receptor (GPCR) allosteric modulation. *J Biol Chem* **287**:650–659.

Christopoulos A (1998) Assessing the distribution of parameters in models of ligand-receptor interaction: to log or not to log. *Trends Pharmacol Sci* **19**:351–357.

Christopoulos A (2002) Allosteric binding sites on cell-surface receptors: novel targets for drug discovery. *Nat Rev Drug Discov* **1**:198–210.

Conklin BR (2007) New tools to build synthetic hormonal pathways. *Proc Natl Acad Sci USA* **104**:4777–4778.

Conn PJ, Jones CK, and Lindsley CW (2009) Subtype-selective allosteric modulators of muscarinic receptors for the treatment of CNS disorders. *Trends Pharmacol Sci* **30**:148–155.

Davey AE, Leach K, Valant C, Conigrave AD, Sexton PM, and Christopoulos A (2012) Positive and negative allosteric modulators promote biased signaling at the calcium-sensing receptor. *Endocrinology* **153**:1232–1241.

Ehlert FJ (1988) Estimation of the affinities of allosteric ligands using radioligand binding and pharmacological null methods. *Mol Pharmacol* **33**:187–194.

Ferguson SM, Eskenazi D, Ishikawa M, Wanat MJ, Phillips PE, Dong Y, Roth BL, and Neumaier JF (2011) Transient neuronal inhibition reveals opposing roles of indirect and direct pathways in sensitization. *Nat Neurosci* **14**:22–24.

Garner AR, Rowland DC, Hwang SY, Baumgaertel K, Roth BL, Kentros C, and Mayford M (2012) Generation of a synthetic memory trace. *Science* **335**: 1513–1516.

Guettier JM, Gautam D, Scarselli M, Ruiz de Azua I, Li JH, Rosemond E, Ma X, Gonzalez FJ, Armbruster BN, and Lu H et al. (2009) A chemical-genetic approach

to study G protein regulation of beta cell function in vivo. *Proc Natl Acad Sci USA* **106**:19197–19202.
Haga K, Kruse AC, Asada H, Yurugi-Kobayashi T, Shiroishi M, Zhang C, Weis WI, Okada T, Kobilka BK, and Haga T et al. (2012) Structure of the human M2 muscarinic acetylcholine receptor bound to an antagonist. *Nature* **482**:547–551.
Jacobson MA, Kreatsoulas C, Pascarella DM, O'Brien JA, and Sur C (2010) The M1 muscarinic receptor allosteric agonists AC-42 and 1-[1′-(2-methylbenzyl)-1,4′-bipiperidin-4-yl]-1,3-dihydro-2H-benzimidazol-2-one bind to a unique site distinct from the acetylcholine orthosteric site. *Mol Pharmacol* **78**:648–657.
Krashes MJ, Koda S, Ye C, Rogan SC, Adams AC, Cusher DS, Maratos-Flier E, Roth BL, and Lowell BB (2011) Rapid, reversible activation of AgRP neurons drives feeding behavior in mice. *J Clin Invest* **121**:1424–1428.
Kruse AC, Hu J, Pan AC, Arlow DH, Rosenbaum DM, Rosemond E, Green HF, Liu T, Chae PS, and Dror RO et al. (2012) Structure and dynamics of the M3 muscarinic acetylcholine receptor. *Nature* **482**:552–556.
Leach K, Sexton PM, and Christopoulos A (2007) Allosteric GPCR modulators: taking advantage of permissive receptor pharmacology. *Trends Pharmacol Sci* **28**:382–389.
Ma L, Seager MA, Wittmann M, Jacobson M, Bickel D, Burno M, Jones K, Graufelds VK, Xu G, and Pearson M et al. (2009) Selective activation of the M1 muscarinic acetylcholine receptor achieved by allosteric potentiation. *Proc Natl Acad Sci USA* **106**:15950–15955.
Maillet EL, Pellegrini N, Valant C, Bucher B, Hibert M, Bourguignon J-J, and Galzi J-L (2007) A novel, conformation-specific allosteric inhibitor of the tachykinin NK2 receptor (NK2R) with functionally selective properties. *FASEB J* **21**:2124–2134.
Marlo JE, Niswender CM, Days EL, Bridges TM, Xiang Y, Rodriguez AL, Shirey JK, Brady AE, Nalywajko T, and Luo Q et al. (2009) Discovery and characterization of novel allosteric potentiators of M1 muscarinic receptors reveals multiple modes of activity. *Mol Pharmacol* **75**:577–588.
Mary S, Damian M, Louet M, Floquet N, Fehrentz JA, Marie J, Martinez J, and Banères JL (2012) Ligands and signaling proteins govern the conformational landscape explored by a G protein-coupled receptor. *Proc Natl Acad Sci USA* **109**:8304–8309.
Mathiesen JM, Ulven T, Martini L, Gerlach LO, Heinemann A, and Kostenis E (2005) Identification of indole derivatives exclusively interfering with a G protein-independent signaling pathway of the prostaglandin D2 receptor CRTH2. *Mol Pharmacol* **68**:393–402.
Motulsky HC.A. (2004). *Fitting Models to Biological Data Using Linear and Nonlinear Regression. A Practical Guide to Curve Fitting*, Oxford University Press, New York.
Nawaratne V, Leach K, Suratman N, Loiacono RE, Felder CC, Armbruster BN, Roth BL, Sexton PM, and Christopoulos A (2008) New insights into the function of M4 muscarinic acetylcholine receptors gained using a novel allosteric modulator and a DREADD (designer receptor exclusively activated by a designer drug). *Mol Pharmacol* **74**:1119–1131.
Pei Y, Rogan SC, Yan F, and Roth BL (2008) Engineered GPCRs as tools to modulate signal transduction. *Physiology (Bethesda)* **23**:313–321.
Ray RS, Corcoran AE, Brust RD, Kim JC, Richerson GB, Nattie E, and Dymecki SM (2011) Impaired respiratory and body temperature control upon acute serotonergic neuron inhibition. *Science* **333**:637–642.
Sasaki K, Suzuki M, Mieda M, Tsujino N, Roth B, and Sakurai T (2011) Pharmacogenetic modulation of orexin neurons alters sleep/wakefulness states in mice. *PLoS ONE* **6**:e20360.
Shirey JK, Brady AE, Jones PJ, Davis AA, Bridges TM, Kennedy JP, Jadhav SB, Menon UN, Xiang Z, and Watson ML et al. (2009) A selective allosteric potentiator of the M1 muscarinic acetylcholine receptor increases activity of medial prefrontal cortical neurons and restores impairments in reversal learning. *J Neurosci* **29**:14271–14286.
Stallaert W, Christopoulos A, and Bouvier M (2011) Ligand functional selectivity and quantitative pharmacology at G protein-coupled receptors. *Expert Opin Drug Discov* **6**:811–825.
Stewart GD, Sexton PM, and Christopoulos A (2010) Prediction of functionally selective allosteric interactions at an M3 muscarinic acetylcholine receptor mutant using *Saccharomyces cerevisiae*. *Mol Pharmacol* **78**:205–214.
Vaidehi N and Kenakin T (2010) The role of conformational ensembles of seven transmembrane receptors in functional selectivity. *Curr Opin Pharmacol* **10**:775–781.
Valant C, Felder CC, Sexton PM, and Christopoulos A (2012a) Probe dependence in the allosteric modulation of a G protein-coupled receptor: implications for detection and validation of allosteric ligand effects. *Mol Pharmacol* **81**:41–52.
Valant C, Gregory KJ, Hall NE, Scammells PJ, Lew MJ, Sexton PM, and Christopoulos A (2008) A novel mechanism of G protein-coupled receptor functional selectivity. Muscarinic partial agonist McN-A-343 as a bitopic orthosteric/allosteric ligand. *J Biol Chem* **283**:29312–29321.
Valant C, Robert Lane J, Sexton PM, and Christopoulos A (2012b) The best of both worlds? Bitopic orthosteric/allosteric ligands of g protein-coupled receptors. *Annu Rev Pharmacol Toxicol* **52**:153–178.
Wess J, Duttaroy A, Zhang W, Gomeza J, Cui Y, Miyakawa T, Bymaster FP, McKinzie L, Felder CC, and Lamping KG et al. (2003) M1-M5 muscarinic receptor knockout mice as novel tools to study the physiological roles of the muscarinic cholinergic system. *Receptors Channels* **9**:279–290.

Address correspondence to: Prof. Arthur Christopoulos Drug Discovery Biology, Monash Institute of Pharmaceutical Sciences, Monash University, 399 Royal Parade, Parkville, Victoria 3052, Australia. E-mail: arthur.christopoulos@monash.edu

Molecular Pharmacology

Supplementary Information

Allosteric Modulation of a Chemogenetically Modified G Protein-Coupled Receptor

Alaa Abdul-Ridha, J. Robert Lane, Patrick M. Sexton, Meritxell Canals and Arthur Christopoulos

Drug Discovery Biology, Monash Institute of Pharmaceutical Sciences and

Department of Pharmacology, Monash University, Parkville, Victoria, 3052, Australia.

Supplementary Figure 1. Structures of compounds used in this study.

Supplementary Figure 2. Ligand binding properties at the M_1 WT and DREADD mAChRs. The equilibrium binding of the antagonist [^{3}H]QNB is inhibited by (A) xanomeline, (B) TBPB, (C) McN-A-343 (D) clozapine and (E) NDMC in membranes of FlpIn CHO cells expressing the WT M_1 mAChR (closed circles) and M_1 DREADD (open circles). All assays were performed using 0.13nM [^{3}H]QNB in the presence of 100μM GppNHp for 1h at 37°C. Data points represent the mean ± S.E. of three independent experiments performed in triplicate. Refer to Table 1 for parameters.

Supplementary Figure 3. Ligand receptor activation properties at the M_1 WT and DREADD mAChRs. Concentration- response curves of intracellular Ca^{2+} mobilization assays for (A) xanomeline, (B) TBPB, (C) McN-A-343 (D) clozapine and (E) NDMC in CHO FlpIn cells stably expressing the WT M_1 mAChR (closed circles) and M_1 DREADD (open circles) at 37°C. Data points represent the mean ± S.E. of three independent experiments performed in duplicate. Refer to Table 1 for parameters.

Supplementary Figure 4. BQCA's allosteric modulation of NDMC is analogous to that of CNO at the M_1 DREADD. Interaction between BQCA and NDMC in (A) [^{3}H]QNB binding inhibition assay, (B) intracellular Ca^{2+} mobilization, (C) ERK1/2 phosphorylation and (D) cAMP accumulation in CHO FlpIn cells stably expressing the M_1 DREADD mAChR. Data points represent the mean ± S.E. of three independent experiments performed in duplicate. Curves drawn through the points in (A) represent the best fit of an allosteric ternary complex model (Equation 1). Curves drawn through the points in (B and C) represent the best fit of an operational allosteric model (Equation 2).

Supplementary Table 1.

Operational model parameters for the allosteric interaction between NDMC and BQCA at the M_1 DREADD. Estimated parameter values represent the mean ± S.E from three experiments performed in duplicate and analysed according to equation 2. All other details are as for Table 3.

	Ca^{2+}	pERK1/2
Log τ_A	2.31±0.06	2.04±0.12
Log τ_B	0.31±0.06	0.24±0.18
	(2)	(1.7)
pK_B	4.05	
Log αβ (αβ)	0.70±0.21 (5)	1.35±0.26 (22)

Supplementary Table 2.

Operational model parameters for the allosteric interactions between BQCA and each of the ligands in the table in the Ca^{2+} mobilisation and ERK1/2 phosphorylation (pERK1/2) signalling pathways at the M_1 WT and DREADD mAChRs. Estimated parameter values represent the mean ± S.E from three experiments performed in duplicate and analysed according to equation 2. All other details are as for Table 3.

	Ca^{2+}				pERK1/2			
	WT		DREADD		WT		DREADD	
Ligand	Log τ_A	Log αβ	Log τ_A	Log αβ	Log τ_A	Log αβ	Log τ_A	Log αβ
ACh	4.78±0.10	4.10±0.20	1.31±0.11	2.92±0.14	4.71±0.07	3.84±0.17	1.53±0.05	2.40±0.07
Xanomeline	2.05±0.04	2.94±0.43	0.86±0.03	0.17±0.16	1.36±0.13	1.20±0.18	0.12±0.3	0.13±0.50
TBPB	1.62±0.05	2.98±0.32	0.91±0.04	0.12±0.37	0.72±0.10	2.75±0.31	0.28±0.04	0.18±0.07
McN-A-343	2.91±0.03	3.25±0.50	1.38±0.15	1.65±0.27	3.01±0.16	3.32±0.41	1.30±0.09	1.42±0.13
CNO	0.78±0.04	-0.22±0.60	2.81±0.04	0.30±0.29	0.44±0.07	-0.23±0.49	2.65±0.10	1.61±0.22
Clozapine	-1.5±0.31	-1.34±0.9	1.24±0.06	0.16±0.52	-0.37±0.10	-1.00±0.90	1.75±0.01	-0.24±0.32
NDMC	1.15±0.07	2.86±0.68	2.31±0.06	0.70±0.21	1.57±0.06	3.33±0.22	2.04±0.12	1.35±0.26

4

Supplementary Figure 1

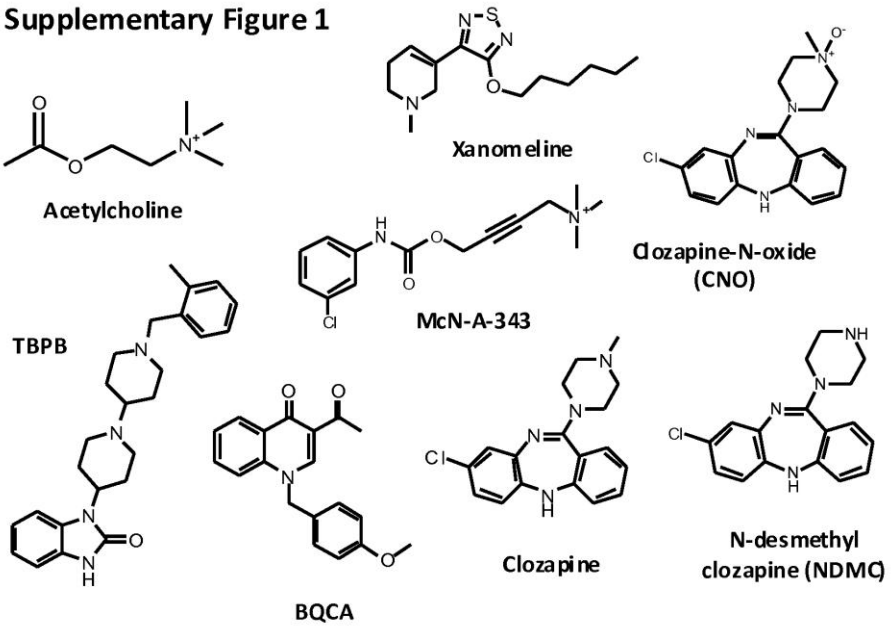

5

Supplementary Figure 2

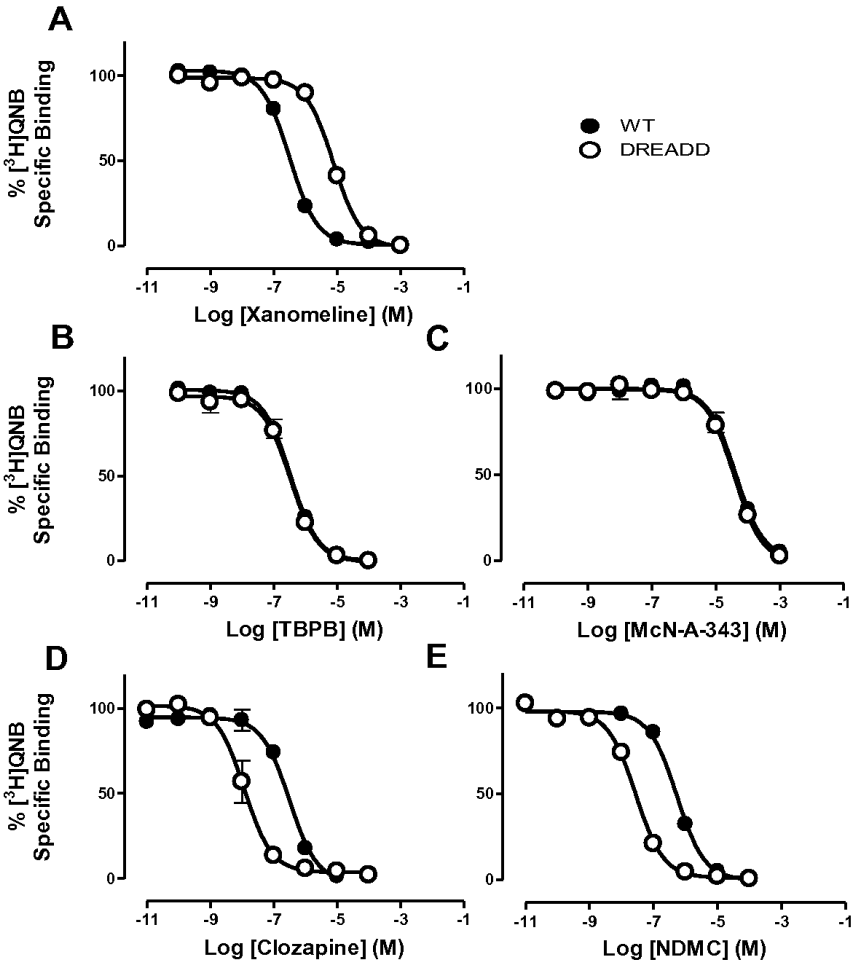

6

Supplementary Figure 3

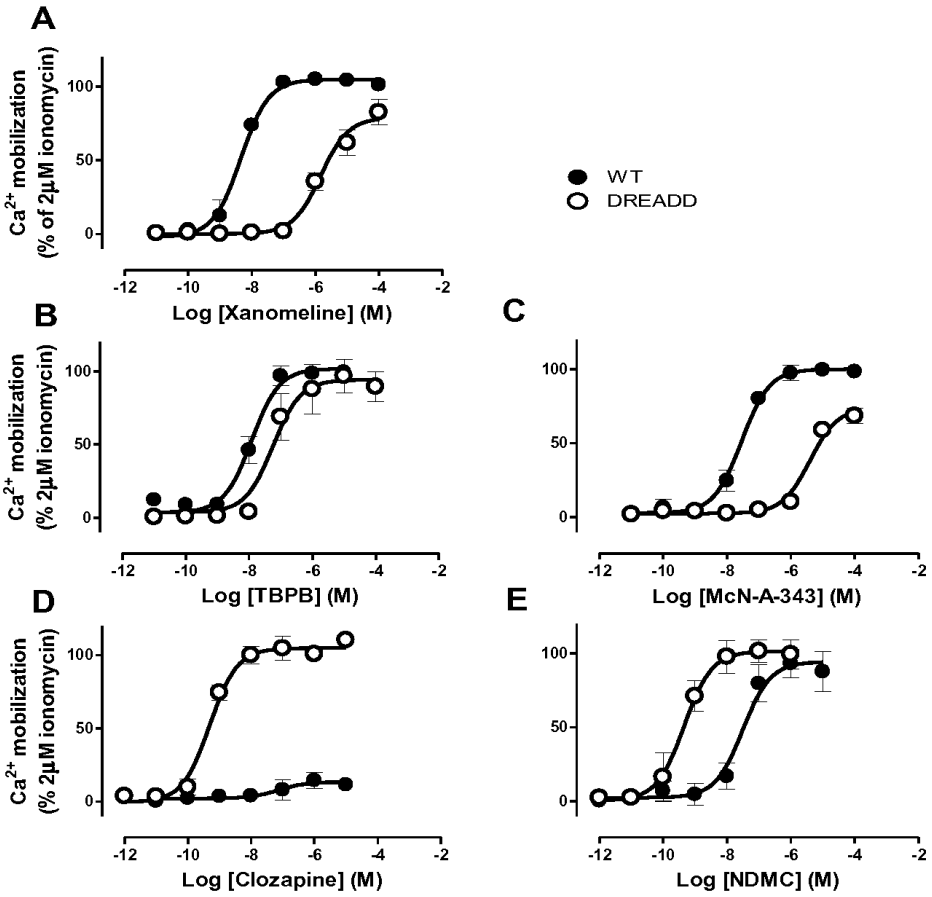

7

Supplementary figure 4

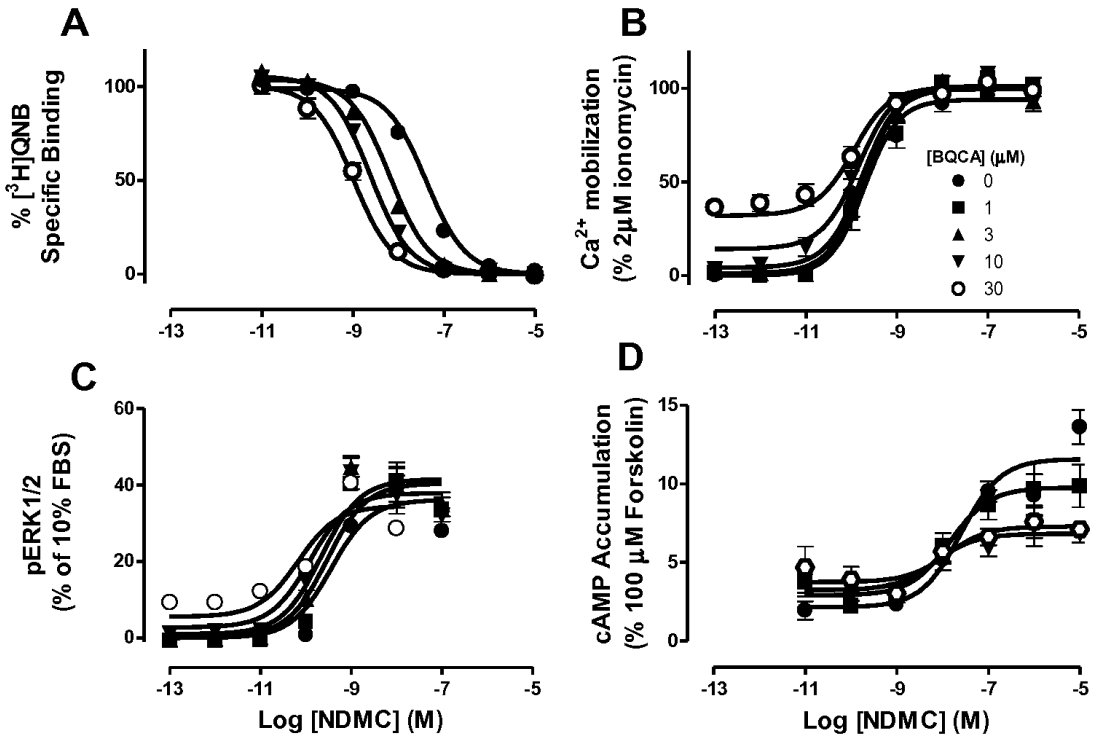

8

CHAPTER 3

Molecular Determinants of Allosteric Modulation at the M_1 Muscarinic Acetylcholine Receptor

Alaa Abdul-Ridha, Laura López, Peter Keov, David M. Thal, Shailesh N. Mistry, Patrick M. Sexton, J. Robert Lane, Meritxell Canals, and Arthur Christopoulos

J. Biol. Chem **289**: 6067-6079, February 2014.

Monash University

Declaration for Thesis Chapter 3

Declaration by candidate

In the case of Chapter 3, the nature and extent of my contribution to the work was the following:

Nature of contribution	**Extent of contribution (%)**
Development of ideas, participated in research design, conducted experiments, performed data analysis, contributed to the writing and editing of the manuscript.	80%

The following co-authors contributed to the work. If co-authors are students at Monash University, the extent of their contribution in percentage terms must be stated:

Name	**Nature of contribution**
Laura López	Performed molecular modelling studies, contributed to the writing and of the manuscript
Peter Keov	Generated some of the mutant receptors (2%)
David M. Thal	Conducted some of the early radioligand binding experiments
Shailesh N. Mistry	Contributed to manuscript preparation
Patrick M. Sexton	Contributed to manuscript preparation
J. Robert Lane	Participated in research design, performed data analysis, contributed to manuscript preparation
Meritxell Canals	Development of ideas, participated in research design, performed data analysis, contributed to manuscript preparation
Arthur Christopoulos	Participated in research design, performed data analysis, contributed to manuscript preparation

The undersigned hereby certify that the above declaration correctly reflects the nature and extent of the candidate's and co-authors' contributions to this work.

Candidate's Signature		**Date**
Main Supervisor's Signature		**Date**

Signal Transduction:

Molecular Determinants of Allosteric Modulation at the M_1 Muscarinic Acetylcholine Receptor

Alaa Abdul-Ridha, Laura López, Peter Keov, David M. Thal, Shailesh N. Mistry, Patrick M. Sexton, J. Robert Lane, Meritxell Canals and Arthur Christopoulos

J. Biol. Chem. 2014, 289:6067-6079.
doi: 10.1074/jbc.M113.539080 originally published online January 17, 2014

THE JOURNAL OF BIOLOGICAL CHEMISTRY VOL. 289, NO. 9, pp. 6067–6079, February 28, 2014

Molecular Determinants of Allosteric Modulation at the M_1 Muscarinic Acetylcholine Receptor*

Received for publication, December 2, 2013, and in revised form, January 16, 2014 Published, JBC Papers in Press, January 17, 2014, DOI 10.1074/jbc.M113.539080

Alaa Abdul-Ridha[‡1], **Laura López**[‡], **Peter Keov**[‡], **David M. Thal**[‡], **Shailesh N. Mistry**[§], **Patrick M. Sexton**[‡2], **J. Robert Lane**[‡], **Meritxell Canals**[‡3], **and Arthur Christopoulos**[‡2,4]

From [‡]*Drug Discovery Biology and* [§]*Medicinal Chemistry, Monash Institute of Pharmaceutical Sciences and Department of Pharmacology, Monash University, Parkville, Victoria 3052, Australia*

Background: BQCA is a selective allosteric modulator of the M_1 mAChR.
Results: Residues that govern BQCA activity were identified using mutagenesis and molecular modeling.
Conclusion: BQCA likely occupies a pocket overlapping prototypical mAChR modulators and gains selectivity through cooperativity with orthosteric ligands.
Significance: Understanding the structural basis of BQCA function can provide insight into the design of more tailored allosteric ligands.

Benzylquinolone carboxylic acid (BQCA) is an unprecedented example of a selective positive allosteric modulator of acetylcholine at the M_1 muscarinic acetylcholine receptor (mAChR). To probe the structural basis underlying its selectivity, we utilized site-directed mutagenesis, analytical modeling, and molecular dynamics to delineate regions of the M_1 mAChR that govern modulator binding and transmission of cooperativity. We identified Tyr-85$^{2.64}$ in transmembrane domain 2 (TMII), Tyr-179 and Phe-182 in the second extracellular loop (ECL2), and Glu-397$^{7.32}$ and Trp-400$^{7.35}$ in TMVII as residues that contribute to the BQCA binding pocket at the M_1 mAChR, as well as to the transmission of cooperativity with the orthosteric agonist carbachol. As such, the BQCA binding pocket partially overlaps with the previously described "common" allosteric site in the extracellular vestibule of the M_1 mAChR, suggesting that its high subtype selectivity derives from either additional contacts outside this region or through a subtype-specific cooperativity mechanism. Mutation of amino acid residues that form the orthosteric binding pocket caused a loss of carbachol response that could be rescued by BQCA. Two of these residues (Leu-102$^{3.29}$ and Asp-105$^{3.32}$) were also identified as indirect contributors to the binding affinity of the modulator. This new insight into the structural basis of binding and function of BQCA can guide the design of new allosteric ligands with tailored pharmacological properties.

* This work was supported in part by National Health and Medical Research Council of Australia Program Grant 519461 (to A. C. and P. M. S.), Project Grant APP1011796 (to M. C.), and Grant APP1011920 (to J. R. L.) and computational studies were supported by Resource Allocation Scheme Grant VR0024 from the Victorian Life Sciences Computation Initiative, Peak Computing Facility, University of Melbourne.
[1] Recipient of an Australian Postgraduate Award scholarship.
[2] Principal Research Fellows of the National Health and Medical Research Council of Australia.
[3] To whom correspondence may be addressed: Drug Discovery Biology, Monash Institute of Pharmaceutical Sciences, Monash University, 399 Royal Parade, Parkville, Victoria 3052, Australia. [redacted]
[4] To whom correspondence may be addressed: Drug Discovery Biology, Monash Institute of Pharmaceutical Sciences, Monash University, 399 Royal Parade, Parkville, Victoria 3052, Australia. [redacted]

G protein-coupled receptors (GPCRs)[5] mediate a multitude of biological functions in response to a variety of ligands, including hormones and neurotransmitters, and play essential roles in all physiological processes (1). As such, GPCRs are important therapeutic targets for numerous diseases (2). Given such importance, an understanding of the structural basis underlying ligand binding and activation of GPCRs is essential to design more effective therapies (3). The recent surge in high resolution family A GPCR crystal structures (4) has provided new insights into the structural and functional diversity of this protein family. This knowledge, combined with information from computational, biochemical, and mutagenesis studies, has not only mapped out the location of orthosteric binding pockets but is starting to unravel the molecular changes that occur upon receptor activation and the mechanisms by which different ligands stabilize distinct conformational states (5, 6).

The M_1 mAChR is a family A GPCR and is one of five mAChR subtypes for which acetylcholine (ACh) is the endogenous orthosteric agonist. The ACh binding pocket is formed by amino acids that are conserved across all five mAChR subtypes and shares structural homology with other functionally unrelated acetylcholine-binding proteins from different species (7). Along with the M_4 mAChR, the M_1 mAChR is an attractive therapeutic target for the treatment of diseases in which cognition is impaired, such as Alzheimer disease and schizophrenia (8). However, because of the highly homologous ACh binding pocket across subtypes, it has been challenging to develop drugs that are sufficiently subtype-selective to avoid undesired activity at other mAChRs. This has spurred intensive efforts to discover allosteric ligands that act at topographically distinct regions on these receptors (9) with more potential to confer subtype selectivity. Despite the wealth of information obtained from GPCR crystal structures, challenges remain in understanding the mode of binding and action of such small molecule

[5] The abbreviations used are: GPCR, G protein-coupled receptor; BQCA, benzylquinolone carboxylic acid; ACh, acetylcholine; mAChR, muscarinic acetylcholine receptor; CCh, carbachol; QNB, quinuclidinyl benzilate; NMS, *N*-methylscopolamine; IP_1, myoinositol 1-phosphate; TM, transmembrane domain; ECL, extracellular loop; MD, molecular dynamics.

allosteric modulators (9). High resolution structures of family A GPCRs bound to allosteric modulators are only starting to be solved (10), and even then the dynamic mechanisms contributing to modulator binding, receptor activation, and transmission of cooperativity between orthosteric and allosteric sites cannot be readily captured in a single structure.

The conserved ACh-binding site in mAChRs is located in the top third of the transmembrane helical bundle of the receptor with ACh contacting inward-facing residues in ECL2 and TMIII–VII (7, 11). In particular, TMIII contains a number of residues that have been implicated in both binding and activation mechanisms of the mAChRs and plays a central role as a structural and functional hub of many GPCRs (1). Accumulated evidence also points toward the existence of a "common" allosteric binding pocket utilized by structurally diverse mAChR allosteric modulators (12–14). This site is located within an extracellular "vestibule" and includes residues from both ECL2 and the extracellular regions of TMII and -VII (12, 13). Interestingly, we recently demonstrated that LY2033298, an allosteric modulator originally described as being a "selective" positive allosteric modulator for ACh at the M_4 mAChR, can also occupy this conserved allosteric pocket at the M_2 mAChR, where it exerts cooperative behavior with alternative orthosteric agonists, such as oxotremorine M, but not with ACh (14). Such probe dependence highlights the fact that selectivity of allosteric agents can actually be attained through two mechanisms, namely the differences in the allosteric site between receptor subtypes or the differences in cooperativity upon binding to a common allosteric site.

With regard to the M_1 mAChR, several selective ligands have been discovered in the past few years (15). Among these, benzylquinolone carboxylic acid (BQCA) is a novel example of a highly selective positive allosteric modulator of ACh binding and function at the M_1 mAChR, displaying very low affinity but a remarkably high cooperativity with ACh (16–18). The unprecedented subtype selectivity of BQCA thus suggests two potential scenarios as follows: (i) that BQCA binds to a completely different site than other mAChR allosteric modulators or (ii) that BQCA achieves subtype-selective cooperativity upon interaction with a conserved or overlapping allosteric site. In this study, we aimed to resolve this issue by site-directed mutagenesis of residues previously shown to be important for orthosteric, allosteric, or bitopic (dual orthosteric-allosteric) ligand binding at either the M_1 mAChR or other mAChR family subtypes. Importantly, we also applied an analytical approach, based on the operational model of agonism (19, 20), to elucidate the effects of the introduced mutations on ligand binding *versus* signaling *versus* transmission of cooperativity. By doing so, we present new evidence for differential effects of distinct receptor regions on each of these molecular properties at the M_1 mAChR.

EXPERIMENTAL PROCEDURES

Materials—Chinese hamster ovary (CHO) FlpIn cells and Dulbecco's modified Eagle's medium (DMEM) were purchased from Invitrogen. Fetal bovine serum (FBS) was purchased from ThermoTrace (Melbourne, Australia). Hygromycin-B was purchased from Roche Applied Science. [^{3}H]Quinuclidinyl benzilate ([^{3}H]QNB; specific activity, 50 Ci/mmol), *N*-[^{3}H]methylscopolamine ([^{3}H]NMS); specific activity, 85 Ci/mmol), and MicroScint scintillation liquid were purchased from PerkinElmer Life Sciences. IP-One assay kit and reagents were purchased from Cisbio (Codolet, France). All other chemicals were purchased from Sigma. BQCA was synthesized in-house at the Monash Institute of Pharmaceutical Sciences.

Cell Culture and Receptor Mutagenesis—Mutations of the c-Myc-hM_1 mAChR sequence were generated using the QuikChange site-directed mutagenesis kit (Agilent Technologies, La Jolla, CA). All mutations were confirmed by DNA sequencing (AGRF, Australia). Mutant c-Myc-hM_1 mAChR DNA constructs were transfected into FlpIn CHO cells (Invitrogen) and selected using 0.2 mg/ml hygromycin for stable expression.

Whole Cell Radioligand Binding Assays—To facilitate a more direct comparison between parameters derived from the analysis of cell-based functional assays (see below), radioligand binding experiments were performed on whole cells rather than membrane preparations. Saturation binding assays were performed using cells plated at 10^4 cells per well in 96-well Isoplates (PerkinElmer Life Sciences). The following day cells were incubated with the orthosteric antagonists [^{3}H]QNB or [^{3}H]NMS in a final volume of 100 μl of HEPES buffer (10 mM HEPES, 145 mM NaCl, 1 mM $MgSO_4 \cdot 7H_2O$, 10 mM glucose, 5 mM KCl, 2 mM $CaCl_2$, 1.5 mM $NaHCO_3$, pH 7.4) for 2 h at room temperature. For competition binding assays, cells were plated at 2.5×10^4 cells per well. The following day, cells were incubated in a final volume of 100 μl of HEPES buffer containing increasing concentrations of the competing cold ligand CCh (in the absence or presence of increasing concentrations of BQCA) for 4 h at 4 °C (to avoid potential confounding effects of competing agonist ligands on receptor internalization while ensuring reactions reach equilibrium) in the presence of 0.3 nM [^{3}H]QNB or [^{3}H]NMS. Nonspecific binding was defined in the presence of 100 μM atropine. For all experiments, termination of the assay was performed by rapid removal of radioligand followed by two 100-μl washes with ice-cold 0.9% NaCl buffer. Radioactivity was determined by addition of 100 μl of Microscint scintillation liquid (PerkinElmer Life Sciences) to each well and counting in a MicroBeta plate reader (PerkinElmer Life Sciences).

IP-One Accumulation Assays—The IP-One assay kit (Cisbio, France) was used for the direct quantitative measurement of myoinositol 1-phosphate (IP_1) in FlpIn CHO cells stably expressing either WT or mutant hM_1 mAChRs. This is a competitive immunoassay that measures the homogeneous time-resolved fluorescence signal transferred between a cryptate-labeled IP_1-specific monoclonal antibody and d_2-labeled IP_1. The fluorescence signal measured is inversely proportional to the concentration of native IP_1.

Briefly, cells were seeded into 384-well proxy-plates at 7,500 cells per well and allowed to grow overnight at 37 °C, 5% CO_2. The following day, cells were stimulated with CCh in IP_1 stimulation buffer (HEPES 10 mM, $CaCl_2$ 1 mM, $MgCl_2$ 0.5 mM, KCl 4.2 mM, NaCl 146 mM, glucose 5.5 mM, LiCl 50 mM, pH 7.4) in the absence or presence of increasing concentrations of BQCA and incubated for 1 h at 37 °C, 5% CO_2. Cells were lysed by the

addition of homogeneous time-resolved fluorescence reagents, the cryptate-labeled anti-IP_1 antibody, and the d_2-labeled IP_1 analog prepared in lysis buffer, followed by incubation for 1 h at room temperature. The emission signals were measured at 590 and 665 nm after excitation at 340 nm using the Envision multilabel plate reader (PerkinElmer Life Sciences), and the signal was expressed as the homogeneous time-resolved fluorescence ratio: $F = ((\text{fluorescence}_{665\text{ nm}}/\text{fluorescence}_{590\text{ nm}}) \times 10^4)$. Experiments using WT M_1 mAChR CHO FlpIn cells were performed in parallel each day.

Computational Methods for the Model of the Ligand-Receptor Complex—The sequence of the hM_1 mAChR was retrieved from the Swiss-Prot database. ClustalX software (21) was used to align the hM_1 mAChR sequence with the crystal structure of the nanobody-stabilized active state of the human β_2 adrenoreceptor (Protein Data Bank code 3P0G) (22). Ballesteros-Weinstein numbering was used for residues in the TMs (23).

The structural model of the receptor was built using the Modeler Version 9.12 suite of programs (24), which yielded 10 candidate models. The conserved disulfide bonds between residues Cys-$98^{3.25}$ at the top of TMIII and the cysteine in the middle of the ECL2 as well as the one between Cys-$391^{6.61}$ and Cys-$394^{7.29}$ in ECL3 present in the template structure were also built and maintained as a constraint for geometric optimization. The best structure was selected from these candidates, according to the Modeler Discrete Optimized Protein Energy (DOPE) assessment score and visual inspection. The resulting receptor structure was optimized using the Duan *et al.* (25) force field and the general Amber force field, and HF/6–31G*-derived restrained electrostatic potential atomic charges were used for the ligands (26).

Docking of the ligands was performed with MOE (Molecular Operating Environment, Chemical Computing Group, Inc.). CCh was docked manually into the receptor model with the protonated nitrogen interacting with $Asp^{3.32}$ and the carbamate group situated toward TMVI resembling the position of the ligands described in the mAChR crystal structures (Protein Data Bank code 3UON (7) and Protein Data Bank code 4DAJ (11)). The allosteric binding site of BQCA was generated using the Alpha site finder. Dummy atoms were created from the obtained α spheres. BQCA docking was carried out using the Induced Fit protocol, with Alpha PMI placement and Affinity dG rescoring. One main BQCA pose was obtained at an allosteric site comprising residues from ECL2, ECL3, TMII, and TMVII at the extracellular surface of the M_1 mAChR. The lowest energy conformation of this pose was selected and subjected to an energy minimization using MMFF94X force field. Molecular dynamics (MD) simulations of the final complex was performed with NAMD2.9 (27) package using the protocol described previously (28).

Data Analysis—All data were analyzed using Prism 6.01 (GraphPad Software, San Diego). Inhibition binding curves between [^{3}H]QNB or [^{3}H]NMS and unlabeled ligands were fitted to a one-site binding model (29). Binding interaction studies with allosteric ligands were fitted to the following allosteric ternary complex model, Equation 1 (30),

$$Y = \frac{B_{max}[A]}{[A] + \left(\frac{K_A K_B}{\alpha'[B] + K_B}\right)\left(1 + \frac{[I]}{K_I} + \frac{[B]}{K_B} + \frac{\alpha[I][B]}{K_I K_B}\right)} \quad \text{(Eq. 1)}$$

where Y is percentage (vehicle control) binding; B_{max} is the total number of receptors; $[A]$, $[B]$, and $[I]$ are the concentrations of radioligand, allosteric modulator, and the orthosteric ligand, respectively; K_A, K_B, and K_I are the equilibrium dissociation constants of the radioligand, allosteric modulator, and orthosteric ligand, respectively. α' and α are the binding cooperativities between the allosteric modulator and radioligand and the allosteric ligand and orthosteric ligand, respectively. Values of α (or α') >1 denote positive cooperativity; values <1 (but >0) denote negative cooperativity, and values $= 1$ denote neutral cooperativity.

Concentration-response curves for the interaction between the allosteric ligand and the orthosteric ligand in the various functional signaling assays were globally fitted to the following operational model of allosterism and agonism, Equation 2 (20),

$$E = \frac{E_m(\tau_A[A](K_B + \alpha\beta[B]) + \tau_B[B]K_A)^n}{([A]K_B + K_A K_B + [B]K_A + \alpha[A][B])^n + (\tau_A[A](K_B + \alpha\beta[B]) + \tau_B[B]K_A)^n} \quad \text{(Eq. 2)}$$

where E_m is the maximum possible cellular response; $[A]$ and $[B]$ are the concentrations of orthosteric and allosteric ligands, respectively; K_A and K_B are the equilibrium dissociation constant of the orthosteric and allosteric ligands, respectively; τ_A and τ_B are operational measures of orthosteric and allosteric ligand efficacy, respectively; α is the binding cooperativity parameter between the orthosteric and allosteric ligand, and β denotes the magnitude of the allosteric effect of the modulator on the efficacy of the orthosteric agonist. In many instances, the individual model parameters of Equation 2 could not be directly estimated via the nonlinear regression algorithm by analysis of the functional data alone, due to parameter redundancy. To facilitate model convergence, we therefore fixed the equilibrium dissociation constant of each ligand to that determined from the whole cell binding assays. This practice assumes that the affinity determined in the whole cell binding assays is not significantly different from the "functional" affinity operative at the level of the signaling assay, which may not always be the case (31), and thus may lead to a systematic error in the estimate of the operational efficacy parameter, τ. However, because only a single pathway (IP_1) is being considered, the *relative* differences between τ values remain valid for statistical comparison purposes.

All affinity, potency, and cooperativity values were estimated as logarithms (32), and statistical comparisons between values were by one-way analysis of variance using a Dunnett's multiple comparison post test to determine significant differences between mutant receptors and the WT M_1 mAChR. A value of $p < 0.05$ was considered statistically significant.

RESULTS

To identify the location of the binding pocket of BQCA and to gain insight into its molecular mechanism of allosteric modulation at the M_1 mAChR, residues from distinct locations

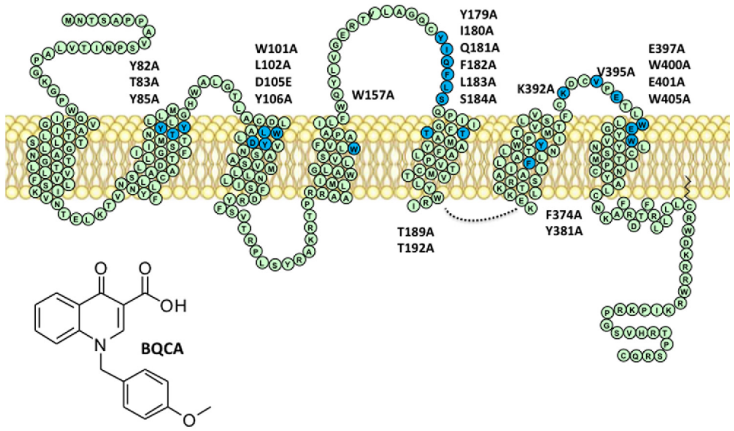

FIGURE 1. **Mutations and ligands investigated in this study.** A *snake* diagram of the human M_1 mAChR highlighting mutated residues and chemical structure of the allosteric modulator BQCA.

within the receptor were mutated to alanine (Fig. 1). This includes residues previously shown to be important for orthosteric, allosteric, or bitopic ligand binding at either the M_1 or other mAChR subtypes (18, 33–35).

Effects of Amino Acid Substitutions on the Binding of Orthosteric Ligands at the M_1 mAChR—Whole cell [^{3}H]NMS saturation binding experiments showed that the majority of the mutations led to a significant reduction in cell surface receptor expression compared with the WT (Table 1). The maximum decrease in receptor expression relative to WT was 3-fold at F374$^{6.44}$A. In agreement with previous reports (36, 37), no [^{3}H]NMS binding was detected when residues Tyr-106$^{3.33}$, Trp-157$^{4.57}$, Tyr-381$^{6.51}$, or Val-395 were mutated to alanine. For these mutant receptors, [^{3}H]QNB was used as the alternative radioligand.

In addition to receptor expression, the equilibrium dissociation constant of orthosteric antagonists [^{3}H]NMS or [^{3}H]QNB (pK_A) or the orthosteric agonist CCh (pK_I) were significantly altered for a large number of mutants (Fig. 2 and Tables 1 and 2). Most notably, and in agreement with previous studies (33, 37, 38), alanine mutation of the TMII residues Tyr-82$^{2.61}$ or Tyr-85$^{2.64}$, and the conserved orthosteric site residues Trp-101$^{3.28}$, Leu-102$^{3.29}$, Asp-105$^{3.32}$, Tyr-106$^{3.33}$, Trp-157$^{4.57}$, Thr-189$^{5.39}$, or Thr-192$^{5.42}$ caused significant reduction in the equilibrium dissociation constants of both CCh and the radiolabeled antagonist used (Fig. 2 and Tables 1 and 2). Mutation of Leu-183 in ECL2 or Val-395 in ECL3 also led to significant decreases in the affinities of both ligands. Consistent with previous findings showing that the Tyr-381$^{6.51}$ residue is able to discriminate between different mAChR antagonists (39, 40), we found that Y381$^{6.51}$A completely abolished [^{3}H]NMS binding, although it showed unaltered affinity for [^{3}H]QNB. Several mutations showed differential effects between the binding of the radioligand and CCh. F182A and E397$^{7.32}$A caused significant reduction in [^{3}H]NMS affinity but had no effect upon the affinity of CCh, whereas I180A and W400$^{7.35}$A only decreased CCh affinity. Mutation of the highly conserved aromatic residues Phe-374$^{6.44}$ and Trp-405$^{7.40}$ as well as the ECL2 residue Gln-181 resulted in substantially enhanced CCh binding affinity, with F374$^{6.44}$A also displaying reduced [^{3}H]NMS binding. Mutation of Phe-374$^{6.44}$ and Trp-405$^{7.40}$ to alanine has been previously shown to cause constitutive receptor activity, which is likely to account for the increase in CCh affinity (38, 40–43). Alanine substitution of Tyr-179, Ser-184$^{5.32}$, Lys-392, and Glu-401$^{7.36}$ did not impact the affinity of either agonist or antagonist. Overall, the change in pK_A of the radiolabeled antagonists tracks with changes in CCh pK_I for the majority of mutations

TABLE 1
Whole cell equilibrium saturation binding parameters for WT and mutant M_1 mAChRs

Values represent the mean ± S.E. from 2 to 5 separate experiments performed in duplicate. B_{max} is the maximum density of binding sites per 10^6 cells in counts/min. pK_A is the negative logarithm of the radioligand equilibrium dissociation constant.

	B_{max}	pK_A
M_1 WT [^{3}H]NMS	300 ± 10	10.04 ± 0.01
M_1 WT [^{3}H]QNB	290 ± 13	9.85 ± 0.03
Y82$^{2.61}$A	225 ± 7	9.76 ± 0.01[a]
T83$^{2.62}$A	302 ± 5	9.95 ± 0.05
Y85$^{2.64}$A	398 ± 10	9.82 ± 0.03[a]
W101$^{3.28}$A	177 ± 1[a]	9.36 ± 0.06[a]
L102$^{3.29}$A	147 ± 12[a]	9.40 ± 0.05[a]
D105$^{3.32}$E	195 ± 12[a]	9.17 ± 0.07[a]
Y106$^{3.33}$A[b]	220 ± 10	9.15 ± 0.20[a]
W157$^{4.57}$A[b]	300 ± 8	9.32 ± 0.09[a]
Y179A	270 ± 14	10.00 ± 0.02
I180A	186 ± 6[a]	9.95 ± 0.03
Q181A	276 ± 8	9.92 ± 0.08
F182A	255 ± 7	9.52 ± 0.05[a]
L183A	300 ± 23	9.31 ± 0.05[a]
S184$^{5.32}$A	246 ± 9[a]	10.04 ± 0.02
T189$^{5.39}$A	390 ± 13[a]	9.56 ± 0.08[a]
T192$^{5.42}$A	402 ± 12[a]	9.76 ± 0.05[a]
F374$^{6.44}$A	90 ± 8[a]	9.29 ± 0.12[a]
Y381$^{6.51}$A[b]	174 ± 15[a]	9.82 ± 0.02
K392A	231 ± 7	9.88 ± 0.09
V395A[b]	315 ± 24	9.30 ± 0.06[a]
E397$^{7.32}$A	237 ± 8[a]	9.82 ± 0.02[a]
W400$^{7.35}$A	138 ± 6[a]	9.95 ± 0.01
E401$^{7.36}$A	236 ± 18[a]	9.97 ± 0.05
W405$^{7.40}$A	189 ± 10[a]	9.95 ± 0.02

[a] Data are significantly different ($p < 0.05$) from WT value as determined by one-way analysis of variance with Dunnett's post hoc test.
[b] Experiments and statistical comparisons are relative to WT [^{3}H]QNB values.

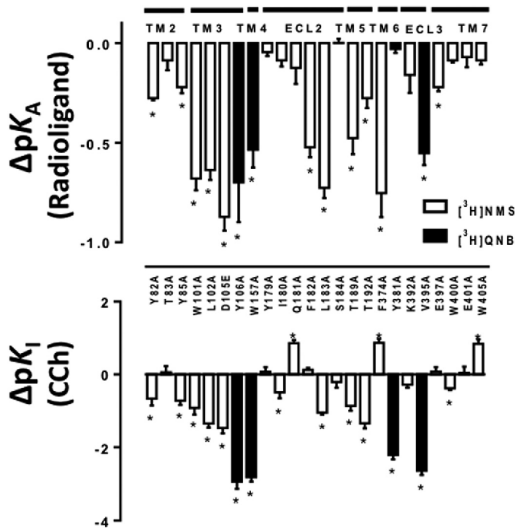

FIGURE 2. **Orthosteric agonist affinity estimates are differentially modified by M_1 mAChR mutations.** *Bars* represent the difference in pK_A of orthosteric antagonist [^{3}H]NMS or [^{3}H]QNB (*top panel*) derived from whole cell saturation binding experiments (Table 1) or the difference in pK_I of the orthosteric agonist CCh (*bottom panel*) derived from whole cell competition binding experiments (Table 2), relative to the WT receptor value for each ligand at each mutant residue. Data represent the mean ± S.E. of three experiments performed in duplicate. *, significantly different from WT, $p < 0.05$, one-way analysis of variance, Dunnett's post hoc test.

TABLE 2

Whole cell equilibrium competition binding parameters for the interaction between [^{3}H]NMS or [^{3}H]QNB, CCh, and BQCA at the WT and mutant M_1 mAChRs

Estimated parameter values represent the mean ± S.E. of 3–4 experiments performed in duplicate and analyzed according to Equation 1.

	CCh pK_I[a]	BQCA pK_B[b]	log α[c]
M_1 WT [^{3}H]NMS	4.56 ± 0.05	4.49 ± 0.09	2.64 ± 0.12
M_1 WT [^{3}H]QNB	4.67 ± 0.20	4.18 ± 0.18	2.31 ± 0.36
$Y82^{2.61}$A	3.89 ± 0.10[d]	4.70 ± 0.08	2.53 ± 0.14
$T83^{2.62}$A	4.62 ± 0.12	4.39 ± 0.18	2.52 ± 0.24
$Y85^{2.64}$A	3.84 ± 0.08[d]	4.32 ± 0.10	2.29 ± 0.13
$W101^{3.28}$A	3.64 ± 0.10[d]	4.38 ± 0.06	2.43 ± 0.11
$L102^{3.29}$A	3.21 ± 0.06[d]	4.12 ± 0.10[d]	2.19 ± 0.12
$D105^{3.32}$E	3.09 ± 0.08[d]	3.79 ± 0.07[d]	1.61 ± 0.1[d]
$Y106^{3.33}$A[e]	1.73 ± 0.10[d]	ND[f]	ND
$W157^{4.57}$A[e]	1.85 ± 0.06[d]	ND	ND
Y179A	4.63 ± 0.07	4.55 ± 0.11	0.52 ± 0.20[d]
I180A	4.07 ± 0.08[d]	5.03 ± 0.08[d]	2.49 ± 0.13
Q181A	5.42 ± 0.05[d]	5.12 ± 0.07[d]	1.79 ± 0.1[d]
F182A	4.68 ± 0.03	4.41 ± 0.07	1.79 ± 0.12[d]
L183A	3.51 ± 0.03[d]	4.23 ± 0.05	2.32 ± 0.08
$S184^{5.32}$A	4.35 ± 0.09	4.70 ± 0.1	2.27 ± 0.15
$T189^{5.39}$A	3.69 ± 0.07[d]	4.68 ± 0.04	1.73 ± 0.11[d]
$T192^{5.42}$A	3.22 ± 0.08[d]	4.06 ± 0.13	2.18 ± 0.15
$F374^{6.44}$A	5.43 ± 0.08[d]	5.38 ± 0.06[d]	1.57 ± 0.15[d]
$Y381^{6.51}$A[e]	2.46 ± 0.06[d]	ND	ND
$K392^{6.62}$A	4.28 ± 0.05	4.40 ± 0.09	2.80 ± 0.12
$V395^{7.30}$A[e]	2.03 ± 0.06[d]	4.31 ± 0.06	1.02 ± 0.25[d]
$E397^{7.32}$A	4.64 ± 0.07	4.66 ± 0.07	1.79 ± 0.13[d]
$W400^{7.35}$A	4.18 ± 0.02[d]	ND	ND
$E401^{7.36}$A	4.60 ± 0.12	4.72 ± 0.08	1.74 ± 0.14[d]
$W405^{7.40}$A	5.40 ± 0.07[d]	5.70 ± 0.05[d]	1.59 ± 0.12[d]

[a] Negative logarithm of the equilibrium dissociation constant of CCh.
[b] Negative logarithm of the equilibrium dissociation constant of BQCA as estimated from Equation 1.
[c] Logarithm of the binding cooperativity factor between BQCA and CCh as estimated from Equation 1; for this analysis, the pK_A of the radiolabeled antagonist for the WT and each of the mutant receptors was constrained to the values listed in Table 1. The cooperativity between BQCA and the radioligand was constrained to −2, consistent with high negative cooperativity between the two ligands.
[d] Data are significantly different ($p < 0.05$) from WT values as determined by one-way analysis of varianc with Dunnett's post hoc test.
[e] Experiments and statistical comparisons are relative to WT [^{3}H]QNB values.
[f] ND means not determined (no modulation of affinity).

tested (Fig. 2). Those that showed the most divergent effects include $Y381^{6.51}$A in the orthosteric pocket, causing a marked decrease in CCh affinity but not that of [^{3}H]QNB and Q181A, $F374^{6.44}$A, and $W405^{7.40}$A that caused an increased affinity for CCh.

Effect of Amino Acid Substitution on BQCA Affinity and on the Transmission of Binding Cooperativity with CCh at the M_1 mAChR—The orthosteric binding pocket is formed by amino acids that are fully conserved across all five mAChR subtypes (7). However, although the importance of these residues for orthosteric ligand binding has been demonstrated in numerous studies and confirmed in our results, less is known about the role of these residues in the actions of allosteric ligands. Mutation of $Trp^{3.28}$ at the M_2 and M_4 mAChRs led to a significant reduction in affinity of the allosteric modulator LY2033298 and its binding cooperativity with ACh (14, 33). To determine whether BQCA behaves in a similar manner to LY2033298 at the equivalent residue in the M_1 mAChR, we performed equilibrium binding studies for the interaction between CCh and BQCA at $W101^{3.28}$A, as well as at other orthosteric pocket residues. An allosteric ternary complex model (Equation 1) was applied to the data to obtain estimates of BQCA affinity at each mutant (pK_B), and its binding cooperativity with CCh (log α) (representative examples of the analysis for different constructs are shown in Fig. 3, and all results are summarized in Fig. 4).

We found that the cooperativity of BQCA with CCh at $W101^{3.28}$A, $L102^{3.29}$A, or $T192^{5.42}$A was not significantly different when compared with the WT receptor estimates (Fig. 4 and Table 2). Although these residues do not form direct contacts with orthosteric ligands, they have been described to constitute a "second shell" that stabilizes the primary binding pocket (3, 44). Interestingly, mutation of orthosteric binding site residues substantially affected the ability of BQCA to modulate CCh affinity; binding cooperativity with CCh was completely abolished at $Y106^{3.33}$A, $W157^{4.57}$A, and $Y381^{6.51}$A and was significantly reduced at $D105^{3.32}$E and $T189^{5.39}$A (Figs. 3*D* and 4 and Table 2). In addition, V395A, which displayed a reduction in affinity for [^{3}H]QNB and CCh similar to that of orthosteric site residues, also caused a significant reduction in binding cooperativity between BQCA and CCh (Table 2 and Fig. 4 (*bottom panel*)). No pK_B estimates for BQCA could be derived from the analysis of the binding interaction data of $Y106^{3.33}$A, $W157^{4.57}$A, or $Y381^{6.51}$A due to the lack of allosteric modulation. The pK_B of BQCA was significantly lower than WT at $L102^{3.29}$A and $D105^{3.32}$E but was unchanged at the remaining orthosteric site mutations (Fig. 4 (*top panel*) and Table 2). These results suggest that residues that form direct contacts with the orthosteric ligand (7) also play a role in the transmission of cooperativity from the allosteric binding site of BQCA.

Equilibrium binding studies for the interaction between CCh and BQCA were also performed on residues previously described to participate in the allosteric modulation of mAChRs. Alanine

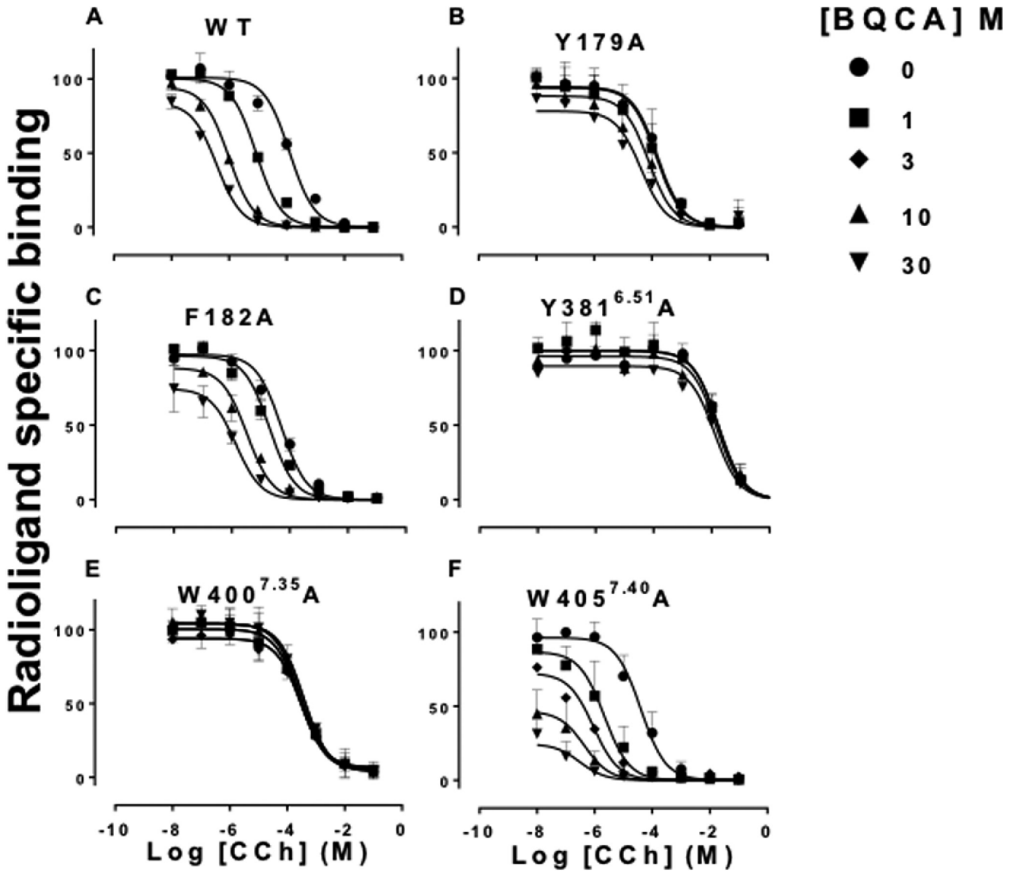

FIGURE 3. **Identification of residues that differentially govern BQCA affinity and binding cooperativity with CCh at the M_1 mAChR.** The *curves* represent competition between [^{3}H]NMS (*A–C*, *E*, and *F*) or [^{3}H]QNB (*D*) and increasing concentrations of CCh in the absence or presence of varying concentrations of BQCA. All assays were performed using 0.3 nM [^{3}H]NMS or [^{3}H]QNB in whole cells expressing the WT or mutant c-Myc-tagged M_1 mAChRs as described under "Experimental Procedures." Data points represent the mean ± S.E. of three independent experiments performed in duplicate. Curves drawn through the *points* in *A–C* and *F* represent the best fit of an allosteric ternary complex model (Equation 1). Parameters obtained from these experiments are listed in Table 2.

substitution of the TMII residues had no affect on the binding cooperativity between BQCA and CCh (Table 2). However, alanine substitution of the ECL2 residues Tyr-179, Gln-181, and Phe-182 significantly reduced the binding cooperativity, with Tyr-179 having the most profound effect (Fig. 3, *B* and *C*, and Table 2). The cooperativity was unaffected at the remaining ECL2 residues I180A, L183A, and S184A (Table 2). However, although I180A did not have a significant effect on cooperativity, it had significant opposing effects on the affinities of CCh and BQCA, with a decrease in the former and an increase in the latter (Figs. 2 and 4 and Table 2).

Mutation of the glutamate residues Glu-397$^{7.32}$ and Glu-401$^{7.36}$, which have been implicated in the binding of allosteric ligands at the mAChRs (34, 45, 46), also caused significant reduction in the binding cooperativity (Table 2). Alanine substitution of the conserved Trp-400$^{7.35}$ residue in TMVII led to complete loss of allosteric modulation even at the highest concentrations of BQCA (Fig. 3*E* and Table 2) confirming the importance of this residue for the binding of allosteric ligands at the M_1 mAChR (18, 40, 47) and suggesting that this is likely to be a residue with which BQCA directly interacts.

Alanine substitution of the conserved aromatic residues Phe-374$^{6.44}$ or Trp-405$^{7.40}$ also led to substantial reductions in the binding cooperativity (Fig. 3*F* and Table 2). Interestingly all three mutations (Q181A, F374$^{6.44}$A, and W405$^{7.40}$A) that led to an increase in CCh affinity also caused an increase in BQCA affinity and a reduction in the binding cooperativity between the two ligands (Figs. 2, 3*F*, and 4 and Table 2). The pK_B estimates obtained from the binding interaction studies at the remaining mutants were not significantly different from WT (Fig. 4 and Table 2). Overall, the binding interaction studies revealed a significant correlation between the changes in affin-

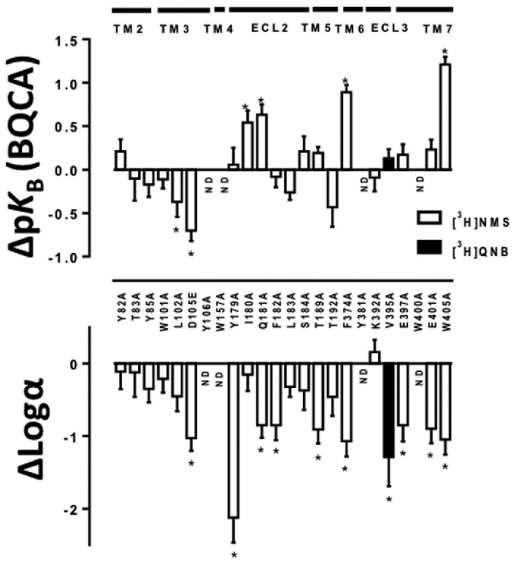

FIGURE 4. **Effects of M_1 mAChR mutations on BQCA affinity and binding cooperativity estimates.** *Bars* represent the difference in pK_B (*top panel*) or binding cooperativity value (log α, *bottom panel*) of BQCA relative to WT as derived from binding interaction experiments with CCh (Table 2). Data represent the mean ± S.E. of three experiments performed in duplicate. *ND*, no modulation by BQCA. *, significantly different from WT, $p < 0.05$, one-way analysis of variance, Dunnett's post hoc test.

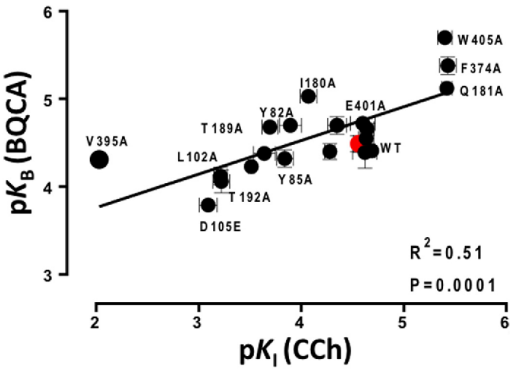

FIGURE 5. **Positive correlation between the changes in orthosteric and allosteric ligand affinities at the M_1 mAChR mutants.** Each point represents the affinity values of BQCA (pK_B) and CCh (pK_I) as determined from whole cell competition binding studies as listed in Table 2.

ities of CCh and BQCA (Fig. 5). Additionally, these data show that residues located in both the putative allosteric and the orthosteric pockets are conformationally linked and contribute to the transmission of binding cooperativity.

Effects of Mutations on Ligand Efficacy and on the Transmission of Functional Cooperativity between CCh and BQCA—To investigate the effects of the selected mutations on the ability of BQCA to modulate signaling efficacy, we determined the concentration-response profile for CCh in the absence and presence of increasing concentrations of BQCA using IP_1 accumulation as a canonical measure of M_1 mAChR activation resulting from preferential activation of $G\alpha_q$ G proteins. The potency (pEC_{50}) and maximal agonist effect (E_{max}) parameters for CCh in the absence of modulator are shown in Table 3. As agonist potency is determined by affinity, signaling efficacy, and receptor density, we applied an operational model of allosterism (Equation 2 (20)) to estimate the effect of each mutation on the operational efficacy (log τ) of CCh and BQCA without the confounding influence of affinity. The estimated log τ values were then corrected for changes in receptor expression and are summarized in Fig. 6 and Table 4. Additionally, analysis of the data with Equation 2 allowed for the estimation of the overall functional allosteric interaction between CCh and BQCA at each mutant (denoted by the parameter log αβ).

As summarized in Fig. 6 (representative examples in Fig. 7), the majority of the M_1 mAChR mutations led to a significant reduction in the signaling efficacy of CCh (log τ_A). Not surprisingly, the most prominent effects were seen for the orthosteric site residues in TMIII, W157$^{4.57}$A in TMIV, and Y381$^{6.51}$A in TMVI, consistent with reduced CCh affinity at these mutants and their importance for orthosteric ligand binding (3). No change in log τ_A was detected at residues for which CCh displayed higher affinity (Q181A, F374$^{6.44}$A, and W405$^{7.40}$A). Interestingly, our analysis indicated that the CCh log τ_A was significantly larger than WT at V395A in ECL3, despite a significant reduction in CCh binding affinity (Figs. 2 and 6 and Tables 1 and 2). BQCA agonism was not detected at any of the mutants with the exception of F374$^{6.44}$A (log τ_B 0.55 ± 0.10) and W405$^{7.40}$A (log τ_B 0.25 ± 0.06), where log τ_B was not significantly different to WT (log τ_B 0.38 ± 0.05) (Fig. 7).

TABLE 3

CCh pEC_{50} and E_{max} values for WT and mutant M_1 mAChRs as measured from the IP_1 accumulation assay

Estimated parameter values represent the mean ± S.E. of three experiments performed in duplicate.

	pEC_{50}[a]	E_{max}
WT	5.72 ± 0.08	100
Y82$^{2.61}$A	4.65 ± 0.20[b]	66.03 ± 7.35[b]
T83$^{2.62}$A	5.27 ± 0.15	20.39 ± 1.35[b]
Y85$^{2.64}$A	4.43 ± 0.06[b]	90.56 ± 5.67
W101$^{3.28}$A	2.95 ± 0.50[b]	10.05 ± 3.40[b]
L102$^{3.29}$A	2.46 ± 0.10[b]	20.00 ± 5.37[b]
D105$^{3.32}$E	NA[c]	NA
Y106$^{3.33}$A	NA	NA
W157$^{4.57}$A	NA	NA
Y179A	4.39 ± 0.14[b]	82.38 ± 4.47
I180A	4.43 ± 0.27[b]	79.92 ± 9.37
Q181A	5.120 ± 0.26	80.00 ± 7.60
F182A	4.85 ± 0.10[b]	82.73 ± 3.85
L183A	3.76 ± 0.14[b]	65.32 ± 5.11[b]
S184$^{5.32}$A	4.89 ± 0.07[b]	85.55 ± 4.00
T189$^{5.39}$A	3.94 ± 0.15[b]	101.00 ± 9.41
T192$^{5.42}$A	3.40 ± 0.20[b]	70.82 ± 9.24
F374$^{6.44}$A	4.74 ± 0.09[b]	105.2 ± 3.55
Y381$^{6.51}$A	3.10 ± 0.30[b]	21.81 ± 3.00[b]
K392$^{6.62}$A	5.37 ± 0.12	91.19 ± 5.66
V395$^{7.30}$A	4.71 ± 0.11[b]	97.23 ± 4.45
E397$^{7.32}$A	5.50 ± 0.21	96.20 ± 8.89
W400$^{7.35}$A	3.50 ± 0.08[b]	71.80 ± 3.70
E401$^{7.36}$A	5.12 ± 0.05	99.00 ± 3.39
W405$^{7.40}$A	5.21 ± 0.05	84.38 ± 1.98

[a] Negative logarithm of the EC_{50} value.
[b] Significantly different ($p < 0.05$), from WT value as determined by one-way analysis of variance with Dunnett's post hoc test.
[c] NA, not applicable (no detectable response).

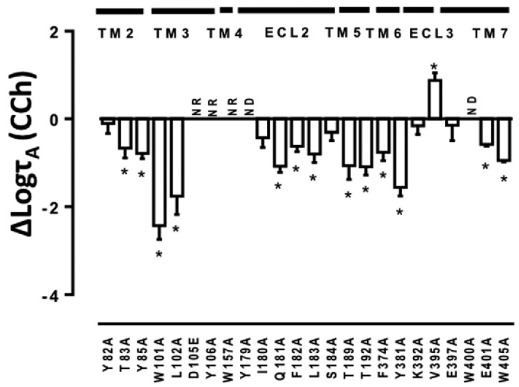

FIGURE 6. **CCh signaling efficacy (log τ_A) estimates are differentially affected by M_1 mAChR mutations.** *Bars* represent the difference in log τ_A of CCh at each mutant relative to the WT receptor value, as derived from application of the operational model of allosterism to the IP_1 interaction data at each mutant (Equation 2). Data represent the mean ± S.E. of three experiments performed in duplicate. *NR* indicates that CCh activity was absent. *ND* indicates that Equation 2 could not be used due to loss of allosteric modulation by BQCA. *, significantly different to WT receptor value, $p < 0.05$, one-way analysis of variance, Dunnett's post hoc test.

TABLE 4

Operational model parameters for the functional allosteric interaction between CCh and BQCA at the WT and mutant M_1 mAChRs measured using IP_1 accumulation

Estimated parameter values represent the mean ± S.E. of three experiments performed in duplicate. Log τ_A and log $\alpha\beta$ values were obtained from analyses of functional interaction data according to Equation 2. For this analysis, the pK_I and pK_B values for CCh and BQCA, respectively, were fixed to those determined from the radioligand binding assays as listed in Table 2.

	log τ_A[a]	log $\alpha\beta$[b]
WT	1.32 ± 0.07	2.03 ± 0.12
$Y82^{2.61}A$	1.21 ± 0.13	1.14 ± 0.17[c]
$T83^{2.62}A$	0.65 ± 0.13[c]	0.73 ± 0.20[c]
$Y85^{2.64}A$	0.53 ± 0.07[c]	1.03 ± 0.09[c]
$W101^{3.28}A$[d]	−1.11 ± 0.18[c]	1.95 ± 0.17
$L102^{3.29}A$[d]	−0.44 ± 0.24[c]	0.98 ± 0.15[c]
$D105^{3.32}E$[d]	−0.69 ± 0.23[c]	0.97 ± 0.20[c]
$Y106^{3.33}A$[d]	−0.79 ± 0.21[c]	1.24 ± 0.10[c]
$W157^{4.57}A$[d]	−2.01 ± 0.20[c]	1.74 ± 0.49
Y179A	ND[e]	ND
I180A	0.89 ± 0.13	1.35 ± 0.18
Q181A	0.24 ± 0.08[c]	0.33 ± 0.12[c]
F182A	0.70 ± 0.07[c]	0.53 ± 0.13[c]
L183A	0.52 ± 0.11[c]	1.26 ± 0.13[c]
$S184^{5.32}A$	1.01 ± 0.11	1.61 ± 0.14
$T189^{5.39}A$	0.25 ± 0.18[c]	0.71 ± 0.12[c]
$T192^{5.42}A$	0.23 ± 0.11[c]	1.76 ± 0.10
$F374^{6.44}A$	0.56 ± 0.11[c]	0.03 ± 0.02[c]
$Y381^{6.51}A$[d]	−0.23 ± 0.11[c]	1.25 ± 0.08[c]
$K392^{6.62}A$	1.16 ± 0.11	1.92 ± 0.14
$V395^{7.30}A$	2.19 ± 0.10[c]	1.46 ± 0.14
$E397^{7.32}A$	1.17 ± 0.20	1.07 ± 0.30[c]
$W400^{7.35}A$	ND	ND
$E401^{7.36}A$	0.74 ± 0.02[c]	0.93 ± 0.04[c]
$W405^{7.40}A$	0.38 ± 0.02[c]	0.47 ± 0.07[c]

[a] Logarithm of operational efficacy parameter for CCh (log τ_A) was corrected for changes in receptor expression to allow comparison with WT.
[b] Logarithm of the functional cooperativity between CCh and BQCA is shown.
[c] Significantly different ($p < 0.05$), from WT value as determined by one-way ANOVA with Dunnett's post hoc test.
[d] pK_B of BQCA was left unconstrained at W101A, L102A, D105E, Y106A, W157A, and Y381A. The log τ_B of BQCA was constrained to −2 at these mutants.
[e] ND, no modulation by BQCA.

A common finding was obtained from the interaction studies between BQCA and CCh at the orthosteric site mutations that substantially impaired CCh signaling ($W101^{3.28}A$, $L102^{3.29}A$, $D105^{3.32}E$, $Y106^{3.33}A$, $W157^{4.57}A$, and $Y381^{6.51}A$). As opposed to the loss of cooperativity between the two ligands seen in the binding interaction studies for the majority of these mutant receptors (Fig. 3*D* and Table 2), BQCA was able to rescue CCh function (Fig. 7*D* and Table 4). An analogous "rescue" of ACh function by LY2033289 has been described at equivalent TMIII residues in the M_4 mAChR (33, 48). This finding indicates that a key part of the mechanism for the positive cooperativity mediated by BQCA on the orthosteric agonist involves a global drive of the receptor toward an active conformation.

The majority of mutant residues that displayed reduced binding cooperativity (log α) between CCh and BQCA also caused a reduction in functional cooperativity (log $\alpha\beta$) between the two ligands (Fig. 8). These include the three residues that showed enhanced affinities for CCh and BQCA (Q181A, $W405^{7.40}A$, and $F374^{6.44}A$), F182A in ECL2 (Fig. 7, *C* and *F*), $T189^{5.39}A$ in TMV, and the two glutamate mutants $E397^{7.32}A$ and $E401^{7.36}A$. The three residues mutated in TMII ($Y82^{2.61}A$, $T83^{2.62}A$, and $Y85^{2.64}A$) and L183A in ECL2 caused significant reductions in functional cooperativity despite their lack of effect on binding cooperativity between CCh and BQCA (Fig. 8 and Table 4), indicating that these residues are likely to play a role in the transmission of functional cooperativity alone. In contrast, the log $\alpha\beta$ between BQCA and CCh at V395A was unchanged, despite significantly reduced binding cooperativity (Fig. 8 and Table 4). Consistent with the findings of Ma *et al.* (18), modulation of CCh efficacy was absent at Y179A and $W400^{7.35}A$ (Figs. 7, *B* and *E*, and 8). These results suggest that Trp-$400^{7.35}$ and Tyr-179 are likely to be residues with which BQCA directly interacts.

Molecular Dynamics Simulations and Ligand Docking—Ligand docking and molecular dynamic simulations were subsequently performed to rationalize our findings. This resulted in one main pose of BQCA in the predicted allosteric site.

The obtained complex for BQCA and CCh bound to the modeled M_1 mAChR is shown in Fig. 9*A*. CCh forms the established salt bridge between the cationic nitrogen and Asp-$105^{3.32}$ and is fixed in a hydrophobic pocket formed by residues Tyr-$106^{3.33}$ in TMIII, Trp-$157^{4.57}$ in TMIV, Tyr-$381^{6.51}$ in TMVI, and Tyr-$404^{7.39}$ and Tyr-$408^{7.43}$ in TMVII (Fig. 9*B*). This is a signature network of interactions in cationic amine receptors (7, 11, 49), rhodopsins (51), and the adenosine A_{2A} receptor (52). Moreover, the orthosteric site is further flanked by the H-bonds formed between Tyr-$106^{3.33}$ and Tyr-$381^{6.51}$, which adds stability to the binding pocket (3), and together with Tyr-$404^{7.39}$ and Tyr-$408^{7.43}$ formed an aromatic lid separating the orthosteric and allosteric pockets. The aromatic ring of Trp-$157^{4.57}$ appears to form a π-π interaction with Tyr-$106^{3.33}$ (Fig. 9*B*), and it has been shown to form direct contact with the aromatic ring of the antagonist QNB (7).

The analysis of the MD trajectories shows the interaction of BQCA with residues located in the allosteric binding site (Fig. 9*C*). This binding site is defined by residues from TMII, TMVII, and ECL2 and is in agreement with our binding and functional studies; in particular, significant effects of the mutation of Tyr-179 in ECL2 and Trp-$400^{7.35}$ in TMVII can be reconciled with this pose. Tyr-179 is predicted to contribute to the stability of BQCA binding via formation of hydrophobic/edge-to-face π-π

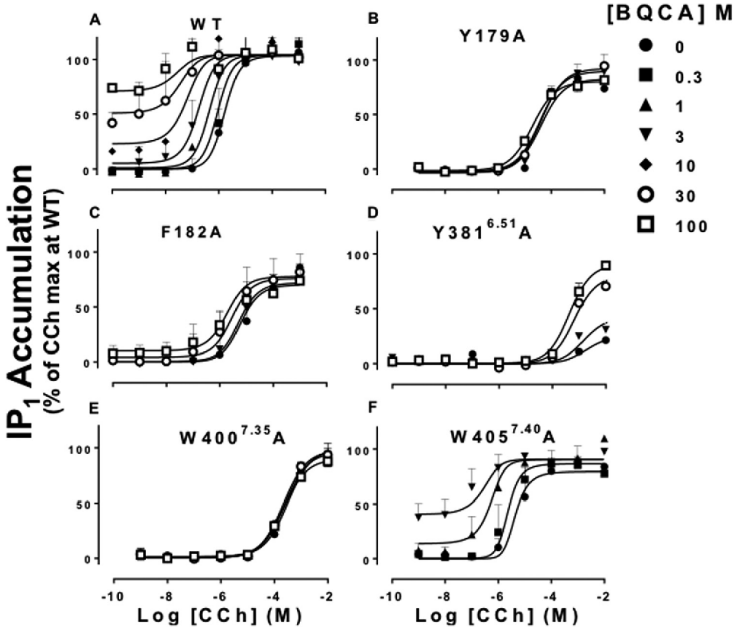

FIGURE 7. **Identification of residues that differentially govern BQCA efficacy and functional cooperativity with CCh at the M_1 mAChR.** Interaction between BQCA and CCh in IP_1 accumulation assay in CHO FlpIn cells stably expressing the WT or mutant M_1 mAChRs. Data points represent the mean ± S.E. of three independent experiments performed in duplicate. *Curves* drawn through the points in *A, C, D,* and *F* represent the best fit of an operational allosteric model (Equation 2 and Table 4) with the affinity of each ligand at each mutant fixed to the value determined from separate binding studies (Table 2).

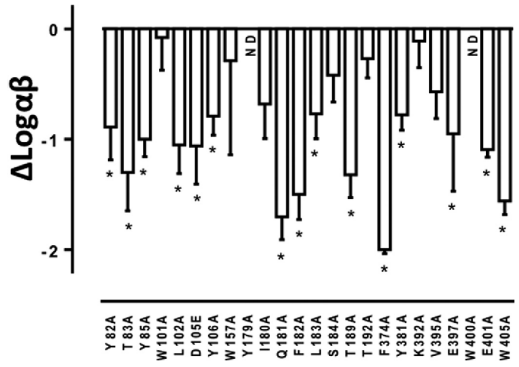

FIGURE 8. **BQCA functional cooperativities are differentially modified by M_1 mAChR mutations.** *Bars* represent the difference in the functional cooperativity value (log $\alpha\beta$, Equation 2) relative to the WT value, as derived from application of the operational model of allosterism to the CCh and BQCA IP_1 interaction data at each mutant (Equation 2) (Table 4). Data represent the mean ± S.E. from three experiments performed in duplicate. *ND,* no modulation by BQCA. * significantly different from WT value, $p < 0.05$, one-way analysis of variance, Dunnett's post test.

interactions with both the bicyclic 4-oxoquinoline core and the benzylic pendant of BQCA. Similarly, Trp-$400^{7.35}$ is predicted to make a π-π interaction with the benzylic pendant. In this model, Glu-$397^{7.32}$ also constrains this moiety of BQCA through a hydrophobic interaction, essentially forming a lid over this part of the allosteric binding site. Tyr-$85^{2.64}$ and Tyr-$82^{2.61}$ are predicted to delimit the allosteric site via extra edge-to-face π-π/hydrophobic interactions with the 4-oxoquinoline ring system (Fig. 9*C*). Although the former residue only affected the functional cooperativity between BQCA and CCh, it has been found to be an important contact residue for prototypical allosteric modulators at the M_2 mAChR (13). Mutation of an adjacent residue at the M_4 mAChR ($193^{2.65}$T) was found to be important for the transmission of cooperativity between ACh and LY2033298 (34), suggesting a contribution of this residue to a conserved allosteric pocket within the mAChR family. Fig. 10 shows the global movements of the ECLs and TMs as well as the movements of the residues to accommodate the binding of BQCA. These include the rotation of the aromatic side chains of Trp-$400^{7.35}$ (Fig. 10, *inset*) and Trp-$405^{7.40}$ that may be facilitating the accompanying shifts in the nearby TMVII residues Glu-$397^{7.32}$ and Glu-$401^{7.36}$ to constrain BQCA into the observed pose. The binding of BQCA also causes subtle movements in the ECLs; the most significant of these appear to be in ECL2 where the aromatic side chains of Tyr-179 and Phe-182 both move closer to BQCA, whereas Gln-181 adopts a horizontal position away from the ligand accessible cavity. These results support our finding that mutation of Glu-$397^{7.32}$, Glu-$401^{7.36}$, Tyr-179, and Phe-182 lead to reduced cooperativity between BQCA and CCh and that mutation of Gln-181 enhances the binding affinity of both ligands.

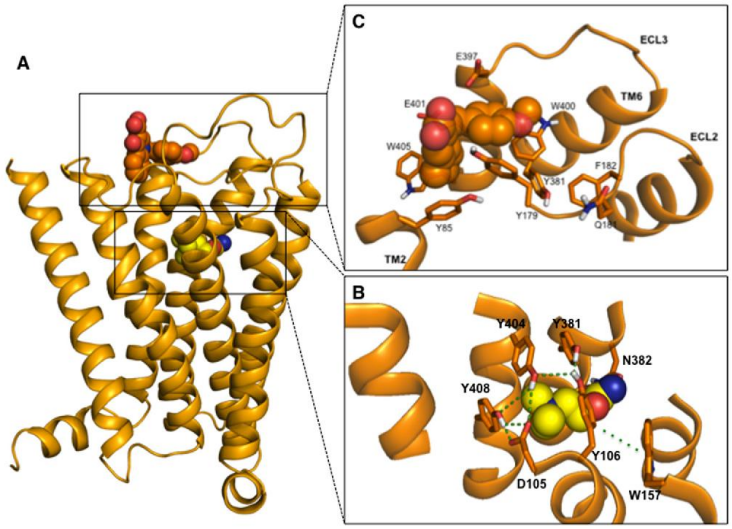

FIGURE 9. **Structural model of the M_1 mAChR in complex with BQCA and CCh.** *A*, overall view of the complex obtained using MD simulations. The ligands are shown in *orange* (BQCA) and *yellow* (CCh) *spheres*. *B*, orthosteric binding site for CCh; *C*, predicted allosteric binding site of BQCA. Important residues are shown by *orange sticks*.

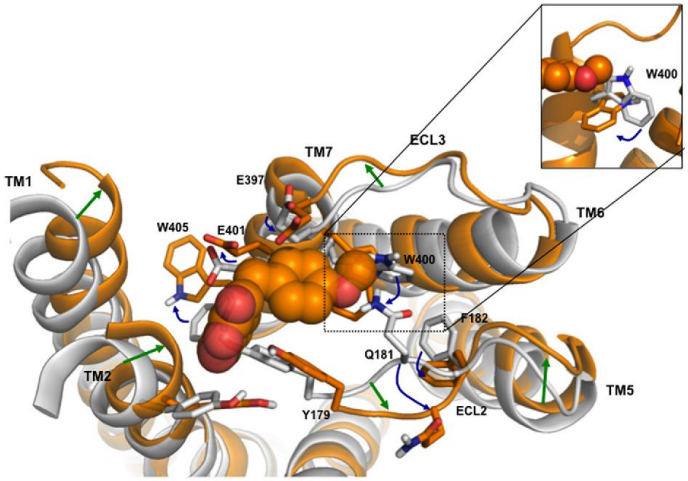

FIGURE 10. **Proposed rearrangement of ECLs and TMs upon BQCA binding to M_1 mAChR.** Extracellular view of the BQC-binding site at the starting position for MD simulations (*gray*) or at the final position of the receptor after 20 ns of MD (*orange*). Important residues involved in BQCA binding or cooperativity are shown as *sticks*. Global movements of TMs and ECLs are shown with *green arrows*, and residue shifts are indicated by *blue arrows*. *Inset* shows the movement of the side chain of Trp-400$^{7.35}$.

DISCUSSION

BQCA demonstrates a number of unique properties relative to previously described allosteric ligands of the mAChR family, including an exquisite selectivity for M_1 mAChRs over other subtypes and a mechanism of action that appears in strict accordance with a two-state model of receptor activity, such that it is a positive modulator of agonists but a negative modulator of antagonists/inverse agonists (16, 17). Moreover, the compound is active *in vivo* (18, 53), providing proof of concept for the validity of allosteric targeting of M_1 mAChRs in the treatment of CNS disorders, and it has been the focus of numerous structure-activity studies (15, 54) aimed at improving its "druggability" and affinity. However, it is now apparent that allosteric modulators can achieve selectivity by more than one mechanism, *i.e.* at the level of structural divergence of an allosteric pocket across GPCR subtypes or via selective cooperativ-

ity at a given subtype despite acting at a "conserved" allosteric site (14). The latter paradigm is best exemplified by the mAChRs, in which are all characterized by an extracellular vestibule that can be recognized by structurally diverse allosteric ligands (12, 13). To better understand the basis of the selectivity of BQCA, we combined mutagenesis with mathematical and molecular modeling to identify potential structural contributors to its binding pocket and its ability to allosterically modulate the binding and signaling of the prototypical orthosteric agonist CCh.

Although no affinity values could be obtained for BQCA at residues where allosteric modulation was abolished (Tyr-$106^{3.33}$, Trp-$157^{4.57}$ and Tyr-$381^{6.51}$ and Trp-$400^{7.35}$), our study identified residues of the M_1 mAChR that contribute to the following: (i) the binding affinity of the modulator; (ii) the cooperativity between the modulator and the orthosteric agonist CCh; (iii) the ability of the modulator to drive the receptor into an active state, and (iv) enhancement of the binding affinity of BQCA.

Alanine substitution of a number of residues from various regions in the receptor caused a decrease in the cooperativity between BQCA and CCh in binding and functional interaction studies (Figs. 4 and 8 and Tables 2 and 4). Such reductions in cooperativity resulted either from mutation of residues that form the proposed allosteric binding pocket or residues conformationally linked to the allosteric site and thus needed for the transmission of cooperativity or receptor activation upon ligand binding. Our MD simulations support this hypothesis and the experimental findings. As shown in Fig. 9, the proposed BQCA pocket is topographically distinct from the orthosteric binding site, and these two sites are separated by a shelf of aromatic residues. The residues that are predicted to form the BQCA binding pocket, mainly from ECL2 (Tyr-179), TMII (Tyr-$85^{2.64}$), and TMVII (Trp-$400^{7.35}$) or those whose mutation to alanine cause significant decreases in cooperativity (Phe-182, Glu-$397^{7.32}$, and Glu-$401^{7.36}$), are equivalent to residues that have been implicated in the binding of several allosteric ligands at mAChRs, as follows : (i) the action of gallamine and the allosteric antagonist MT7 at the M_1 mAChR (40, 47); (ii) the action of LY2033298 at the M_4 mAChR (34), and (iii) the action of $C_{7/3}$-phth, gallamine, alcuronium, McN-A-343, alkane-bisammonium, and caracurine V-type allosteric modulators at the M_2 mAChR (13, 35, 42, 55–57).

The only residue in the proposed BQCA binding pocket that leads to complete loss of modulation in both functional and binding assays is Trp-$400^{7.35}$. This suggests that the π-π interaction of the benzylic pendant of BQCA and the aromatic side chain of Trp-$400^{7.35}$ makes either a major contribution to BQCA binding and/or maintaining the structure of the local binding pocket of BQCA. Other residues, such as Tyr-179, Tyr-$82^{2.61}$, and Tyr-$85^{2.64}$, while predicted in our MD simulations to interact with BQCA, appear to have a predominant role in the transmission of BQCA's modulator action on orthosteric ligands such that their mutation to alanine impairs the transmission of cooperativity but does not lead to a significant loss of binding affinity. Of interest, a recent molecular dynamics study identified two binding centers in the extracellular vestibule of the M_2 mAChR, each defined by a pair of aromatic residues (center 1, Tyr-177^{ECL2} and $Trp^{7.35}$; center 2, $Tyr^{2.61}$ and $Tyr^{2.64}$) (13). It is noteworthy that we identified these residues as key contributors for the binding and function of BQCA. Furthermore, $Tyr^{2.64}$ and $Trp^{7.35}$ are conserved across all mAChR receptor subtypes; $Tyr^{2.61}$ is conserved across all but the M_3 mAChR (where it is replaced by a similarly aromatic phenylalanine residue), and Tyr-179 is only present at the M_1 and M_2 mAChRs but is a phenylalanine at the M_3 and M_4 mAChRs. This is consistent with BQCA sharing a common binding site with other prototypical mAChR allosteric modulators. Glu-$397^{7.32}$ and Glu-$401^{7.36}$ are not conserved across the mAChR family and were predicted by our modeling experiments to make minimal interaction with BQCA. Mutation of these residues had no effect on BQCA binding affinity but decreased cooperativity with CCh. This suggests that such residues may govern the subtype-specific cooperative effect of BQCA upon orthosteric ligand binding from a conserved allosteric pocket.

The observation of a correlation between the change in CCh binding affinity (pK_I) and BQCA binding affinity (pK_B) is entirely consistent with our previous description of the mechanism of BQCA within the confines of a strict two-state model (Fig. 5) (17). Furthermore, the finding that the orthosteric site residues shown in Fig. 9*B* lead to complete loss (Y$106^{3.33}$A, W$157^{4.57}$A, and Y$381^{6.51}$A), or significant reduction (D$105^{3.32}$A) in the binding cooperativity between CCh and BQCA is a striking example of a conformationally linked mechanism for the transmission of cooperativity. The efficacy of CCh was severely reduced when each of these residues was mutated, but this was "rescued" by BQCA. Furthermore, these additional functional interaction data confirmed the ability of BQCA to bind to this set of mutant receptors, a conclusion that could not be drawn from the binding data alone. This highlights the importance of using both binding and functional assays to characterize the effect of mutations upon allosteric ligand function.

Given that an analogous observation was made for the action of the positive allosteric modulator, LY2033298, at a functionally impaired M_4 mAChR double mutant containing the Y$113^{3.33}$C (48) or the D$112^{3.32}$E mutation (33), our results indicate that BQCA may share similarities in mechanism of action and may bind to a site that is spatially conserved between the M_4 the M_1 mAChRs. However, the very high selectivity of BQCA for the M_1 mAChR (as opposed to LY2033298 that acts at both the M_2 and M_4 mAChRs) indicates that although the allosteric sites of these two ligands share some epitopes, they may engage additional distinct residues either in their mode of binding or transmission of cooperativity to the orthosteric site.

In addition to regions of the receptor that were primarily important for the binding of BQCA and transmission of cooperativity, we also identified mutations that caused a significant enhancement in the affinities of both CCh and BQCA (Q181A, F$374^{6.44}$A, and W$405^{7.40}$A). Previous studies have reported increases in CCh affinity at Q181A (36, 40), whereas others have reported constitutive receptor activity when residues 6.44 and 7.40 are mutated to alanine (41, 43). The movement of the side chain of $Phe^{6.44}$ is coupled to an outward movement of TMVI upon β_2-adrenergic receptor activation (58), and it has been reported to be a microswitch in GPCR activation (50). It

has also been suggested that Trp-405$^{7.40}$ restricts thermal motions of the extracellular domain of TMVII of mAChRs (3).

In summary, we have identified key regions in the M_1 mAChR that are involved in the binding and signaling of CCh and BQCA, and in the transmission of cooperativity between the orthosteric and an allosteric binding site. We propose that some of the structural determinants of these effects are analogous to those of other family A GPCRs, but the unique selectivity of BQCA arises from the additional involvement of nonconserved residues (*e.g.* Glu-397$^{7.32}$ and Glu-401$^{7.36}$) and/or selective cooperativity with agonists at the M_1 mAChR. Therefore, our results provide further understanding of the structural basis of allosteric modulation that may be of general application to GPCR drug discovery and that can help guide the more rational design of allosteric ligands that target this distinct site. In particular, they challenge an important concept often associated with allosteric targeting of GPCRs, namely that selective modulators gain subtype selectivity through their binding to a site that is not conserved across a receptor subfamily. Rather, as highlighted in our study, selective cooperativity via interaction with a conserved allosteric site is also possible. Given the increasing number of GPCR crystal structures now being solved, it should thus be appreciated that structure-based drug design using *in silico* screening for novel allosteric modulators will not, in and of itself, guarantee a desired level of selectivity without complementation by additional structure-function approaches as described herein.

Acknowledgments—We are grateful to Dr. Ann Stewart for generating some of the M_1 mAChR mutants and Briana J. Davie for the synthesis of BQCA.

REFERENCES

1. Venkatakrishnan, A. J., Deupi, X., Lebon, G., Tate, C. G., Schertler, G. F., and Babu, M. M. (2013) Molecular signatures of G-protein-coupled receptors. *Nature* **494,** 185–194
2. Lagerström, M. C., and Schiöth, H. B. (2008) Structural diversity of G protein-coupled receptors and significance for drug discovery. *Nat. Rev. Drug Discov.* **7,** 339–357
3. Hulme, E. C. (2013) GPCR activation: a mutagenic spotlight on crystal structures. *Trends Pharmacol. Sci.* **34,** 67–84
4. Stevens, R. C., Cherezov, V., Katritch, V., Abagyan, R., Kuhn, P., Rosen, H., and Wüthrich, K. (2013) The GPCR Network: a large-scale collaboration to determine human GPCR structure and function. *Nat. Rev. Drug Discov.* **12,** 25–34
5. Miao, Y., Nichols, S. E., Gasper, P. M., Metzger, V. T., and McCammon, J. A. (2013) Activation and dynamic network of the M2 muscarinic receptor. *Proc. Natl. Acad. Sci. U.S.A.* **110,** 10982–10987
6. Wacker, D., Wang, C., Katritch, V., Han, G. W., Huang, X.-P., Vardy, E., McCorvy, J. D., Jiang, Y., Chu, M., Siu, F. Y., Liu, W., Xu, H. E., Cherezov, V., Roth, B. L., and Stevens, R. C. (2013) Structural features for functional selectivity at serotonin receptors. *Science* **340,** 615–619
7. Haga, K., Kruse, A. C., Asada, H., Yurugi-Kobayashi, T., Shiroishi, M., Zhang, C., Weis, W. I., Okada, T., Kobilka, B. K., Haga, T., and Kobayashi, T. (2012) Structure of the human M2 muscarinic acetylcholine receptor bound to an antagonist. *Nature* **482,** 547–551
8. Conn, P. J., Christopoulos, A., and Lindsley, C. W. (2009) Allosteric modulators of GPCRs: a novel approach for the treatment of CNS disorders. *Nat. Rev. Drug Discov.* **8,** 41–54
9. Conn, P. J., Jones, C. K., and Lindsley, C. W. (2009) Subtype-selective allosteric modulators of muscarinic receptors for the treatment of CNS disorders. *Trends Pharmacol. Sci.* **30,** 148–155
10. Tan, Q., Zhu, Y., Li, J., Chen, Z., Han, G. W., Kufareva, I., Li, T., Ma, L., Fenalti, G., Li, J., Zhang, W., Xie, X., Yang, H., Jiang, H., Cherezov, V., Liu, H., Stevens, R. C., Zhao, Q., and Wu, B. (2013) Structure of the CCR5 chemokine receptor–HIV entry inhibitor maraviroc complex. *Science* **341,** 1387–1390
11. Kruse, A. C., Hu, J., Pan, A. C., Arlow, D. H., Rosenbaum, D. M., Rosemond, E., Green, H. F., Liu, T., Chae, P. S., Dror, R. O., Shaw, D. E., Weis, W. I., Wess, J., and Kobilka, B. K. (2012) Structure and dynamics of the M3 muscarinic acetylcholine receptor. *Nature* **482,** 552–556
12. De Amici, M., Dallanoce, C., Holzgrabe, U., Tränkle, C., and Mohr, K. (2010) Allosteric ligands for G protein-coupled receptors: A novel strategy with attractive therapeutic opportunities. *Med. Res. Rev.* **30,** 463–549
13. Dror, R. O., Green, H. F., Valant, C., Borhani, D. W., Valcourt, J. R., Pan, A. C., Arlow, D. H., Canals, M., Lane, J. R., Rahmani, R., Baell, J. B., Sexton, P. M., Christopoulos, A., and Shaw, D. E. (2013) Structural basis for modulation of a G-protein-coupled receptor by allosteric drugs. *Nature* **503,** 295–299
14. Valant, C., Felder, C. C., Sexton, P. M., and Christopoulos, A. (2012) Probe dependence in the allosteric modulation of a g protein-coupled receptor: implications for detection and validation of allosteric ligand effects. *Mol. Pharmacol.* **81,** 41–52
15. Davie, B. J., Christopoulos, A., and Scammells, P. J. (2013) Development of M1 mAChR allosteric and bitopic ligands: prospective therapeutics for the treatment of cognitive deficits. *ACS Chem. Neurosci.* **4,** 1026–1048
16. Abdul-Ridha, A., Lane, J. R., Sexton, P. M., Canals, M., and Christopoulos, A. (2013) Allosteric modulation of a chemogenetically modified G protein-coupled receptor. *Mol. Pharmacol.* **83,** 521–530
17. Canals, M., Lane, J. R., Wen, A., Scammells, P. J., Sexton, P. M., and Christopoulos, A. (2012) A Monod-Wyman-Changeux mechanism can explain G protein-coupled receptor (GPCR) allosteric modulation. *J. Biol. Chem.* **287,** 650–659
18. Ma, L., Seager, M. A., Seager M, Wittmann, M., Jacobson, M., Bickel, D., Burno, M., Jones, K., Graufelds, V. K., Xu, G., Pearson, M., McCampbell, A., Gaspar, R., Shughrue, P., Danziger, A., Regan, C., Flick, R., Pascarella, D., Garson, S., Doran, S., Kreatsoulas, C., Veng, L., Lindsley, C. W., Shipe, W., Kuduk, S., Sur, C., Kinney, G., Seabrook, G. R., and Ray, W. J. (2009) Selective activation of the M1 muscarinic acetylcholine receptor achieved by allosteric potentiation. *Proc. Natl. Acad. Sci. U.S.A.* **106,** 15950–15955
19. Black, J. W., and Leff, P. (1983) Operational models of pharmacological agonism. *Proc. R. Soc. Lond. B Biol. Sci.* **220,** 141–162
20. Leach, K., Sexton, P. M., and Christopoulos, A. (2007) Allosteric GPCR modulators: taking advantage of permissive receptor pharmacology. *Trends Pharmacol. Sci.* **28,** 382–389
21. Thompson, J. D., Gibson, T. J., Plewniak, F., Jeanmougin, F., and Higgins, D. G. (1997) The CLUSTAL_X windows interface: flexible strategies for multiple sequence alignment aided by quality analysis tools. *Nucleic Acids Res.* **25,** 4876–4882
22. Rasmussen, S. G., Choi, H. J., Fung, J. J., Pardon, E., Casarosa, P., Chae, P. S., Devree, B. T., Rosenbaum, D. M., Thian, F. S., Kobilka, T. S., Schnapp, A., Konetzki, I., Sunahara, R. K., Gellman, S. H., Pautsch, A., Steyaert, J., Weis, W. I., and Kobilka, B. K. (2011) Structure of a nanobody-stabilized active state of the β_2 adrenoceptor. *Nature* **469,** 175–180
23. Ballesteros, J. A., and Weinstein, H. (1995) in *Methods in Neurosciences* (Stuart, C. S., ed) pp. 366–428, Academic Press, New York
24. Sali, A., and Blundell, T. L. (1993) Comparative protein modelling by satisfaction of spatial restraints. *J. Mol. Biol.* **234,** 779–815
25. Duan, Y., Wu, C., Chowdhury, S., Lee, M. C., Xiong, G., Zhang, W., Yang, R., Cieplak, P., Luo, R., Lee, T., Caldwell, J., Wang, J., and Kollman, P. (2003) A point-charge force field for molecular mechanics simulations of proteins based on condensed-phase quantum mechanical calculations. *J. Comput. Chem.* **24,** 1999–2012
26. Wang, J., Wolf, R. M., Caldwell, J. W., Kollman, P. A., and Case, D. A. (2004) Development and testing of a general amber force field. *J. Comput. Chem.* **25,** 1157–1174
27. Phillips, J. C., Braun, R., Wang, W., Gumbart, J., Tajkhorshid, E., Villa, E., Chipot, C., Skeel, R. D., Kalé, L., and Schulten, K. (2005) Scalable molecular dynamics with NAMD. *J. Comput. Chem.* **26,** 1781–1802

28. Shonberg, J., Herenbrink, C. K., López, L., Christopoulos, A., Scammells, P. J., Capuano, B., and Lane, J. R. (2013) A structure-activity analysis of biased agonism at the dopamine D2 receptor. *J. Med. Chem.* **56,** 9199–9221
29. Motulsky H. J., and Christopoulos, A. (2003) Fitting models to biological data using linear and nonlinear regression. *A Practical Guide to Curve Fitting*, GraphPad Software Inc., San Diego
30. Leach, K., Loiacono, R. E., Felder, C. C., McKinzie, D. L., Mogg, A., Shaw, D. B., Sexton, P. M., and Christopoulos, A. (2010) Molecular mechanisms of action and *in vivo* validation of an M4 muscarinic acetylcholine receptor allosteric modulator with potential antipsychotic properties. *Neuropsychopharmacology* **35,** 855–869
31. Kenakin, T., and Christopoulos, A. (2013) Signalling bias in new drug discovery: detection, quantification and therapeutic impact. *Nat. Rev. Drug Discov.* **12,** 205–216
32. Christopoulos, A. (1998) Assessing the distribution of parameters in models of ligand-receptor interaction: to log or not to log. *Trends Pharmacol. Sci.* **19,** 351–357
33. Leach, K., Davey, A. E., Felder, C. C., Sexton, P. M., and Christopoulos, A. (2011) The role of transmembrane domain 3 in the actions of orthosteric, allosteric, and atypical agonists of the m4 muscarinic acetylcholine receptor. *Mol. Pharmacol.* **79,** 855–865
34. Nawaratne, V., Leach, K., Felder, C. C., Sexton, P. M., and Christopoulos, A. (2010) Structural determinants of allosteric agonism and modulation at the M4 muscarinic acetylcholine receptor: identification of ligand-specific and global activation mechanisms. *J. Biol. Chem.* **285,** 19012–19021
35. Valant, C., Gregory, K. J., Hall, N. E., Scammells, P. J., Lew, M. J., Sexton, P. M., and Christopoulos, A. (2008) A novel mechanism of G protein-coupled receptor functional selectivity. Muscarinic partial agonist McN-A-343 as a bitopic orthosteric/allosteric ligand. *J. Biol. Chem.* **283,** 29312–29321
36. Goodwin, J. A., Hulme, E. C., Langmead, C. J., and Tehan, B. G. (2007) Roof and floor of the muscarinic binding pocket: variations in the binding modes of orthosteric ligands. *Mol. Pharmacol.* **72,** 1484–1496
37. Lu, Z.-L., and Hulme, E. C. (1999) The functional topography of transmembrane domain 3 of the M1 muscarinic acetylcholine receptor, revealed by scanning mutagenesis. *J. Biol. Chem.* **274,** 7309–7315
38. Lu, Z.-L., Saldanha, J. W., and Hulme, E. C. (2001) Transmembrane domains 4 and 7 of the M1 muscarinic acetylcholine receptor are critical for ligand binding and the receptor activation switch. *J. Biol. Chem.* **276,** 34098–34104
39. Avlani, V. A., Langmead, C. J., Guida, E., Wood, M. D., Tehan, B. G., Herdon, H. J., Watson, J. M., Sexton, P. M., and Christopoulos, A. (2010) Orthosteric and allosteric modes of interaction of novel selective agonists of the M1 muscarinic acetylcholine receptor. *Mol. Pharmacol.* **78,** 94–104
40. Matsui, H., Lazareno, S., and Birdsall, N. J. (1995) Probing of the location of the allosteric site on m1 muscarinic receptors by site-directed mutagenesis. *Mol. Pharmacol.* **47,** 88–98
41. Daval, S. B., Kellenberger, E., Bonnet, D., Utard, V., Galzi, J. L., and Ilien, B. (2013) Exploration of the orthosteric/allosteric interface in human m1 muscarinic receptors by bitopic fluorescent ligands. *Mol. Pharmacol.* **84,** 71–85
42. Prilla, S., Schrobang, J., Ellis, J., Höltje, H.-D., and Mohr, K. (2006) Allosteric interactions with muscarinic acetylcholine receptors: complex role of the conserved tryptophan M2422Trp in a critical cluster of amino acids for baseline affinity, subtype selectivity, and cooperativity. *Mol. Pharmacol.* **70,** 181–193
43. Spalding, T. A., Burstein, E. S., Henderson, S. C., Ducote, K. R., and Brann, M. R. (1998) Identification of a ligand-dependent switch within a muscarinic receptor. *J. Biol. Chem.* **273,** 21563–21568
44. Hulme, E. C., Lu, Z. L., Saldanha, J. W., and Bee, M. S. (2003) Structure and activation of muscarinic acetylcholine receptors. *Biochem. Soc. Trans.* **31,** 29–34
45. Lebois, E. P., Bridges, T. M., Lewis, L. M., Dawson, E. S., Kane, A. S., Xiang, Z., Jadhav, S. B., Yin, H., Kennedy, J. P., Meiler, J., Niswender, C. M., Jones, C. K., Conn, P. J., Weaver, C. D., and Lindsley, C. W. (2010) Discovery and characterization of novel subtype-selective allosteric agonists for the investigation of M(1) receptor function in the central nervous system. *ACS Chem. Neurosci.* **1,** 104–121
46. May, L. T., Avlani, V. A., Langmead, C. J., Herdon, H. J., Wood, M. D., Sexton, P. M., and Christopoulos, A. (2007) Structure-function studies of allosteric agonism at M2 muscarinic acetylcholine receptors. *Mol. Pharmacol.* **72,** 463–476
47. Marquer, C., Fruchart-Gaillard, C., Letellier, G., Marcon, E., Mourier, G., Zinn-Justin, S., Ménez, A., Servent, D., and Gilquin, B. (2011) Structural model of ligand-G protein-coupled receptor (GPCR) complex based on experimental double mutant cycle data. *J. Biol. Chem.* **286,** 31661–31675
48. Nawaratne, V., Leach, K., Suratman, N., Loiacono, R. E., Felder, C. C., Armbruster, B. N., Roth, B. L., Sexton, P. M., and Christopoulos, A. (2008) New insights into the function of M4 muscarinic acetylcholine receptors gained using a novel allosteric modulator and a DREADD (designer receptor exclusively activated by a designer drug). *Mol. Pharmacol.* **74,** 1119–1131
49. Cherezov, V., Rosenbaum, D. M., Hanson, M. A., Rasmussen, S. G., Thian, F. S., Kobilka, T. S., Choi, H. J., Kuhn, P., Weis, W. I., Kobilka, B. K., and Stevens, R. C. (2007) High-resolution crystal structure of an engineered human β2-adrenergic G protein-coupled receptor. *Science* **318,** 1258–1265
50. Valentin-Hansen, L., Holst, B., Frimurer, T. M., and Schwartz, T. W. (2012) PheVI:09 (Phe6.44) as a sliding microswitch in seven-transmembrane (7TM) G protein-coupled receptor activation. *J. Biol. Chem.* **287,** 43516–43526
51. Choe, H. W., Kim, Y. J., Park, J. H., Morizumi, T., Pai, E. F., Krauss, N., Hofmann, K. P., Scheerer, P., and Ernst, O. P. (2011) Crystal structure of metarhodopsin II. *Nature* **471,** 651–655
52. Lebon, G., Warne, T., Edwards, P. C., Bennett, K., Langmead, C. J., Leslie, A. G., and Tate, C. G. (2011) Agonist-bound adenosine A2A receptor structures reveal common features of GPCR activation. *Nature* **474,** 521–525
53. Shirey, J. K., Brady, A. E., Jones, P. J., Davis, A. A., Bridges, T. M., Kennedy, J. P., Jadhav, S. B., Menon, U. N., Xiang, Z., Watson, M. L., Christian, E. P., Doherty, J. J., Quirk, M. C., Snyder, D. H., Lah, J. J., Levey, A. I., Nicolle, M. M., Lindsley, C. W., and Conn, P. J. (2009) A selective allosteric potentiator of the M1 muscarinic acetylcholine receptor increases activity of medial prefrontal cortical neurons and restores impairments in reversal learning. *J. Neurosci.* **29,** 14271–14286
54. Mistry, S. N., Valant, C., Sexton, P. M., Capuano, B., Christopoulos, A., and Scammells, P. J. (2013) Synthesis and pharmacological profiling of analogues of benzyl quinolone carboxylic acid (BQCA) as allosteric modulators of the M1 muscarinic receptor. *J. Med. Chem.* **56,** 5151–5172
55. Huang, X. P., Prilla, S., Mohr, K., and Ellis, J. (2005) Critical amino acid residues of the common allosteric site on the M2 muscarinic acetylcholine receptor: more similarities than differences between the structurally divergent agents gallamine and bis(ammonio)alkane-type hexamethylene-bis-[dimethyl-(3-phthalimidopropyl)ammonium]dibromide. *Mol. Pharmacol.* **68,** 769–778
56. May, L. T., Leach, K., Sexton, P. M., and Christopoulos, A. (2007) Allosteric modulation of G protein-coupled receptors. *Annu. Rev. Pharmacol. Toxicol.* **47,** 1–51
57. Voigtländer, U., Jöhren, K., Mohr, M., Raasch, A., Tränkle, C., Buller, S., Ellis, J., Höltje, H. D., and Mohr, K. (2003) Allosteric site on muscarinic acetylcholine receptors: identification of two amino acids in the muscarinic M2 receptor that account entirely for the M2/M5 subtype selectivities of some structurally diverse allosteric ligands in *N*-methylscopolamine-occupied receptors. *Mol. Pharmacol.* **64,** 21–31
58. Rasmussen, S. G., DeVree, B. T., Zou, Y., Kruse, A. C., Chung, K. Y., Kobilka, T. S., Thian, F. S., Chae, P. S., Pardon, E., Calinski, D., Mathiesen, J. M., Shah, S. T., Lyons, J. A., Caffrey, M., Gellman, S. H., Steyaert, J., Skiniotis, G., Weis, W. I., Sunahara, R. K., and Kobilka, B. K. (2011) Crystal structure of the β2 adrenergic receptor-Gs protein complex. *Nature* **477,** 549–555

CHAPTER 4

Mechanistic Insights into Allosteric Structure-Function Relationships at the M_1 Muscarinic Acetylcholine Receptor

Alaa Abdul-Ridha, J. Robert Lane, Shailesh N. Mistry, Laura López, Patrick M. Sexton, Peter Scammells, Arthur Christopoulos and Meritxell Canals

J. Biol. Chem, **298**: 33701-33711, November 2014.

Monash University

Declaration for Thesis Chapter 4

Declaration by candidate

In the case of Chapter 4, the nature and extent of my contribution to the work was the following:

Nature of contribution	**Extent of contribution (%)**
Development of ideas, participated in research design, conducted experiments, performed data analysis, contributed to the writing and editing of the manuscript.	70%

The following co-authors contributed to the work. If co-authors are students at Monash University, the extent of their contribution in percentage terms must be stated:

Name	**Nature of contribution**
J. Robert Lane	Participated in research design, performed data analysis, contributed to manuscript preparation
Shailesh N. Mistry	Participated in research design, performed compound synthesis, contributed to manuscript preparation
Laura López	Performed molecular modelling studies, contributed to the writing and editing of the manuscript
Patrick M. Sexton	Contributed to manuscript preparation
Peter J. Scammells	Participated in research design, performed compound synthesis, contributed to manuscript preparation
Arthur Christopoulos	Participated in research design, performed data analysis, contributed to manuscript preparation
Meritxell Canals	Development of ideas, participated in research design, performed data analysis, contributed to manuscript preparation

The undersigned hereby certify that the above declaration correctly reflects the nature and extent of the candidate's and co-authors' contributions to this work.

Candidate's Signature		**Date**
Main Supervisor's Signature		**Date**

Signal Transduction:

Mechanistic Insights into Allosteric Structure-Function Relationships at the M 1 Muscarinic Acetylcholine Receptor

Alaa Abdul-Ridha, J. Robert Lane, Shailesh N. Mistry, Laura López, Patrick M. Sexton, Peter J. Scammells, Arthur Christopoulos and Meritxell Canals

J. Biol. Chem. 2014, 289:33701-33711.
doi: 10.1074/jbc.M114.604967 originally published online October 17, 2014

THE JOURNAL OF BIOLOGICAL CHEMISTRY VOL. 289, NO. 48, pp. 33701–33711, November 28, 2014

Mechanistic Insights into Allosteric Structure-Function Relationships at the M_1 Muscarinic Acetylcholine Receptor*[S]

Received for publication, August 19, 2014, and in revised form, October 6, 2014 Published, JBC Papers in Press, October 17, 2014, DOI 10.1074/jbc.M114.604967

Alaa Abdul-Ridha[‡1,2], **J. Robert Lane**[‡1,3], **Shailesh N. Mistry**[§], **Laura López**[‡], **Patrick M. Sexton**[‡4], **Peter J. Scammells**[§], **Arthur Christopoulos**[‡4,5], **and Meritxell Canals**[‡6]

From the Departments of [‡]*Drug Discovery Biology and* [§]*Medicinal Chemistry, Monash Institute of Pharmaceutical Sciences and Department of Pharmacology, Monash University, Parkville, Victoria 3052, Australia*

Background: Selective and potent positive allosteric modulators (PAMs) of the M_1 mAChR have been recently described.
Results: Use of structural analogues and mutagenic mapping identified the mechanistic basis for increased PAM activity.
Conclusion: Combined analytical, structure-function, and modeling approaches uncover allosteric mechanisms at the M_1 mAChR.
Significance: New chemical space can be explored in the development of tailored M_1 mAChR PAMs.

Benzylquinolone carboxylic acid (BQCA) is the first highly selective positive allosteric modulator (PAM) for the M_1 muscarinic acetylcholine receptor (mAChR), but it possesses low affinity for the allosteric site on the receptor. More recent drug discovery efforts identified 3-((1*S*,2*S*)-2-hydroxycyclohexyl)-6-((6-(1-methyl-1*H*-pyrazol-4-yl)pyridin-3-yl)methyl)benzo[*h*]-quinazolin-4(3*H*)-one (referred to herein as benzoquinazolinone 12) as a more potent M_1 mAChR PAM with a structural ancestry originating from BQCA and related compounds. In the current study, we optimized the synthesis of and fully characterized the pharmacology of benzoquinazolinone 12, finding that its improved potency derived from a 50-fold increase in allosteric site affinity as compared with BQCA, while retaining a similar level of positive cooperativity with acetylcholine. We then utilized site-directed mutagenesis and molecular modeling to validate the allosteric binding pocket we previously described for BQCA as a shared site for benzoquinazolinone 12 and provide a molecular basis for its improved activity at the M_1 mAChR. This includes a key role for hydrophobic and polar interactions with residues Tyr-179, in the second extracellular loop (ECL2) and Trp-400$^{7.35}$ in transmembrane domain (TM) 7. Collectively, this study highlights how the properties of affinity and cooperativity can be differentially modified on a common structural scaffold and identifies molecular features that can be exploited to tailor the development of M_1 mAChR-targeting PAMs.

G protein-coupled receptors (GPCRs)[7] are the largest class of cell surface receptors and mediate major physiological processes. With over 800 GPCRs encoded by the human genome, they are the target of more than 30% of currently marketed drugs (1). The M_1 mAChR is one of five muscarinic receptor subtypes that belong to the family A GPCRs (2). Numerous drug discovery efforts have focused on developing selective ligands for this receptor subtype as potential therapies for neurocognitive disorders, such as Alzheimer's disease and schizophrenia (3, 4). Efforts aimed at targeting the highly conserved orthosteric (ACh) binding site have largely failed because of a lack of ligand subtype selectivity, whereas those targeting topographically distinct allosteric sites have proven more fruitful (5, 6). However, allosteric ligands can display complex behaviors, modulating orthosteric ligand affinity or efficacy and/or displaying direct agonism in their own right. A surge in family A GPCR crystal structures has provided considerable insights into the location of orthosteric binding pockets and the molecular mechanisms underlying ligand binding and receptor activation (7, 8). Of particular interest, the recent solution of a crystal structure of the M_2 mAChR co-bound with an allosteric modulator and an orthosteric agonist has given the first snapshot of a mechanism by which a modulator can act to enhance orthosteric agonist affinity (9). However, such information is currently lacking for other GPCRs, and both the structural and dynamic bases of how allosteric modulation is transmitted between spatially distinct binding sites remain largely unexplored. Thus, a combination of structure-activity and structure-function studies of GPCR allostery remains a vital approach to addressing some of these challenges, provided that this approach is enriched by analytical methods that can dissect

* This work was funded by National Health and Medical Research Council of Australia Program Grants APP1055134 (to A. C. and P. M. S.) and APP1049564 (to J. R. L.). The computational studies were supported by resource allocation scheme Grant VR0024 of the Victorian Life Sciences Computation Initiative on its Peak Computing Facility at the University of Melbourne.
[S] This article contains supplemental materials.
[1] These authors contributed equally to this work.
[2] Recipient of an Australian Postgraduate Award scholarship.
[3] R.D. Wright NHMRC Career Development Fellow.
[4] Principal Research Fellows of the National Health and Medical Research Council of Australia.
[5] To whom correspondence may be addressed: Drug Discovery Biology, Monash Inst. of Pharmaceutical Sciences, Monash University, 381 Royal Parade, Parkville, Victoria 3052, Australia [redacted]
[6] M.C. is a Monash Fellow. To whom correspondence may be addressed: Drug Discovery Biology, Monash Inst. of Pharmaceutical Sciences, Monash University, 381 Royal Parade, Parkville, Victoria 3052, Australia [redacted]

[7] The abbreviations used are: GPCR, G protein-coupled receptor; ACh, acetylcholine; ANOVA, analysis of variance; BQCA, benzylquinolone carboxylic acid; CCh, carbachol; mAChR, muscarinic acetylcholine receptor; TM, transmembrane domain; NMS, *N*-methylscopolamine.

structural effects on ligand binding from transmission of cooperativity and receptor activation.

In a recent study, we combined site-directed mutagenesis, analytical modeling, and molecular dynamics to delineate regions of the M_1 mAChR governing actions of the prototypical positive allosteric modulator, BQCA (10). This compound has emerged as a useful tool because it displays absolute subtype selectivity for the M_1 mAChR, has a very high positive cooperativity with ACh, displays a mechanism of action that appears in strict accordance with a simple two-state model of receptor activity (11), and has shown *in vivo* efficacy (6, 12). We identified several residues that contribute to the BQCA binding pocket as well as to the transmission of cooperativity with the orthosteric agonist, carbachol. Such residues were located in the ECL2 and at the top of TM2 and TM7. The BQCA binding pocket was proposed to partially overlap with the previously described "common" allosteric site in the extracellular vestibule of mAChRs (9, 13–16), suggesting that its high subtype selectivity derives from either additional contacts outside this region or through a subtype-specific cooperativity mechanism (17).

Unfortunately, both the therapeutic utility of BQCA and potential for deeper mechanistic insights into M_1 mAChR allostery afforded by this molecule remain limited, because BQCA has a very low affinity for the M_1 mAChR in the absence of co-bound agonist (11) and poor aqueous solubility. This has mechanistic implications in that it limits the ability to utilize loss of function mutagenesis approaches to distinguish key residues that govern modulator affinity (thus directly contributing to the allosteric binding site) *versus* residues that contribute to the transmission of the allosteric effect (thus indirectly contributing to the observed potency and selectivity). Such insights would be greatly facilitated by the availability of higher affinity allosteric probes. Encouragingly, recent drug discovery efforts resulted in the disclosure of putative allosteric M_1 mAChR ligands with higher functional potency than BQCA, although the mechanism of action remains to be definitively established for a number of these compounds (18–23). One such compound, 3-((1*S*,2*S*)-2-hydroxycyclohexyl)-6-((6-(1-methyl-1*H*-pyrazol-4-yl)pyridin-3-yl)methyl)benzo[*h*]quinazolin-4(3*H*)-one, referred to herein as benzoquinazolinone 12 (see Fig. 1), is of particular interest, because it is structurally derived from BQCA but has been reported to have substantially higher functional potency, on the basis of preliminary characterization (24, 25). However, its ultimate mechanism of action and the structural basis for its higher potency remain undetermined.

In the current study, we developed an optimized synthesis of benzoquinazolinone 12, report the first comprehensive pharmacological characterization of its allosteric properties, and use site-directed mutagenesis of specific M_1 mAChR amino acid residues to determine ligand-receptor interactions that govern the actions of this compound at the M_1 mAChR and explain its improved allosteric properties in comparison to BQCA. We also contextualize our experimental findings using molecular modeling and find that many of the key residues that form the allosteric binding pocket at the M_1 mAChR are structurally conserved in other mAChR subtypes (9, 13–15) and even other GPCRs (26, 27). Collectively, our results highlight how allosteric selectivity can be attained not only via selective affinity for a defined binding pocket but also by differential cooperativity between subtypes and can provide the basis for the design of novel M_1 mAChR-selective allosteric ligands.

EXPERIMENTAL PROCEDURES

Materials—CHO FlpIn cells and DMEM were purchased from Invitrogen. FBS was purchased from ThermoTrace (Melbourne, Australia). Hygromycin-B was purchased from Roche. [^{3}H]*N*-methylscopolamine ([^{3}H]NMS); specific activity, 84.1 Ci/mmol) and MicroScint scintillation liquid were purchased from PerkinElmer Life Sciences. IP-One assay kit and reagents were purchased from Cisbio (Codolet, France). All other chemicals were purchased from Sigma-Aldrich. BQCA and benzoquinazolinone 12 were synthesized in house as described in the supplemental materials.

Cell Culture and Receptor Mutagenesis—Mutations of the c-myc-hM_1 mAChR sequence were generated using the QuikChange site-directed mutagenesis kit (Agilent Technologies, La Jolla, CA) following the manufacturer's instructions. All mutations were confirmed by DNA sequencing (Australian Genome Research Facility, Melbourne, Australia). Mutant c-myc-hM_1 mAChR DNA constructs were transfected into FlpIn CHO cells (Invitrogen) and selected using 0.2 mg/ml hygromycin for stable expression.

Whole Cell Radioligand Binding Assays—Saturation binding assays were performed using cells plated at 10^4 cells per well in 96-well Isoplates (PerkinElmer Life Sciences). The following day, the cells were incubated with the orthosteric antagonist [^{3}H]NMS in a final volume of 100 μl of HEPES buffer (10 mM HEPES, 145 mM NaCl, 1 mM $MgSO_4{\cdot}7H_2O$, 10 mM glucose, 5 mM KCl, 2 mM $CaCl_2$, 1.5 mM $NaHCO_3$, pH 7.4) for 2 h at room temperature. For competition binding assays, cells were plated at 2.5×10^4 cells/well. The following day, cells were incubated in a final volume of 100 μl of HEPES buffer containing increasing concentrations of the competing cold ligand ACh (in the absence or presence of increasing concentrations of the allosteric modulator) in a humidified incubator for 1.5 h at 37 °C in the presence of 0.3 nM [^{3}H]NMS. Nonspecific binding was defined in the presence of 100 μM atropine. For all experiments, termination of the assay was performed by rapid removal of radioligand followed by two 100-μl washes with ice-cold 0.9% NaCl buffer. Radioactivity was determined by addition of 100 μl of Microscint scintillation liquid (PerkinElmer Life Sciences) to each well and counting in a MicroBeta plate reader (PerkinElmer Life Sciences).

IP-One Accumulation Assays—The IP-One assay kit (Cisbio, France) was used for the direct quantitative measurement of *myo*-inositol 1 phosphate (IP_1) in FlpIn CHO cells stably expressing either WT or mutant hM_1 mAChRs. Cells were seeded into 384-well Proxy plates (PerkinElmer Life Sciences) at 7,500 cells/well. The following day cells were stimulated with ACh in IP_1 stimulation buffer (10 mM HEPES, 1 mM $CaCl_2$, 0.5 mM $MgCl_2$, 4.2 mM KCl, 146 mM NaCl, 5.5 mM glucose, 50 mM LiCl, pH 7.4) in the absence or presence of increasing concentrations of the allosteric modulator and incubated for 1 h at 37 °C, 5% CO_2. Cells were lysed by the addition of homogenous time resolved FRET reagents, the cryptate-labeled anti-IP_1 antibody, and the d_2-labeled IP_1 analogue, followed by incuba-

tion for 1 h at room temperature. The emission signals were measured at 590 and 665 nm after excitation at 340 nm using the Envision multilabel plate reader (PerkinElmer Life Sciences), and the signal was expressed as the homogenous time resolved FRET ratio: $F = ((\text{fluorescence}_{665\ nm}/\text{fluorescence}_{590\ nm}) \times 10^4)$. Experiments using WT M_1 mAChR CHO FlpIn cells were performed in parallel each day.

Computational Methods for the Model of the Ligand-Receptor Complex—Our previously described hM_1 mAChR model was used for the structural study (10). Docking of the ligands was performed using MOE (Molecular Operating Environment Chemical Computing Group). ACh was docked manually into the receptor model with the quaternized nitrogen of the choline head group interacting with $Asp^{3.32}$ and the ester group situated toward TMIII–TMVI, resembling the position of the ligands described in the mAChR crystal structures (Protein Data Bank codes 3UON (28) and 4DAJ (29)). Benzoquinazolinone 12 was docked into the hM_1 mAChR allosteric binding site described for BQCA. The complex was subjected to an energy minimization using MMFF94X force field and was further refined by means of MD simulations (performed with NAMD2.9 (30) package) using a previously described protocol (31).

Data Analysis—All data were analyzed using Prism 6.01 (GraphPad Software, San Diego, CA). Inhibition binding curves between [^{3}H]NMS and unlabeled ligands were fitted to a one-site binding model (32). Binding interaction studies with allosteric ligands were fitted to the following allosteric ternary complex model (33),

$$Y = \frac{B_{max}[A]}{[A] + \left(\frac{K_A K_B}{\alpha'[B] + K_B}\right)\left(1 + \frac{[I]}{K_I} + \frac{[B]}{K_B} + \frac{\alpha[I][B]}{K_I K_B}\right)} \quad \text{(Eq. 1)}$$

where Y is the percentage (vehicle control) binding, B_{max} is the total number of receptors; [A], [B], and [I] are the concentrations of radioligand, allosteric modulator, and the orthosteric ligand, respectively; and K_A, K_B, and K_I are the equilibrium dissociation constants of the radioligand, allosteric modulator, and orthosteric ligand, respectively. α' and α are the binding cooperativities between the allosteric modulator and radioligand and the allosteric ligand and orthosteric ligand, respectively. Values of α (or α') that are >1 denote positive cooperativity, values of <1 (but >0) denote negative cooperativity, and a value of 1 denotes neutral cooperativity.

Concentration-response curves for the interaction between the allosteric ligand and the orthosteric ligand in the IP-One accumulation assays were globally fitted to the following operational model of allosterism and agonism (34),

$$E = \frac{E_m(\tau_A[A](K_B + \alpha\beta[B]) + \tau_B[B]K_A)^n}{([A]K_B + K_A K_B + [B]K_A + \alpha[A][B])^n + (\tau_A[A](K_B + \alpha\beta[B]) + \tau_B[B]K_A)^n} \quad \text{(Eq. 2)}$$

where E_m is the maximum possible cellular response; [A] and [B] are the concentrations of orthosteric and allosteric ligands, respectively; K_A and K_B are the equilibrium dissociation constant of the orthosteric and allosteric ligands, respectively; τ_A and τ_B are operational measures of orthosteric and allosteric ligand efficacy, respectively, α is the binding cooperativity parameter between the orthosteric and allosteric ligand, and β denotes the magnitude of the allosteric effect of the modulator on the efficacy of the orthosteric agonist. In many instances, the individual model parameters of Equation 2 could not be directly estimated via the nonlinear regression algorithm by analysis of the functional data alone, because of parameter redundancy. To facilitate model convergence, therefore, we fixed the equilibrium dissociation constant of each ligand to that determined from the whole cell binding assays. This practice assumes that the affinity determined in the whole cell binding assays is not significantly different from the "functional" affinity operative at the level of the signaling assay, which may not always be the case (35) and thus may lead to a systematic error in the estimate of the operational efficacy parameter, τ. However, because only a single pathway (IP_1) is being considered, the *relative* differences between τ values remain valid for statistical comparison purposes.

All affinity, potency, and cooperativity values were estimated as logarithms (36), and statistical comparisons between values were by one-way analysis of variance using a Dunnett's multiple comparison post test to determine significant differences between mutant receptors and the WT M_1 mAChR. A value of $p < 0.05$ was considered statistically significant.

RESULTS

Identification of Benzoquinazolinone 12 as a Selective Positive Allosteric Modulator of the M_1 mAChR with Higher Affinity than BQCA—In a patent from Merck (25), a series of aryl methyl benzoquinazolinone compounds were disclosed as selective positive allosteric modulators of the M_1 mAChR. One such compound, 3-((1*S*,2*S*)-2-hydroxycyclohexyl)-6-((6-(1-methyl-1*H*-pyrazol-4-yl)pyridin-3-yl)methyl)benzo[*h*]quinazolin-4(3*H*)-one (referred to herein as benzoquinazolinone 12; Fig. 1*A*), was identified as a potent and selective modulator based on its ability to potentiate a single EC_{20} concentration of ACh in a calcium mobilization assay (25, 37). We developed an optimized synthesis, improving the overall yield (Scheme S1 in the supplemental materials) of this compound, followed by detailed pharmacological characterization. We performed whole cell equilibrium competition binding using the radiolabeled antagonist [^{3}H]NMS to study the interaction between ACh and benzoquinazolinone 12. An allosteric ternary complex model (Equation 1) was applied to the data to obtain estimates of modulator affinity for the M_1 mAChR (pK_B), and its binding cooperativity with ACh (Log α) (Fig. 2 and Table 1). This revealed that compared with the prototypical M_1 mAChR positive allosteric modulator BQCA, benzoquinazolinone 12 displays a greater than 50-fold increase in affinity for the M_1 mAChR (Fig. 1*B*, $K_B = 15\ \mu M$ and $K_B = 0.3\ \mu M$, for BQCA and benzoquinazolinone 12, respectively) while maintaining a similar level of positive cooperativity with ACh (Fig. 2*A* and Table 1). Interestingly, the modulator displayed high negative cooperativity with the inverse agonist radioligand, which is also a property shared by BQCA (11). Moreover, we confirmed the absolute subtype selectivity of benzoquinazolinone 12 in bind-

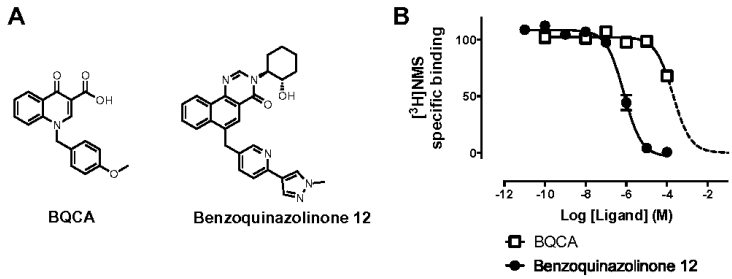

FIGURE 1. *A*, chemical structure of M_1 mAChR-selective positive allosteric modulators. *Left panel*, BQCA. *Right panel*, benzoquinazolinone 12. *B*, BQCA and benzoquinazolinone 12 inhibit the equilibrium binding of [^{3}H]NMS. Data points represent the means ± S.E. of three independent experiments performed in triplicate.

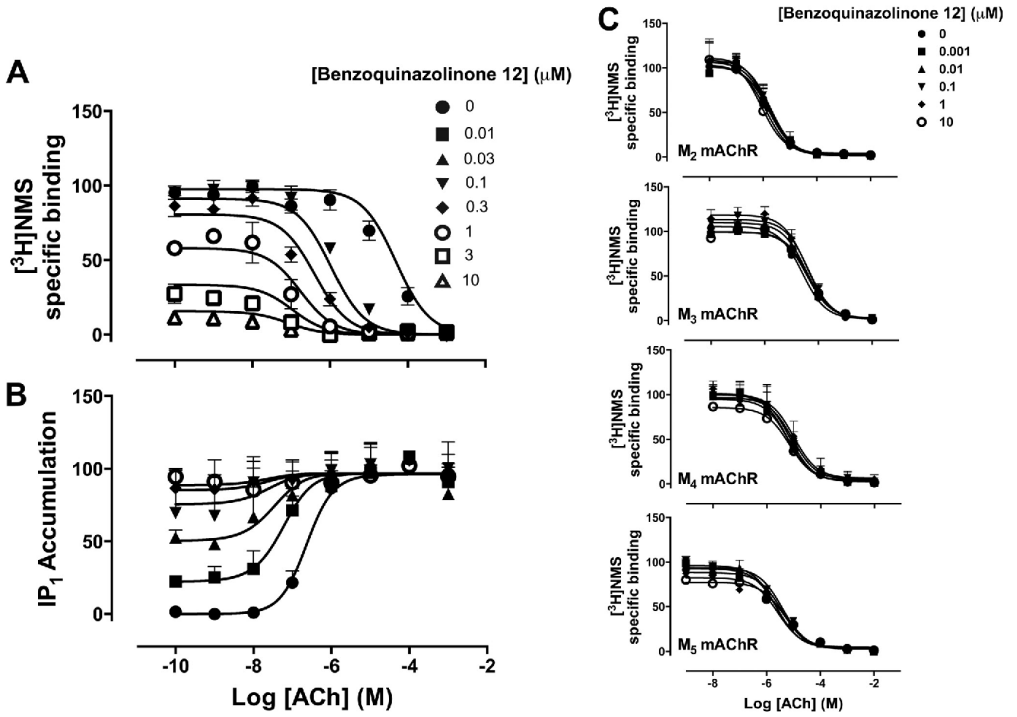

FIGURE 2. **Pharmacological characterization of benzoquinazolinone 12, a high affinity positive allosteric modulator of the M_1 mAChR.** *A*, whole cell radioligand competition binding between [^{3}H]NMS and increasing concentrations of ACh in the absence or presence of increasing concentrations of benzoquinazolinone 12 in CHO FlpIn cells stably expressing WT M_1 mAChR. *B*, interaction between ACh and benzoquinazolinone 12 in an IP_1 accumulation assay in CHO FlpIn cells stably expressing WT M_1 mAChR. *C*, whole cell radioligand competition binding between [^{3}H]NMS and increasing concentrations of ACh in the absence or presence of increasing concentrations of benzoquinazolinone 12 in CHO FlpIn cells stably expressing WT M_{2-5} mAChR. The *curves* in *A* and *C* represent the best fit of an allosteric ternary complex model (Equation 1). The *curves* in *B* represent the best fit of an operational allosteric model (Equation 2).

ing studies using cells expressing the M_2, M_3, M_4, and M_5 mAChRs. As shown in Fig. 2*C*, benzoquinazolinone 12 does not modulate the affinity of ACh at any of these receptor subtypes. We next extended our characterization of this ligand to functional assays. Using IP_1 accumulation as a canonical measure of M_1 mAChR activation resulting from preferential activation of $G\alpha_q$ proteins, and analysis of the data by applying an operational model of allostery (Equation 2), we found that both functional cooperativity (Log $\alpha\beta$) and the intrinsic efficacy (Log τ_B) of benzoquinazolinone 12 were similar to those determined for BQCA (Table 1 and Fig. 2*B*). It was of interest, therefore, to determine the structural basis of the improved allosteric action of benzoquinazolinone 12 as compared with BQCA at the level of receptor residues that this ligand engages and confirm whether benzoquinazolinone 12 engages the same allosteric site as that which we have proposed for BQCA (10).

Effect of Amino Acid Substitution to Ala on the Binding and Function of Benzoquinazolinone 12—As shown above, our pharmacological characterization revealed that benzoquinazolinone 12 displayed a 50-fold increase in allosteric site affinity as compared with BQCA (Table 1). Using a structure-function approach, we next sought to investigate whether benzoquinazolinone 12 binds to the same allosteric pocket as BQCA and the ligand-receptor interactions that govern its binding affinity and cooperativity with ACh.

We focused our investigation on the three amino acid residues we recently identified as contributing to the BQCA binding pocket at the M_1 mAChR (Tyr-$85^{2.64}$ in TM2, Tyr-179 in ECL2, and Trp-$400^{7.35}$ in TM7) (10). In addition, we included Tyr-$82^{2.61}$ in TM2, which is conserved in the related M_2 mAChR and previously identified to contribute to the binding pocket of several allosteric modulators at that subtype (9, 13, 15). Each of these aromatic residues was mutated to Ala, and the mutant M_1 mAChRs were stably expressed in FlpIn CHO cells. Only $W400^{7.35}$A showed >50% reduction in cell surface receptor expression compared with the WT (Table 2). The equilibrium dissociation constants of the orthosteric antagonist [^{3}H]NMS (pK_A) and the orthosteric agonist ACh (pK_I) were significantly reduced at $Y82^{2.61}$A and $Y85^{2.64}$A, whereas only ACh affinity was reduced at $W400^{7.35}$A (Table 2), consistent with previously published findings (13, 14, 38–40).

We then investigated the effect of each of these mutations on the affinity and function of benzoquinazolinone 12. Binding interaction studies revealed that although the affinity of BQCA (pK_B) and its binding cooperativity with ACh (Log α) were not affected by the $Y82^{2.61}$A mutation, benzoquinazolinone 12 displayed a significantly reduced affinity at this mutant receptor with no significant change in its binding cooperativity with ACh (Tables 3 and 4 and Fig. 3, *top* and *middle panels*). Similarly, the pK_B and Log α of BQCA were not affected by the $Y85^{2.64}$A mutation; however, the pK_B (but not the binding cooperativity) of benzoquinazolinone 12 were significantly lower compared with WT. A Tyr in ECL2 (Tyr-179 in the M_1 mAChR) has been found in numerous studies to be involved in the binding of allosteric ligands at the mAChR family (10, 12–15). As shown in Tables 3 and 4 and Fig. 3 (*top* and *middle panels*), mutation of this residue has a profound effect on both BQCA and benzoquinazolinone 12, although mechanistically the effect on BQCA appears to be via reduced cooperativity with ACh, whereas the effect on benzoquinazolinone 12 is a ~100-fold reduction in its affinity for the allosteric site. In contrast, Ala substitution of the conserved Trp-$400^{7.35}$ residue in TM7 completely abolished the binding of both BQCA and benzoquinazolinone 12 (Table 3 and Fig. 3, *top* and *middle panels*), suggesting that this residue is a key direct contributor to the allosteric binding pocket. It is also interesting to note that the binding cooperativity between ACh with benzoquinazolinone 12 was not significantly different from WT at any of the Ala mutants with the exception of $W400^{7.35}$A. As such, these aromatic residues appear to be critical for the binding of benzoquinazolinone 12 but do not participate in the transfer of cooperativity between benzoquinazolinone 12 and the ACh binding site.

Analysis of the allosteric modulator effects at the Ala mutants using an IP_1 accumulation assay revealed that the functional cooperativity (Log $\alpha\beta$) of benzoquinazolinone 12 with ACh is increased at $Y82^{2.61}$A but not affected by Ala substitution at Tyr-$85^{2.64}$ (Table 4 and Fig. 3, *bottom panel*). At both Y179A and $W400^{7.35}$A, BQCA showed no potentiation of ACh. However, in the case of benzoquinazolinone 12 at Y179A,

TABLE 1

Allosteric modulator pharmacological parameters at the WT M_1 mAChR

Estimated parameter values represent the means ± S.E. of three experiments performed in duplicate. pK_B and Log α values were obtained from analysis of the binding interaction data with Equation 1, whereas Log $\alpha\beta$ and Log τ_B values were obtained from analysis of functional interaction data according to Equation 2.

Ligand	pK_B[a]	Log α[b]	Log $\alpha\beta$[c]	Log τ_B[d]
BQCA	4.82 ± 0.09	1.90 ± 0.14	1.54 ± 0.15	0.35 ± 0.07
Benzoquinazolinone 12	6.55 ± 0.03[e]	2.14 ± 0.06	1.79 ± 0.21	0.87 ± 0.20

[a] Negative logarithm of the equilibrium dissociation constant of the modulator
[b] Logarithm of the binding cooperativity factor between the modulator and ACh as estimated by Equation 1; for this analysis, the pK_A of [^{3}H]NMS was constrained to 9.92, and the cooperativity between [^{3}H]NMS with each of the modulators was constrained to −2, consistent with high negative cooperativity between the two ligands.
[c] Logarithm of the functional cooperativity between ACh and the modulator.
[d] Logarithm of the operational efficacy parameter for the modulator.
[e] Significantly different ($p < 0.05$), from BQCA as determined by one-way ANOVA with Dunnett's post hoc test.

TABLE 2

Whole cell equilibrium binding and functional parameters for [^{3}H]NMS and ACh at the WT and mutant M_1 mAChRs

The values represent the means ± S.E. of three experiments performed in duplicate. ND, not determined.

	B_{max}[a]	pK_A[b]	pK_I[c]	pEC_{50}[d]	Log τ_A[e]
M_1 WT	415 ± 15	9.92 ± 0.01	5.11 ± 0.08	6.56 ± 0.11	1.74 ± 0.05
$Y82^{2.61}$A	225 ± 7[f,g]	9.76 ± 0.01[f,g]	4.29 ± 0.07[g]	5.64 ± 0.10[g]	1.02 ± 0.08[g]
$Y85^{2.64}$A	398 ± 10[f]	9.82 ± 0.03[f,g]	4.65 ± 0.06[g]	5.23 ± 0.08[g]	0.57 ± 0.05[g]
Y179A	270 ± 14[f,g]	10.00 ± 0.02[f]	5.05 ± 0.08	5.37 ± 0.12[g]	0.82 ± 0.03[g]
$W400^{7.35}$A	138 ± 6[f,g]	9.95 ± 0.01[f]	4.62 ± 0.08[g]	4.84 ± 0.04[g]	ND
$Y82^{2.61}$F	280 ± 12[g]	10.39 ± 0.01[g]	5.24 ± 0.08	5.59 ± 0.09[g]	0.96 ± 0.06[g]
$Y85^{2.64}$F	295 ± 12[g]	10.04 ± 0.01	4.98 ± 0.09	5.54 ± 0.08[g]	1.09 ± 0.05[g]
Y179F	280 ± 10[g]	9.95 ± 0.07	5.24 ± 0.08	5.68 ± 0.10[g]	0.94 ± 0.08[g]
Y179W	304 ± 8[g]	9.85 ± 0.03	5.08 ± 0.09	5.42 ± 0.09[g]	0.86 ± 0.09[g]
$W400^{7.35}$F	170 ± 12[g]	10.04 ± 0.01	4.82 ± 0.07	5.29 ± 0.09[g]	1.00 ± 0.03[g]
$W400^{7.35}$Y	230 ± 16[g]	10.31 ± 0.05[g]	5.21 ± 0.05	5.86 ± 0.06[g]	1.28 ± 0.06[g]

[a] Maximum density of binding sites per 10^4 cells in counts/min.
[b] Negative logarithm of [^{3}H]NMS equilibrium dissociation constant.
[c] Negative logarithm of ACh equilibrium dissociation constant.
[d] Negative logarithm of the EC_{50} value.
[e] Logarithm of the operational efficacy parameter for ACh as estimated by Equation 2, corrected for changes in receptor expression to allow comparison with WT.
[f] Values taken from the results of Abdul-Ridha *et al.* (10).
[g] Significantly different ($p < 0.05$), from WT value as determined by one-way ANOVA with Dunnett's post hoc test.

TABLE 3

Allosteric modulator equilibrium dissociation constants (pK_B) and binding cooperativity (Log α) estimates for the interaction with ACh at the WT and mutant M_1 mAChRs

Estimated parameter values represent the means ± S.E. of three or four experiments performed in duplicate. pK_B is the negative logarithm of the equilibrium dissociation constant of the modulator, as estimated by Equation 1 from binding interaction studies with ACh; for this analysis, the pK_A of [^{3}H]NMS for the WT and each of the mutants was constrained to the values listed in Table II. The cooperativity between [^{3}H]NMS with each of the modulators was constrained to −2, consistent with high negative cooperativity between the two ligands. ND, not determined (no allosteric modulation).

	pK_B		Log α	
	BQCA	Benzoquinazolinone 12	BQCA	Benzoquinazolinone 12
M_1 WT	4.82 ± 0.06	6.55 ± 0.03	1.90 ± 0.14	2.14 ± 0.06
$Y82^{2.61}A$	4.73 ± 0.06	5.28 ± 0.03[a]	1.96 ± 0.14	2.62 ± 0.15
$Y85^{2.64}A$	4.86 ± 0.08	5.37 ± 0.06[a]	1.53 ± 0.13	2.08 ± 0.11
Y179A	4.68 ± 0.08	4.56 ± 0.19[a]	−0.16 ± 0.28[a]	2.18 ± 0.22
$W400^{7.35}A$	ND	ND	ND	ND
$Y82^{2.61}F$	4.99 ± 0.07	5.67 ± 0.07[a]	1.72 ± 0.14	2.23 ± 0.14
$Y85^{2.64}F$	4.66 ± 0.00	5.86 ± 0.06[a]	1.35 ± 0.15	2.09 ± 0.15
Y179F	4.72 ± 0.07	6.15 ± 0.05[a]	1.88 ± 0.13	2.04 ± 0.13
Y179W	5.06 ± 0.05	6.69 ± 0.04	2.11 ± 0.13	1.78 ± 0.14
$W400^{7.35}F$	4.44 ± 0.08[a]	5.22 ± 0.08[a]	0.83 ± 0.16[a]	2.25 ± 0.15
$W400^{7.35}Y$	4.27 ± 0.10[a]	5.34 ± 0.07[a]	1.50 ± 0.10	2.06 ± 0.14

[a] Significantly different ($p < 0.05$), from WT value as determined by one-way ANOVA with Dunnett's post hoc test.

TABLE 4

Functional cooperativity (Log $\alpha\beta$) estimates for the interaction between the allosteric modulators and ACh at the WT and mutant M_1 mAChRs

Estimated parameter values represent the means ± S.E. of three or four experiments performed in duplicate. Log $\alpha\beta$ is the logarithm of the functional cooperativity factor between the modulator and ACh as estimated by Equation 2. For this analysis, the pK_i values for ACh were fixed to those determined from the radioligand binding assays as listed in Table 2. ND, not determined (no allosteric modulation).

	Log $\alpha\beta$	
	BQCA	Benzoquinazolinone 12
M_1 WT	1.54 ± 0.15	1.79 ± 0.21
$Y82^{2.61}A$	1.93 ± 0.10	2.76 ± 0.27[a]
$Y85^{2.64}A$	1.49 ± 0.04	1.96 ± 0.04
Y179A	ND	1.82 ± 0.14
$W400^{7.35}A$	ND	ND
$Y82^{2.61}F$	1.46 ± 0.20	2.01 ± 0.32
$Y85^{2.64}F$	0.58 ± 0.08[a]	1.82 ± 0.23
Y179F	1.26 ± 0.15	2.15 ± 0.30
Y179W	1.68 ± 0.11	2.53 ± 0.23
$W400^{7.35}F$	0.45 ± 0.07[a]	0.90 ± 0.11
$W400^{7.35}Y$	1.10 ± 0.11	0.57 ± 0.09[a]

[a] Significantly different ($p < 0.05$), from WT value as determined by one-way ANOVA with Dunnett's post hoc test.

potentiation was similar to WT but was abolished at the $W400^{7.35}A$ mutation. The intrinsic efficacy (Log τ_B) of both BQCA and benzoquinazolinone 12 was abolished at each of the M_1 mAChR Ala mutants with the exception of benzoquinazolinone 12 at $Y82^{2.61}A$, where Log τ_B (0.73 ± 0.20) was unchanged relative to WT values (Table 1).

The combined data from the Ala mutation experiments reveal that Tyr-179 in ECL2 and Trp-$400^{7.35}$, residues shown to be of key importance for the activity of BQCA, are also important for the binding of benzoquinazolinone 12. This is consistent with both ligands binding to the same allosteric site within the M_1 mAChR. Furthermore, these results reveal that mutation of Tyr-179 reduces benzoquinazolinone 12 binding affinity but not cooperativity. It is interesting to note that although BQCA was unaffected by both $Y82^{2.61}A$ and $Y85^{2.64}A$ mutations, this was not the case for benzoquinazolinone 12. As such, the replacement of the methoxy group with an aromatic substituent at the 4-position of the benzylic pendant of BQCA or the replacement of the carboxylic acid with the corresponding 3-((1*S*,2*S*)-2-hydroxycyclohexyl) group present in benzoquinazolinone 12 must confer sensitivity to mutation of these TM2 residues.

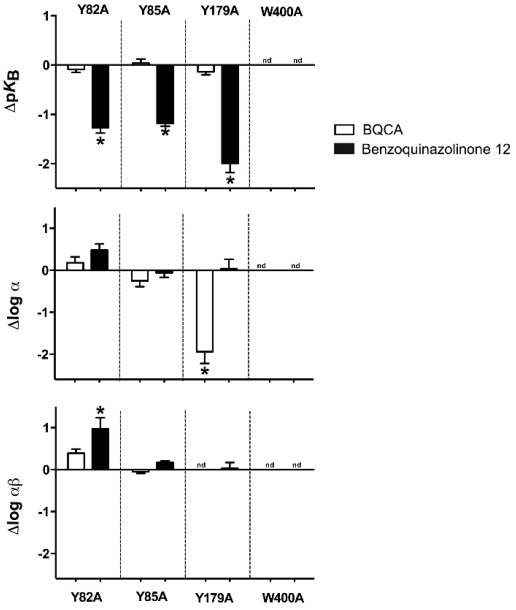

FIGURE 3. **Effect of M_1 mAChR Ala mutations on the binding and function of BQCA and benzoquinazolinone 12.** The *bars* represent the difference for each mutant receptor in allosteric ligand affinity (pK_B, *top panel*), binding cooperativity value (Log α, *middle panel*), or functional cooperativity value (Log $\alpha\beta$, *bottom panel*) of BQCA and benzoquinazolinone 12 relative to WT. The values are derived from interaction experiments in [^{3}H]NMS radioligand binding and IP_1 accumulation (Tables 3 and 4). *, significantly different ($p < 0.05$) from WT as determined by one-way ANOVA with Dunnett's post hoc test. *nd*, not determined (no allosteric modulation).

Molecular Dynamics Simulations and Ligand Docking of Benzoquinazolinone 12 and Comparison with BQCA—To rationalize our findings, we performed ligand docking and molecular dynamic simulations. This resulted in one main pose of benzoquinazolinone 12 in an M_1 mAChR in which ACh was co-bound. This was then compared with the complex of BQCA with carbachol (CCh) bound to the M_1 mAChR obtained using the same methodology in our previous study (10). The complex

for benzoquinazolinone 12 and ACh bound to the modeled M_1 mAChR is shown in Fig. 4. As for CCh in our previous study and analogous to that observed in receptor crystal structure of the M_2 mAChR in complex with the agonist iperoxo (9), Asp-$105^{3.32}$ engages the quaternized choline head group of ACh. Furthermore, ACh lies within a hydrophobic pocket formed by residues Tyr-$106^{3.33}$, Trp-$157^{4.57}$, Tyr-$381^{6.51}$, and Tyr-$408^{7.43}$. In the BQCA-bound complex, stability is added to this binding pocket through a network of hydrogen bond interactions between Tyr-$381^{6.51}$, Tyr-$106^{3.33}$, and Tyr-$404^{7.39}$ (10). These Tyr residues essentially form an aromatic lid over ACh via cation-π interactions. It is interesting to note that in the case of the complex with benzoquinazolinone 12 bound, although the interaction between Tyr-$381^{6.51}$ and Tyr-$106^{3.33}$ is maintained, Tyr-$404^{7.39}$ faces TM2 and interacts with Tyr-$82^{2.61}$ (Fig. 4).

Analysis of the molecular dynamics trajectories reveals that both BQCA and benzoquinazolinone 12 adopt a similar pose (Fig. 5). In both cases, the binding site for the ligands is defined by residues from TM2, TM7, and ECL2 and is in agreement with our mutagenesis studies. In particular, the significant effects of the mutation of Tyr-179 to Ala in ECL2 and Trp-$400^{7.35}$ in TM7 on the pharmacology of BQCA and benzoquinazolinone 12 can be reconciled with the poses of each ligand. In both BQCA and benzoquinazolinone 12 complexes, Tyr-179 is predicted to contribute to the stable binding of the compounds via hydrophobic/edge to face π-π interactions with the bicyclic 4-oxoquinoline core of BQCA or tricyclic benzo-[*h*]quinazolin-4(3*H*)-one core of benzoquinazolinone 12. In addition, the hydroxyl group of Tyr-179 may form a polar or potential hydrogen bond interaction with the OH group of the 3-((1*S*,2*S*)-2-hydroxycyclohexyl) moiety of benzoquinazolinone 12. This interaction cannot take place in the BQCA bound complex, because BQCA does not bear the corresponding amide moiety. Trp-$400^{7.35}$ is predicted to interact with the benzylic pendant of both BQCA and benzoquinazolinone 12. However, in the BQCA bound complex, Trp-$400^{7.35}$ is positioned horizontally below the benzylic pendant of BQCA and is predicted to make a π-π stacking interaction with this moiety (Fig. 5*A*). In comparison, to accommodate the additional *N*-methylpyrazole substituent of benzoquinazolinone 12, Trp-$400^{7.35}$ is positioned in a more vertical orientation and extends toward TM6. This orientation allows the following interactions: (*a*) edge to face π-π/hydrophobic interactions with the *N*-methylpyrazole substituent of benzoquinazolinone 12, (*b*) hydrophobic sandwich of pyrazole substituent between Trp-$400^{7.35}$ and Tyr-179, (*c*) a π-π stacking interaction with Phe-182 in ECL2,

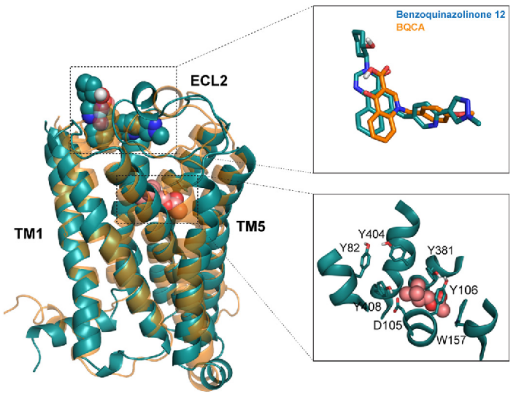

FIGURE 4. **Structural homology model of the M_1 mAChR complex co-bound with CCh-BQCA (*orange*) or ACh-benzoquinazolinone 12 (*blue*).** The overall structure of the BQCA-bound M_1 mAChR model (*orange*) is similar to that of the benzoquinazolinone 12-bound M_1 mAChR model (*blue*). ACh (*pink*), BQCA (*orange*), and benzoquinazolinone 12 (*blue*) are shown as *spheres* colored according to element. *Top inset*, overlay of the BQCA (*orange*) and benzoquinazolinone 12 (*blue*) poses represented as stick structures. *Bottom inset*, ACh binding site in benzoquinazolinone 12-bound M_1 mAChR complex model. Important residues are shown as *sticks*.

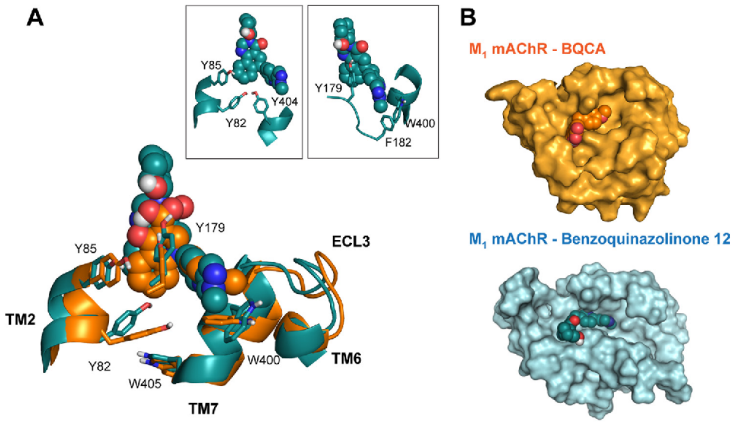

FIGURE 5. **Proposed arrangement of the binding sites of BQCA and benzoquinazolinone 12 at the M_1 mAChR.** *A*, extracellular view of the binding sites of BQCA and benzoquinazolinone 12. BQCA (*orange*) and benzoquinazolinone 12 (*blue*) are shown as *spheres* colored according to element. Important residues are shown as sticks. *Insets*, positions of Tyr-$2^{2.61}$, Tyr-$85^{2.64}$, Tyr-$404^{7.39}$, Tyr-179, Phe-182, and Trp-$400^{7.35}$ in the ACh-benzoquinazolinone 12-bound M_1 mAChR model. *B*, extracellular view of the BQCA-bound (*orange*) and benzoquinazolinone 12-bound (*blue*) M_1 mAChR models showing a tighter pocket for benzoquinazolinone 12 as compared with that predicted for BQCA.

which appears to pull ECL2 toward TM7, creating a tighter allosteric binding pocket as compared with that observed in the BQCA bound complex (Fig. 5, *A* and *B*). The additional interactions observed in the complex with benzoquinazolinone 12 can explain, in part, the increased affinity of benzoquinazolinone 12 as compared with BQCA. The TM2 residues Tyr-85$^{2.64}$ and Tyr-82$^{2.61}$ are predicted to delimit the allosteric site in both complexes via edge to face π-π/hydrophobic interactions with the 4-oxoquinoline ring system in the case of BQCA. However, the tricyclic core of benzoquinazolinone 12 is closer to TM2 (Fig. 5*A*), allowing π interactions with both residues, which may also contribute to the higher binding affinity of benzoquinazolinone 12. In agreement with this pose, mutation of both Tyr-85$^{2.64}$ and Tyr-82$^{2.61}$ caused a greater than 10-fold loss of affinity for benzoquinazolinone 12, whereas no effect upon the affinity of BQCA was observed. The closer interaction of Tyr-82$^{2.61}$ with benzoquinazolinone 12 may allow for increased ligand-receptor hydrophobic interactions that may account for the higher binding affinity of this ligand at the allosteric binding site (Fig. 5, *A* and *B*). Of interest, Tyr-82$^{2.61}$ makes a H-bond interaction with Tyr-404$^{7.39}$, one of the residues that forms the aromatic 'lid' over the CCh binding site in the BQCA bound complex. As such, this interaction may provide part of the cooperative mechanism through which binding of benzoquinazolinone 12 to the allosteric pocket modulates the shape of and ligand receptor interactions within the orthosteric pocket.

Effect of Conservative Amino Acid Substitution on the Binding and Function of BQCA and Benzoquinazolinone 12—Our mutagenesis and modeling studies highlight the particular importance of Tyr-85$^{2.64}$ and Tyr-82$^{2.61}$ in TM2, Tyr-179 in ECL2, and Trp-400$^{7.35}$ in TM7. However, such an Ala scanning approach, although useful to highlight the importance of individual residues for the binding of a ligand, can only give limited information regarding the nature of these interactions. In particular our modeling studies suggested that Tyr-85$^{2.64}$, Tyr-82$^{2.61}$, and Tyr-179 might participate in a hydrogen bond network with the ligand and/or with other residues in the complex with benzoquinazolinone 12 but not in the BQCA complex. To further understand the contribution of each of the aromatic amino acid residues to the allosteric binding pocket, we tested the effects of more subtle amino acid substitutions on ligand binding and function. We mutated each Tyr residue (Tyr-82$^{2.61}$, Tyr-85$^{2.64}$, and Tyr-179) or Trp-400$^{7.35}$ to Phe. In addition, we mutated Tyr-179 to Trp with the expectation that this larger, bicyclic aromatic residue would be able to make stronger interactions with the benzylic pendant of both ligands as suggested from our BQCA analogues SAR data (41), Ala mutation data, and modeling results. We compared the effects of these mutations upon the pharmacology of both BQCA and benzoquinazolinone 12 (Fig. 6).

As with the Ala substitutions, we first tested the effects of the mutants on orthosteric ligand binding and cell surface receptor expression. Whole cell [^{3}H]NMS saturation binding experiments showed that all the mutations led to a significant reduction in cell surface receptor expression compared with the WT (Table 2). The maximum decrease in receptor expression relative to WT was ~2-fold at Trp-400$^{7.35}$F. In addition to receptor expression, the equilibrium dissociation constant of the

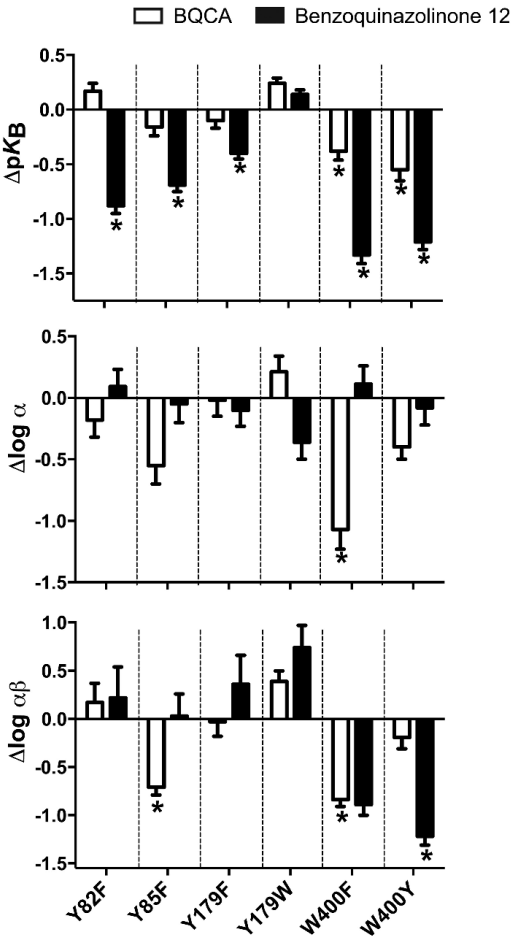

FIGURE 6. **Effect of M_1 mAChR conservative mutations on the binding and function of BQCA and benzoquinazolinone 12.** The *bars* represent the difference for each mutant receptor in allosteric ligand affinity (pK_B, *top panel*), binding cooperativity value (Log α, *middle panel*), or functional cooperativity value (Log $\alpha\beta$, *bottom panel*) of BQCA and benzoquinazolinone 12 relative to WT. The values are derived from interaction experiments in [^{3}H]NMS radioligand binding and IP_1 accumulation (Tables 3 and 4). *, significantly different ($p < 0.05$) from WT as determined by one-way ANOVA with Dunnett's post hoc test.

orthosteric antagonist [^{3}H]NMS (pK_A) or the orthosteric agonist ACh (pK_I) were also determined (Table 2). Y82$^{2.61}$F and W400$^{7.35}$Y caused slight but significant increases in [^{3}H]NMS affinity. The remaining mutants had no effect on orthosteric ligand binding. The potency (EC_{50}) of ACh in IP_1 assays was significantly reduced at all the mutants, likely because of the reduction in receptor surface expression (Table 2).

To determine the effects of each mutant on allosteric ligand binding affinity (pK_B) and cooperativity (Log α) with ACh, we performed whole cell binding interaction studies for both BQCA and benzoquinazolinone 12. The pK_B and Log α of

BQCA were unchanged at the Tyr to Phe mutants (Y85$^{2.64}$F, Y82$^{2.61}$F, and Y179F) (Table 3), suggesting that the ability of these residues to make hydrophobic, rather than polar, interactions is predominant for their role in BQCA binding and function. In contrast, substitution of the conserved aromatic residue Trp-400 to less bulky aromatic amino acids (W400$^{7.35}$F and W400$^{7.35}$Y) caused significant reductions in BQCA and benzoquinazolinone 12 binding affinity (Table 3). Interestingly, substitution of Tyr-85$^{2.64}$ and Tyr-82$^{2.61}$ in TM2 and Tyr-179 in ECL2 to Phe resulted in significant decreases in the binding affinity of benzoquinazolinone 12. This suggests that the ability to make polar interactions has a significant contribution to their role in the binding of benzoquinazolinone 12 and is in agreement with the network of interactions predicted by our modeling experiments. Replacement of Tyr-179 with a Trp did not significantly change the affinity of either BQCA or benzoquinazolinone 12. The binding cooperativity of BQCA with ACh was only reduced at W400$^{7.35}$F (Table 3). Interestingly, and in agreement with the results at the corresponding Ala mutants, the binding cooperativity of benzoquinazolinone 12 with ACh was not significantly changed at any of these conservative mutants (Table 3).

We extended our study to look at the effect of these mutations upon the action of BQCA and benzoquinazolinone 12 in a functional assay. Analysis of the allosteric potentiation of ACh by BQCA in an IP_1 accumulation assay revealed that the functional cooperativity was profoundly reduced at Y85$^{2.64}$F and W400$^{7.35}$F, although benzoquinazolinone 12 showed reduced cooperativity with ACh at W400$^{7.35}$Y but not the other mutations. Both ligands showed unchanged cooperativity at Y179W (Table 4), in agreement with the binding results.

DISCUSSION

Significant efforts have been directed at the discovery of novel selective ligands of the M_1 mAChR as a therapeutic approach for neurocognitive disorders, such as Alzheimer's disease (3, 42). From these efforts, the compounds that display the most exquisite selectivity target an allosteric site of this receptor, as exemplified by BQCA (6, 12). More recently, benzoquinazolinone 12, an analogue of BQCA, was described as a modulator with improved allosteric activity (25). We have now provided a detailed characterization of benzoquinazolinone 12, demonstrating that its increase in activity at the M_1 mAChR as compared with BQCA is largely derived from an approximately 50-fold increase in affinity, whereas both functional and binding cooperativity with ACh are not substantially changed. Furthermore, benzoquinazolinone 12 not only displays high positive cooperativity with agonist binding but also high negative cooperativity with the binding of the orthosteric antagonist [^{3}H]NMS. Thus, benzoquinazolinone 12 appears to conform to the classic Monod-Wyman-Changeux mechanism of action previously described for BQCA (11).

Our previous SAR study of derivatives of BQCA revealed four discrete areas of structural modification that conferred distinct effects on the allosteric activity of these compounds (41). Alternative substitution of the 5- and 8-positions of the quinolone ring appeared to modulate intrinsic efficacy (τ_B); isosteric replacement of the carboxylic acid moiety or amide derivatives modulated cooperativity parameters (α and β) and, finally, replacement of the pendant *N*-alkyl group modulated affinity (pK_B). The ability to enrich allosteric SAR by dissecting these molecular parameters can also be used to link these parameters to receptor structural information, thus yielding new insights into the structural basis of allostery. In the current study, we applied this approach to explore the structural basis of the improved allosteric activity of benzoquinazolinone 12 at the M_1 mAChR in comparison to BQCA. This is important, because the location and nature of the allosteric site for most GPCRs remains poorly characterized. Our combined mutagenesis and molecular modeling experiments provide evidence that BQCA and benzoquinazolinone 12 occupy a similar pocket of the M_1 mAChR. In our previous study, we proposed that Tyr-179 (in ECL2) and Trp-400$^{7.35}$ were of key importance for the activity of BQCA (10). In the current work, we confirmed this result and found that the W400$^{7.35}$A mutation abrogated detectable binding of compound benzoquinazolinone 12, whereas the compound also displayed a 100-fold decrease in affinity at the Y179A mutant. However, this latter mutation had no effect upon the cooperativity of benzoquinazolinone 12. In agreement with the role of Tyr-179 as a determinant of both BQCA and benzoquinazolinone 12 affinity or transmission of cooperativity, our modeling studies reveal that this residue provides hydrophobic/edge to face π-π interactions with the bicyclic core of BQCA or tricyclic core of benzoquinazolinone 12, although the rotameric orientation of the residue differs slightly depending on the molecule bound. Indeed, mutation of this Tyr to the aromatic residues Phe or Trp had no effect, confirming that Tyr-179 makes predominantly hydrophobic interactions with both ligands. Trp-400$^{7.35}$ is predicted to interact with the benzylic pendant of both BQCA and benzoquinazolinone 12. Indeed, the importance of this interaction is validated both by our structure-function analysis and by the SAR of BQCA derivatives (41) and benzoquinazolinone 12. The mutation of Trp-400$^{7.35}$ to Ala completely abolished detectable binding of all allosteric modulators in this study. Furthermore, the additional aromatic substitution of the 4-position of the benzylic pendant conferred a gain in affinity. Such substitutions would enhance the ability of these ligands to make hydrophobic interactions with Trp-400$^{7.35}$. In agreement with this hypothesis, the conservative mutation of Trp-400$^{7.35}$ to the smaller Phe or Tyr conferred decreases in affinity. In the BQCA-bound complex Trp-400$^{7.35}$ is positioned horizontally below the benzylic pendant of BQCA and makes a π-π stacking interaction with this moiety. In comparison, to accommodate the additional pyrazole substituent of benzoquinazolinone 12, Trp-400$^{7.35}$ is positioned in a more vertical orientation and extends toward TM6. This change in orientation allows the pyrazole substituent of benzoquinazolinone 12 to make hydrophobic interactions with both Trp-400$^{7.35}$ and Tyr-179. Of interest, in the M_2 mAChR crystal structure, Trp-422$^{7.35}$ adopts a vertical conformation in the presence of the positive allosteric modulator LY2119620 and a horizontal conformation with iperoxo alone. The vertical conformation of this residue in the M_2-iperoxo-LY2119620 complex allows it to engage in an aromatic stacking interaction with the modulator (9).

The TM2 residues Tyr-85$^{2.64}$ and Tyr-82$^{2.61}$ are predicted to line the allosteric pocket in both BQCA and benzoquinazolinone 12-bound complexes. However, the tricyclic core of benzoquinazolinone 12 is predicted to be closer to TM2, conferring stronger interactions with both residues, which may contribute to the higher binding affinity of benzoquinazolinone 12. In agreement with this pose, mutation of both Tyr-85$^{2.64}$ and Tyr-82$^{2.61}$ to Ala caused a greater than 10-fold loss of affinity for benzoquinazolinone 12, whereas no effect upon the affinity of BQCA was observed. Tyr-82$^{2.61}$ was predicted to make a H-bond interaction with Tyr-404$^{7.39}$ in the benzoquinazolinone 12-bound complex but not in the BQCA-bound complex. Interestingly, mutation of Tyr-82$^{2.61}$ to Phe caused a significant decrease in the pK_B of benzoquinazolinone 12 for the mutant receptor but not BQCA. Tyr$^{7.39}$ has been shown to play a key role in the binding of the orthosteric ligand iperoxo in the active structure of the M_2 mAChR, forming an aromatic lid over the ligand amine, an interaction present in our BQCA bound complex. Indeed, this residue has been shown to play an important role in orthosteric ligand binding at a number of GPCRs. Of interest, mutation of the corresponding residue in the M_4 mAChR caused a significant decrease in the binding cooperativity of the positive allosteric modulator LY2033298 with ACh (14). This suggests that this residue is also important for transfer of cooperativity between the allosteric and orthosteric binding sites. It is also interesting to note that the additional pyrimidinone ring in benzoquinazolinone 12 is predicted to be positioned above the allosteric binding pocket. Although the functional significance of this portion of the modulator has not yet been investigated through structure-activity relationships, a recent report by Kuduk *et al.* (44) highlights the importance of the intramolecular hydrogen bond between the 4-oxo moiety and 3-carboxylic acid group present in bicyclic BQCA-type scaffolds, suggesting that this hydrogen bond is key for allosteric activity. We hypothesize that the pyrimidinone ring that forms part of the tricyclic core in benzoquinazolinone 12 formalizes the rigidity imparted by this intramolecular hydrogen bond.

Dror *et al.* (13) recently used molecular dynamics to identify two binding centers in the extra cellular vestibule of the M_2 mAChR that are implicated in the binding of several structurally diverse positive and negative allosteric modulators, each of the binding centers is defined by a pair of aromatic residues (Centre 1 Tyr-177^{ECL2} and Trp$^{7.35}$, Centre 2 Tyr$^{2.61}$, and Tyr$^{2.64}$). Additionally, the M_2 mAChR crystal structure co-bound by the orthosteric agonist iperoxo and the positive allosteric modulator LY2119620 shows that the aromatic rings of the modulator are situated directly between Tyr-177 in ECL2 and Trp-422$^{7.35}$, forming a three-layered aromatic stack (9). A previous mutagenesis study implicated Tyr-177 as a contact for the LY2119620 congener LY2033298 at the M_2 mAChRs (43). We identified the equivalent M_1 mAChR residues as key contributors for the binding and function of BQCA (10) and benzoquinazolinone 12. In particular, because benzoquinazolinone 12 displays significantly higher affinity than BQCA, we were able to demonstrate that Tyr-179 has a major role in the binding of allosteric ligands or in the transfer of cooperativity. Tyr$^{2.64}$ and Trp$^{7.35}$ are conserved across all mAChR receptor subtypes, Tyr$^{2.61}$ is conserved across all but the M_3 mAChR (where it is a similarly aromatic Phe residue), and Tyr-179 is only present at the M_1 and M_2 mAChRs but is a Phe at the M_3 and M_4 mAChRs. This is consistent with BQCA and its analogues sharing a common binding site with other prototypical mAChR allosteric modulators. Although these findings provide insight into the location of the binding pocket for mAChR allosteric modulators, they do not explain how some of these ligands achieve subtype selectivity. As we hypothesized in our earlier studies, it is likely that receptor subtype selectivity is achieved via selective cooperativity of the modulators with the orthosteric ligands.

In summary, our combined mutagenesis and molecular dynamics simulations have validated the allosteric binding pocket we previously described for BQCA and provided a mechanistic basis for observed SAR of M_1 mAChR positive allosteric modulators. In particular, we have demonstrated that benzoquinazolinone 12 displays a significant increase in affinity at the M_1 mAChR and identified the ligand-receptor interactions that confer this increase. These insights will provide the basis for the development of novel M_1 mAChR selective allosteric ligands that explore new chemical space.

Acknowledgment—We are grateful to Dr. Ann Stewart for technical assistance.

REFERENCES

1. Katritch, V., Cherezov, V., and Stevens, R. C. (2013) Structure-function of the G protein-coupled receptor superfamily. *Annu. Rev. Pharmacol. Toxicol.* **53**, 531–556
2. Kruse, A. C., Hu, J., Kobilka, B. K., and Wess, J. (2014) Muscarinic acetylcholine receptor X-ray structures: potential implications for drug development. *Curr. Opin. Pharmacol.* **16**, 24–30
3. Conn, P. J., Christopoulos, A., and Lindsley, C. W. (2009) Allosteric modulators of GPCRs: a novel approach for the treatment of CNS disorders. *Nat. Rev. Drug Discov.* **8**, 41–54
4. Jones, C. K., Byun, N., and Bubser, M. (2012) Muscarinic and nicotinic acetylcholine receptor agonists and allosteric modulators for the treatment of schizophrenia. *Neuropsychopharmacology* **37**, 16–42
5. Byun, N. E., Grannan, M., Bubser, M., Barry, R. L., Thompson, A., Rosanelli, J., Gowrishankar, R., Kelm, N. D., Damon, S., Bridges, T. M., Melancon, B. J., Tarr, J. C., Brogan, J. T., Avison, M. J., Deutch, A. Y., Wess, J., Wood, M. R., Lindsley, C. W., Gore, J. C., Conn, P. J., and Jones, C. K. (2014) Antipsychotic drug-like effects of the selective M4 muscarinic acetylcholine receptor positive allosteric modulator VU0152100. *Neuropsychopharmacology* **39**, 1578–1593
6. Shirey, J. K., Brady, A. E., Jones, P. J., Davis, A. A., Bridges, T. M., Kennedy, J. P., Jadhav, S. B., Menon, U. N., Xiang, Z., Watson, M. L., Christian, E. P., Doherty, J. J., Quirk, M. C., Snyder, D. H., Lah, J. J., Levey, A. I., Nicolle, M. M., Lindsley, C. W., and Conn, P. J. (2009) A selective allosteric potentiator of the M1 muscarinic acetylcholine receptor increases activity of medial prefrontal cortical neurons and restores impairments in reversal learning. *J. Neurosci.* **29**, 14271–14286
7. Stevens, R. C., Cherezov, V., Katritch, V., Abagyan, R., Kuhn, P., Rosen, H., and Wüthrich, K. (2013) The GPCR Network: a large-scale collaboration to determine human GPCR structure and function. *Nat. Rev. Drug Discov.* **12**, 25–34
8. Venkatakrishnan, A. J., Deupi, X., Lebon, G., Tate, C. G., Schertler, G. F., and Babu, M. M. (2013) Molecular signatures of G-protein-coupled receptors. *Nature* **494**, 185–194
9. Kruse, A. C., Ring, A. M., Manglik, A., Hu, J., Hu, K., Eitel, K., Hübner, H., Pardon, E., Valant, C., Sexton, P. M., Christopoulos, A., Felder, C. C., Gmeiner, P., Steyaert, J., Weis, W. I., Garcia, K. C., Wess, J., and Kobilka, B. K. (2013) Activation and allosteric modulation of a muscarinic acetylcholine receptor. *Nature* **504**, 101–106
10. Abdul-Ridha, A., López, L., Keov, P., Thal, D. M., Mistry, S. N., Sexton,

P. M., Lane, J. R., Canals, M., and Christopoulos, A. (2014) Molecular determinants of allosteric modulation at the M1 muscarinic acetylcholine receptor. *J. Biol. Chem.* **289,** 6067–6079
11. Canals, M., Lane, J. R., Wen, A., Scammells, P. J., Sexton, P. M., and Christopoulos, A. (2012) A Monod-Wyman-Changeux mechanism can explain G protein-coupled receptor (GPCR) allosteric modulation. *J. Biol. Chem.* **287,** 650–659
12. Ma, L., Seager, M. A., Wittmann, M., Jacobson, M., Bickel, D., Burno, M., Jones, K., Graufelds, V. K., Xu, G., Pearson, M., McCampbell, A., Gaspar, R., Shughrue, P., Danziger, A., Regan, C., Flick, R., Pascarella, D., Garson, S., Doran, S., Kreatsoulas, C., Veng, L., Lindsley, C. W., Shipe, W., Kuduk, S., Sur, C., Kinney, G., Seabrook, G. R., and Ray, W. J. (2009) Selective activation of the M1 muscarinic acetylcholine receptor achieved by allosteric potentiation. *Proc. Natl. Acad. Sci. U.S.A.* **106,** 15950–15955
13. Dror, R. O., Green, H. F., Valant, C., Borhani, D. W., Valcourt, J. R., Pan, A. C., Arlow, D. H., Canals, M., Lane, J. R., Rahmani, R., Baell, J. B., Sexton, P. M., Christopoulos, A., and Shaw, D. E. (2013) Structural basis for modulation of a G-protein-coupled receptor by allosteric drugs. *Nature* **503,** 295–299
14. Nawaratne, V., Leach, K., Felder, C. C., Sexton, P. M., and Christopoulos, A. (2010) Structural determinants of allosteric agonism and modulation at the M4 muscarinic acetylcholine receptor: identification of ligand-specific and global activation mechanisms. *J. Biol. Chem.* **285,** 19012–19021
15. May, L. T., Avlani, V. A., Langmead, C. J., Herdon, H. J., Wood, M. D., Sexton, P. M., and Christopoulos, A. (2007) Structure-function studies of allosteric agonism at M2 muscarinic acetylcholine receptors. *Mol. Pharmacol.* **72,** 463–476
16. Matsui, H., Lazareno, S., and Birdsall, N. J. (1995) Probing of the location of the allosteric site on m1 muscarinic receptors by site-directed mutagenesis. *Mol. Pharmacol.* **47,** 88–98
17. Lazareno, S., Dolezal, V., Popham, A., and Birdsall, N. J. (2004) Thiochrome enhances acetylcholine affinity at muscarinic M4 receptors: receptor subtype selectivity via cooperativity rather than affinity. *Mol. Pharmacol.* **65,** 257–266
18. Lebois, E. P., Bridges, T. M., Lewis, L. M., Dawson, E. S., Kane, A. S., Xiang, Z., Jadhav, S. B., Yin, H., Kennedy, J. P., Meiler, J., Niswender, C. M., Jones, C. K., Conn, P. J., Weaver, C. D., and Lindsley, C. W. (2010) Discovery and characterization of novel subtype-selective allosteric agonists for the investigation of M_1 receptor function in the central nervous system. *ACS Chem. Neurosci.* **1,** 104–121
19. Melancon, B. J., Tarr, J. C., Panarese, J. D., Wood, M. R., and Lindsley, C. W. (2013) Allosteric modulation of the M1 muscarinic acetylcholine receptor: improving cognition and a potential treatment for schizophrenia and Alzheimer's disease. *Drug Discovery Today* **18,** 1185–1199
20. Tarr, J. C., Turlington, M. L., Reid, P. R., Utley, T. J., Sheffler, D. J., Cho, H. P., Klar, R., Pancani, T., Klein, M. T., Bridges, T. M., Morrison, R. D., Blobaum, A. L., Xiang, Z., Daniels, J. S., Niswender, C. M., Conn, P. J., Wood, M. R., and Lindsley, C. W. (2012) Targeting selective activation of M1 for the treatment of Alzheimer's disease: further chemical optimization and pharmacological characterization of the M1 positive allosteric modulator ML169. *ACS Chem. Neurosci.* **3,** 884–895
21. Foster, D. J., Choi, D. L., Conn, P. J., and Rook, J. M. (2014) Activation of M1 and M4 muscarinic receptors as potential treatments for Alzheimer's disease and schizophrenia. *Neuropsychiatr. Dis. Treat.* **10,** 183–191
22. Nickols, H. H., and Conn, P. J. (2014) Development of allosteric modulators of GPCRs for treatment of CNS disorders. *Neurobiol. Dis.* **61,** 55–71
23. Nathan, P. J., Watson, J., Lund, J., Davies, C. H., Peters, G., Dodds, C. M., Swirski, B., Lawrence, P., Bentley, G. D., O'Neill, B. V., Robertson, J., Watson, S., Jones, G. A., Maruff, P., Croft, R. J., Laruelle, M., and Bullmore, E. T. (2013) The potent M1 receptor allosteric agonist GSK1034702 improves episodic memory in humans in the nicotine abstinence model of cognitive dysfunction. *Int. J. Neuropsychopharmacol.* **16,** 721–731
24. Kuduk, S. D., and Beshore, D. C. (2012) Novel M1 allosteric ligands: a patent review. *Expert. Opin. Ther. Pat.* **22,** 1385–1398
25. Kuduk, S. D., Beshore, D. C., DiMarco, C. N., and Greshock, T. J. (May 27, 2010) U. S. Patent WO 2010/059773
26. Kennedy, D. P., McRobb, F. M., Leonhardt, S. A., Purdy, M., Figler, H., Marshall, M. A., Chordia, M., Figler, R., Linden, J., Abagyan, R., and Yeager, M. (2014) The second extracellular loop of the adenosine A1 receptor mediates activity of allosteric enhancers. *Mol. Pharmacol.* **85,** 301–309
27. Ragnarsson, L., Wang, C. I., Andersson, A., Fajarningsih, D., Monks, T., Brust, A., Rosengren, K. J., and Lewis, R. J. (2013) Conopeptide rho-TIA defines a new allosteric site on the extracellular surface of the α1B-adrenoceptor. *J. Biol. Chem.* **288,** 1814–1827
28. Haga, K., Kruse, A. C., Asada, H., Yurugi-Kobayashi, T., Shiroishi, M., Zhang, C., Weis, W. I., Okada, T., Kobilka, B. K., Haga, T., and Kobayashi, T. (2012) Structure of the human M2 muscarinic acetylcholine receptor bound to an antagonist. *Nature* **482,** 547–551
29. Kruse, A. C., Hu, J., Pan, A. C., Arlow, D. H., Rosenbaum, D. M., Rosemond, E., Green, H. F., Liu, T., Chae, P. S., Dror, R. O., Shaw, D. E., Weis, W. I., Wess, J., and Kobilka, B. K. (2012) Structure and dynamics of the M3 muscarinic acetylcholine receptor. *Nature* **482,** 552–556
30. Phillips, J. C., Braun, R., Wang, W., Gumbart, J., Tajkhorshid, E., Villa, E., Chipot, C., Skeel, R. D., Kalé, L., and Schulten, K. (2005) Scalable molecular dynamics with NAMD. *J. Comput. Chem.* **26,** 1781–1802
31. Shonberg, J., Herenbrink, C. K., López, L., Christopoulos, A., Scammells, P. J., Capuano, B., and Lane, J. R. (2013) A structure-activity analysis of biased agonism at the dopamine D2 receptor. *J. Med. Chem.* **56,** 9199–9221
32. Motulsky H, C. A. (2004) *Fitting Models to Biological Data Using Linear and Nonlinear Regression: A Practical Guide to Curve Fitting*, Oxford University Press, New York
33. Leach, K., Loiacono, R. E., Felder, C. C., McKinzie, D. L., Mogg, A., Shaw, D. B., Sexton, P. M., and Christopoulos, A. (2010) Molecular mechanisms of action and in vivo validation of an M4 muscarinic acetylcholine receptor allosteric modulator with potential antipsychotic properties. *Neuropsychopharmacology* **35,** 855–869
34. Leach, K., Sexton, P. M., and Christopoulos, A. (2007) Allosteric GPCR modulators: taking advantage of permissive receptor pharmacology. *Trends Pharmacol. Sci.* **28,** 382–389
35. Kenakin, T., and Christopoulos, A. (2013) Signalling bias in new drug discovery: detection, quantification and therapeutic impact. *Nat. Rev. Drug Discov.* **12,** 205–216
36. Christopoulos, A. (1998) Assessing the distribution of parameters in models of ligand-receptor interaction: to log or not to log. *Trends Pharmacol. Sci.* **19,** 351–357
37. Kuduk, S. D., Chang, R. K., Di Marco, C. N., Ray, W. J., Ma, L., Wittmann, M., Seager, M. A., Koeplinger, K. A., Thompson, C. D., Hartman, G. D., and Bilodeau, M. T. (2011) Quinolizidinone carboxylic acid selective M1 allosteric modulators: SAR in the piperidine series. *Bioorg. Med. Chem. Lett.* **21,** 1710–1715
38. Hulme, E. C., Lu, Z. L., Saldanha, J. W., and Bee, M. S. (2003) Structure and activation of muscarinic acetylcholine receptors. *Biochem. Soc. Trans.* **31,** 29–34
39. Lebon, G., Langmead, C. J., Tehan, B. G., and Hulme, E. C. (2009) Mutagenic mapping suggests a novel binding mode for selective agonists of M1 muscarinic acetylcholine receptors. *Mol. Pharmacol.* **75,** 331–341
40. Keov, P., López, L., Devine, S. M., Valant, C., Lane, J. R., Scammells, P. J., Sexton, P. M., and Christopoulos, A. (2014) Molecular mechanisms of bitopic ligand engagement with the M1 muscarinic acetylcholine receptor. *J. Biol. Chem.* **289,** 23817–23837
41. Mistry, S. N., Valant, C., Sexton, P. M., Capuano, B., Christopoulos, A., and Scammells, P. J. (2013) Synthesis and pharmacological profiling of analogues of benzyl quinolone carboxylic acid (BQCA) as allosteric modulators of the M1 muscarinic receptor. *J. Med. Chem.* **56,** 5151–5172
42. Conn, P. J., Jones, C. K., and Lindsley, C. W. (2009) Subtype-selective allosteric modulators of muscarinic receptors for the treatment of CNS disorders. *Trends Pharmacol. Sci.* **30,** 148–155
43. Valant, C., Felder, C. C., Sexton, P. M., and Christopoulos, A. (2012) Probe dependence in the allosteric modulation of a g protein-coupled receptor: implications for detection and validation of allosteric ligand effects. *Mol. Pharmacol.* **81,** 41–52
44. Kuduk, S. D., Di Marco, C. N., Saffold, J. R., Ray, W. J., Ma, L., Wittmann, M., Koeplinger, K. A., Thompson, C. D., Hartman, G. D., Bilodeau, M.T., and Beshore, D. C. (2014) Identification of a methoxynaphtalene scaffold as a core replacement in quinolizidinone amide M1 positive allosteric modulators. *Bioorg. Med. Chem. Lett.* **24,** 1417–1420

Appendix S1: Supplementary Methods

Mechanistic Insights into Allosteric Structure-Function Relationships at the M_1 Muscarinic Acetylcholine Receptor

Alaa Abdul-Ridha[1]*, J. Robert Lane[1]*, Shailesh N. Mistry[2], Laura López[1], Patrick M. Sexton[1], Peter J. Scammells[2], Arthur Christopoulos[1§] and Meritxell Canals[1§]

[1]Drug Discovery Biology or [2]Medicinal Chemistry, Monash Institute of Pharmaceutical Sciences and Department of Pharmacology, Monash University, Parkville, Victoria, 3052, Australia.

Running Title: *Structure-function analysis of M_1 receptor allosteric ligands*

[§]To whom correspondence should be addressed: Dr. Meritxell Canals or Prof. Arthur Christopoulos, Drug Discovery Biology, Monash Institute of Pharmaceutical Sciences, Monash University, 381 Royal Parade, Parkville, Victoria 3052, Australia. Phone: (03) 9903 9067, [redacted]

* These authors contributed equally to this manuscript

Key words: muscarinic acetylcholine receptor, allosteric modulation, cell signaling, drug discovery.

Abbreviations. DIPEA, *N,N*-diisopropylethylamine; DMF, *N,N*-dimethylformamide; DMF-DMA, *N,N*-dimethylformamide, dimethylacetal; DMSO, dimethylsulfoxide; FCC, flash column chromatography; HCTU, *O*-(*1H*-6-chlorobenzotriazole-1-yl)-1,1,3,3-tetramethyluronium hexafluorophosphate; PE, petroleum spirits 40-60; THF, tetrahydrofuran.

Synthesis of compounds. 1-(4-Methoxybenzyl)-4-oxo-1,4-dihydroquinoline-3-carboxylic acid **(BQCA)**, was taken from our in-house library from stocks, with synthesis according our previously reported protocols for the 4-oxoquinoline-3-carboxylic acid series.[1]

Scheme S1. Optimised synthesis of 3-((1*S*,2*S*)-2-hydroxycyclohexyl)-6-((6-(1-methyl-1*H*-pyrazol-4-yl)pyridin-3-yl)methyl)benzo[*h*]quinazolin-4(3*H*)-one (12).

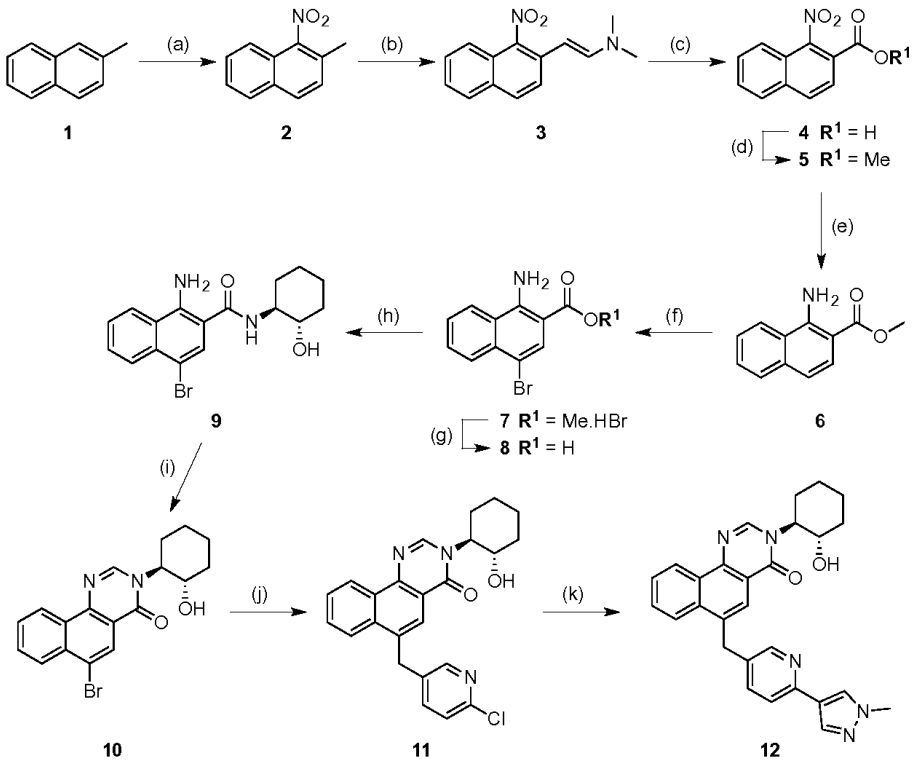

[a] Reagents and conditions: (a) i. AcOH, 0 °C; ii. fuming $HNO_{3\,(aq)}$ dropwise, 0 °C, 47%; (b) DMF-DMA, 140 °C, 89%; (c) i. K_2CO_3, $^tBuOH/H_2O$ 1:1, rt; ii. $KMnO_4$, rt, 93%; (d) MeOH, cat. concentrated $H_2SO_{4\,(aq)}$, reflux, 89%; (e) 10% Pd/C, H_2, ThalesNano H-Cube®, MeOH/EtoAc or MeOH/THF, 83%; (f) i. 1,4-dioxane, CCl_4 1:1, 0 °C; ii. Br_2, 1,4-dioxane/CCl_4 1:1, dropwise, 0 °C, 85%; (g) i. $LiOH.H_2O$, THF/water 1:1, rt; ii. 55 °C, 100%; (h) HCTU, (*1S,2S*)-2-aminocyclohexanol hydrochloride, DIPEA, DMF, rt, 97%; (i) DMF-DMA, 85 °C, 98%; (j) i. cat. $Pd(P(^tBu)_3)_2$, degassed anhydrous THF, 0 °C; ii. 0.5M (2-chloro-5-pyridyl)methylzinc chloride/THF, 0 °C to rt, 79%; (k) 1-methyl-4-(4,4,5,5-tetramethyl-1,3,2-dioxaborolan-2-yl)-*1H*-pyrazole, cat. $PdCl_2(PPh_3)_2$, 1M $Na_2CO_{3\,(aq)}$/THF 1:3 degassed, 100 °C, 65%.

The synthesis of 3-((1*S*,2*S*)-2-hydroxycyclohexyl)-6-((6-(1-methyl-1*H*-pyrazol-4-yl)pyridin-3-yl)methyl)benzo[*h*]quinazolin-4(3*H*)-one **(12)** was adapted from that reported in the literature[2] (Scheme S1). Initially, commercially available 2-methylnaphthalene (**1**) underwent nitration using previously reported conditions, with the desired 1-nitro regioisomer **2**, being isolated through recrystallization from MeOH.[3] Functionalisation of the methyl group of **2** was possible through heating with DMF-DMA at 140 °C, introducing a *N,N*-dimethylenamine moiety, to give **3**.[4] This underwent clean $KMnO_4$ mediated oxidation, affording 1-nitro-2-naphthoic acid (**4)** in excellent yield. Subsequent Fischer esterification of **4**, in the presence of catalytic concentrated $H_2SO_{4\,(aq)}$ refluxing in MeOH, gave the corresponding methyl ester **5**. A ThalesNano H-Cube® was employed, using a 10% Pd/C cartridge, to reduce the nitro group of **5**, affording the aniline derivative **6** in good yield. Selective mono-bromination in the 4-position of **6**, using Br_2 in a mixture of 1,4-dioxane/CCl_4 afforded **7** in excellent yield as the hydrobromide salt. Basic hydrolysis of **7** was achieved in quantitative yield in the presence of excess $LiOH.H_2O$ in THF/water at 55 °C, to give the amino acid **8** in the unsalted form.

Subsequent HCTU-mediated coupling of **8** with (1*S*, 2*S*)-2-aminocycohexanol proceeded smoothly, affording the corresponding amide **9** in near-quantitative yield. The target benzo[*h*]quinazolin-4(3*H*)-one core was obtained through cyclisation of **9**, by heating in DMF-DMA at 85 °C, giving **10**.

The commercial availability of 0.5 M (2-chloro-5-pyridyl)methylzinc chloride/THF allowed a Negishi coupling to be employed to facilitate sp^2-sp^3 aryl/alkyl C-C bond formation, providing 2-chloropyridyl derivative **11** in good yield. The success of this particular transformation was found to be heavily reliant on the age and quality of the zincate solution, and could only be carried out using the more hindered $Pd(P(^tBu)_3)_2$ catalyst.

Finally, Suzuki chemistry was employed to install the *N*-methylpyrazolyl group to the 2-position of the pyridine ring, affording the desired target compound, benzoquinazolinone **12**.

General Chemistry Methods: Chemicals and solvents were purchased from standard suppliers and used without further purification. Davisil® silica gel (40-63μm), for flash column chromatography (FCC) was supplied by Grace Davison Discovery Sciences (Victoria, Australia) and deuterated solvents were purchased from Cambridge Isotope Laboratories, Inc. (USA, distributed by Novachem PTY. Ltd, Victoria, Australia).

Unless otherwise stated, reactions were carried out at ambient temperature. Reactions were monitored by thin layer chromatography on commercially available precoated aluminium-backed plates (Merck Kieselgel 60 F_{254}). Visualisation was by examination under UV light (254 and 366 nm). General staining carried out with $KMnO_4$ or phosphomolybdic acid. A solution of Ninhydrin (in ethanol) was used to visualize primary and secondary amines. All organic extracts collected after aqueous work-up procedures were dried over anhydrous $MgSO_4$ or Na_2SO_4 before gravity filtering and evaporation to dryness. Organic solvents were evaporated *in vacuo* at ≤ 40°C (water bath temperature). Purification using preparative layer chromatography (PLC) was carried out on Analtech preparative TLC plates (200 mm x 200 mm x 2 mm).

^1H and ^{13}C NMR spectra were recorded on a Bruker Avance Nanobay III 400MHz Ultrashield Plus spectrometer at 400.13 MHz and 100.62 MHz, respectively. Chemical shifts (δ) are recorded in parts per million (ppm) with reference to the chemical shift of the

deuterated solvent. Coupling constants (J) and carbon-fluorine coupling constants (J_{CF}) are recorded in Hz and the significant multiplicities described by singlet (s), doublet (d), triplet (t), quadruplet (q), broad (br), multiplet (m), doublet of doublets (dd), doublet of triplets (dt). Spectra were assigned using appropriate COSY, distortionless enhanced polarisation transfer (DEPT), HSQC and HMBC sequences. Specific optical rotation was determined using a Jasco P-2000 polarimeter.

LCMS were run to verify reaction outcome and purity using either system A or B. **System A:** an Agilent 6100 Series Single Quad coupled to an Agilent 1200 Series HPLC. The following buffers were used; buffer A: 0.1% formic acid in H_2O; buffer B: 0.1% formic acid in MeCN. The following gradient was used with a Phenomenex Luna 3µM C8(2) 15 x 4.6 mm column, and a flow rate of 0.5 mL/min and total run time of 12 min; 0–4 min 95% buffer A and 5% buffer B, 4–7 min 0% buffer A and 100% buffer B, 7–12 min 95% buffer A and 5% buffer B. Mass spectra were acquired in positive and negative ion mode with a scan range of 0–1000 *m/z* at 5V. UV detection was carried out at 254 nm. **System B:** an Agilent 6120 Series Single Quad coupled to an Agilent 1260 Series HPLC. The following buffers were used; buffer A: 0.1% formic acid in H_2O; buffer B: 0.1% formic acid in MeCN. The following gradient was used with a Poroshell 120 EC-C18 50 x 3.0 mm 2.7 micron column, and a flow rate of 0.5 mL/min and total run time of 5 min; 0–1 min 95% buffer A and 5% buffer B, from 1-2.5 min up to 0% buffer A and 100% buffer B, held at this composition until 3.8 min, 3.8–4 min 95% buffer A and 5% buffer B, held until 5 min at this composition. Mass spectra were acquired in positive and negative ion mode with a scan range of 100–1000 *m/z*. UV detection was carried out at 214 and 254 nm. All retention times (t_R) are quoted in minutes.

Preparative HPLC was performed using an Agilent 1260 infinity coupled with a binary preparative pump and Agilent 1260 FC-PS fraction collector, using Agilent OpenLAB CDS software (Rev C.01.04), and an Altima 5µM C8 22 x 250 mm column. The following buffers

were used; buffer A: H_2O; buffer B: MeCN, with sample being run at a gradient of 5% buffer B to 100% buffer B over 20 min, at a flow rate of 20 mL/min All screening compounds were of > 95% purity unless specified in the individual monologue.

2-Methyl-1-nitronaphthalene (2).[3] 2-Methylnaphthalene **(1)** (14.2 g, 100 mmol) was dissolved in glacial AcOH (50 mL) and cooled to 0 °C, over an ice bath, with stirring. Fuming $HNO_{3\,(aq)}$ (8 mL) was added dropwise to this solution and stirring was continued in the ice bath for 2 hours, over which time a yellow precipitate formed. TLC analysis (EtOAc/PE 2:8) indicated starting material had been consumed. The mixture was dilute with water (150 mL), then extracted with DCM (3 x 50 mL). The combined organic layers were then washed with sat. $NaHCO_{3(aq)}$ (200 mL). After drying over $MgSO_4$, the organic layers were concentrated under reduced pressure to give 19.2 g of crude yellow solid. This was recrystallized from MeOH (20 mL) to give an initial crop of 6.20 g of pale yellow crystals (collected by vacuum filtration). The filtrate was concentrated, then passed through a plug of silica gel (eluent EtOAc/PE 5:95). The resulting filtrate was again concentrated under reduced pressure and recrystallized from MeOH to give a further 2.627 g of pale yellow crystals. Total yield 8.827 g (47%) as pale yellow crystalline solid. ^{1}H NMR (400 MHz, $CDCl_3$) δ 7.94 – 7.83 (m, 2H), 7.76 – 7.69 (m, 1H), 7.61 (ddd, J = 8.5/6.9/1.3 Hz, 1H), 7.54 (ddd, J = 8.0/6.9/1.2 Hz, 1H), 7.37 (d, J = 8.5 Hz, 1H), 2.51 (s, 3H); ^{13}C NMR (101 MHz, $CDCl_3$) δ 148.95, 132.41, 130.58, 128.67, 128.26, 128.10, 127.67, 126.80, 124.85, 121.41, 17.99.

***N,N*-Dimethyl-2-(1-nitronaphthalen-2-yl)ethen-1-amine (3).**[4] 2-Methyl-1-nitronaphthalene **(2)** (3.505 g, 18.72 mmol) was dissolved in anhydrous DMF (30 mL) under an atmosphere of nitrogen at room temperature. To this stirred solution was added DMF-DMA (3.347 g, 28.09 mmol, 1.5 eq). The mixture was heated at 140 °C for 7 hours, then cooled and stirred at room temperature overnight. TLC analysis (EtOAc/PE 3:7) after this

time indicated that starting material still remained, so DMF-DMA (0.669 mg, 5.62 mmol, 0.3 eq) was added, and heating continued at 140 °C for 1 hour. The mixture was cooled, then concentrated under reduced pressure. The residue was washed with hexanes, and the resulted precipitate collected by filtration (vacuum), with further washings of hexanes. After drying, 4.04 g (89%) of bright red solid were obtained. ^{1}H NMR (400 MHz, $CDCl_3$) δ 7.73 (d, J = 8.1 Hz, 1H), 7.70 (d, J = 9.0 Hz, 1H), 7.57 (dd, J = 8.4/0.5 Hz, 1H), 7.54 – 7.45 (m, 2H), 7.37 (ddd, J = 8.0/6.9/1.1 Hz, 1H), 7.02 (d, J = 13.4 Hz, 1H), 5.15 (d, J = 13.4 Hz, 1H), 2.91 (s, 6H); ^{13}C NMR (101 MHz, $CDCl_3$) δ 144.40, 144.36, 130.12, 130.03, 128.49, 127.92, 125.07, 121.50, 121.02, 120.80, 89.34, 40.84; *m/z* MS (TOF ES$^+$) does not fly; LC-MS t_R: 5.46 (system A).

1-Nitro-2-naphthoic acid (4).[2] *N,N*-Dimethyl-2-(1-nitronaphthalen-2-yl)ethen-1-amine **(3)** (3.696 g, 15.26 mmol) and K_2CO_3 (5.271 g, 38.14 mmol, 2.5 eq) were dispersed in *tert*-butanol/water (1:1, 110 mL) at room temperature, with stirring. To this was slowly added $KMnO_4$ (6.027 g, 38.14 mmol, 2.5 eq), before stirring the resulting mixture at room temperature for 72 hours. TLC analysis (EtOAc/PE 3:7) indicated starting material had disappeared, so the mixture was filtered (vacuum) and the collected precipitate washed with water (100 mL). The filtrate was concentrated under reduced pressure until ~100 mL of liquid remained, then acidified with 2M $HCl_{(aq)}$ to pH 2. The resulting precipitate was collected by filtration (vacuum) with washings of water to give 3.084 g (93%) of pale yellow solid. ^{1}H NMR (400 MHz, DMSO) δ 14.21 (s, 1H), 8.31 (d, J = 8.4 Hz, 1H), 8.26 – 8.16 (m, 1H), 8.03 (d, J = 8.6 Hz, 1H), 7.87 – 7.77 (m, 2H), 7.76 – 7.68 (m, 1H); ^{13}C NMR (101 MHz, DMSO) δ 164.44, 147.90, 135.16, 130.98, 129.92, 129.62, 128.45, 125.18, 123.07, 121.77, 120.23; *m/z* MS (TOF ES$^+$) $C_{11}H_6NO_3$ [M-OH]$^+$ calcd 200.0; found 200.1; LC-MS t_R: 5.27 (system A).

Methyl 1-nitro-2-naphthoate (5). 1-Nitro-2-naphthoic acid **(4)** (3.273 g, 15.07 mmol) was dissolved in MeOH, with addition of concentrated $H_2SO_{4\,(aq)}$ (1 mL). The resulting solution was refluxed overnight. TLC analysis (MeOH/DCM 1:9) indicated starting material had been consumed after this time. The mixture was cooled and concentrated under reduced pressure. The resulting residue was diluted with care using excess sat. $NaHCO_{3\,(aq)}$, and the resulting precipitate collected by filtration (vacuum), and washed with water before allowing to dry, to give 3.103 g (89%) pale brown solid. ^{1}H NMR (400 MHz, $CDCl_3$) δ 8.08 – 7.99 (m, 2H), 7.99 – 7.92 (m, 1H), 7.84 – 7.76 (m, 1H), 7.74 – 7.66 (m, 2H), 3.97 (s, 3H); ^{13}C NMR (101 MHz, $CDCl_3$) δ 164.06, 150.02, 135.97, 130.51, 129.63, 129.45, 128.21, 125.16, 124.23, 122.97, 119.37, 53.34; *m/z* MS (TOF ES$^+$) $C_{11}H_6NO_4$ $[M\text{-}CH_3]^+$ calcd 216.0; found 216.1; LC-MS t_R: 5.70 (system A).

Methyl 1-amino-2-naphthoate (6). Methyl 1-nitro-2-naphthoate **(5)** (3.047 g, 13.18 mmol) was dissolved in MeOH/EtOAc (1:1, 240 mL) and cycled through a ThalesNano H-Cube®, using a 10% Pd/C cartridge. The mixture was split into two batches, with the first batch continuously cycled (reaction mixture exhaust fed directly back into reactor feed) through at 1 mL min^{-1} at 35 °C under 10 bar of H_2 pressure for 3.5 hours. The second batch was cycled through at 2 mL min^{-1} at 40 °C under 20 bar of H_2 pressure for 5.5 hours. In both cases, regular LCMS analysis was used to monitor reaction progression. The second batch failed to react completely due to a fault developing with the machine (though LCMS analysis indicated almost complete conversion had taken place). The batches were combined and concentrated under reduced pressure, before dissolving the residue in DCM (50 mL). This was extracted with 1M $HCl_{(aq)}$ (2 x 30 mL), and the combined aqueous layers neutralized with sat. $NaHCO_{3\,(aq)}$, before extraction with DCM (3 x 30 mL). After concentration of the secondary organic extract under reduced pressure, it was noted that much of the desired product was still trapped in the original DCM layer. The organic layers were combined and

concentrated down under reduced pressure, and the resulting residue purified by FCC (eluent DCM/PE 1:1) to give the desired aniline as 1.67 yellow solid; in addition to 0.786 g of unreduced nitro starting material. This was dissolved in THF (5 mL) and MeOH (45 mL) and passed through the ThalesNano H-Cube® (Full H_2 setting, 1 mL min^{-1}, 25 °C) until LCMS analysis indicated conversion was complete. The reaction mixture was concentrated under reduced pressure, and the residue purified by FCC (eluent EtOAc/PE 0:100 to 30:70), to give 520 mg of yellow solid. Total yield 2.19 g (83%) yellow solid. ^{1}H NMR (400 MHz, $CDCl_3$) δ 7.91 (dd, *J* = 8.4/0.9 Hz, 1H), 7.88 (d, *J* = 8.9 Hz, 1H), 7.79 – 7.70 (m, 1H), 7.55 (ddd, *J* = 8.1/6.9/1.2 Hz, 1H), 7.47 (ddd, *J* = 8.3/6.9/1.4 Hz, 1H), 7.09 (d, *J* = 8.9 Hz, 1H), 7.23 – 6.10 (m, 2H), 3.92 (s, 3H); ^{13}C NMR (101 MHz, $CDCl_3$) δ 169.49, 148.99, 136.58, 128.65, 128.56, 126.68, 125.41, 123.27, 121.66, 116.11, 104.27, 51.68; *m/z* MS (TOF ES^+) $C_{12}H_{12}NO_2$ $[MH]^+$ calcd 202.1; found 202.1; LC-MS t_R: 5.62 (system A).

Methyl 1-amino-4-bromo-2-naphthoate hydrobromide (7).[2] Methyl 1-amino-2-naphthoate **(6)** (2.19 g, 10.88 mmol) was dissolved in 1,4-dioxane/CCl_4 (1:1, 50 mL) and cooled with stirring to 0 °C in an ice bath. A solution of Br_2 (1.739 g, 10.88 mmol, 1 eq) in 1,4-dioxane/CCl_4 (1:1, 10 mL) was added in a dropwise fashion and stirring was continued at 0 °C for 2.5 hours. TLC analysis (DCM) after this time indicated starting material had been consumed. The formed precipitate was collected by filtration (vacuum) and washed with Et_2O, to give 2.456 g of peach solid. The filtrate was concentrated, and the residue redissolved in DCM, before adding excess PE, to effect further precipitation. The resultant precipitate was collected as before, with washings of PE, to give a combined yield of 3.333 g (85%) of peach solid as the hydrobromide salt. ^{1}H NMR (400 MHz, DMSO) δ 8.44 (d, *J* = 8.2 Hz, 1H), 8.01 (dd, *J* = 8.3/0.9 Hz, 1H), 8.00 (s, 1H), 7.77 (ddd, *J* = 8.2/6.9/1.0 Hz, 1H), 7.61 (ddd, *J* = 8.3/7.0/1.2 Hz, 1H), 6.85 (s, 3H), 3.84 (s, 3H); ^{13}C NMR (101 MHz, DMSO) δ 167.43, 149.99, 133.61, 130.42, 129.56, 126.66, 126.11, 124.32, 124.24, 105.53, 102.36,

51.72; *m/z* MS (TOF ES$^+$) $C_{12}H_{11}BrNO_2$ $[MH]^+$ calcd 280.0; found 280.0; LC-MS t_R: 4.18 (system B).

1-Amino-4-bromo-2-naphthoic acid (8). Methyl 1-amino-4-bromo-2-naphthoate hydrobromide **(7)** (3.33 g, 9.23 mmol) was dissolved in THF/water (1:1, 60 mL), and the flask atmosphere purged with nitrogen. The flask was stirred at room temperature for 5 minutes, before addition of $LiOH.H_2O$ (1.162 g, 27.70 mmol, 3 eq), with stirring continued for 72 hours at room temperature. TLC analysis (EtOAc) after this time, indicated conversion was almost complete, so $LiOH.H_2O$ (775 mg, 2 eq) was added, and the mixture heated at 55 °C for 6 hours. A final addition of $LiOH.H_2O$ (775 mg, 2 eq) was made, before continuing stirring at 55 °C overnight. TLC analysis (DCM) indicated conversion was complete. The mixture was concentrated under reduced pressure to remove THF, then acidified with 2M $HCl_{(aq)}$ to pH 2. The resulting precipitate was collected by filtration (vacuum), with washings of water. After overnight drying in a desiccator (compound was found to retain moisture with air-drying), 2.679 g (quantitative yield) of beige solid were obtained. ^{1}H NMR (400 MHz, DMSO) δ 12.77 (s, 1H), 8.41 (d, *J* = 8.2 Hz, 1H), 8.25 – 7.81 (m, 2H), 8.00 (s, 1H), 8.00 (dd, *J* = 8.4/0.9 Hz, 1H), 7.75 (ddd, *J* = 8.2/6.9/1.0 Hz, 1H), 7.60 (ddd, *J* = 8.2/6.9, 1.2 Hz, 1H); ^{13}C NMR (101 MHz, DMSO) δ 169.19, 150.09, 133.59, 130.39, 130.14, 126.59, 125.87, 124.39, 124.11, 105.16, 103.21. *m/z* MS (TOF ES$^+$) $C_{11}H_9BrNO_2$ $[MH]^+$ calcd 266.0; found 266.1; LC-MS t_R: 3.71 (system B).

1-Amino-4-bromo-*N*-((*1S,2S*)-2-hydroxycyclohexyl)-2-naphthamide (9). 1-Amino-4-bromo-2-naphthoic acid **(8)** (1.00 g, 3.76 mmol), HCTU (1.71 g, 4.13 mmol, 1.1 eq) and (*1S, 2S*)-2-aminocyclohexanol hydrochloride (626 mg, 4.13 mmol, 1.1 eq) were stirred in DMF (7 mL) at room temperature for 5 minutes, before adding DIPEA (1.215 g, 1.638 mL, 9.40 mmol, 2.5 eq). The mixture was stirred at room temperature for 24 hours (though TLC

analysis (EtOAc) indicated complete consumption of starting material after 1.5 hours). The mixture was diluted with excess water, and the resulting precipitate collected by filtration (vacuum) and washed with water. After drying 1.32 g (97%) of off-white solid was obtained. ^{1}H NMR (400 MHz, DMSO) δ 8.32 (d, *J* = 8.4 Hz, 1H), 8.08 (d, *J* = 8.1 Hz, 2H), 8.06 (s, 1H), 7.99 (dd, *J* = 8.4/0.8 Hz, 1H), 7.76 (s, 2H), 7.68 (ddd, *J* = 8.2/7.0/0.8 Hz, 1H), 7.54 (ddd, *J* = 8.2/6.8/1.1 Hz, 1H), 3.76 – 3.57 (m, 1H), 3.54 – 3.37 (m, 1H), 2.03 – 1.76 (m, 2H), 1.76 – 1.54 (m, 2H), 1.41 – 1.04 (m, 4H); ^{13}C NMR (101 MHz, DMSO) δ 167.97, 147.41, 132.51, 129.05, 129.02, 126.27, 125.40, 124.64, 123.78, 108.34, 105.35, 70.97, 55.03, 34.62, 31.36, 24.59, 24.26; *m/z* MS (TOF ES$^+$) $C_{17}H_{20}BrN_2O_2$ $[MH]^+$ calcd 363.1; found 363.1; LC-MS t_R: 3.70 (system B).

6-Bromo-3-((*1S,2S*)-2-hydroxycyclohexyl)benzo[*h*]quinazolin-4(*3H*)-one (10). 1-Amino-4-bromo-*N*-((*1S,2S*)-2-hydroxycyclohexyl)-2-naphthamide **(9)** (8.66 g, 23.84 mmol) was dispersed in DMF-DMA (40 mL) and heated at 85 °C for 4 hours. LCMS analysis indicated starting material had been consumed. The mixture was cooled and carefully quenched with water (very exothermic), and the resulting precipitate collected by filtration (vacuum) before washing with water. After drying under air, 8.679 g (98%) of off-white solid was obtained. ^{1}H NMR (400 MHz, DMSO) δ 9.00 (dd, *J* = 8.2/0.7 Hz, 1H), 8.74 (s, 1H), 8.35 (s, 1H), 8.26 (d, *J* = 8.1 Hz, 1H), 7.95 (ddd, *J* = 8.3/7.0/1.3 Hz, 1H), 7.87 (ddd, *J* = 8.1/7.1/1.1 Hz, 1H), 5.01 (d, *J* = 5.3 Hz, 1H), 4.48 (s, 1H), 4.03 (s, 1H), 2.24 – 1.57 (m, 5H), 1.54 – 1.02 (m, 3H); ^{13}C NMR (101 MHz, DMSO) δ 159.37, 147.60, 145.35, 133.27, 130.84, 130.52, 128.26, 127.79, 126.84, 125.16, 125.03, 120.15, 68.92, 35.10, 30.11, 25.02, 23.94. *m/z* MS (TOF ES$^+$) $C_{18}H_{18}BrN_2O_2$ $[MH]^+$ calcd 373.1; found 373.1; LC-MS t_R: 3.94 (system B).

6-((6-Chloropyridin-3-yl)methyl)-3-((*1S,2S*)-2-hydroxycyclohexyl)benzo[*h*]quinazolin-4(*3H*)-one (11). 6-Bromo-3-((*1S,2S*)-2-hydroxycyclohexyl)benzo[*h*]quinazolin-4(*3H*)-one

(10) (513 mg, 1.37 mmol) was dispersed in anhydrous THF (0.5 mL) under an atmosphere of nitrogen, before degassing under a stream of nitrogen for 5 minutes at room temperature. $Pd(P(^tBu)_3)_2$ (21 mg, 0.04 mmol, 0.03 eq) was added, and the flask sealed, re-evacuated and purged with nitrogen, before cooling to 0 °C over an ice bath. (2-Chloro-5-pyridyl)methylzinc chloride in THF (0.5 M, 3.44 mL, 1.72 mmol, 1.25 eq) was added, and stirring continued at 0 °C for 5 minutes. The mixture was then allowed to warm to room temperature, and stirred for 1 hour, before re-cooling to 0 °C and quenching with water. The resulting slurry diluted with water (20 mL), then extracted with EtOAc (3 x 20 mL). The combined organic layers were washed with brine (20 mL) then concentrated under reduced pressure, and the residue purified by FCC (eluent EtOAc/PE 30:70 to 100:0) to give 452 mg (79%) of pale yellow solid. ^{1}H NMR (400 MHz, DMSO) δ 9.05 – 8.93 (m, 1H), 8.67 (s, 1H), 8.44 (d, *J* = 2.1 Hz, 1H), 8.17 (dd, *J* = 7.5/1.6 Hz, 1H), 7.97 (s, 1H), 7.85 – 7.71 (m, 2H), 7.66 (dd, *J* = 8.3/2.5 Hz, 1H), 7.41 (dd, *J* = 8.3/0.4 Hz, 1H), 4.98 (d, *J* = 5.4 Hz, 1H), 4.57 (s, 2H), 4.78 – 4.26 (m, 1H), 4.03 (s, 1H), 2.18 – 1.60 (m, 5H), 1.53 – 1.19 (m, 3H); ^{13}C NMR (101 MHz, DMSO) δ 160.25, 149.91, 148.20, 146.49, 145.00, 139.87, 135.54, 134.90, 133.80, 129.80, 129.51, 128.00, 127.02, 125.08, 124.44, 124.12, 122.36, 69.89, 35.20, 34.21, 30.59, 25.07, 23.99; *m/z* MS (TOF ES$^+$) $C_{24}H_{23}ClN_3O_2$ $[MH]^+$ calcd 420.2; found 420.2; LC-MS t_R: 3.47 (system B).

3-((*1S,2S*)-2-Hydroxycyclohexyl)-6-((6-(1-methyl-*1H*-pyrazol-4-yl)pyridin-3-yl)methyl)benzo[*h*]quinazolin-4(*3H*)-one (12). 6-((6-Chloropyridin-3-yl)methyl)-3-((*1S,2S*)-2-hydroxycyclohexyl)benzo[*h*]quinazolin-4(*3H*)-one **(11)** (6.758 g, 16.09 mmol) and 1-methyl-4-(4,4,5,5-tetramethyl-1,3,2-dioxaborolan-2-yl)-*1H*-pyrazole (5.023 g, 24.14 mmol, 1.5 eq) was dispersed in 1M $Na_2CO_{3\,(aq)}$ (30 mL) and THF (90 mL). The mixture was sonicated for 5 minutes, before degassing under a steady stream of nitrogen for 5 minutes. $PdCl_2(PPh_3)_2$ (1.130 g, 1.61 mmol, 0.1 eq) was added and the mixture heated at 100 °C under

a reflux condenser in an atmosphere of nitrogen for 22 hours. The mixture was cooled, and concentrated under reduced pressure to remove THF, then diluted with water (100 mL), before extraction with EtOAc (3 x 100 mL). The combined organic layers were passed through a bed of celite to remove spent catalyst, then washed with brine (100 mL), before drying over $MgSO_4$ and concentrating under reduced pressure. Initial attempted purification of the residue by FCC (eluent MeOH/DCM 0:100 to 5:95) gave poor mass recovery, and product with minor impurities present. The Celite bed was rewashed with DCM, and the resulting filtrate washed with brine before concentration under reduced pressure. TLC analysis (MeOH/DCM 5:95) indicated both the columned product and DCM concentrate contained the desired product with relatively minor impurities. These was combined and recrystallised from EtOH/water, to give a total of 4.901 g (65%) of off-white shiny solid. ^{1}H NMR (400 MHz, DMSO) δ 8.99 (dd, J = 8.1/1.4 Hz, 1H), 8.66 (s, 1H), 8.51 (d, J = 1.4 Hz, 1H), 8.28 – 8.15 (m, 2H), 7.97 (s, 1H), 7.92 (d, J = 0.7 Hz, 1H), 7.84 – 7.70 (m, 2H), 7.61 – 7.43 (m, 2H), 4.98 (d, J = 5.4 Hz, 1H), 4.53 (s, 2H), 4.71 – 4.22 (m, 1H), 4.18 – 3.92 (m, 1H), 3.86 (s, 3H), 2.14 – 1.58 (m, 5H), 1.48 – 1.26 (m, 3H); ^{13}C NMR (101 MHz, DMSO) δ 160.27, 149.79, 149.50, 146.57, 144.87, 136.88, 136.83, 135.54, 133.95, 132.79, 129.77, 129.39, 129.23, 126.92, 125.02, 124.52, 122.61, 122.10, 119.03, 115.15, 68.58, 38.68, 35.20, 34.90, 30.36, 25.07, 23.98; *m/z* MS (TOF ES$^+$) $C_{28}H_{28}N_5O_2$ $[MH]^+$ calcd 466.2; found 466.3; LC-MS t_R: 3.08 (system B); $[\alpha]_D^{27}$ = + 23.29° (0.69, DMSO).

References

(1) Mistry, S. N.; Valant, C.; Christopoulos, A.; Sexton, P. M.; Capuano, B.; Scammells, P. J. Synthesis and Pharmacological Profiling of Analogues of Benzyl Quinolone Carboxylic Acid (BQCA) as Allosteric Modulators of the M_1 Muscarinic Receptor. *J. Med. Chem.* **2013**, 5151–5172.

(2) Kuduk, S. D.; Beshore, D. C.; Di Marco, C. N.; Greshock, T. J. Aryl Methyl Benzoquinazolinone M1 Receptor Positive Allosteric Modulators. WO 2010/059773, May 27, 2010.

(3) Buehler, S.; Lagoja, I.; Giegrich, H.; Stengele, K. P.; Pfleiderer, W. New Types of Very Efficient Photolabile Protecting Groups Based Upon the [2- (2- Nitrophenyl) Propoxy] Carbonyl (NPPOC) Moiety. *Helv. Chim. Acta* **2004**, *87*, 620–659.

(4) Riesgo, E. C.; Jin, X.; Thummel, R. P. Introduction of Benzo[H]Quinoline and 1,10-Phenanthroline Subunits by Friedländer Methodology. *J. Org. Chem.* **1997**, *61*, 3017–3022.

CHAPTER 5

General Discussion

A large body of evidence from pre-clinical and clinical studies support the implication of the M_1 mAChR in the cognitive processes of learning and memory (Conn et al., 2009; Wess et al., 2007). As a result, the M_1 mAChR has long been an attractive therapeutic target for diseases where such processes are impaired such as AD and schizophrenia (see Chapter 1). In the quest to find selective ligands for this receptor, the positive allosteric modulator BQCA was discovered. BQCA represents a valuable and selective pharmacological tool for *in vivo* and *in vitro* studies and is the first allosteric GPCR ligand proven to behave according to a strict two-state Monod-Wyman-Changeux (MWC) model of receptor activation at the M_1 mAChR (Canals et al., 2012; Canals et al., 2011; Monod et al., 1963; Monod et al., 1965). The unique nature of BQCAs' behaviour has provided a framework for the study and classification of allosteric modulators across different GPCR families (Canals et al., 2012).

The distinctive and predictable manner by which BQCA behaves is exploited in Chapter 2 to investigate the nature of allosteric modulation at the M_1 DREADD, a chemogenetically modified M_1 mAChR designed as a tool to investigate the physiological outcomes of activation of this receptor *in vivo* upon CNO administration (see Chapters 1 and 2). A comprehensive analysis of the allosteric interaction of BQCA with CNO, ACh and a number of structurally and functionally diverse M_1 mAChR ligands was performed at multiple signaling pathways linked to the M_1 WT and DREADD mAChRs.

Initial pharmacological characterisation of the various ligands in binding and Ca^{2+} mobilisation assays revealed different profiles of receptor binding and activation at the M_1 DREADD that suggest multiple modes of receptor engagement. The mutations at the M_1 DREADD caused the orthosteric ligands ACh and xanomeline to lose affinity and potency, while the opposite effects were observed for CNO and its close structural analogues NDMC and clozapine, whereby both properties were significantly enhanced. Interestingly, the affinity and potency of the bitopic ligand TBPB (Keov et al., 2014; Keov et al., 2013) was

unaffected by the M_1 DREADD mutations. Unlike TBPB, however, McN-A-343, a partial M_1 mAChR agonist that has been shown to be bitopic at the M_2 mAChR (Valant et al., 2008), displayed reduced potency and efficacy at the M_1 DREADD that was not due to a loss of binding affinity, suggesting that McN-A-343 is unable to mediate receptor transition into an active state at the M_1 DREADD.

The key findings in Chapter 2 were observed in the allosteric interaction studies of BQCA with both the cognate and the synthetic agonists at the M_1 DREADD. As expected, BQCA displayed key characteristics of allostery within a two-state system at the WT M_1 mAChR, such as positive modulation of co-bound orthosteric or bitopic agonists, and different degrees of cooperativity depending on the intrinsic efficacy of the co-bound ligand and the magnitude of stimulus-response coupling of the studied signal pathway (Canals et al., 2012; Canals et al., 2011; Monod et al., 1963; Monod et al., 1965). The allosteric modulation at the M_1 DREADD was not compatible with a two-state model in that no correlation could be observed between the strength of cooperativity and the degree of signaling efficacy of co-bound ligands, suggesting that the behaviour of the DREADD with respect to allosteric modulation is a result of multiple, distinct, receptor conformations. Moreover, the allosteric modulation of the CNO-bound DREADD receptor is not equivalent to the corresponding modulation of the ACh-bound WT receptor. BQCA was found to engender stimulus bias at the M_1 DREADD, by remarkably behaving as a neutral allosteric modulator of CNO efficacy in the pERK1/2 pathway while having negative modulation in the $Ca2^+$ mobilisation and IP_1 pathways. The same pattern of biased modulation was observed in the interaction of BQCA with NDMC suggesting that a unique receptor conformation is stabilised by CNO and its analogues in combination with BQCA at the M_1 DREADD that is distinct from that stabilized by ACh and BQCA at the M_1 WT mAChR.

Given that GPCRs are known to adopt a range of biologically active states, rather than simply two states (active or inactive) (Mary et al., 2012; Vaidehi and Kenakin, 2010), it may be questionable as to how BQCA behaves in a manner consistent with a two-state model. In this regard, it is likely that BQCA changes the abundance but not the nature of the different states, shifting the overall abundance of receptors to active microstates and resulting in what appears to be a "two-state" system at the macroscopic level. A change in the nature of the microstates, in addition to their abundance, would manifest as biased modulation and may be the reason for the observed biased engendered by BQCA at the M_1 DREADD.

Collectively, the findings in Chapter 2 suggest that the DREADD receptor may not be a valid approach to study the actions of BQCA *in vivo* since the signalling outcomes produced in the presence of CNO will not be reflecting those of the native receptor. In addition, the higher cooperativity of BQCA with ACh means that it still will preferentially enhance the actions of endogenous ACh over the synthetic ligand CNO at the modified receptor *in vivo*. Even in the event where the DREADD is introduced into a transgenic animal with a knock-out background, the potential for the interaction of endogenous ACh with the DREADD remains in the presence of BQCA. As a consequence, the spatio-temporal control that was a key advantage of this approach may be compromised and, thus, the interpretation of such *in vivo* experiments would be extremely challenging and caution must be exercised when interpreting studies of allosteric modulation using DREADDs. In addition, selective allosteric ligands, may be sufficient on their own to provide control over cellular activity in a defined special and temporal manner, eliminating the need to design chemogenetic tools such as the DREADD.

The recent surge in high resolution Family A GPCR crystal structures has provided tremendous insights into the structural and functional characteristics of this protein family (Venkatakrishnan et al., 2013). Such insights, combined with knowledge from mutagenesis

and computational studies have been able to map out the precise location of orthosteric ligand binding pockets in addition to revealing molecular changes that occur upon receptor activation and the mechanisms by which different ligands stabilise distinct receptor conformations (Haga et al., 2012; Jaakola et al., 2008; Katritch et al., 2013; Kruse et al., 2012b; Miao et al., 2013; Wacker et al., 2013; Wang et al., 2013a). Despite the abundance of information obtained from GPCR crystal structures, challenges remain in understanding the mode of action and binding of small molecule allosteric ligands. To understand allosterism from such an approach, multiple structures need to be solved; the orthosteric ligand-bound structure, the allosteric ligand-bound structure and the structure with both sites occupied. To understand probe dependence, these structures need to be solved for different orthosteric and allosteric ligand pairs. The former approach has been recently partially demonstrated for the M_2 mAChR, where crystal structures have been solved in complex with either the orthosteric antagonist (QNB) alone (Haga et al., 2012), the orthosteric agonist (iperoxo) alone (Kruse et al., 2013) or iperoxo co-bound with the M_2 mAChR PAM, LY2119620 (Kruse et al., 2013). However, no crystal structure with LY2119620 alone has been solved. While these structures offered insights into the structural basis of mAChR activation and allosteric modulation by a small drug-like molecule, they offer only a single snapshot of an active mAChR and the information may be limited to the M_2 mAChR. Moreover, the general limitation of GPCR crystals is that they are static structures and cannot translate information on the dynamic nature of ligand-receptor interactions. Therefore, even with the availability of crystal structures (Haga et al., 2012; Kruse et al., 2013), structure-function studies are still required to validate and understand how certain allosteric ligand-receptor interactions observed in crystal structures contribute to ligand activity. Consequently, combining information from structure-function studies that determine the importance of certain ligand-receptor

interactions, with information from crystallographic studies provides an ideal approach to both understanding allosteric ligand activity and for guiding rational drug design.

Despite the numerous favourable features of BQCA; its high M_1 mAChR selectivity, its unique mode of action and high cooperativity with ACh, this compound is still limited as a pharmacological tool by its low affinity for the receptor (~100μM) and poor aqueous solubility (Canals et al., 2012). Such limitations greatly restrict its *in vivo* and potentially, therapeutic utility. Moreover, the mechanism by which BQCA achieves its M_1 mAChR selectivity and the structural basis of its binding and function remain poorly understood. Knowledge of receptor interactions that govern the selectivity and mechanism of action of BQCA can provide considerable guidance in the rational design of allosteric ligands with improved pharmacological characteristics. Nonetheless, being the first selective PAM for the M_1 mAChR, BQCA represents a very useful starting point to understand allosteric modulation at this receptor.

To determine the structural basis of BQCA selectivity and to understand allosteric ligand-receptor interactions at the M_1 mAChR, a structure-function approach is applied in Chapter 3 to investigate the role certain amino acids play in the function of BQCA. Site-directed mutagenesis is performed by substituting amino acid side chains into Ala, or 'side-chain deletion'. This method is useful to verify the role of individual residues in ligand activity and intermolecular interactions at a particular receptor.

Using this approach, there have been a number of structure-function studies at the M_1 mAChR and other mAChR subtypes that investigated the molecular determinants of binding and function of allosteric modulators (Huang et al., 2005; Leach et al., 2011; Matsui et al., 1995; May et al., 2007a; Nawaratne et al., 2010; Prilla et al., 2006; Stewart et al., 2010; Valant et al., 2012a; Voigtlander et al., 2003). Evidence from these studies indicated that mAChRs have an allosteric binding site located extracellularly to the TM-bound orthosteric

pocket and that residues at positions 2.61, 2.64, 3.28, 5.24-5.27, 5.29, 7.32, 7.35 and 7.36 contribute to the allosteric modulator binding site, and or play a role in cooperativity. These studies also suggested that residues in the orthosteric pocket may contribute indirectly to the function of allosteric ligands (Hulme, 2013; Leach et al., 2011; Nawaratne et al., 2010). This information provided the basis for the rationale to introduce mutations into a selected number of amino acids at the M_1 mAChR in the current project.

Chapter 3 elucidated the effects of the introduced mutations on the affinity, efficacy and cooperativity of BQCA and identified differential effects of distinct receptor regions on each of the molecular properties at the M_1 mAChR. Specifically, BQCA was found to occupy an allosteric pocket in the extracellular vestibule of the M_1 mAChR and interact with residues at the top of TM2 (Tyr85$^{2.64}$), ECL2 (Tyr179 and Phe182) and the top of TM7 (Glu397$^{7.32}$ and Trp400$^{7.35}$). Molecular dynamic simulation studies with BQCA confirmed the contribution of each of these residues to the allosteric binding pocket. These findings are particularly interesting as they highlight that the BQCA binding pocket partially overlaps with the previously described "common" allosteric site identified for a number of allosteric ligands at other mAChR subtypes. The results suggest that BQCA achieves selectivity by "selective cooperativity" with the orthosteric agonist at the M_1 mAChR, despite binding at a "conserved" allosteric site. The conservation within the allosteric site likely results from the fact that amino acid residues at positions 2.64 and 7.35 are identical across all mAChR receptor subtypes; while Tyr179 is only present at the M_1 and M_2 mAChRs but is still an aromatic residue (Phe) at the M_3 and M_4 mAChRs.

The studies in Chapter 3 also identified that Ala substitution of a number of residues from various regions in the receptor caused a decrease in the cooperativity between BQCA and CCh in binding and functional interaction studies. Such reductions in cooperativity resulted either from mutation of residues that contributed directly to the allosteric binding pocket

(Tyr85$^{2.64}$, Tyr179, Phe182, Glu397$^{7.32}$ and Trp400$^{7.35}$) or residues conformationally linked to the allosteric site and thus needed for the transmission of cooperativity or receptor activation upon ligand binding. For example, Ala substitution of Glu397$^{7.32}$ and Glu401$^{7.36}$, both of which are not conserved across the mAChR family and, as predicted by the modelling experiments, make minimal interactions with BQCA, had no effect on BQCA binding affinity but decreased cooperativity with CCh. Such residues may govern the subtype-specific cooperative effect of BQCA upon orthosteric ligand binding from a conserved allosteric pocket. Furthermore, mutation of the highly conserved orthosteric site residues (D105$^{3.32}$, Y106$^{3.33}$, W157$^{4.57}$ and Y381$^{6.51}$), led to complete loss or significant reduction in the binding cooperativity between CCh and BQCA, highlighting the importance of the orthosteric site residues for the transmission of binding cooperativity and demonstrating a striking example of a conformationally linked mechanism for the transmission of cooperativity. Moreover, the significantly impaired signaling efficacy of CCh at these mutants was "rescued" by BQCA, suggesting that BQCA becomes an "efficacy only" modulator when such residues are mutated. These findings emphasise the importance of using both binding and functional assays to characterize the effect of mutations upon allosteric ligand function. Interestingly, similar observations were noted in Chapter 2, whereby at the DREADD (which contains a mutation at the orthosteric site residue Tyr106$^{3.33}$), BQCA lost the ability to potentiate the affinity of ACh, while "rescuing" the impaired signaling efficacy of ACh at this receptor.

Recent compelling evidence from: (1) an atomic scale molecular dynamics simulations study at the M_2 mAChR, which identified the mode of binding of a number of prototypical allosteric ligands (Dror et al., 2013), and (2) a study that solved the crystal structure of the M_2 mAChR with iperoxo and the PAM LY2119620 (described above) (Kruse et al., 2013),

highlight the importance of the TM2 residues Tyr$^{2.61}$ and Tyr$^{2.64}$, Tyr177 in ECL2 (residue 179 at the M_1 mAChR) and Trp$^{7.35}$ in TM7 for the binding of the allosteric ligands examined.

In Chapter 3, the molecular models predict that the TM2 residues Tyr82$^{2.61}$ and Tyr85$^{2.64}$, and Tyr179 in ECL2, interact directly with BQCA. Despite this, mutation of these residues to Ala did not cause a significant decrease in BQCA binding affinity, rather, only led to a decrease in the transmission of BQCA's cooperativity with the orthosteric agonist. Given the contribution of these residues to the BQCA binding pocket as suggested by the model in Chapter 3, and the findings in Dror et al., (2013) and Kruse et al., (2013), it may be hypothesised that these residues in fact do contribute to the binding affinity of BQCA, but this is not detected in our study for two main reasons. First, a decrease in the binding affinity of an inherently low affinity ligand, such as BQCA, is difficult to detect experimentally. This is evident by the fact that BQCA is unable to completely displace the binding of the radiolabeled antagonists [^{3}H]QNB and [^{3}H]NMS. Second, the affinity (pK_B) values determined for BQCA in Chapter 3 are estimates of the ATCM from binding interaction studies, rather than direct measurements. Therefore, the low affinity of BQCA restricts the prospect of gaining mechanistic insights of modulator activity from structure-function studies. As seen in Chapter 3, it is difficult to distinguish key residues that govern modulator affinity (thus directly contributing the allosteric binding site), versus residues that contribute to the transmission of the allosteric effect (thus indirectly contributing to the observed potency and selectivity). Such insights would be greatly facilitated by the availability of higher affinity allosteric probes.

Fortunately, numerous structure-activity studies focusing at improving the "druggability" and affinity of BQCA have resulted in the disclosure of a number of putative allosteric M_1 mAChR ligands with higher functional potency than BQCA (Foster et al., 2014). In a patent from Merck (Kuduk and Beshore, 2012; Kuduk et al., 2010a), benzoquinazolinone 12 was

disclosed amongst a number of aryl methyl benzoquinazolinone compounds. This compound was of particular interest to our study because it is structurally related to BQCA and on the basis of preliminary studies, has been reported to have a substantially higher functional potency than BQCA. However, nothing is known about its mechanism of action or the structural basis of its function.

In Chapter 4, we developed an optimised chemical synthesis of benzoquinazolinone 12 (performed by S.N Mistry, see Chapter 4 declaration), improving the overall yield of this compound. This was followed by the first comprehensive pharmacological characterisation of the allosteric properties of benzoquinazolinone 12, which confirmed its M_1 mAChR selectivity. Moreover, analysis of the allosteric actions of this compound revealed that, compared to BQCA, it displayed a greater than 50-fold increase in affinity for the M_1 mAChR while maintaining a similar level of efficacy and positive cooperativity with ACh.

Given these findings, it was of interest to determine the structural basis of the improved allosteric action of benzoquinazolinone 12 as compared to BQCA at the level of receptor residues that this ligand engages and confirm whether benzoquinazolinone 12 engages the same allosteric site as that which has been proposed for BQCA. Moreover, we took advantage of the high affinity of benzoquinazolinone 12 to overcome the limitations posed by BQCA and to gain deeper mechanistic insights of modulator activity from structure-function studies.

The studies in Chapter 4 focused on the four amino acids (Tyr82$^{2.61}$ and Tyr85$^{2.64}$, Tyr179 and Trp400$^{7.35}$) reported to contribute the binding of BQCA and other mAChR allosteric modulators. The results from the Ala mutation experiments reveal the importance of Tyr179 and Trp400$^{7.35}$ for the binding of benzoquinazolinone 12 and BQCA, consistent with both ligands binding to the same allosteric site within the M_1 mAChR. Ala mutation of all the three Tyr residues found them to be critical for the binding of benzoquinazolinone 12 but not

for the transfer of cooperativity with the ACh binding site. This is in contrast to the results with BQCA, which found these residues to be important for the transmission of cooperativity with the orthosteric site rather than binding affinity. It is interesting to note that while BQCA was minimally affected by both Tyr82$^{2.61}$Ala and Tyr85$^{2.64}$Ala mutations, this was not the case for benzoquinazolinone 12. As such, the replacement of the methoxy group with an aromatic substituent at the 4-position of the benzylic pendant of BQCA, or the replacement of the carboxylic acid with the corresponding 3- ((1*S*,2*S*)-2-hydroxycyclohexyl) group present in benzoquinazolinone 12 must confer the difference sensitivity to mutation of these TM2 residues. However, this may reflect the fact that a reduction in binding affinity at these mutants can only be detected by the improved affinity window offered by the high affinity of benzoquinazolinone 12. Additionally, the different effects observed for BQCA and benzoquinazolinone 12 could due to limitations in the ternary complex model used to analyse the binding data and not to differences in the way the compounds interact with the receptor.

Our experimental findings were rationalised in molecular dynamic simulations which showed that both BQCA and benzoquinazolinone 12 adopt a similar pose within the allosteric pocket. However, while both ligands are predicted to interact with similar residues, certain additional interactions appear to take place with benzoquinazolinone 12, accounting for the higher affinity of this compound. In addition, the aromatic side chain of Trp400$^{7.35}$ is predicted to adopt a different orientation in the benzoquinazolinone 12-bound model, facilitating a number of additional interactions of certain residues with benzoquinazolinone 12 that do not take place with BQCA. The closer interaction of the tricyclic core of benzoquinazolinone 12 to the TM2 residues Tyr82$^{2.61}$ and Tyr85$^{2.64}$ may also contribute to the higher affinity of this ligand. This may also explain the greater than 10-fold loss of affinity for benzoquinazolinone 12 when these residues are mutated to Ala while no effect upon BQCA's affinity was

observed. The modelling studies additionally suggested that the hydroxyl group on Tyr82$^{2.61}$, Tyr85$^{2.64}$ and Tyr179 might participate in a hydrogen bond network with benzoquinazolinone 12 and/or with other residues in the complex in the benzoquinazolinone 12 but not the BQCA-bound complex. While these results provide insight into ligand-receptor interactions, it should be noted that the homology model used to predict these interactions is limited as it is based on the crystal structure of the nanobody-stabilised active-state human β_2 adrenergic receptor (see Chapter 3 and 4 Experimental Procedures section) and the interactions predicted remain to be validated upon the availability of an M_1 mAChR crystal structure. Therefore, caution must be exercised if the information generated in this model is to be used for future structure-based drug design.

While the Ala scanning approach proved useful in identifying the importance of individual residues for the binding of BQCA and benzoquinazolinone 12, the information provided regarding the nature of these interactions is limited. Further insights were gained into the contribution of each of the aromatic amino acid residues to the allosteric binding pocket when the effects of more subtle amino acid substitutions were tested on ligand binding and function. Each of the Tyr residues (Y82$^{2.61}$, Y85$^{2.64}$ and Y179) were mutated to Phe in order to maintain the aromaticity of the side chain of these amino acids while removing their hydroxyl group. The effects of these mutations were subsequently compared upon the pharmacology of both BQCA and benzoquinazolinone 12. At the Tyr-to-Phe mutations, the binding and function of BQCA were unaffected, suggesting that the ability of these residues to make hydrophobic rather than polar interactions with the modulator. In contrast, the same mutations resulted in significant decreases in the binding affinity of benzoquinazolinone 12, suggesting that the significant role these residues play in the binding of benzoquinazolinone 12 is via polar interactions and giving support to the network of polar interactions predicted by the modelling studies. Therefore, the network of polar interactions formed between

benzoquinazolinone 12 and Tyr residues in the allosteric binding pocket may also contribute to the higher affinity of this compound in comparison to BQCA.

Collectively, the studies in Chapters 3 and 4 identified key regions in the M_1 mAChR that are involved in the binding and function of BQCA and benzoquinazolinone 12, and provide an unprecedented insight into the structural basis of allosteric modulation at this receptor which may be of general application to GPCR drug discovery. The combined mutagenesis and molecular dynamics simulations studies provide a mechanistic basis for observed structure-activity relationship of M_1 mAChR positive allosteric modulators. In particular, the studies demonstrated that benzoquinazolinone 12 displays a significant increase in affinity at the M_1 mAChR and identified the ligand-receptor interactions that confer this increase. These insights will provide the basis for the development of novel M_1 mAChR selective allosteric ligands or guide the improvement of existing allosteric ligands.

A key property often associated with allosteric targeting of GPCRs is that selective modulators gain subtype selectivity through their binding to a site that is not conserved across a receptor subfamily. However, the findings in Chapters 3 and 4 challenge this concept and show that selective cooperativity via interaction with a conserved allosteric site may account for the selectivity of BQCA and benzoquinazolinone 12. However, the mechanism by which this "selective cooperativity" is achieved remains to be elucidated. Given the findings in this thesis and other recent studies that the allosteric binding site in the extracellular vestibule of mAChRs is conserved between subtypes, it may be hypothesised that this site has evolved to harbour yet undiscovered endogenous allosteric ligands for mAChRs. Indeed, early studies on the M_2 mAChR reported that certain endogenous peptides, such as dynorphin A, protamine, myelin basic protein and major basic protein display allosteric behaviour in their interactions at this receptor (Hu and el-Fakahany, 1993; Hu et al., 1992; Jacoby et al., 1993). However, further studies are required to validate these findings.

Given the vast insights gained from structure function studies described herein, and the increasing number of GPCR crystal structures being solved, it should thus be appreciated that structure-based drug design using *in silico* screening for novel allosteric modulators is not sufficient to produce ligands with desired functions and a high level of selectivity. Rather, drug discovery efforts should complement their findings from in *in silico* screening with structure-function studies. Although the *in vivo* efficacy of benzoquinazolinone 12 is yet to be determined, the binding pocket described for this ligand and BQCA may be used to perform virtual ligand screening to identify new allosteric modulators, or refine existing modulators to improve their selectivity and/function.

While M_1 mAChR PAMs have been the focus of many studies, selective M_1 mAChR NAMs may potentially be beneficial in diseases where cholinergic neurotransmission is augmented. For example, mAChR antagonists are among the treatments used for Parkinson's disease (Xiang et al., 2012), however, the clinical utility of these compounds is significantly limited by their central and peripheral adverse effects. Similar to positive allosteric ligands, the structure-function information provided in the current thesis may guide the development of new selective M_1 mAChR NAMs.

In conclusion, the studies in this thesis have identified the molecular determinants of allosteric modulation at the M_1 mAChR, determined the structural basis of the improved function of novel allosteric modulators and provided new insights into allosteric modulation at a chemogenetically modified M_1 mAChR. These studies may facilitate the future development of selective therapies. With the first M_1 mAChR PAM (MK-7622) recently reaching the clinical trial stage (Conn et al., 2014), the future of M_1 mAChR PAMs looks promising.

CHAPTER 6

References

Abdul-Ridha A, Lane JR, Mistry SN, Lopez L, Sexton PM, Scammells PJ, Christopoulos A and Canals M (2014a) Mechanistic insights into allosteric structure-function relationships at the M1 muscarinic acetylcholine receptor. *J Biol Chem* **289**(48): 33701-33711.

Abdul-Ridha A, Lane JR, Sexton PM, Canals M and Christopoulos A (2013) Allosteric Modulation of a Chemogenetically Modified G Protein-Coupled Receptor. *Mol Pharmacol* **83**(2): 521-530.

Abdul-Ridha A, López L, Keov P, Thal DM, Mistry SN, Sexton PM, Lane JR, Canals M and Christopoulos A (2014b) Molecular Determinants of Allosteric Modulation at the M1 Muscarinic Acetylcholine Receptor. *J. Biol. Chem.* **289**(9): 6067-6079.

Adams JP and Sweatt JD (2002) Molecular psychology: roles for the ERK MAP kinase cascade in memory. *Annu Rev Pharmacol Toxicol* **42**: 135-163.

Akam EC, Challiss RA and Nahorski SR (2001) G(q/11) and G(i/o) activation profiles in CHO cells expressing human muscarinic acetylcholine receptors: dependence on agonist as well as receptor-subtype. *Br J Pharmacol* **132**(4): 950-958.

Alexander GM, Rogan SC, Abbas AI, Armbruster BN, Pei Y, Allen JA, Nonneman RJ, Hartmann J, Moy SS, Nicolelis MA, McNamara JO and Roth BL (2009) Remote control of neuronal activity in transgenic mice expressing evolved G protein-coupled receptors. *Neuron* **63**(1): 27-39.

Allman K, Page KM, Curtis CA and Hulme EC (2000) Scanning mutagenesis identifies amino acid side chains in transmembrane domain 5 of the M(1) muscarinic receptor that participate in binding the acetyl methyl group of acetylcholine. *Mol Pharmacol* **58**(1): 175-184.

Alvarez-Curto E, Prihandoko R, Tautermann CS, Zwier JM, Pediani JD, Lohse MJ, Hoffmann C, Tobin AB and Milligan G (2011) Developing chemical genetic approaches to explore G protein-coupled receptor function: validation of the use of a receptor activated solely by synthetic ligand (RASSL). *Mol Pharmacol* **80**(6): 1033-1046.

Anagnostaras SG, Murphy GG, Hamilton SE, Mitchell SL, Rahnama NP, Nathanson NM and Silva AJ (2003) Selective cognitive dysfunction in acetylcholine M1 muscarinic receptor mutant mice. *Nat Neurosci* **6**(1): 51-58.

Antony J, Kellershohn K, Mohr-Andra M, Kebig A, Prilla S, Muth M, Heller E, Disingrini T, Dallanoce C, Bertoni S, Schrobang J, Trankle C, Kostenis E, Christopoulos A, Holtje HD, Barocelli E, De Amici M, Holzgrabe U and Mohr K (2009) Dualsteric GPCR targeting: a novel route to binding and signaling pathway selectivity. *FASEB J.* **23**(2): 442-450.

Armbruster BN (2007) Evolving the lock to fit the key to create a family of G protein-coupled receptors potently activated by an inert ligand. *Proc. Natl. Acad. Sci. USA* **12**: 5163-5168.

Armbruster BN, Li X, Pausch MH, Herlitze S and Roth BL (2007) Evolving the lock to fit the key to create a family of G protein-coupled receptors potently activated by an inert ligand. *Proc Natl Acad Sci U S A* **104**(12): 5163-5168.

Auld DS, Kornecook TJ, Bastianetto S and Quirion R (2002) Alzheimer's disease and the basal forebrain cholinergic system: relations to beta-amyloid peptides, cognition, and treatment strategies. *Prog Neurobiol* **68**(3): 209-245.

Avlani VA, Gregory KJ, Morton CJ, Parker MW, Sexton PM and Christopoulos A (2007) Critical role for the second extracellular loop in the binding of both orthosteric and allosteric G protein-coupled receptor ligands. *J Biol Chem* **282**(35): 25677-25686.

Avlani VA, Langmead CJ, Guida E, Wood MD, Tehan BG, Herdon HJ, Watson JM, Sexton PM and Christopoulos A (2010) Orthosteric and allosteric modes of interaction of novel selective agonists of the M1 muscarinic acetylcholine receptor. *Mol Pharmacol* **78**(1): 94-104.

Ballard C, Gauthier S, Corbett A, Brayne C, Aarsland D and Jones E (2011) Alzheimer's disease. *Lancet* **377**(9770): 1019-1031.

Ballesteros JA and Weinstein H (1995) Integrated methods for the construction of three-dimensional models and computational probing of structure-function relations in G protein-coupled receptors, in *Methods Neurosci* (Stuart CS ed) pp 366-428, Academic Press.

Baumgold J (1992) Muscarinic receptor-mediated stimulation of adenylyl cyclase. *Trends Pharmacol Sci* **13**(9): 339-340.

Baumgold J, Paek R and Yasumoto T (1992) Agents that stimulate phosphoinositide turnover also elevate cAMP in SK-N-SH human neuroblastoma cells. *Life Sci* **50**(23): 1755-1759.

Becnel J, Johnson O, Majeed Zana R, Tran V, Yu B, Roth Bryan L, Cooper Robin L, Kerut Edmund K and Nichols Charles D (2013) DREADDs in Drosophila: A Pharmacogenetic Approach for Controlling Behavior, Neuronal Signaling, and Physiology in the Fly. *Cell Reports* **4**(5): 1049-1059.

Bence K, Ma W, Kozasa T and Huang XY (1997) Direct stimulation of Bruton's tyrosine kinase by G(q)-protein alpha-subunit. *Nature* **389**(6648): 296-299.

Berkeley JL, Gomeza J, Wess J, Hamilton SE, Nathanson NM and Levey AI (2001) M1 Muscarinic Acetylcholine Receptors Activate Extracellular Signal-Regulated Kinase in CA1 Pyramidal Neurons in Mouse Hippocampal Slices. *Mol Cell Neurosci* **18**(5): 512-524.

Berkeley JL and Levey AI (2000) Muscarinic activation of mitogen-activated protein kinase in PC12 cells. *J Neurochem* **75**(2): 487-493.

Bernstein LS, Ramineni S, Hague C, Cladman W, Chidiac P, Levey AI and Hepler JR (2004) RGS2 Binds Directly and Selectively to the M1 Muscarinic Acetylcholine Receptor Third Intracellular Loop to Modulate Gq/11α Signaling. *J Biol Chem* **279**(20): 21248-21256.

Berstein G, Blank JL, Smrcka AV, Higashijima T, Sternweis PC, Exton JH and Ross EM (1992) Reconstitution of agonist-stimulated phosphatidylinositol 4,5-bisphosphate hydrolysis using purified m1 muscarinic receptor, Gq/11, and phospholipase C-beta 1. *J Biol Chem* **267**(12): 8081-8088.

Bhanot P, Brink M, Samos CH, Hsieh JC, Wang Y, Macke JP, Andrew D, Nathans J and Nusse R (1996) A new member of the frizzled family from Drosophila functions as a Wingless receptor. *Nature* **382**(6588): 225-230.

Birdsall NJ, Farries T, Gharagozloo P, Kobayashi S, Lazareno S and Sugimoto M (1999) Subtype-selective positive cooperative interactions between brucine analogs and acetylcholine at muscarinic receptors: functional studies. *Mol Pharmacol* **55**(4): 778-786.

Bjarnadottir TK, Fredriksson R, Hoglund PJ, Gloriam DE, Lagerstrom MC and Schioth HB (2004) The human and mouse repertoire of the adhesion family of G-protein-coupled receptors. *Genomics* **84**(1): 23-33.

Black JW and Leff P (1983) Operational Models of Pharmacological Agonism. *Proc Biol Sci* **220**(1219): 141-162.

Blin N, Yun J and Wess J (1995) Mapping of single amino acid residues required for selective activation of Gq/11 by the m3 muscarinic acetylcholine receptor. *J Biol Chem* **270**(30): 17741-17748.

Bluml K, Mutschler E and Wess J (1994a) Functional role in ligand binding and receptor activation of an asparagine residue present in the sixth transmembrane domain of all muscarinic acetylcholine receptors. *J Biol Chem* **269**(29): 18870-18876.

Bluml K, Mutschler E and Wess J (1994b) Functional role of a cytoplasmic aromatic amino acid in muscarinic receptor-mediated activation of phospholipase C. *J Biol Chem* **269**(15): 11537-11541.

Bluml K, Mutschler E and Wess J (1994c) Insertion mutagenesis as a tool to predict the secondary structure of a muscarinic receptor domain determining specificity of G-protein coupling. *Proc Natl Acad Sci USA* **91**(17): 7980-7984.

Bock A, Merten N, Schrage R, Dallanoce C, Bätz J, Klöckner J, Schmitz J, Matera C, Simon K, Kebig A, Peters L, Müller A, Schrobang-Ley J, Tränkle C, Hoffmann C, De Amici M, Holzgrabe U, Kostenis E and Mohr K (2012) The allosteric vestibule of a seven transmembrane helical receptor controls G-protein coupling. *Nat Commun* **3**: 1044.

Bock A and Mohr K (2013) Dualsteric GPCR targeting and functional selectivity: the paradigmatic M2 muscarinic acetylcholine receptor. *Drug discovery today. Technologies* **10**(2): e245-e252.

Bodick NC, Offen WW, Levey AI, Cutler NR, Gauthier SG, Satlin A, Shannon HE, Tollefson GD, Rasmussen K, Bymaster FP, Hurley DJ, Potter WZ and Paul SM (1997a) Effects of xanomeline, a selective muscarinic receptor agonist, on cognitive function and behavioral symptoms in Alzheimer disease. *Arch Neurol* **54**(4): 465-473.

Bodick NC, Offen WW, Shannon HE, Satterwhite J, Lucas R, van Lier R and Paul SM (1997b) The selective muscarinic agonist xanomeline improves both the cognitive deficits and behavioral symptoms of Alzheimer disease. *Alzheimer Dis Assoc Disord* **11 Suppl 4**: S16-22.

Bohr C HK, KroghA (1904) Übereinen in biologischen Beziehung wichtigen Einfluss, den die Kohlensäurespannung des Blutes auf dessen Sauer-stoffbindung übt. . *Skand. Arch. Physiol* **16**: 402-412.

Bondar A and Lazar J (2014) Dissociated GαGTP and Gβγ Protein Subunits Are the Major Activated Form of Heterotrimeric Gi/o Proteins. *J Biol Chem* **289**(3): 1271-1281.

Bonner TI, Buckley NJ, Young AC and Brann MR (1987) Identification of a family of muscarinic acetylcholine receptor genes. *Science* **237**(4814): 527-532.

Bouvier M (2001) Oligomerization of G-protein-coupled transmitter receptors. *Nat Rev Neurosci* **2**(4): 274-286.

Bouvier M, Hausdorff WP, De Blasi A, O'Dowd BF, Kobilka BK, Caron MG and Lefkowitz RJ (1988) Removal of phosphorylation sites from the beta 2-adrenergic receptor delays onset of agonist-promoted desensitization. *Nature* **333**(6171): 370-373.

Bridges TM, Kennedy JP, Noetzel MJ, Breininger ML, Gentry PR, Conn PJ and Lindsley CW (2010) Chemical lead optimization of a pan Gq mAChR M1, M3, M5 positive allosteric modulator (PAM) lead. Part II: Development of a potent and highly selective M1 PAM. *Bioorg. Med. Chem. Lett.* **20**(6): 1972-1975.

Brown DA (2010) Muscarinic acetylcholine receptors (mAChRs) in the nervous system: some functions and mechanisms. *J Mol Neurosci* **41**(3): 340-346.

Brusa R, Gamalero SR, Genazzani E and Eva C (1995) In primary neuronal cultures muscarinic m1 and m3 receptor mRNA levels are regulated by agonists, partial agonists and antagonists. *Eur J Pharmacol* **289**(1): 9-16.

Bruysters M, Jongejan A, Akdemir A, Bakker RA and Leurs R (2005) A G(q/11)-coupled mutant histamine H(1) receptor F435A activated solely by synthetic ligands (RASSL). *J Biol Chem* **280**(41): 34741-34746.

Buchanan KA, Petrovic MM, Chamberlain SE, Marrion NV and Mellor JR (2010) Facilitation of long-term potentiation by muscarinic M(1) receptors is mediated by inhibition of SK channels. *Neuron* **68**(5): 948-963.

Budzik B, Garzya V, Shi D, Foley JJ, Rivero RA, Langmead CJ, Watson J, Wu Z, Forbes IT and Jin J (2010a) 2' biaryl amides as novel and subtype selective M1 agonists. Part I: Identification, synthesis, and initial SAR. *Bioorg. Med. Chem. Lett.* **20**(12): 3540-3544.

Budzik B, Garzya V, Shi D, Walker G, Lauchart Y, Lucas AJ, Rivero RA, Langmead CJ, Watson J, Wu Z, Forbes IT and Jin J (2010b) 2' biaryl amides as novel and subtype selective M1 agonists. Part II: Further optimization and profiling. *Bioorg. Med. Chem. Lett.* **20**(12): 3545-3549.

Budzik B, Garzya V, Shi D, Walker G, Woolley-Roberts M, Pardoe J, Lucas A, Tehan B, Rivero RA, Langmead CJ, Watson J, Wu Z, Forbes IT and Jin J (2010c) Novel N-Substituted Benzimidazolones as Potent, Selective, CNS-Penetrant, and Orally Active M1 mAChR Agonists. *ACS Med. Chem. Lett.* **1**(6): 244-248.

Buller S, Zlotos DP, Mohr K and Ellis J (2002) Allosteric site on muscarinic acetylcholine receptors: a single amino acid in transmembrane region 7 is critical to the subtype selectivities of caracurine V derivatives and alkane-bisammonium ligands. *Mol Pharmacol* **61**(1): 160-168.

Burford NT and Nahorski SR (1996) Muscarinic m1 receptor-stimulated adenylate cyclase activity in Chinese hamster ovary cells is mediated by Gs alpha and is not a consequence of phosphoinositidase C activation. *Biochem J* **315 (Pt 3)**: 883-888.

Burstein ES, Spalding TA and Brann MR (1996) Amino acid side chains that define muscarinic receptor/G-protein coupling. Studies of the third intracellular loop. *J Biol Chem* **271**(6): 2882-2885.

Burstein ES, Spalding TA and Brann MR (1998a) The second intracellular loop of the m5 muscarinic receptor is the switch which enables G-protein coupling. *J Biol Chem* **273**(38): 24322-24327.

Burstein ES, Spalding TA and Brann MR (1998b) Structure/function relationships of a G-protein coupling pocket formed by the third intracellular loop of the m5 muscarinic receptor. *Biochemistry* **37**(12): 4052-4058.

Butcher AJ, Kong KC, Prihandoko R and Tobin AB (2012) Physiological role of G-protein coupled receptor phosphorylation. *Handb Exp Pharmacol*(208): 79-94.

Caccamo A, Fisher A and LaFerla FM (2009) M1 agonists as a potential disease-modifying therapy for Alzheimer's disease. *Curr Alzheimer Res* **6**(2): 112-117.

Caccamo A, Oddo S, Billings LM, Green KN, Martinez-Coria H, Fisher A and LaFerla FM (2006) M1 receptors play a central role in modulating AD-like pathology in transgenic mice. *Neuron* **49**(5): 671-682.

Calabresi P, Centonze D, Gubellini P, Pisani A and Bernardi G (1998) Endogenous ACh enhances striatal NMDA-responses via M1-like muscarinic receptors and PKC activation. *Eur J Neurosci* **10**(9): 2887-2895.

Canals M, Lane JR, Wen A, Scammells PJ, Sexton PM and Christopoulos A (2012) A Monod-Wyman-Changeux Mechanism Can Explain G Protein-coupled Receptor (GPCR) Allosteric Modulation. *J Biol Chem* **287**(1): 650-659.

Canals M, Sexton PM and Christopoulos A (2011) Allostery in GPCRs: 'MWC' revisited. *Trends Biochem. Sci.* **36**(12): 663-672.

Cannon DM, Klaver JK, Gandhi SK, Solorio G, Peck SA, Erickson K, Akula N, Savitz J, Eckelman WC, Furey ML, Sahakian BJ, McMahon FJ and Drevets WC (2011) Genetic variation in cholinergic muscarinic-2 receptor gene modulates M2 receptor binding in vivo and accounts for reduced binding in bipolar disorder. *Mol Psych* **16**(4): 407-418.

Cantrell AR, Ma JY, Scheuer T and Catterall WA (1996) Muscarinic modulation of sodium current by activation of protein kinase C in rat hippocampal neurons. *Neuron* **16**(5): 1019-1026.

Carr DB and Surmeier DJ (2007) M1 muscarinic receptor modulation of Kir2 channels enhances temporal summation of excitatory synaptic potentials in prefrontal cortex pyramidal neurons. *J Neurophysiol* **97**(5): 3432-3438.

Caruana DA, Warburton EC and Bashir ZI (2011) Induction of activity-dependent LTD requires muscarinic receptor activation in medial prefrontal cortex. *J Neurosci* **31**(50): 18464-18478.

Caulfield MP and Birdsall NJ (1998) International Union of Pharmacology. XVII. Classification of muscarinic acetylcholine receptors. *Pharmacol Rev* **50**(2): 279-290.

Challiss RAJ and Wess J (2011) Receptors: GPCR-G protein preassembly? *Nat Chem Biol* **7**(10): 657-658.

Chambon C, Jatzke C, Wegener N, Gravius A and Danysz W (2012) Using cholinergic M1 receptor positive allosteric modulators to improve memory via enhancement of brain cholinergic communication. *Eur J Pharmacol* **697**(1-3): 73-80.

Chambon C, Wegener N, Gravius A and Danysz W (2011) A new automated method to assess the rat recognition memory: validation of the method. *Behav Brain Res* **222**(1): 151-157.

Chan WY, McKinzie DL, Bose S, Mitchell SN, Witkin JM, Thompson RC, Christopoulos A, Lazareno S, Birdsall NJ, Bymaster FP and Felder CC (2008) Allosteric modulation of the muscarinic M4 receptor as an approach to treating schizophrenia. *Proc Natl Acad Sci USA* **105**(31): 10978-10983.

Chandrashekar J, Mueller KL, Hoon MA, Adler E, Feng L, Guo W, Zuker CS and Ryba NJP (2000) T2Rs Function as Bitter Taste Receptors. *Cell* **100**(6): 703-711.

Charlton SJ and Vauquelin G (2010) Elusive equilibrium: the challenge of interpreting receptor pharmacology using calcium assays. *Br J Pharmacol* **161**(6): 1250-1265.

Cherezov V, Rosenbaum DM, Hanson MA, Rasmussen SG, Thian FS, Kobilka TS, Choi HJ, Kuhn P, Weis WI, Kobilka BK and Stevens RC (2007) High-resolution crystal structure of an engineered human beta2-adrenergic G protein-coupled receptor. *Science* **318**(5854): 1258-1265.

Chien EY, Liu W, Zhao Q, Katritch V, Han GW, Hanson MA, Shi L, Newman AH, Javitch JA, Cherezov V and Stevens RC (2010) Structure of the human dopamine D3 receptor in complex with a D2/D3 selective antagonist. *Science* **330**(6007): 1091-1095.

Choe HW, Kim YJ, Park JH, Morizumi T, Pai EF, Krauss N, Hofmann KP, Scheerer P and Ernst OP (2011a) Crystal structure of metarhodopsin II. *Nature* **471**(7340): 651-655.

Choe HW, Park JH, Kim YJ and Ernst OP (2011b) Transmembrane signaling by GPCRs: insight from rhodopsin and opsin structures. *Neuropharmacology* **60**(1): 52-57.

Christopoulos A (2002) Allosteric binding sites on cell-surface receptors: novel targets for drug discovery. *Nat Rev Drug Discov* **1**(3): 198-210.

Christopoulos A (2014) Advances in GPCR Allostery: From Function to Structure. *Mol Pharmacol* **86**(5): 463-478.

Christopoulos A, Changeux J-P, Catterall WA, Fabbro D, Burris TP, Cidlowski JA, Olsen RW, Peters JA, Neubig RR, Pin J-P, Sexton PM, Kenakin TP, Ehlert FJ, Spedding M and Langmead CJ (2014) International Union of Basic and Clinical Pharmacology. XC. Multisite Pharmacology: Recommendations for the Nomenclature of Receptor Allosterism and Allosteric Ligands. *Pharmacol Rev* **66**(4): 918-947.

Christopoulos A and Kenakin T (2002) G protein-coupled receptor allosterism and complexing. *Pharmacol Rev* **54**(2): 323-374.

Christopoulos A, Lanzafame A and Mitchelson F (1998) Allosteric interactions at muscarinic cholinoceptors. *Clin Exp Pharmacol Physiol* **25**(3-4): 185-194.

Christopoulos A, Sorman JL, Mitchelson F and El-Fakahany EE (1999) Characterization of the subtype selectivity of the allosteric modulator heptane-1,7-bis-(dimethyl-3'-phthalimidopropyl) ammonium bromide (C7/3-phth) at cloned muscarinic acetylcholine receptors. *Biochem Pharmacol* **57**(2): 171-179.

Cianfrocca R, Tocci P, Semprucci E, Spinella F, Di Castro V, Bagnato A and Rosanò L β-Arrestin 1 is required for endothelin-1-induced NF-κB activation in ovarian cancer cells. *Life Sci*(0).

Claing A, Perry SJ, Achiriloaie M, Walker JK, Albanesi JP, Lefkowitz RJ and Premont RT (2000) Multiple endocytic pathways of G protein-coupled receptors delineated by GIT1 sensitivity. *Proc Natl Acad Sci USA* **97**(3): 1119-1124.

Clark AL and Mitchelson F (1976) The inhibitory effect of gallamine on muscarinic receptors. *Br J Pharmacol* **58**(3): 323-331.

Comps-Agrar L, Kniazeff J, Norskov-Lauritsen L, Maurel D, Gassmann M, Gregor N, Prezeau L, Bettler B, Durroux T, Trinquet E and Pin JP (2011) The oligomeric state sets GABA(B) receptor signalling efficacy. *EMBO J* **30**(12): 2336-2349.

Conn PJ, Jones CK and Lindsley CW (2009) Subtype-selective allosteric modulators of muscarinic receptors for the treatment of CNS disorders. *Trends Pharmacol. Sci.* **30**(3): 148-155.

Conn PJ, Lindsley CW, Meiler J and Niswender CM (2014) Opportunities and challenges in the discovery of allosteric modulators of GPCRs for treating CNS disorders. *Nat Rev Drug Discov* **13**(9): 692-708.

Coso OA, Chiariello M, Kalinec G, Kyriakis JM, Woodgett J and Gutkind JS (1995) Transforming G protein-coupled receptors potently activate JNK (SAPK). Evidence for a divergence from the tyrosine kinase signaling pathway. *J Biol Chem* **270**(10): 5620-5624.

Coso OA, Teramoto H, Simonds WF and Gutkind JS (1996) Signaling from G protein-coupled receptors to c-Jun kinase involves beta gamma subunits of heterotrimeric G proteins acting on a Ras and Rac1-dependent pathway. *J Biol Chem* **271**(8): 3963-3966.

Coward P, Wada HG, Falk MS, Chan SD, Meng F, Akil H and Conklin BR (1998) Controlling signaling with a specifically designed Gi-coupled receptor. *Proc Natl Acad Sci USA* **95**(1): 352-357.

Curtis CA, Wheatley M, Bansal S, Birdsall NJ, Eveleigh P, Pedder EK, Poyner D and Hulme EC (1989) Propylbenzilylcholine mustard labels an acidic residue in transmembrane helix 3 of the muscarinic receptor. *J Biol Chem* **264**(1): 489-495.

Daaka Y, Luttrell LM and Lefkowitz RJ (1997) Switching of the coupling of the beta2-adrenergic receptor to different G proteins by protein kinase A. *Nature* **390**(6655): 88-91.

Daiss JO, Duda-Johner S, Burschka C, Holzgrabe U, Mohr K and Tacke R (2002) N+/Si Replacement as a Tool for Probing the Pharmacophore of Allosteric Modulators of Muscarinic M2 Receptors: Synthesis, Allosteric Potency, and Positive Cooperativity of Silicon-Based W84 Derivatives. *Organometallics* **21**(5): 803-811.

Daub H, Wallasch C, Lankenau A, Herrlich A and Ullrich A (1997) Signal characteristics of G protein-transactivated EGF receptor. *EMBO J* **16**(23): 7032-7044.

Daval SB, Kellenberger E, Bonnet D, Utard V, Galzi JL and Ilien B (2013) Exploration of the orthosteric/allosteric interface in human m1 muscarinic receptors by bitopic fluorescent ligands. *Mol Pharmacol* **84**(1): 71-85.

Davenport AP, Alexander SP, Sharman JL, Pawson AJ, Benson HE, Monaghan AE, Liew WC, Mpamhanga CP, Bonner TI, Neubig RR, Pin JP, Spedding M and Harmar AJ (2013) International Union of Basic and Clinical Pharmacology. LXXXVIII. G protein-coupled receptor list: recommendations for new pairings with cognate ligands. *Pharmacol Rev* **65**(3): 967-986.

Davie BJ, Christopoulos A and Scammells PJ (2013) Development of M1 mAChR Allosteric and Bitopic Ligands: Prospective Therapeutics for the Treatment of Cognitive Deficits. *ACS Chem. Neurosci.* **4**(7): 1026-1048.

Davis AA, Fritz JJ, Wess J, Lah JJ and Levey AI (2010) Deletion of M1 Muscarinic Acetylcholine Receptors Increases Amyloid Pathology In Vitro and In Vivo. *J Neurosci* **30**(12): 4190-4196.

De Amici M, Dallanoce C, Holzgrabe U, Tränkle C and Mohr K (2010) Allosteric ligands for G protein-coupled receptors: A novel strategy with attractive therapeutic opportunities. *Med Res Rev* **30**(3): 463-549.

Debburman SK, Kunapuli P, Benovic JL and Hosey MM (1995) Agonist-dependent phosphorylation of human muscarinic receptors in Spodoptera frugiperda insect cell membranes by G protein-coupled receptor kinases. *Mol Pharmacol* **47**(2): 224-233.

Defea K (2008) Beta-arrestins and heterotrimeric G-proteins: collaborators and competitors in signal transduction. *Br J Pharmacol* **153 Suppl 1**: S298-309.

Di Chiara G, Morelli M and Consolo S (1994) Modulatory functions of neurotransmitters in the striatum: ACh/dopamine/NMDA interactions. *Trends Neurosci.* **17**(6): 228-233.

Digby GJ, Noetzel MJ, Bubser M, Utley TJ, Walker AG, Byun NE, Lebois EP, Xiang Z, Sheffler DJ, Cho HP, Davis AA, Nemirovsky NE, Mennenga SE, Camp BW, Bimonte-Nelson HA, Bode J, Italiano K, Morrison R, Daniels JS, Niswender CM, Olive MF, Lindsley CW, Jones CK and Conn PJ (2012a) Novel allosteric agonists of M1 muscarinic acetylcholine receptors induce brain region-specific responses that correspond with behavioral effects in animal models. *J Neurocie* **32**(25): 8532-8544.

Digby GJ, Utley TJ, Lamsal A, Sevel C, Sheffler DJ, Lebois EP, Bridges TM, Wood MR, Niswender CM, Lindsley CW and Conn PJ (2012b) Chemical Modification of the M1 Agonist VU0364572 Reveals Molecular Switches in Pharmacology and a Bitopic Binding Mode. *ACS Chem. Neurosci.* **3**(12): 1025-1036.

Disingrini T, Muth M, Dallanoce C, Barocelli E, Bertoni S, Kellershohn K, Mohr K, De Amici M and Holzgrabe U (2006) Design, synthesis, and action of oxotremorine-related hybrid-type allosteric modulators of muscarinic acetylcholine receptors. *J Med Chem* **49**(1): 366-372.

Dore AS, Okrasa K, Patel JC, Serrano-Vega M, Bennett K, Cooke RM, Errey JC, Jazayeri A, Khan S, Tehan B, Weir M, Wiggin GR and Marshall FH (2014) Structure of class C GPCR metabotropic glutamate receptor 5 transmembrane domain. *Nature* **511**(7511): 557-562.

Dorr P, Westby M, Dobbs S, Griffin P, Irvine B, Macartney M, Mori J, Rickett G, Smith-Burchnell C, Napier C, Webster R, Armour D, Price D, Stammen B, Wood A and Perros M (2005)

Maraviroc (UK-427,857), a potent, orally bioavailable, and selective small-molecule inhibitor of chemokine receptor CCR5 with broad-spectrum anti-human immunodeficiency virus type 1 activity. *Antimicrob Agents Chemother* **49**(11): 4721-4732.

Dror RO, Green HF, Valant C, Borhani DW, Valcourt JR, Pan AC, Arlow DH, Canals M, Lane JR, Rahmani R, Baell JB, Sexton PM, Christopoulos A and Shaw DE (2013) Structural basis for modulation of a G-protein-coupled receptor by allosteric drugs. *Nature* **503**(7475): 295-299.

Dunlap J and Brown JH (1983) Heterogeneity of binding sites on cardiac muscarinic receptors induced by the neuromuscular blocking agents gallamine and pancuronium. *Mol Pharmacol* **24**(1): 15-22.

Eglen R (2012) Overview of Muscarinic Receptor Subtypes, in *Muscarinic Receptors* (Fryer AD, Christopoulos A and Nathanson NM eds) pp 3-28, Springer Berlin Heidelberg.

Eglen RM (2005) Muscarinic receptor subtype pharmacology and physiology. *Prog Med Chem* **43**: 105-136.

Eglen RM (2006) Muscarinic receptor subtypes in neuronal and non-neuronal cholinergic function. *Auton Autacoid Pharmacol* **26**(3): 219-233.

Eglen RM and Nahorski SR (2000) The muscarinic M(5) receptor: a silent or emerging subtype? *Br J Pharmacol* **130**(1): 13-21.

Egorov AV, Angelova PR, Heinemann U and Muller W (2003) Ca2+-independent muscarinic excitation of rat medial entorhinal cortex layer V neurons. *Eur J Neuroci* **18**(12): 3343-3351.

Ehlert FJ (1985) The relationship between muscarinic receptor occupancy and adenylate cyclase inhibition in the rabbit myocardium. *Mol Pharmacol* **28**(5): 410-421.

Ehlert FJ (1988) Estimation of the affinities of allosteric ligands using radioligand binding and pharmacological null methods. *Mol Pharmacol* **33**(2): 187-194.

Ehlert FJ (2005) Analysis of allosterism in functional assays. *J Pharmacol Exp Ther* **315**(2): 740-754.

Ehlert FJ, Ragan P, Chen A, Roeske WR and Yamamura HI (1982) Modulation of benzodiazepine receptor binding: insight into pharmacological efficacy. *Eur J Pharmacol* **78**(2): 249-253.

El-Asmar L, Springael JY, Ballet S, Andrieu EU, Vassart G and Parmentier M (2005) Evidence for negative binding cooperativity within CCR5-CCR2b heterodimers. *Mol Pharmacol* **67**(2): 460-469.

Ellis J, Huyler J and Brann MR (1991) Allosteric regulation of cloned m1-m5 muscarinic receptor subtypes. *Biochem Pharmacol* **42**(10): 1927-1932.

Ellis J, Pediani JD, Canals M, Milasta S and Milligan G (2006) Orexin-1 receptor-cannabinoid CB1 receptor heterodimerization results in both ligand-dependent and -independent coordinated alterations of receptor localization and function. *J Biol Chem* **281**(50): 38812-38824.

Ellis J and Seidenberg M (1992) Two allosteric modulators interact at a common site on cardiac muscarinic receptors. *Mol Pharmacol* **42**(4): 638-641.

Espada S, Rojo AI, Salinas M and Cuadrado A (2009) The muscarinic M1 receptor activates Nrf2 through a signaling cascade that involves protein kinase C and inhibition of GSK-3beta: connecting neurotransmission with neuroprotection. *J Neurochem* **110**(3): 1107-1119.

Espinoza-Fonseca LM and Trujillo-Ferrara JG (2005) Identification of multiple allosteric sites on the M1 muscarinic acetylcholine receptor. *FEBS Lett* **579**(30): 6726-6732.

Espinoza-Fonseca LM and Trujillo-Ferrara JG (2006) The existence of a second allosteric site on the M1 muscarinic acetylcholine receptor and its implications for drug design. *Bioorg. Med. Chem. Lett.* **16**(5): 1217-1220.

Evans BA, Broxton N, Merlin J, Sato M, Hutchinson DS, Christopoulos A and Summers RJ (2011) Quantification of functional selectivity at the human alpha(1A)-adrenoceptor. *Mol Pharmacol* **79**(2): 298-307.

Falkenburger BH, Jensen JB and Hille B (2010) Kinetics of M1 muscarinic receptor and G protein signaling to phospholipase C in living cells. *J Gen Physiol* **135**(2): 81-97.

Farrell MS, Pei Y, Wan Y, Yadav PN, Daigle TL, Urban DJ, Lee H-M, Sciaky N, Simmons A, Nonneman RJ, Huang X-P, Hufeisen SJ, Guettier J-M, Moy SS, Wess J, Caron MG, Calakos N and Roth BL (2013) A G[alpha]s DREADD Mouse for Selective Modulation of cAMP Production in Striatopallidal Neurons. *Neuropsychopharmacology* **38**(5): 854-862.

Fatkenheuer G, Pozniak AL, Johnson MA, Plettenberg A, Staszewski S, Hoepelman AI, Saag MS, Goebel FD, Rockstroh JK, Dezube BJ, Jenkins TM, Medhurst C, Sullivan JF, Ridgway C, Abel S, James IT, Youle M and van der Ryst E (2005) Efficacy of short-term monotherapy with maraviroc, a new CCR5 antagonist, in patients infected with HIV-1. *Nat Med* **11**(11): 1170-1172.

Felder CC (1995) Muscarinic acetylcholine receptors: signal transduction through multiple effectors. *FASEB J.* **9**(8): 619-625.

Felder CC, Bymaster FP, Ward J and DeLapp N (2000) Therapeutic opportunities for muscarinic receptors in the central nervous system. *J Med Chem* **43**(23): 4333-4353.

Felder CC, Kanterman RY, Ma AL and Axelrod J (1989) A transfected m1 muscarinic acetylcholine receptor stimulates adenylate cyclase via phosphatidylinositol hydrolysis. *J Biol Chem* **264**(34): 20356-20362.

Felder CC, Ma AL, Liotta LA and Kohn EC (1991) The antiproliferative and antimetastatic compound L651582 inhibits muscarinic acetylcholine receptor-stimulated calcium influx and arachidonic acid release. *JPET* **257**(3): 967-971.

Felsch JS, Cachero TG and Peralta EG (1998) Activation of protein tyrosine kinase PYK2 by the m1 muscarinic acetylcholine receptor. *Proc Natl Acad Sci USA* **95**(9): 5051-5056.

Ferguson SM, Eskenazi D, Ishikawa M, Wanat MJ, Phillips PE, Dong Y, Roth BL and Neumaier JF (2011) Transient neuronal inhibition reveals opposing roles of indirect and direct pathways in sensitization. *Nat Neurosci* **14**(1): 22-24.

Ferguson SS, Downey WE, 3rd, Colapietro AM, Barak LS, Menard L and Caron MG (1996) Role of beta-arrestin in mediating agonist-promoted G protein-coupled receptor internalization. *Science* **271**(5247): 363-366.

Ferré S, Casadó V, Devi LA, Filizola M, Jockers R, Lohse MJ, Milligan G, Pin J-P and Guitart X (2014) G Protein–Coupled Receptor Oligomerization Revisited: Functional and Pharmacological Perspectives. *Pharmacol Rev* **66**(2): 413-434.

Fink-Jensen A, Fedorova I, Wortwein G, Woldbye DP, Rasmussen T, Thomsen M, Bolwig TG, Knitowski KM, McKinzie DL, Yamada M, Wess J and Basile A (2003) Role for M5 muscarinic acetylcholine receptors in cocaine addiction. *J Neurosci Res* **74**(1): 91-96.

Fisher A (2007) M1 Muscarinic Agonists: A Comprehensive Therapy Against Major Hallmarks of Alzheimer's Disease, in *Pharmacol Mech Alzheimer's Ther* pp 50-63, Springer New York.

Fisher A, Michaelson DM, Brandeis R, Haring R, Chapman S and Pittel Z (2000) M1 muscarinic agonists as potential disease-modifying agents in Alzheimer's disease. Rationale and perspectives. *Annals New York Acad Sci* **920**: 315-320.

Flynn DD, Ferrari-DiLeo G, Mash DC and Levey AI (1995) Differential regulation of molecular subtypes of muscarinic receptors in Alzheimer's disease. *J Neurochem* **64**(4): 1888-1891.

Foord SM, Bonner TI, Neubig RR, Rosser EM, Pin JP, Davenport AP, Spedding M and Harmar AJ (2005) International Union of Pharmacology. XLVI. G protein-coupled receptor list. *Pharmacol Rev* **57**(2): 279-288.

Foster DJ, Choi DL, Conn PJ and Rook JM (2014) Activation of M1 and M4 muscarinic receptors as potential treatments for Alzheimer's disease and schizophrenia. *Neuropsy Dis Trtment* **10**: 183-191.

Frank M, Thumer L, Lohse MJ and Bunemann M (2005) G Protein activation without subunit dissociation depends on a G{alpha}(i)-specific region. *J Biol Chem* **280**(26): 24584-24590.

Fredriksson R, Lagerstrom MC, Lundin LG and Schioth HB (2003) The G-protein-coupled receptors in the human genome form five main families. Phylogenetic analysis, paralogon groups, and fingerprints. *Mol Pharmacol* **63**(6): 1256-1272.

Galvez T, Urwyler S, Prezeau L, Mosbacher J, Joly C, Malitschek B, Heid J, Brabet I, Froestl W, Bettler B, Kaupmann K and Pin JP (2000) Ca(2+) requirement for high-affinity gamma-aminobutyric acid (GABA) binding at GABA(B) receptors: involvement of serine 269 of the GABA(B)R1 subunit. *Mol Pharmacol* **57**(3): 419-426.

Gamper N and Shapiro MS (2007) Regulation of ion transport proteins by membrane phosphoinositides. *Nat Rev Neurosci* **8**(12): 921-934.

Garner AR, Rowland DC, Hwang SY, Baumgaertel K, Roth BL, Kentros C and Mayford M (2012) Generation of a Synthetic Memory Trace. *Science* **335**(6075): 1513-1516.

Gautam D, Heard TS, Cui Y, Miller G, Bloodworth L and Wess J (2004) Cholinergic stimulation of salivary secretion studied with M1 and M3 muscarinic receptor single- and double-knockout mice. *Mol Pharmacol* **66**(2): 260-267.

Gautam D, Jeon J, Li JH, Han SJ, Hamdan FF, Cui Y, Lu H, Deng C, Gavrilova O and Wess J (2008) Metabolic roles of the M3 muscarinic acetylcholine receptor studied with M3 receptor mutant mice: a review. *J Recep Sig Transd* **28**(1-2): 93-108.

Gavalas A, Lan T-H, Liu Q, Corrêa IR, Javitch JA and Lambert NA (2013) Segregation of Family A G Protein–Coupled Receptor Protomers in the Plasma Membrane. *Mol Pharmacol* **84**(3): 346-352.

Gerber DJ, Sotnikova TD, Gainetdinov RR, Huang SY, Caron MG and Tonegawa S (2001) Hyperactivity, elevated dopaminergic transmission, and response to amphetamine in M1 muscarinic acetylcholine receptor-deficient mice. *Proc Natl Acad Sci USA* **98**(26): 15312-15317.

Gether U and Kobilka BK (1998) G protein-coupled receptors. II. Mechanism of agonist activation. *J Biol Chem* **273**(29): 17979-17982.

Ghamari-Langroudi M and Bourque CW (2004) Muscarinic receptor modulation of slow afterhyperpolarization and phasic firing in rat supraoptic nucleus neurons. *J Neurosci* **24**(35): 7718-7726.

Giessel AJ and Sabatini BL (2010) M1 muscarinic receptors boost synaptic potentials and calcium influx in dendritic spines by inhibiting postsynaptic SK channels. *Neuron* **68**(5): 936-947.

Gilman AG (1987) G proteins: transducers of receptor-generated signals. *Annu Rev Biochem* **56**: 615-649.

Gimpl G, Burger K and Fahrenholz F (1997) Cholesterol as modulator of receptor function. *Biochem* **36**(36): 10959-10974.

Gnagey AL, Seidenberg M and Ellis J (1999) Site-directed mutagenesis reveals two epitopes involved in the subtype selectivity of the allosteric interactions of gallamine at muscarinic acetylcholine receptors. *Mol Pharmacol* **56**(6): 1245-1253.

Gomeza J, Shannon H, Kostenis E, Felder C, Zhang L, Brodkin J, Grinberg A, Sheng H and Wess J (1999a) Pronounced pharmacologic deficits in M2 muscarinic acetylcholine receptor knockout mice. *Proc Natl Acad Sci USA* **96**(4): 1692-1697.

Gomeza J, Zhang L, Kostenis E, Felder C, Bymaster F, Brodkin J, Shannon H, Xia B, Deng C and Wess J (1999b) Enhancement of D1 dopamine receptor-mediated locomotor stimulation in M(4) muscarinic acetylcholine receptor knockout mice. *Proc Natl Acad Sci USA* **96**(18): 10483-10488.

Goodwin JA, Hulme EC, Langmead CJ and Tehan BG (2007) Roof and floor of the muscarinic binding pocket: variations in the binding modes of orthosteric ligands. *Mol Pharmacol* **72**(6): 1484-1496.

Gregory KJ, Hall NE, Tobin AB, Sexton PM and Christopoulos A (2010) Identification of orthosteric and allosteric site mutations in M2 muscarinic acetylcholine receptors that contribute to ligand-selective signaling bias. *J Biol Chem* **285**(10): 7459-7474.

Gregory KJ, Sexton PM and Christopoulos A (2007) Allosteric modulation of muscarinic acetylcholine receptors. *Curr Neuropharmacol* **5**(3): 157-167.

Gudermann T, Grosse R and Schultz G (2000) Contribution of receptor/G protein signaling to cell growth and transformation. *Naunyn Schmiedebergs Arch Pharmacol* **361**(4): 345-362.

Guettier JM, Gautam D, Scarselli M, Ruiz de Azua I, Li JH, Rosemond E, Ma X, Gonzalez FJ, Armbruster BN, Lu H, Roth BL and Wess J (2009) A chemical-genetic approach to study G protein regulation of beta cell function in vivo. *Proc Natl Acad Sci USA* **106**(45): 19197-19202.

Gulledge AT, Park SB, Kawaguchi Y and Stuart GJ (2007) Heterogeneity of phasic cholinergic signaling in neocortical neurons. *J Neurophysiol* **97**(3): 2215-2229.

Gulledge AT and Stuart GJ (2005) Cholinergic inhibition of neocortical pyramidal neurons. *J Neurosci* **25**(44): 10308-10320.

Gurwitz D, Haring R, Heldman E, Fraser CM, Manor D and Fisher A (1994) Discrete activation of transduction pathways associated with acetylcholine m1 receptor by several muscarinic ligands. *Eur J Pharmacol* **267**(1): 21-31.

Gutkind JS (1998) The Pathways Connecting G Protein-coupled Receptors to the Nucleus through Divergent Mitogen-activated Protein Kinase Cascades. *J Biol Chem* **273**(4): 1839-1842.

Gutkind JS (2000) Regulation of mitogen-activated protein kinase signaling networks by G protein-coupled receptors. *Sci STKE* **2000**(40): re1.

Haga K, Kameyama K, Haga T, Kikkawa U, Shiozaki K and Uchiyama H (1996) Phosphorylation of Human m1 Muscarinic Acetylcholine Receptors by G Protein-coupled Receptor Kinase 2 and Protein Kinase C. *J Biol Chem* **271**(5): 2776-2782.

Haga K, Kruse AC, Asada H, Yurugi-Kobayashi T, Shiroishi M, Zhang C, Weis WI, Okada T, Kobilka BK, Haga T and Kobayashi T (2012) Structure of the human M2 muscarinic acetylcholine receptor bound to an antagonist. *Nature* **482**(7386): 547-551.

Hagan JJ, Jansen JH and Broekkamp CL (1987) Blockade of spatial learning by the M1 muscarinic antagonist pirenzepine. *Psychopharmacology* **93**(4): 470-476.

Hagan JJ, van der Heijden B and Broekkamp CL (1988) The relative potencies of cholinomimetics and muscarinic antagonists on the rat iris in vivo: effects of pH on potency of pirenzepine and telenzepine. *Naunyn-Schmiedeberg's Arch Pharmacol* **338**(5): 476-483.

Haj-Dahmane S and Andrade R (1998) Ionic mechanism of the slow afterdepolarization induced by muscarinic receptor activation in rat prefrontal cortex. *J Neurophysiol* **80**(3): 1197-1210.

Hall DA (2000) Modeling the functional effects of allosteric modulators at pharmacological receptors: an extension of the two-state model of receptor activation. *Mol Pharmacol* **58**(6): 1412-1423.

Hamilton SE, Loose MD, Qi M, Levey AI, Hille B, McKnight GS, Idzerda RL and Nathanson NM (1997) Disruption of the m1 receptor gene ablates muscarinic receptor-dependent M current regulation and seizure activity in mice. *Proc Natl Acad Sci USA* **94**(24): 13311-13316.

Hamilton SE and Nathanson NM (2001) The M1 Receptor Is Required for Muscarinic Activation of Mitogen-activated Protein (MAP) Kinase in Murine Cerebral Cortical Neurons. *J Biol Chem* **276**(19): 15850-15853.

Hammer R, Berrie CP, Birdsall NJ, Burgen AS and Hulme EC (1980) Pirenzepine distinguishes between different subclasses of muscarinic receptors. *Nature* **283**(5742): 90-92.

Han SJ, Hamdan FF, Kim SK, Jacobson KA, Bloodworth LM, Li B and Wess J (2005) Identification of an agonist-induced conformational change occurring adjacent to the ligand-binding pocket of the M(3) muscarinic acetylcholine receptor. *J Biol Chem* **280**(41): 34849-34858.

Han Y, Moreira IS, Urizar E, Weinstein H and Javitch JA (2009) Allosteric communication between protomers of dopamine class A GPCR dimers modulates activation. *Nat Chem Biol* **5**(9): 688-695.

Hanson MA, Roth CB, Jo E, Griffith MT, Scott FL, Reinhart G, Desale H, Clemons B, Cahalan SM, Schuerer SC, Sanna MG, Han GW, Kuhn P, Rosen H and Stevens RC (2012) Crystal Structure of a Lipid G Protein–Coupled Receptor. *Science* **335**(6070): 851-855.

Hao W, Xing-Jun W, Yong-Yao C, Liang Z, Yang L and Hong-Zhuan C (2005) Up-regulation of M1 muscarinic receptors expressed in CHOm1 cells by panaxynol via cAMP pathway. *Neurosci letters* **383**(1–2): 121-126.

Harikumar KG, Ball AM, Sexton PM and Miller LJ (2010) Importance of lipid-exposed residues in transmembrane segment four for family B calcitonin receptor homo-dimerization. *Regul Pep* **164**(2-3): 113-119.

Harikumar KG, Wootten D, Pinon DI, Koole C, Ball AM, Furness SGB, Graham B, Dong M, Christopoulos A, Miller LJ and Sexton PM (2012) Glucagon-like peptide-1 receptor dimerization differentially regulates agonist signaling but does not affect small molecule allostery. *Proc Natl Acad Sci USA* **109**(45): 18607-18612.

Haring R, Fisher A, Marciano D, Pittel Z, Kloog Y, Zuckerman A, Eshhar N and Heldman E (1998) Mitogen-Activated Protein Kinase-Dependent and Protein Kinase C-Dependent Pathways Link the m1 Muscarinic Receptor to β-Amyloid Precursor Protein Secretion. *J Neurochem* **71**(5): 2094-2103.

Hasselmo ME (2006) The role of acetylcholine in learning and memory. *Curr Opin Neurobiol* **16**(6): 710-715.

Heitz F, Holzwarth JA, Gies JP, Pruss RM, Trumpp-Kallmeyer S, Hibert MF and Guenet C (1999) Site-directed mutagenesis of the putative human muscarinic M2 receptor binding site. *Eur J Pharmacol* **380**(2-3): 183-195.

Hern JA, Baig AH, Mashanov GI, Birdsall B, Corrie JE, Lazareno S, Molloy JE and Birdsall NJ (2010) Formation and dissociation of M1 muscarinic receptor dimers seen by total internal reflection fluorescence imaging of single molecules. *Proc Natl Acad Sci USA* **107**(6): 2693-2698.

Hersch SM, Gutekunst CA, Rees HD, Heilman CJ and Levey AI (1994) Distribution of m1-m4 muscarinic receptor proteins in the rat striatum: light and electron microscopic immunocytochemistry using subtype-specific antibodies. *J Neurosci* **14**(5 Pt 2): 3351-3363.

Hersch SM and Levey AI (1995) Diverse pre- and post-synaptic expression of m1-m4 muscarinic receptor proteins in neurons and afferents in the rat neostriatum. *Life Sci.* **56**(11-12): 931-938.

Hildebrand ME, David LS, Hamid J, Mulatz K, Garcia E, Zamponi GW and Snutch TP (2007) Selective inhibition of Cav3.3 T-type calcium channels by Galphaq/11-coupled muscarinic acetylcholine receptors. *J Biol Chem* **282**(29): 21043-21055.

Hill-Eubanks D, Burstein ES, Spalding TA, Brauner-Osborne H and Brann MR (1996) Structure of a G-protein-coupling domain of a muscarinic receptor predicted by random saturation mutagenesis. *J Biol Chem* **271**(6): 3058-3065.

Hill JJ and Peralta EG (2001) Inhibition of a Gi-activated Potassium Channel (GIRK1/4) by the Gq-coupled m1 Muscarinic Acetylcholine Receptor. *J Biol Chem* **276**(8): 5505-5510.

Hill SJ, May LT, Kellam B and Woolard J (2014) Allosteric interactions at adenosine A1 and A3 receptors: new insights into the role of small molecules and receptor dimerization. *Br J Pharmacol* **171**(5): 1102-1113.

Hille B (1994) Modulation of ion-channel function by G-protein-coupled receptors. *Trends Neurosci.* **17**(12): 531-536.

Hock C, Maddalena A, Raschig A, Muller-Spahn F, Eschweiler G, Hager K, Heuser I, Hampel H, Muller-Thomsen T, Oertel W, Wienrich M, Signorell A, Gonzalez-Agosti C and Nitsch RM (2003) Treatment with the selective muscarinic m1 agonist talsaclidine decreases cerebrospinal fluid levels of A beta 42 in patients with Alzheimer's disease. *Amyloid* **10**(1): 1-6.

Hollenstein K, Kean J, Bortolato A, Cheng RKY, Dore AS, Jazayeri A, Cooke RM, Weir M and Marshall FH (2013) Structure of class B GPCR corticotropin-releasing factor receptor 1. *Nature* **499**(7459): 438-443.

Hu J and el-Fakahany EE (1993) Allosteric interaction of dynorphin and myelin basic protein with muscarinic receptors. *Pharmacology* **47**(6): 351-359.

Hu J, Hu K, Liu T, Stern MK, Mistry R, Challiss RAJ, Costanzi S and Wess J (2013) Novel Structural and Functional Insights into M3 Muscarinic Receptor Dimer/Oligomer Formation. *J Biol Chem* **288**(48): 34777-34790.

Hu J, Wang SZ, Forray C and el-Fakahany EE (1992) Complex allosteric modulation of cardiac muscarinic receptors by protamine: potential model for putative endogenous ligands. *Mol Pharmacol* **42**(2): 311-321.

Hu J, Wang Y, Zhang X, Lloyd JR, Li JH, Karpiak J, Costanzi S and Wess J (2010) Structural basis of G protein-coupled receptor-G protein interactions. *Nat Chem Biol* **6**(7): 541-548.

Huang X-Y, Morielli AD and Peralta EG (1993) Tyrosine kinase-dependent suppression of a potassium channel by the G protein-coupled m1 muscarinic acetylcholine receptor. *Cell* **75**(6): 1145-1156.

Huang XP, Prilla S, Mohr K and Ellis J (2005) Critical amino acid residues of the common allosteric site on the M2 muscarinic acetylcholine receptor: more similarities than differences between the structurally divergent agents gallamine and bis(ammonio)alkane-type hexamethylene-bis-[dimethyl-(3-phthalimidopropyl)ammonium]dibromide. *Mol Pharmacol* **68**(3): 769-778.

Huang Y and Mucke L (2012) Alzheimer Mechanisms and Therapeutic Strategies. *Cell* **148**(6): 1204-1222.

Hulme EC (2013) GPCR activation: a mutagenic spotlight on crystal structures. *Trends Pharmacol. Sci.* **34**(1): 67-84.

Hulme EC, Birdsall NJ and Buckley NJ (1990) Muscarinic receptor subtypes. *Annu. Rev. Pharmacol. Toxicol.* **30**: 633-673.

Hulme EC, Lu ZL, Bee M, Curtis CA and Saldanha J (2001) The conformational switch in muscarinic acetylcholine receptors. *Life Sci.* **68**(22-23): 2495-2500.

Hulme EC, Lu ZL and Bee MS (2003a) Scanning mutagenesis studies of the M1 muscarinic acetylcholine receptor. *Receptors Channels* **9**(4): 215-228.

Hulme EC, Lu ZL, Saldanha JW and Bee MS (2003b) Structure and activation of muscarinic acetylcholine receptors. *Biochem Socie Transd* **31**(Pt 1): 29-34.

Ishibashi M, Yamazaki Y, Miledi R and Sumikawa K (2014) Nicotinic and muscarinic agonists and acetylcholinesterase inhibitors stimulate a common pathway to enhance GluN2B-NMDAR responses. *Proc Natl Acad Sci USA* **111**(34): 12538-12543.

Jaakola VP, Griffith MT, Hanson MA, Cherezov V, Chien EY, Lane JR, Ijzerman AP and Stevens RC (2008) The 2.6 angstrom crystal structure of a human A2A adenosine receptor bound to an antagonist. *Science* **322**(5905): 1211-1217.

Jacobson MA, Kreatsoulas C, Pascarella DM, O'Brien JA and Sur C (2010) The M1 muscarinic receptor allosteric agonists AC-42 and 1-[1'-(2-methylbenzyl)-1,4'-bipiperidin-4-yl]-1,3-dihydro-2H-benzimidazol- 2-one bind to a unique site distinct from the acetylcholine orthosteric site. *Mol Pharmacol* **78**(4): 648-657.

Jacoby DB, Gleich GJ and Fryer AD (1993) Human eosinophil major basic protein is an endogenous allosteric antagonist at the inhibitory muscarinic M2 receptor. *J Clin Invst* **91**(4): 1314-1318.

Jain S, Ruiz de Azua I, Lu H, White MF, Guettier JM and Wess J (2013) Chronic activation of a designer G(q)-coupled receptor improves beta cell function. *J Clin Invest* **123**(4): 1750-1762.

Jakubik J, Bacakova L, el-Fakahany EE and Tucek S (1995) Subtype selectivity of the positive allosteric action of alcuronium at cloned M1-M5 muscarinic acetylcholine receptors. *JPET* **274**(3): 1077-1083.

Jansson CC, Kukkonen J and Akerman KE (1991) Muscarinic receptor-linked elevation of cAMP in SH-SY5Y neuroblastoma cells is mediated by Ca2+ and protein kinase C. *Biochim Biophys Acta* **1095**(3): 255-260.

Jiang S, Wang Y, Ma Q, Zhou A, Zhang X and Zhang Y-w (2012) M1 muscarinic acetylcholine receptor interacts with BACE1 and regulates its proteosomal degradation. *Neurosci letters* **515**(2): 125-130.

Johnson DE, Yamazaki H, Ward KM, Schmidt AW, Lebel WS, Treadway JL, Gibbs EM, Zawalich WS and Rollema H (2005) Inhibitory effects of antipsychotics on carbachol-enhanced insulin secretion from perifused rat islets: role of muscarinic antagonism in antipsychotic-induced diabetes and hyperglycemia. *Diabetes* **54**(5): 1552-1558.

Johnson DJ, Forbes IT, Watson SP, Garzya V, Stevenson GI, Walker GR, Mudhar HS, Flynn ST, Wyman PA, Smith PW, Murkitt GS, Lucas AJ, Mookherjee CR, Watson JM, Gartlon JE, Bradford AM and Brown F (2010) The discovery of a series of N-substituted 3-(4-piperidinyl)-1,3-benzoxazolinones and oxindoles as highly brain penetrant, selective muscarinic M1 agonists. *Bioorg. Med. Chem. Lett.* **20**(18): 5434-5438.

Jones AL, Mowry BJ, McLean DE, Mantzioris BX, Pender MP and Greer JM (2014) Elevated levels of autoantibodies targeting the M1 muscarinic acetylcholine receptor and neurofilament medium in sera from subgroups of patients with schizophrenia. *J Neuroimmunol* **269**(1–2): 68-75.

Jones CK, Brady AE, Davis AA, Xiang Z, Bubser M, Tantawy MN, Kane AS, Bridges TM, Kennedy JP, Bradley SR, Peterson TE, Ansari MS, Baldwin RM, Kessler RM, Deutch AY, Lah JJ, Levey AI, Lindsley CW and Conn PJ (2008) Novel selective allosteric activator of the M1 muscarinic acetylcholine receptor regulates amyloid processing and produces antipsychotic-like activity in rats. *J Neuroscie* **28**(41): 10422-10433.

Jones CK, Byun N and Bubser M (2012) Muscarinic and nicotinic acetylcholine receptor agonists and allosteric modulators for the treatment of schizophrenia. *Neuropsychopharmacology* **37**(1): 16-42.

Jones PG, Curtis CA and Hulme EC (1995) The function of a highly-conserved arginine residue in activation of the muscarinic M1 receptor. *Eur J Pharmacol* **288**(3): 251-257.

Jones SV (1996) Modulation of the inwardly rectifying potassium channel IRK1 by the m1 muscarinic receptor. *Mol Pharmacol* **49**(4): 662-667.

Kamsler A, McHugh TJ, Gerber D, Huang SY and Tonegawa S (2010) Presynaptic m1 muscarinic receptors are necessary for mGluR long-term depression in the hippocampus. *Proc Natl Acad Sci USA* **107**(4): 1618-1623.

Kanba S, Kanba KS, McKinney M, Pfenning M, Abraham R, Nomura S, Enloes L, Mackey S and Richelson E (1990) Desensitization of muscarinic M1 receptors of murine neuroblastoma cells (clone N1E-115) without receptor down-regulation and protein kinase C activity. *Biochem Pharmacol* **40**(5): 1005-1014.

Kanba S, Kanba KS and Richelson E (1986) The protein kinase C activator, 12-O-tetradecanoylphorbol-13-acetate (TPA), inhibits muscarinic (M1) receptor-mediated inositol phosphate release and cyclic GMP formation in murine neuroblastoma cells (clone N1E-115). *Eur J Pharmacol* **125**(1): 155-156.

Karunarathne WKA, Giri L, Kalyanaraman V and Gautam N (2013) Optically triggering spatiotemporally confined GPCR activity in a cell and programming neurite initiation and extension. *Proc Natl Acad Sci USA* **110**(17): E1565-E1574.

Katritch V, Cherezov V and Stevens RC (2013) Structure-Function of the G Protein–Coupled Receptor Superfamily. *Annu Rev Pharmacol Toxicol* **53**(1): 531-556.

Katritch V, Fenalti G, Abola EE, Roth BL, Cherezov V and Stevens RC (2014) Allosteric sodium in class A GPCR signaling. *Trends Biochem. Sci.* **39**(5): 233-244.

Katz A, Wu D and Simon MI (1992) Subunits beta gamma of heterotrimeric G protein activate beta 2 isoform of phospholipase C. *Nature* **360**(6405): 686-689.

Kebig A, Kostenis E, Mohr K and Mohr-Andra M (2009) An optical dynamic mass redistribution assay reveals biased signaling of dualsteric GPCR activators. *J Recep Signal Transduct Res* **29**(3-4): 140-145.

Kebig A and Mohr K (2008) [Cinacalcet - an allosteric enhancer at the Ca2+-receptor]. *Dtsch Med Wochenschr* **133**(33): 1681-1683.

Kenakin T (1995a) Agonist-receptor efficacy. I: Mechanisms of efficacy and receptor promiscuity. *Trends Pharmacol. Sci.* **16**(6): 188-192.

Kenakin T (1995b) Agonist-receptor efficacy. II. Agonist trafficking of receptor signals. *Trends Pharmacol. Sci.* **16**(7): 232-238.

Kenakin T (2005) New concepts in drug discovery: collateral efficacy and permissive antagonism. *Nature Rev Drug Discov* **4**(11): 919-927.

Kenakin T (2007) Functional selectivity through protean and biased agonism: who steers the ship? *Mol Pharmacol* **72**(6): 1393-1401.

Kenakin T (2008) Functional selectivity in GPCR modulator screening. *Comb Chem High Throughput Screen* **11**(5): 337-343.

Kenakin T (2010) G protein coupled receptors as allosteric proteins and the role of allosteric modulators. *J Recep Signal Transduct Res* **30**(5): 313-321.

Kenakin T and Christopoulos A (2013) Signalling bias in new drug discovery: detection, quantification and therapeutic impact. *Nat Rev Drug Discov* **12**(3): 205-216.

Keov P, López L, Devine SM, Valant C, Lane JR, Scammells PJ, Sexton PM and Christopoulos A (2014) Molecular Mechanisms of Bitopic Ligand Engagement with the M1 Muscarinic Acetylcholine Receptor. *J Biol Chem*(In Press).

Keov P, Sexton PM and Christopoulos A (2011) Allosteric modulation of G protein-coupled receptors: a pharmacological perspective. *Neuropharmacology* **60**(1): 24-35.

Keov P, Valant C, Devine SM, Lane JR, Scammells PJ, Sexton PM and Christopoulos A (2013) Reverse Engineering of the Selective Agonist TBPB Unveils Both Orthosteric and Allosteric Modes of Action at the M1 Muscarinic Acetylcholine Receptor. *Mol Pharmacol* **84**(3): 425-437.

Khan MR, Anisuzzaman AS, Semba S, Ma Y, Uwada J, Hayashi H, Suzuki Y, Takano T, Ikeuchi H, Uchino M, Maemoto A, Ushikubi F, Muramatsu I and Taniguchi T (2013a) M1 is a major subtype of muscarinic acetylcholine receptors on mouse colonic epithelial cells. *J Gastroenterol* **48**(8): 885-896.

Khan SM, Sleno R, Gora S, Zylbergold P, Laverdure J-P, Labbé J-C, Miller GJ and Hébert TE (2013b) The Expanding Roles of Gβγ Subunits in G Protein–Coupled Receptor Signaling and Drug Action. *Pharmacol Rev* **65**(2): 545-577.

Kniazeff J, Prezeau L, Rondard P, Pin JP and Goudet C (2011) Dimers and beyond: The functional puzzles of class C GPCRs. *Pharmacol Ther* **130**(1): 9-25.

Kobrinsky E, Mirshahi T, Zhang H, Jin T and Logothetis DE (2000) Receptor-mediated hydrolysis of plasma membrane messenger PIP2 leads to K+-current desensitization. *Nature Cell Biol* **2**(8): 507-514.

Kohout TA, Nicholas SL, Perry SJ, Reinhart G, Junger S and Struthers RS (2004) Differential desensitization, receptor phosphorylation, beta-arrestin recruitment, and ERK1/2 activation by the two endogenous ligands for the CC chemokine receptor 7. *J Biol Chem* **279**(22): 23214-23222.

Kolakowski LF, Jr. (1994) GCRDb: a G-protein-coupled receptor database. *Receptors Channels* **2**(1): 1-7.

Koman A, Cazaubon S, Adem A, Couraud PO and Strosberg AD (1993) Different regulatory patterns of M1 and M2 muscarinic receptor subtype RNA in SH-SY5Y human neuroblastoma induced by phorbol ester or DMSO. *Neurosci letters* **149**(1): 79-82.

Kong KC, Butcher AJ, McWilliams P, Jones D, Wess J, Hamdan FF, Werry T, Rosethorne EM, Charlton SJ, Munson SE, Cragg HA, Smart AD and Tobin AB (2010) M3-muscarinic receptor promotes insulin release via receptor phosphorylation/arrestin-dependent activation of protein kinase D1. *Proc Natl Acad Sci USA* **107**(49): 21181-21186.

Kooistra AJ, Kuhne S, de Esch IJP, Leurs R and de Graaf C (2013) A structural chemogenomics analysis of aminergic GPCRs: lessons for histamine receptor ligand design. *Br J Pharmacol* **170**(1): 101-126.

Kostenis E, Gomeza J, Lerche C and Wess J (1997) Genetic analysis of receptor-Galphaq coupling selectivity. *J Biol Chem* **272**(38): 23675-23681.

Krashes MJ, Koda S, Ye C, Rogan SC, Adams AC, Cusher DS, Maratos-Flier E, Roth BL and Lowell BB (2011) Rapid, reversible activation of AgRP neurons drives feeding behavior in mice. *J Clin Invest* **121**(4): 1424-1428.

Krasnoperov VG, Bittner MA, Beavis R, Kuang Y, Salnikow KV, Chepurny OG, Little AR, Plotnikov AN, Wu D, Holz RW and Petrenko AG (1997) alpha-Latrotoxin stimulates exocytosis by the interaction with a neuronal G-protein-coupled receptor. *Neuron* **18**(6): 925-937.

Kruse AC, Hu J, Kobilka BK and Wess J (2014a) Muscarinic acetylcholine receptor X-ray structures: potential implications for drug development. *Curr Opin Pharmacol* **16**(0): 24-30.

Kruse AC, Hu J, Pan AC, Arlow DH, Rosenbaum DM, Rosemond E, Green HF, Liu T, Chae PS, Dror RO, Shaw DE, Weis WI, Wess J and Kobilka BK (2012a) Structure and dynamics of the M3 muscarinic acetylcholine receptor. *Nature* **482**(7386): 552-556.

Kruse AC, Hu J, Pan AC, Arlow DH, Rosenbaum DM, Rosemond E, Green HF, Liu T, Chae PS, Dror RO, Shaw DE, Weis WI, Wess J and Kobilka BK (2012b) Structure and dynamics of the M3 muscarinic acetylcholine receptor. *Nature* **482**(7386): 552-556.

Kruse AC, Kobilka BK, Gautam D, Sexton PM, Christopoulos A and Wess J (2014b) Muscarinic acetylcholine receptors: novel opportunities for drug development. *Nature Rev Drug Discov*.

Kruse AC, Ring AM, Manglik A, Hu J, Hu K, Eitel K, Hubner H, Pardon E, Valant C, Sexton PM, Christopoulos A, Felder CC, Gmeiner P, Steyaert J, Weis WI, Garcia KC, Wess J and Kobilka BK (2013) Activation and allosteric modulation of a muscarinic acetylcholine receptor. *Nature* **504**(7478): 101-106.

Kuduk SD and Beshore DC (2012) Novel M1 allosteric ligands: a patent review. *Expert Opin Ther Pat* **22**(12): 1385-1398.

Kuduk SD, Beshore DC, DiMarco CN and Greshock TJ (2010a) Aryl methyl benzoquinazolinone M1 receptor positive allosteric modulators. Merck & Co. WO059773.

Kuduk SD, Chang RK, Di Marco CN, Ray WJ, Ma L, Wittman M, Seager MA, Koeplinger KA, Thompson CD, Hartman GD and Bilodeau MT (2010b) Quinolizidinone Carboxylic Acids as CNS Penetrant, Selective M1 Allosteric Muscarinic Receptor Modulators. *ACS Med. Chem. Lett.* **1**: 263-267.

Kuduk SD, Chang RK, Di Marco CN, Ray WJ, Ma L, Wittmann M, Seager MA, Koeplinger KA, Thompson CD, Hartman GD and Bilodeau MT (2011) Quinolizidinone carboxylic acid selective M1 allosteric modulators: SAR in the piperidine series. *Bioorg. Med. Chem. Lett.* **21**(6): 1710-1715.

Kuduk SD, Chang RK, Greshock TJ, Ray WJ, Ma L, Wittmann M, Koeplinger KA, Seager MA, Thompson CD, Hartman G and Bilodeau MT (2012) Identification of Amides as Carboxylic Acid Surrogates for Quinolizidinone-Based M1 Positive Allosteric Modulators. *ACS Med. Chem. Lett.* **3**: 1070-1074.

Kuduk SD, Di Marco CN, Saffold JR, Ray WJ, Ma L, Wittmann M, Koeplinger KA, Thompson CD, Hartman GD, Bilodeau MT and Beshore DC (2014) Identification of a methoxynaphthalene scaffold as a core replacement in quinolizidinone amide M(1) positive allosteric modulators. *Bioorg. Med. Chem. Lett.* **24**(5): 1417-1420.

Lagerstrom MC and Schioth HB (2008a) Structural diversity of G protein-coupled receptors and significance for drug discovery. *Nat Rev Drug Discov* **7**(4): 339-357.

Lagerstrom MC and Schioth HB (2008b) Structural diversity of G protein-coupled receptors and significance for drug discovery. *Nat Rev Drug Discov*

7(4): 339-357.

Lahmy V, Meunier J, Malmstrom S, Naert G, Givalois L, Kim SH, Villard V, Vamvakides A and Maurice T (2013) Blockade of Tau Hyperphosphorylation and A[beta]1-42 Generation by the Aminotetrahydrofuran Derivative ANAVEX2-73, a Mixed Muscarinic and [sigma]1 Receptor Agonist, in a Nontransgenic Mouse Model of Alzheimer/'s Disease. *Neuropsychopharmacology* **38**(9): 1706-1723.

Lameh J, Philip M, Sharma YK, Moro O, Ramachandran J and Sadee W (1992) Hm1 muscarinic cholinergic receptor internalization requires a domain in the third cytoplasmic loop. *J Biol Chem* **267**(19): 13406-13412.

Lane JR, Abdul-Ridha A and Canals M (2013a) Regulation of G protein-coupled receptors by allosteric ligands. *ACS Chem. Neurosci.*

Lane JR, Donthamsetti P, Shonberg J, Draper-Joyce CJ, Dentry S, Michino M, Shi L, López L, Scammells PJ, Capuano B, Sexton PM, Javitch JA and Christopoulos A (2014) A new mechanism of allostery in a G protein-coupled receptor dimer. *Nat Chem Biol* **10**(9): 745-752.

Lane JR, Sexton PM and Christopoulos A (2013b) Bridging the gap: bitopic ligands of G-protein-coupled receptors. *Trends Pharmacol. Sci.* **34**(1): 59-66.

Langmead CJ, Austin NE, Branch CL, Brown JT, Buchanan KA, Davies CH, Forbes IT, Fry VA, Hagan JJ, Herdon HJ, Jones GA, Jeggo R, Kew JN, Mazzali A, Melarange R, Patel N, Pardoe J, Randall AD, Roberts C, Roopun A, Starr KR, Teriakidis A, Wood MD, Whittington M, Wu Z and Watson J (2008a) Characterization of a CNS penetrant, selective M1 muscarinic receptor agonist, 77-LH-28-1. *Br J Pharmacol* **154**(5): 1104-1115.

Langmead CJ and Christopoulos A (2006) Allosteric agonists of 7TM receptors: expanding the pharmacological toolbox. *Trends Pharmacol. Sci.* **27**(9): 475-481.

Langmead CJ and Christopoulos A (2014) Functional and structural perspectives on allosteric modulation of GPCRs. *Curr Opin Cell Biol* **27**: 94-101.

Langmead CJ, Fry VA, Forbes IT, Branch CL, Christopoulos A, Wood MD and Herdon HJ (2006) Probing the molecular mechanism of interaction between 4-n-butyl-1-[4-(2-methylphenyl)-4-oxo-1-butyl]-piperidine (AC-42) and the muscarinic M(1) receptor: direct pharmacological evidence that AC-42 is an allosteric agonist. *Mol Pharmacol* **69**(1): 236-246.

Langmead CJ, Watson J and Reavill C (2008b) Muscarinic acetylcholine receptors as CNS drug targets. *Pharmacol Ther* **117**(2): 232-243.

Lanzafame A, Christopoulos A and Mitchelson F (1997) Three allosteric modulators act at a common site, distinct from that of competitive antagonists, at muscarinic acetylcholine M2 receptors. *JPET* **282**(1): 278-285.

Lanzafame AA, Christopoulos A and Mitchelson F (2003) Cellular signaling mechanisms for muscarinic acetylcholine receptors. *Receptors Channels* **9**(4): 241-260.

Lanzafame AA, Sexton PM and Christopoulos A (2006) Interaction studies of multiple binding sites on m4 muscarinic acetylcholine receptors. *Mol Pharmacol* **70**(2): 736-746.

Lazareno S and Birdsall NJ (1995) Detection, quantitation, and verification of allosteric interactions of agents with labeled and unlabeled ligands at G protein-coupled receptors: interactions of strychnine and acetylcholine at muscarinic receptors. *Mol Pharmacol* **48**(2): 362-378.

Lazareno S, Dolezal V, Popham A and Birdsall NJ (2004) Thiochrome enhances acetylcholine affinity at muscarinic M4 receptors: receptor subtype selectivity via cooperativity rather than affinity. *Mol Pharmacol* **65**(1): 257-266.

Lazareno S, Gharagozloo P, Kuonen D, Popham A and Birdsall NJ (1998) Subtype-selective positive cooperative interactions between brucine analogues and acetylcholine at muscarinic receptors: radioligand binding studies. *Mol Pharmacol* **53**(3): 573-589.

Lazareno S, Popham A and Birdsall NJ (2000) Allosteric interactions of staurosporine and other indolocarbazoles with N-[methyl-(3)H]scopolamine and acetylcholine at muscarinic receptor subtypes: identification of a second allosteric site. *Mol Pharmacol* **58**(1): 194-207.

Lazareno S, Popham A and Birdsall NJ (2002) Analogs of WIN 62,577 define a second allosteric site on muscarinic receptors. *Mol Pharmacol* **62**(6): 1492-1505.

Leach K, Davey AE, Felder CC, Sexton PM and Christopoulos A (2011) The role of transmembrane domain 3 in the actions of orthosteric, allosteric, and atypical agonists of the m4 muscarinic acetylcholine receptor. *Mol Pharmacol* **79**(5): 855-865.

Leach K, Loiacono RE, Felder CC, McKinzie DL, Mogg A, Shaw DB, Sexton PM and Christopoulos A (2010) Molecular mechanisms of action and in vivo validation of an M4 muscarinic acetylcholine receptor allosteric modulator with potential antipsychotic properties. *Neuropsychopharmacology* **35**(4): 855-869.

Leach K, Sexton PM and Christopoulos A (2007) Allosteric GPCR modulators: taking advantage of permissive receptor pharmacology. *Trends Pharmacol. Sci.* **28**(8): 382-389.

Leach K, Simms J, Sexton PM and Christopoulos A (2012) Structure-function studies of muscarinic acetylcholine receptors. *Handb Exp Pharmacol*(208): 29-48.

Lebois EP, Bridges TM, Lewis LM, Dawson ES, Kane AS, Xiang Z, Jadhav SB, Yin H, Kennedy JP, Meiler J, Niswender CM, Jones CK, Conn PJ, Weaver CD and Lindsley CW (2010) Discovery and characterization of novel subtype-selective allosteric agonists for the investigation of M(1) receptor function in the central nervous system. *ACS Chem. Neurosci.* **1**(2): 104-121.

Lebois EP, Digby GJ, Sheffler DJ, Melancon BJ, Tarr JC, Cho HP, Miller NR, Morrison R, Bridges TM, Xiang Z, Daniels JS, Wood MR, Conn PJ and Lindsley CW (2011) Development of a highly selective, orally bioavailable and CNS penetrant M1 agonist derived from the MLPCN probe ML071. *Bioorg. Med. Chem. Lett.* **21**(21): 6451-6455.

Lee CH, Shin IC, Kang JS, Koh HC, Ha JH and Min CK (1998a) Differential coupling of G alpha q family of G-protein to muscarinic M1 receptor and neurokinin-2 receptor. *Arch Pharm Res* **21**(4): 423-428.

Lee KB, Pals-Rylaarsdam R, Benovic JL and Hosey MM (1998b) Arrestin-independent internalization of the m1, m3, and m4 subtypes of muscarinic cholinergic receptors. *J Biol Chem* **273**(21): 12967-12972.

Lee NH, Earle-Hughes J and Fraser CM (1994) Agonist-mediated destabilization of m1 muscarinic acetylcholine receptor mRNA. Elements involved in mRNA stability are localized in the 3'-untranslated region. *J Biol Chem* **269**(6): 4291-4298.

Lee NH and el-Fakahany EE (1991a) Allosteric antagonists of the muscarinic acetylcholine receptor. *Biochem Pharmacol* **42**(2): 199-205.

Lee NH and el-Fakahany EE (1991b) Allosteric interactions at the m1, m2 and m3 muscarinic receptor subtypes. *JPET* **256**(2): 468-479.

Leff P (1995) The two-state model of receptor activation. *Trends Pharmacol. Sci.* **16**(3): 89-97.

Lefkowitz RJ (2013) Arrestins come of age: a personal historical perspective. *Progress in molecular biology and translational science* **118**: 3-18.

Levey AI (1993) Immunological localization of m1-m5 muscarinic acetylcholine receptors in peripheral tissues and brain. *Life Sci* **52**(5-6): 441-448.

Levey AI, Kitt CA, Simonds WF, Price DL and Brann MR (1991) Identification and localization of muscarinic acetylcholine receptor proteins in brain with subtype-specific antibodies. *J Neurosci* **11**(10): 3218-3226.

Liao DL, Hong CJ, Chen HM, Chen YE, Lee SM, Chang CY, Chen H and Tsai SJ (2003) Association of muscarinic m1 receptor genetic polymorphisms with psychiatric symptoms and cognitive function in schizophrenic patients. *Neuropsychobiology* **48**(2): 72-76.

Lin A and DeFea KA (2013) β-Arrestin-kinase scaffolds: turn them on or turn them off? *Wiley Interdiscipl Rev: Sys Biol Med* **5**(2): 231-241.

Lin AL, Zhu B, Zhang W, Dang H, Zhang BX, Katz MS and Yeh CK (2008) Distinct pathways of ERK activation by the muscarinic agonists pilocarpine and carbachol in a human salivary cell line. *Am J Physiol Cell Physiol* **294**(6): C1454-1464.

Lin HH, Stacey M, Saxby C, Knott V, Chaudhry Y, Evans D, Gordon S, McKnight AJ, Handford P and Lea S (2001) Molecular analysis of the epidermal growth factor-like short consensus repeat domain-mediated protein-protein interactions: dissection of the CD97-CD55 complex. *J Biol Chem* **276**(26): 24160-24169.

Lin K, Wang D and Sadée W (2002) Serum Response Factor Activation by Muscarinic Receptors via RhoA: NOVEL PATHWAY SPECIFIC TO M1 SUBTYPE INVOLVING CALMODULIN, CALCINEURIN, AND Pyk2. *J Biol Chem* **277**(43): 40789-40798.

Liu J, Conklin BR, Blin N, Yun J and Wess J (1995) Identification of a receptor/G-protein contact site critical for signaling specificity and G-protein activation. *Proc Natl Acad Sci USA* **92**(25): 11642-11646.

Liu L, Heneghan JF, Michael GJ, Stanish LF, Egertová M and Rittenhouse AR (2008) L- and N-current but not M-current inhibition by M1 muscarinic receptors requires DAG lipase activity. *J Cell Physiol* **216**(1): 91-100.

Liu W, Chun E, Thompson AA, Chubukov P, Xu F, Katritch V, Han GW, Roth CB, Heitman LH, IJzerman AP, Cherezov V and Stevens RC (2012) Structural Basis for Allosteric Regulation of GPCRs by Sodium Ions. *Science* **337**(6091): 232-236.

Lohse MJ, Lefkowitz RJ, Caron MG and Benovic JL (1989) Inhibition of beta-adrenergic receptor kinase prevents rapid homologous desensitization of beta 2-adrenergic receptors. *Proc Natl Acad Sci USA* **86**(9): 3011-3015.

Lu Z-L and Hulme EC (1999a) The Functional Topography of Transmembrane Domain 3 of the M1 Muscarinic Acetylcholine Receptor, Revealed by Scanning Mutagenesis. *J Biol Chem* **274**(11): 7309-7315.

Lu Z-L, Saldanha JW and Hulme EC (2001a) Transmembrane Domains 4 and 7 of the M1Muscarinic Acetylcholine Receptor Are Critical for Ligand Binding and the Receptor Activation Switch. *J Biol Chem* **276**(36): 34098-34104.

Lu ZL, Curtis CA, Jones PG, Pavia J and Hulme EC (1997) The role of the aspartate-arginine-tyrosine triad in the m1 muscarinic receptor: mutations of aspartate 122 and tyrosine 124 decrease receptor expression but do not abolish signaling. *Mol Pharmacol* **51**(2): 234-241.

Lu ZL and Hulme EC (1999b) The functional topography of transmembrane domain 3 of the M1 muscarinic acetylcholine receptor, revealed by scanning mutagenesis. *The Journal of biological chemistry* **274**(11): 7309-7315.

Lu ZL, Saldanha JW and Hulme EC (2001b) Transmembrane domains 4 and 7 of the M(1) muscarinic acetylcholine receptor are critical for ligand binding and the receptor activation switch. *J Biol Chem* **276**(36): 34098-34104.

Luttrell LM, Ferguson SS, Daaka Y, Miller WE, Maudsley S, Della Rocca GJ, Lin F, Kawakatsu H, Owada K, Luttrell DK, Caron MG and Lefkowitz RJ (1999) Beta-arrestin-dependent formation of beta2 adrenergic receptor-Src protein kinase complexes. *Science* **283**(5402): 655-661.

Luttrell LM and Kenakin TP (2011) Refining efficacy: allosterism and bias in G protein-coupled receptor signaling. *Methods Mol Biol* **756**: 3-35.

Luttrell LM, Roudabush FL, Choy EW, Miller WE, Field ME, Pierce KL and Lefkowitz RJ (2001) Activation and targeting of extracellular signal-regulated kinases by beta-arrestin scaffolds. *Proc Natl Acad Sci USA* **98**(5): 2449-2454.

Ma L, Seager MA, Wittmann M, Jacobson M, Bickel D, Burno M, Jones K, Graufelds VK, Xu G, Pearson M, McCampbell A, Gaspar R, Shughrue P, Danziger A, Regan C, Flick R, Pascarella D, Garson S, Doran S, Kreatsoulas C, Veng L, Lindsley CW, Shipe W, Kuduk S, Sur C, Kinney G, Seabrook GR and Ray WJ (2009) Selective activation of the M1 muscarinic acetylcholine receptor achieved by allosteric potentiation. *Proc Natl Acad Sci USA* **106**(37): 15950-15955.

Mahajan R, Ha J, Zhang M, Kawano T, Kozasa T and Logothetis DE (2013) A Computational Model Predicts That G{beta}{gamma} Acts at a Cleft Between Channel Subunits to Activate GIRK1 Channels. *Sci. Signal.* **6**(288): ra69-.

Mahler SV, Vazey EM, Beckley JT, Keistler CR, McGlinchey EM, Kaufling J, Wilson SP, Deisseroth K, Woodward JJ and Aston-Jones G (2014) Designer receptors show role for ventral pallidum input to ventral tegmental area in cocaine seeking. *Nat Neurosci* **17**(4): 577-585.

Mangelus M, Kroyter A, Galron R and Sokolovsky M (2001) Reactive oxygen species regulate signaling pathways induced by M1 muscarinic receptors in PC12M1 cells. *J Neurochem* **76**(6): 1701-1711.

Marinissen MJ, Servitja JM, Offermanns S, Simon MI and Gutkind JS (2003) Thrombin protease-activated receptor-1 signals through Gq- and G13-initiated MAPK cascades regulating c-Jun expression to induce cell transformation. *J Biol Chem* **278**(47): 46814-46825.

Marino MJ and Conn PJ (2002) Direct and indirect modulation of the N-methyl D-aspartate receptor. *Curr Drug Targets CNS Neurol Disord* **1**(1): 1-16.

Marino MJ, Rouse ST, Levey AI, Potter LT and Conn PJ (1998) Activation of the genetically defined m1 muscarinic receptor potentiates N-methyl-D-aspartate (NMDA) receptor currents in hippocampal pyramidal cells. *Proc Natl Acad Sci USA* **95**(19): 11465-11470.

Marlo JE, Niswender CM, Days EL, Bridges TM, Xiang Y, Rodriguez AL, Shirey JK, Brady AE, Nalywajko T, Luo Q, Austin CA, Williams MB, Kim K, Williams R, Orton D, Brown HA, Lindsley CW, Weaver CD and Conn PJ (2009) Discovery and characterization of novel allosteric potentiators of M1 muscarinic receptors reveals multiple modes of activity. *Mol Pharmacol* **75**(3): 577-588.

Mary S, Damian M, Louet M, Floquet N, Fehrentz JA, Marie J, Martinez J and Baneres JL (2012) Ligands and signaling proteins govern the conformational landscape explored by a G protein-coupled receptor. *Proc Natl Acad Sci USA* **109**(21): 8304-8309.

Massot O, Rousselle JC, Fillion MP, Grimaldi B, Cloez-Tayarani I, Fugelli A, Prudhomme N, Seguin L, Rousseau B, Plantefol M, Hen R and Fillion G (1996) 5-hydroxytryptamine-moduline, a new endogenous cerebral peptide, controls the serotonergic activity via its specific interaction with 5-hydroxytryptamine1B/1D receptors. *Mol Pharmacol* **50**(4): 752-762.

Matsui H, Lazareno S and Birdsall NJ (1995) Probing of the location of the allosteric site on m1 muscarinic receptors by site-directed mutagenesis. *Mol Pharmacol* **47**(1): 88-98.

Mattingly RR and Macara IG (1996) Phosphorylation-dependent activation of the Ras-GRF/CDC25Mm exchange factor by muscarinic receptors and G-protein beta gamma subunits. *Nature* **382**(6588): 268-272.

May LT, Avlani VA, Langmead CJ, Herdon HJ, Wood MD, Sexton PM and Christopoulos A (2007a) Structure-Function Studies of Allosteric Agonism at M2 Muscarinic Acetylcholine Receptors. *Mol Pharmacol* **72**(2): 463-476.

May LT, Leach K, Sexton PM and Christopoulos A (2007b) Allosteric modulation of G protein-coupled receptors. *Annu Rev Pharmacol Toxicol* **47**: 1-51.

McCormick DA and Prince DA (1986) Mechanisms of action of acetylcholine in the guinea-pig cerebral cortex in vitro. *J Physiol* **375**: 169-194.

McCormick DA, Wang Z and Huguenard J (1993) Neurotransmitter control of neocortical neuronal activity and excitability. *Cereb Cortex* **3**(5): 387-398.

McCormick DA and Williamson A (1989) Convergence and divergence of neurotransmitter action in human cerebral cortex. *Proc Natl Acad Sci USA* **86**(20): 8098-8102.

McDonald PH, Chow CW, Miller WE, Laporte SA, Field ME, Lin FT, Davis RJ and Lefkowitz RJ (2000) Beta-arrestin 2: a receptor-regulated MAPK scaffold for the activation of JNK3. *Science* **290**(5496): 1574-1577.

Medeiros R, Kitazawa M, Caccamo A, Baglietto-Vargas D, Estrada-Hernandez T, Cribbs DH, Fisher A and LaFerla FM (2011) Loss of muscarinic M1 receptor exacerbates Alzheimer's disease-like pathology and cognitive decline. *Am J Pathol* **179**(2): 980-991.

Melancon BJ, Poslusney MS, Gentry PR, Tarr JC, Sheffler DJ, Mattmann ME, Bridges TM, Utley TJ, Daniels JS, Niswender CM, Conn PJ, Lindsley CW and Wood MR (2013a) Isatin replacements applied to the highly selective, muscarinic M1 PAM ML137: continued optimization of an MLPCN probe molecule. *Bioorg. Med. Chem. Lett.* **23**(2): 412-416.

Melancon BJ, Tarr JC, Panarese JD, Wood MR and Lindsley CW (2013b) Allosteric modulation of the M1 muscarinic acetylcholine receptor: improving cognition and a potential treatment for schizophrenia and Alzheimer's disease. *Drug Discov Today* **18**(23–24): 1185-1199.

Miao Y and McCammon JA (2013) Enhanced Conformational Sampling of M2 Muscarinic Acetylcholine Receptor for Designing Selective Allosteric Drugs. *Biophysical J* **104**(2, Supplement 1): 26a.

Miao Y, Nichols SE, Gasper PM, Metzger VT and McCammon JA (2013) Activation and dynamic network of the M2 muscarinic receptor. *Proc Natl Acad Sci USA* **110**(27): 10982-10987.

Michaelides M, Anderson SAR, Ananth M, Smirnov D, Thanos PK, Neumaier JF, Wang G-J, Volkow ND and Hurd YL (2013) Whole-brain circuit dissection in free-moving animals reveals cell-specific mesocorticolimbic networks. *J Clin Invest* **123**(12): 5342-5350.

Michal P, El-Fakahany EE and Doležal V (2007) Muscarinic M2 Receptors Directly Activate Gq/11 and Gs G-Proteins. *JPET* **320**(2): 607-614.

Michel AD, Delmendo RE, Lopez M and Whiting RL (1990) On the interaction of gallamine with muscarinic receptor subtypes. *Eur J Pharmacol* **182**(2): 335-345.

Migeon JC and Nathanson NM (1994) Differential regulation of cAMP-mediated gene transcription by m1 and m4 muscarinic acetylcholine receptors. Preferential coupling of m4 receptors to Gi alpha-2. *J Biol Chem* **269**(13): 9767-9773.

Migeon JC, Thomas SL and Nathanson NM (1995) Differential coupling of m2 and m4 muscarinic receptors to inhibition of adenylyl cyclase by Gi alpha and G(o)alpha subunits. *J Biol Chem* **270**(27): 16070-16074.

Miller EK and Cohen JD (2001) An integrative theory of prefrontal cortex function. *Annu Rev Neurosc* **24**: 167-202.

Milligan G (2013) The Prevalence, Maintenance, and Relevance of G Protein–Coupled Receptor Oligomerization. *Mol Pharmacol* **84**(1): 158-169.

Milligan G and Kostenis E (2006) Heterotrimeric G-proteins: a short history. *Br J Pharmacol* **147 Suppl 1**: S46-55.

Mistry SN, Valant C, Sexton PM, Capuano B, Christopoulos A and Scammells PJ (2013) Synthesis and pharmacological profiling of analogues of benzyl quinolone carboxylic acid (BQCA) as allosteric modulators of the M1 muscarinic receptor. *J Med Chem* **56**(12): 5151-5172.

Miyakawa T, Yamada M, Duttaroy A and Wess J (2001) Hyperactivity and intact hippocampus-dependent learning in mice lacking the M1 muscarinic acetylcholine receptor. *J Neurosci* **21**(14): 5239-5250.

Mohan S, Kutilek S, Zhang C, Shen HG, Kodama Y, Srivastava AK, Wergedal JE, Beamer WG and Baylink DJ (2000) Comparison of bone formation responses to parathyroid hormone(1-34), (1-31), and (2-34) in mice. *Bone* **27**(4): 471-478.

Mohr K, Trankle C, Kostenis E, Barocelli E, De Amici M and Holzgrabe U (2010) Rational design of dualsteric GPCR ligands: quests and promise. *Br J Pharmacol* **159**(5): 997-1008.

Monod J, Changeux JP and Jacob F (1963) Allosteric proteins and cellular control systems. *J Mol Biol* **6**: 306-329.

Monod J and Jacob F (1961) Teleonomic mechanisms in cellular metabolism, growth, and differentiation. *Cold Spring Harb Symp Quant Biol* **26**: 389-401.

Monod J, Wyman J and Changeux JP (1965) On the Nature of Allosteric Transitions: A Plausible Model. *J Mol Biol* **12**: 88-118.

Moro O, Lameh J and Sadee W (1993) Serine- and threonine-rich domain regulates internalization of muscarinic cholinergic receptors. *J Biol Chem* **268**(10): 6862-6865.

Mundell SJ and Benovic JL (2000) Selective regulation of endogenous G protein-coupled receptors by arrestins in HEK293 cells. *J Biol Chem* **275**(17): 12900-12908.

Munoz-Torrero D (2008) Acetylcholinesterase inhibitors as disease-modifying therapies for Alzheimer's disease. *Curr Med Chem* **15**(24): 2433-2455.

Murakami M and Kouyama T (2008) Crystal structure of squid rhodopsin. *Nature* **453**(7193): 363-367.

Murone M, Rosenthal A and de Sauvage FJ (1999) Sonic hedgehog signaling by the patched-smoothened receptor complex. *Curr Biol* **9**(2): 76-84.

Nakajima K and Wess J (2012) Design and functional characterization of a novel, arrestin-biased designer G protein-coupled receptor. *Mol Pharmacol* **82**(4): 575-582.

Nathan PJ, Watson J, Lund J, Davies CH, Peters G, Dodds CM, Swirski B, Lawrence P, Bentley GD, O'Neill BV, Robertson J, Watson S, Jones GA, Maruff P, Croft RJ, Laruelle M and Bullmore ET (2013) The potent M1 receptor allosteric agonist GSK1034702 improves episodic memory in

humans in the nicotine abstinence model of cognitive dysfunction. *Neuropsychopharmacology* **16**(4): 721-731.

Nathanson NM (2000) A multiplicity of muscarinic mechanisms: enough signaling pathways to take your breath away. *Proc Natl Acad Sci USA* **97**(12): 6245-6247.

Nawaratne V, Leach K, Felder CC, Sexton PM and Christopoulos A (2010) Structural determinants of allosteric agonism and modulation at the M4 muscarinic acetylcholine receptor: identification of ligand-specific and global activation mechanisms. *J Biol Chem* **285**(25): 19012-19021.

Nawaratne V, Leach K, Suratman N, Loiacono RE, Felder CC, Armbruster BN, Roth BL, Sexton PM and Christopoulos A (2008) New insights into the function of M4 muscarinic acetylcholine receptors gained using a novel allosteric modulator and a DREADD (designer receptor exclusively activated by a designer drug). *Mol Pharmacol* **74**(4): 1119-1131.

Neer EJ (1995) Heterotrimeric G proteins: organizers of transmembrane signals. *Cell* **80**(2): 249-257.

Nelson CD, Perry SJ, Regier DS, Prescott SM, Topham MK and Lefkowitz RJ (2007) Targeting of Diacylglycerol Degradation to M1 Muscarinic Receptors by ß-Arrestins. *Science* **315**(5812): 663-666.

Nenasheva TA, Neary M, Mashanov GI, Birdsall NJ, Breckenridge RA and Molloy JE (2013) Abundance, distribution, mobility and oligomeric state of M(2) muscarinic acetylcholine receptors in live cardiac muscle. *J Mol Cell Cardiol* **57**: 129-136.

Neubig RR, Spedding M, Kenakin T and Christopoulos A (2003) International Union of Pharmacology Committee on Receptor Nomenclature and Drug Classification. XXXVIII. Update on terms and symbols in quantitative pharmacology. *Pharmacol Rev* **55**(4): 597-606.

Neves SR, Ram PT and Iyengar R (2002) G protein pathways. *Science* **296**(5573): 1636-1639.

Nichols CD and Roth BL (2009) Engineered G-protein Coupled Receptors are Powerful Tools to Investigate Biological Processes and Behaviors. *Front Mol Neurosci* **2**: 16.

Nickols HH and Conn PJ (2014) Development of allosteric modulators of GPCRs for treatment of CNS disorders. *Neurobiol Dis* **61**(0): 55-71.

Nomura J, Hosoi T, Okuma Y and Nomura Y (2003) The presence and functions of muscarinic receptors in human T cells: the involvement in IL-2 and IL-2 receptor system. *Life Sci* **72**(18-19): 2121-2126.

O'Neill PR, Karunarathne WKA, Kalyanaraman V, Silvius JR and Gautam N (2012) G-protein signaling leverages subunit-dependent membrane affinity to differentially control βγ translocation to intracellular membranes. *Proc Natl Acad Sci USA* **109**(51): E3568–E3577.

Odagaki Y, Kinoshita M and Toyoshima R (2013) Pharmacological characterization of M1 muscarinic acetylcholine receptor-mediated Gq activation in rat cerebral cortical and hippocampal membranes. *Naunyn-Schmiedeberg's Arch Pharmacol* **386**(11): 937-947.

Offermanns S, Wieland T, Homann D, Sandmann J, Bombien E, Spicher K, Schultz G and Jakobs KH (1994) Transfected muscarinic acetylcholine receptors selectively couple to Gi-type G proteins and Gq/11. *Mol Pharmacol* **45**(5): 890-898.

Olianas MC, Dedoni S and Onali P (2013) Coincidence Signaling of Dopamine D₁-Like and M₁ Muscarinic Receptors in the Regulation of Cyclic AMP Formation and CREB Phosphorylation in Mouse Prefrontal Cortex. *Neurosignals* **21**(1-2): 61-74.

Origlia N, Kuczewski N, Aztiria E, Gautam D, Wess J and Domenici L (2006) Muscarinic acetylcholine receptor knockout mice show distinct synaptic plasticity impairments in the visual cortex. *J Physiol* **577**(Pt 3): 829-840.

Overington JP, Al-Lazikani B and Hopkins AL (2006) How many drug targets are there? *Nat Rev Drug Discov* **5**(12): 993-996.

Page KM, Curtis CA, Jones PG and Hulme EC (1995) The functional role of the binding site aspartate in muscarinic acetylcholine receptors, probed by site-directed mutagenesis. *Eur J Pharmacol* **289**(3): 429-437.

Palczewski K, Kumasaka T, Hori T, Behnke CA, Motoshima H, Fox BA, Le Trong I, Teller DC, Okada T, Stenkamp RE, Yamamoto M and Miyano M (2000) Crystal structure of rhodopsin: A G protein-coupled receptor. *Science* **289**(5480): 739-745.

Paule MG, Rowland AS, Ferguson SA, Chelonis JJ, Tannock R, Swanson JM and Castellanos FX (2000) Attention deficit/hyperactivity disorder: characteristics, interventions and models. *Neurotoxicol Teratol* **22**(5): 631-651.

Pearce B, Morrow C and Murphy S (1988) Characteristics of phorbol ester- and agonist-induced down-regulation of astrocyte receptors coupled to inositol phospholipid metabolism. *J Neurochem* **50**(3): 936-944.

Pei Y, Rogan SC, Yan F and Roth BL (2008) Engineered GPCRs as tools to modulate signal transduction. *Physiology* **23**: 313-321.

Peralta EG, Ashkenazi A, Winslow JW, Ramachandran J and Capon DJ (1988) Differential regulation of PI hydrolysis and adenylyl cyclase by muscarinic receptor subtypes. *Nature* **334**(6181): 434-437.

Peretto I, Petrillo P and Imbimbo BP (2009) Medicinal chemistry and therapeutic potential of muscarinic M3 antagonists. *Med Chem Rev* **29**(6): 867-902.

Pierce KL, Premont RT and Lefkowitz RJ (2002) Seven-transmembrane receptors. *Nat Rev Mol Cell Biol* **3**(9): 639-650.

Pioszak AA, Harikumar KG, Parker NR, Miller LJ and Xu HE (2010) Dimeric arrangement of the parathyroid hormone receptor and a structural mechanism for ligand-induced dissociation. *J Biol Chem* **285**(16): 12435-12444.

Pitcher JA, Freedman NJ and Lefkowitz RJ (1998) G protein-coupled receptor kinases. *Annu Rev Biochem* **67**: 653-692.

Poslusney MS, Melancon BJ, Gentry PR, Sheffler DJ, Bridges TM, Utley TJ, Daniels JS, Niswender CM, Conn PJ, Lindsley CW and Wood MR (2013) Spirocyclic replacements for the isatin in the highly selective, muscarinic M1 PAM ML137: the continued optimization of an MLPCN probe molecule. *Bioorg. Med. Chem. Lett.* **23**(6): 1860-1864.

Pou C, Mannoury la Cour C, Stoddart LA, Millan MJ and Milligan G (2012) Functional Homomers and Heteromers of Dopamine D2L and D3 Receptors Co-exist at the Cell Surface. *J Biol Chem* **287**(12): 8864-8878.

Prenzel N, Zwick E, Daub H, Leserer M, Abraham R, Wallasch C and Ullrich A (1999) EGF receptor transactivation by G-protein-coupled receptors requires metalloproteinase cleavage of proHB-EGF. *Nature* **402**(6764): 884-888.

Price MR, Baillie GL, Thomas A, Stevenson LA, Easson M, Goodwin R, McLean A, McIntosh L, Goodwin G, Walker G, Westwood P, Marrs J, Thomson F, Cowley P, Christopoulos A, Pertwee RG and Ross RA (2005) Allosteric modulation of the cannabinoid CB1 receptor. *Mol Pharmacol* **68**(5): 1484-1495.

Prilla S, Schrobang J, Ellis J, Höltje H-D and Mohr K (2006) Allosteric Interactions with Muscarinic Acetylcholine Receptors: Complex Role of the Conserved Tryptophan M2422Trp in a Critical Cluster of Amino Acids for Baseline Affinity, Subtype Selectivity, and Cooperativity. *Mol Pharmacol* **70**(1): 181-193.

Pyne NJ and Pyne S (2011) Receptor tyrosine kinase-G-protein-coupled receptor signalling platforms: out of the shadow? *Trends Pharmacol. Sci.* **32**(8): 443-450.

Pyne NJ, Waters C, Moughal NA, Sambi BS and Pyne S (2003) Receptor tyrosine kinase-GPCR signal complexes. *Biochem Soc Trans* **31**(Pt 6): 1220-1225.

Qin K, Dong C, Wu G and Lambert NA (2011) Inactive-state preassembly of Gq-coupled receptors and Gq heterotrimers. *Nat Chem Biol* **7**(10): 740-747.

Rajagopal S, Rajagopal K and Lefkowitz RJ (2010) Teaching old receptors new tricks: biasing seven-transmembrane receptors. *Nat Rev Drug Discov* **9**(5): 373-386.

Rasmussen SG, Choi HJ, Fung JJ, Pardon E, Casarosa P, Chae PS, Devree BT, Rosenbaum DM, Thian FS, Kobilka TS, Schnapp A, Konetzki I, Sunahara RK, Gellman SH, Pautsch A, Steyaert J, Weis

WI and Kobilka BK (2011a) Structure of a nanobody-stabilized active state of the beta(2) adrenoceptor. *Nature* **469**(7329): 175-180.

Rasmussen SG, Choi HJ, Rosenbaum DM, Kobilka TS, Thian FS, Edwards PC, Burghammer M, Ratnala VR, Sanishvili R, Fischetti RF, Schertler GF, Weis WI and Kobilka BK (2007) Crystal structure of the human beta2 adrenergic G-protein-coupled receptor. *Nature* **450**(7168): 383-387.

Rasmussen SG, DeVree BT, Zou Y, Kruse AC, Chung KY, Kobilka TS, Thian FS, Chae PS, Pardon E, Calinski D, Mathiesen JM, Shah ST, Lyons JA, Caffrey M, Gellman SH, Steyaert J, Skiniotis G, Weis WI, Sunahara RK and Kobilka BK (2011b) Crystal structure of the beta2 adrenergic receptor-Gs protein complex. *Nature* **477**(7366): 549-555.

Ray RS, Corcoran AE, Brust RD, Kim JC, Richerson GB, Nattie E and Dymecki SM (2011) Impaired Respiratory and Body Temperature Control Upon Acute Serotonergic Neuron Inhibition. *Science* **333**(6042): 637-642.

Ray RS, Corcoran AE, Brust RD, Soriano LP, Nattie EE and Dymecki SM (2013) Egr2-neurons control the adult respiratory response to hypercapnia. *Brain Res.* **1511**: 115-125.

Redfern CH, Coward P, Degtyarev MY, Lee EK, Kwa AT, Hennighausen L, Bujard H, Fishman GI and Conklin BR (1999) Conditional expression and signaling of a specifically designed Gi-coupled receptor in transgenic mice. *Nat Biotech* **17**(2): 165-169.

Reid PR, Bridges TM, Sheffler DJ, Cho HP, Lewis LM, Days E, Daniels JS, Jones CK, Niswender CM, Weaver CD, Conn PJ, Lindsley CW and Wood MR (2011) Discovery and optimization of a novel, selective and brain penetrant M1 positive allosteric modulator (PAM): the development of ML169, an MLPCN probe. *Bioorg. Med. Chem. Lett.* **21**(9): 2697-2701.

Richardson RM and Hosey MM (1990) Agonist-independent phosphorylation of purified cardiac muscarinic cholinergic receptors by protein kinase C. *Biochem* **29**(37): 8555-8561.

Ritter SL and Hall RA (2009) Fine-tuning of GPCR activity by receptor-interacting proteins. *Nat Rev. Mol Cell Biol* **10**(12): 819-830.

Rocheville M, Lange DC, Kumar U, Patel SC, Patel RC and Patel YC (2000) Receptors for dopamine and somatostatin: formation of hetero-oligomers with enhanced functional activity. *Science* **288**(5463): 154-157.

Rondard P, Goudet C, Kniazeff J, Pin JP and Prezeau L (2011) The complexity of their activation mechanism opens new possibilities for the modulation of mGlu and GABAB class C G protein-coupled receptors. *Neuropharmacology* **60**(1): 82-92.

Salgado H, Bellay T, Nichols JA, Bose M, Martinolich L, Perrotti L and Atzori M (2007) Muscarinic M2 and M1 receptors reduce GABA release by Ca2+ channel modulation through activation of PI3K/Ca2+ -independent and PLC/Ca2+ -dependent PKC. *J Neurophysiol* **98**(2): 952-965.

Samama P, Cotecchia S, Costa T and Lefkowitz RJ (1993) A mutation-induced activated state of the beta 2-adrenergic receptor. Extending the ternary complex model. *J Biol Chem* **268**(7): 4625-4636.

Sams AG, Hentzer M, Mikkelsen GK, Larsen K, Bundgaard C, Plath N, Christoffersen CT and Bang-Andersen B (2010) Discovery of N-{1-[3-(3-oxo-2,3-dihydrobenzo[1,4]oxazin-4-yl)propyl]piperidin-4-yl}-2-p henylacetamide (Lu AE51090): an allosteric muscarinic M1 receptor agonist with unprecedented selectivity and procognitive potential. *J Med Chem* **53**(17): 6386-6397.

Sandmann J, Peralta EG and Wurtman RJ (1991) Coupling of transfected muscarinic acetylcholine receptor subtypes to phospholipase D. *J Biol Chem* **266**(10): 6031-6034.

Santini F, Penn RB, Gagnon AW, Benovic JL and Keen JH (2000) Selective recruitment of arrestin-3 to clathrin coated pits upon stimulation of G protein-coupled receptors. *J Cell Sci* **113 (Pt 13)**: 2463-2470.

Sasaki K, Suzuki M, Mieda M, Tsujino N, Roth B and Sakurai T (2011) Pharmacogenetic modulation of orexin neurons alters sleep/wakefulness states in mice. *PLoS One* **6**(5): e20360.

Scarr E, Gibbons AS, Neo J, Udawela M and Dean B (2013) Cholinergic connectivity: it's implications for psychiatric disorders. *Frontiers Cell Neurosc* **7**.

Scarr E, Sundram S, Keriakous D and Dean B (2007) Altered hippocampal muscarinic M4, but not M1, receptor expression from subjects with schizophrenia. *Biol Psych* **61**(10): 1161-1170.

Scarselli M, Li B, Kim S-K and Wess J (2007) Multiple Residues in the Second Extracellular Loop Are Critical for M3 Muscarinic Acetylcholine Receptor Activation. *J Biol Chem* **282**(10): 7385-7396.

Scheerer P, Park JH, Hildebrand PW, Kim YJ, Krauss N, Choe HW, Hofmann KP and Ernst OP (2008) Crystal structure of opsin in its G-protein-interacting conformation. *Nature* **455**(7212): 497-502.

Schelshorn D, Joly F, Mutel S, Hampe C, Breton B, Mutel V and Lutjens R (2012) Lateral allosterism in the glucagon receptor family: glucagon-like peptide 1 induces G-protein-coupled receptor heteromer formation. *Mol Pharmacol* **81**(3): 309-318.

Schetz JA, Chu A and Sibley DR (1999) Zinc modulates antagonist interactions with D2-like dopamine receptors through distinct molecular mechanisms. *JPET* **289**(2): 956-964.

Schrage R, Seemann WK, Klöckner J, Dallanoce C, Racké K, Kostenis E, De Amici M, Holzgrabe U and Mohr K (2013) Agonists with supraphysiological efficacy at the muscarinic M2 ACh receptor. *Br J Pharmacol* **169**(2): 357-370.

Selyanko AA, Hadley JK, Wood IC, Abogadie FC, Jentsch TJ and Brown DA (2000) Inhibition of KCNQ1-4 potassium channels expressed in mammalian cells via M1 muscarinic acetylcholine receptors. *J Physiol* **522**(3): 349-355.

Sexton PM and Wootten D (2013) Structural biology: meet the B family. *Nature* **499**(7459): 417-418.

Sheffler DJ, Sevel C, Le U, Lovell KM, Tarr JC, Carrington SJ, Cho HP, Digby GJ, Niswender CM, Conn PJ, Hopkins CR, Wood MR and Lindsley CW (2013) Further exploration of M(1) allosteric agonists: subtle structural changes abolish M(1) allosteric agonism and result in pan-mAChR orthosteric antagonism. *Bioorg. Med. Chem. Lett.* **23**(1): 223-227.

Shekhar A, Potter WZ, Lightfoot J, Lienemann J, Dube S, Mallinckrodt C, Bymaster FP, McKinzie DL and Felder CC (2008) Selective muscarinic receptor agonist xanomeline as a novel treatment approach for schizophrenia. *Am J Psychiatry* **165**(8): 1033-1039.

Shimamura T, Shiroishi M, Weyand S, Tsujimoto H, Winter G, Katritch V, Abagyan R, Cherezov V, Liu W, Han GW, Kobayashi T, Stevens RC and Iwata S (2011) Structure of the human histamine H1 receptor complex with doxepin. *Nature* **475**(7354): 65-70.

Shinoe T, Matsui M, Taketo MM and Manabe T (2005) Modulation of synaptic plasticity by physiological activation of M1 muscarinic acetylcholine receptors in the mouse hippocampus. *J Neurosci* **25**(48): 11194-11200.

Shirey JK, Brady AE, Jones PJ, Davis AA, Bridges TM, Kennedy JP, Jadhav SB, Menon UN, Xiang Z, Watson ML, Christian EP, Doherty JJ, Quirk MC, Snyder DH, Lah JJ, Levey AI, Nicolle MM, Lindsley CW and Conn PJ (2009) A selective allosteric potentiator of the M1 muscarinic acetylcholine receptor increases activity of medial prefrontal cortical neurons and restores impairments in reversal learning. *J Neurosci* **29**(45): 14271-14286.

Shmuel M, Nodel-Berner E, Hyman T, Rouvinski A and Altschuler Y (2007) Caveolin 2 Regulates Endocytosis and Trafficking of the M1 Muscarinic Receptor in MDCK Epithelial Cells. *Mol Biol Cell* **18**(5): 1570-1585.

Shockley MS, Burford NT, Sadée W and Lameh J (1997) Residues Specifically Involved in Down-Regulation but Not Internalization of the m1 Muscarinic Acetylcholine Receptor. *J Neurochem* **68**(2): 601-609.

Shonberg J, Herenbrink CK, López L, Christopoulos A, Scammells PJ, Capuano B and Lane JR (2013) A Structure–Activity Analysis of Biased Agonism at the Dopamine D2 Receptor. *J Med Chem* **56**(22): 9199-9221.

Shukla AK, Manglik A, Kruse AC, Xiao K, Reis RI, Tseng W-C, Staus DP, Hilger D, Uysal S, Huang L-Y, Paduch M, Tripathi-Shukla P, Koide A, Koide S, Weis WI, Kossiakoff AA, Kobilka BK and Lefkowitz RJ (2013) Structure of active [bgr]-arrestin-1 bound to a G-protein-coupled receptor phosphopeptide. *Nature* **497**(7447): 137-141.

Shukla AK, Westfield GH, Xiao K, Reis RI, Huang L-Y, Tripathi-Shukla P, Qian J, Li S, Blanc A, Oleskie AN, Dosey AM, Su M, Liang C-R, Gu L-L, Shan J-M, Chen X, Hanna R, Choi M, Yao XJ, Klink BU, Kahsai AW, Sidhu SS, Koide S, Penczek PA, Kossiakoff AA, Woods Jr VL, Kobilka BK, Skiniotis G and Lefkowitz RJ (2014) Visualization of arrestin recruitment by a G-protein-coupled receptor. *Nature* **advance online publication**.

Siddiquee K, Hampton J, McAnally D, May LT and Smith LH (2013) The apelin receptor inhibits the angiotensin II type 1 receptor via allosteric trans-inhibition. *Br J Pharmacol* **168**(5): 1104-1117.

Silvano E, Millan MJ, Mannoury la Cour C, Han Y, Duan L, Griffin SA, Luedtke RR, Aloisi G, Rossi M, Zazzeroni F, Javitch JA and Maggio R (2010) The tetrahydroisoquinoline derivative SB269,652 is an allosteric antagonist at dopamine D3 and D2 receptors. *Mol Pharmacol* **78**(5): 925-934.

Siu FY, He M, de Graaf C, Han GW, Yang D, Zhang Z, Zhou C, Xu Q, Wacker D, Joseph JS, Liu W, Lau J, Cherezov V, Katritch V, Wang MW and Stevens RC (2013) Structure of the human glucagon class B G-protein-coupled receptor. *Nature* **499**(7459): 444-449.

Smith CJ, Perry EK, Perry RH, Candy JM, Johnson M, Bonham JR, Dick DJ, Fairbairn A, Blessed G and Birdsall NJ (1988) Muscarinic cholinergic receptor subtypes in hippocampus in human cognitive disorders. *J Neurochem* **50**(3): 847-856.

Smith NJ and Milligan G (2010) Allostery at G protein-coupled receptor homo- and heteromers: uncharted pharmacological landscapes. *Pharmacol Rev* **62**(4): 701-725.

Spalding TA, Birdsall NJ, Curtis CA and Hulme EC (1994) Acetylcholine mustard labels the binding site aspartate in muscarinic acetylcholine receptors. *J Biol Chem* **269**(6): 4092-4097.

Spalding TA, Ma JN, Ott TR, Friberg M, Bajpai A, Bradley SR, Davis RE, Brann MR and Burstein ES (2006) Structural requirements of transmembrane domain 3 for activation by the M1 muscarinic receptor agonists AC-42, AC-260584, clozapine, and N-desmethylclozapine: evidence for three distinct modes of receptor activation. *Mol Pharmacol* **70**(6): 1974-1983.

Spalding TA, Trotter C, Skjaerbaek N, Messier TL, Currier EA, Burstein ES, Li D, Hacksell U and Brann MR (2002) Discovery of an ectopic activation site on the M(1) muscarinic receptor. *Mol Pharmacol* **61**(6): 1297-1302.

Srivastava A, Yano J, Hirozane Y, Kefala G, Gruswitz F, Snell G, Lane W, Ivetac A, Aertgeerts K, Nguyen J, Jennings A and Okada K (2014) High-resolution structure of the human GPR40 receptor bound to allosteric agonist TAK-875. *Nature* **513**(7516): 124-127.

Stallaert W, Christopoulos A and Bouvier M (2011) Ligand functional selectivity and quantitative pharmacology at G protein-coupled receptors. *Expert Opin Drug Discov* **6**(8): 811-825.

Stehno-Bittel L, Krapivinsky G, Krapivinsky L, Perez-Terzic C and Clapham DE (1995) The G Protein βγ Subunit Transduces the Muscarinic Receptor Signal for Ca2+ Release in Xenopus Oocytes. *J Biol Chem* **270**(50): 30068-30074.

Steinfeld T, Mammen M, Smith JA, Wilson RD and Jasper JR (2007) A novel multivalent ligand that bridges the allosteric and orthosteric binding sites of the M2 muscarinic receptor. *Mol Pharmacol* **72**(2): 291-302.

Sterin-Borda L, Ganzinelli S, Berra A and Borda E (2003) Novel insight into the mechanisms involved in the regulation of the m1 muscarinic receptor, iNOS and nNOS mRNA levels. *Neuropharmacology* **45**(2): 260-269.

Stewart GD, Sexton PM and Christopoulos A (2010) Prediction of functionally selective allosteric interactions at an M3 muscarinic acetylcholine receptor mutant using Saccharomyces cerevisiae. *Mol Pharmacol* **78**(2): 205-214.

Stockton JM, Birdsall NJ, Burgen AS and Hulme EC (1983) Modification of the binding properties of muscarinic receptors by gallamine. *Mol Pharmacol* **23**(3): 551-557.

Street M, Marsh SJ, Stabach PR, Morrow JS, Brown DA and Buckley NJ (2006) Stimulation of Gαq-coupled M1 muscarinic receptor causes reversible spectrin redistribution mediated by PLC, PKC and ROCK. *J Cell Sci* **119**(8): 1528-1536.

Suh BC and Hille B (2005) Regulation of ion channels by phosphatidylinositol 4,5-bisphosphate. *Curr Opin Neurobiol* **15**(3): 370-378.

Suh PG, Park JI, Manzoli L, Cocco L, Peak JC, Katan M, Fukami K, Kataoka T, Yun S and Ryu SH (2008) Multiple roles of phosphoinositide-specific phospholipase C isozymes. *BMB Rep* **41**(6): 415-434.

Sun Y, Cheng Z, Ma L and Pei G (2002) Beta-arrestin2 is critically involved in CXCR4-mediated chemotaxis, and this is mediated by its enhancement of p38 MAPK activation. *J Biol Chem* **277**(51): 49212-49219.

Sur C, Mallorga PJ, Wittmann M, Jacobson MA, Pascarella D, Williams JB, Brandish PE, Pettibone DJ, Scolnick EM and Conn PJ (2003) N-desmethylclozapine, an allosteric agonist at muscarinic 1 receptor, potentiates N-methyl-D-aspartate receptor activity. *Proc Natl Acad Sci USA* **100**(23): 13674-13679.

Swaminath G, Lee TW and Kobilka B (2003) Identification of an allosteric binding site for Zn2+ on the beta2 adrenergic receptor. *J Biol Chem* **278**(1): 352-356.

Takasu H, Gardella TJ, Luck MD, Potts JT, Jr. and Bringhurst FR (1999) Amino-terminal modifications of human parathyroid hormone (PTH) selectively alter phospholipase C signaling via the type 1 PTH receptor: implications for design of signal-specific PTH ligands. *Biochemistry* **38**(41): 13453-13460.

Tan Q, Zhu Y, Li J, Chen Z, Han GW, Kufareva I, Li T, Ma L, Fenalti G, Li J, Zhang W, Xie X, Yang H, Jiang H, Cherezov V, Liu H, Stevens RC, Zhao Q and Wu B (2013) Structure of the CCR5 Chemokine Receptor–HIV Entry Inhibitor Maraviroc Complex. *Science* **341**(6152): 1387-1390.

Tarr JC, Turlington ML, Reid PR, Utley TJ, Sheffler DJ, Cho HP, Klar R, Pancani T, Klein MT, Bridges TM, Morrison RD, Blobaum AL, Xiang Z, Daniels JS, Niswender CM, Conn PJ, Wood MR and Lindsley CW (2012) Targeting Selective Activation of M1 for the Treatment of Alzheimer's Disease: Further Chemical Optimization and Pharmacological Characterization of the M1 Positive Allosteric Modulator ML169. *ACS Chem. Neurosci.* **3**(11): 884-895.

Tautermann CS, Kiechle T, Seeliger D, Diehl S, Wex E, Banholzer R, Gantner F, Pieper MP and Casarosa P (2013) Molecular basis for the long duration of action and kinetic selectivity of tiotropium for the muscarinic M3 receptor. *J Med Chem* **56**(21): 8746-8756.

Taylor SJ, Chae HZ, Rhee SG and Exton JH (1991) Activation of the beta 1 isozyme of phospholipase C by alpha subunits of the Gq class of G proteins. *Nature* **350**(6318): 516-518.

Thiele A (2013) Muscarinic signaling in the brain. *Annu Rev Neurosci* **36**: 271-294.

Thomas DR, Dada A, Jones GA, Deisz RA, Gigout S, Langmead CJ, Werry TD, Hendry N, Hagan JJ, Davies CH and Watson JM (2010) N-desmethylclozapine (NDMC) is an antagonist at the human native muscarinic M1 receptor. *Neuropharmacology* **58**(8): 1206-1214.

Thomas EA, Carson MJ, Neal MJ and Sutcliffe JG (1997) Unique allosteric regulation of 5-hydroxytryptamine receptor-mediated signal transduction by oleamide. *Proc Natl Acad Sci USA* **94**(25): 14115-14119.

Thomas RL, Mistry R, Langmead CJ, Wood MD and Challiss RAJ (2008) G Protein Coupling and Signaling Pathway Activation by M1 Muscarinic Acetylcholine Receptor Orthosteric and Allosteric Agonists. *JPET* **327**(2): 365-374.

Tolbert LM and Lameh J (1996) Human muscarinic cholinergic receptor Hm1 internalizes via clathrin-coated vesicles. *J Biol Chem* **271**(29): 17335-17342.

Trankle C, Mies-Klomfass E, Cid MH, Holzgrabe U and Mohr K (1998) Identification of a [3H]Ligand for the common allosteric site of muscarinic acetylcholine M2 receptors. *Mol Pharmacol* **54**(1): 139-145.

Trendelenburg AU, Gomeza J, Klebroff W, Zhou H and Wess J (2003) Heterogeneity of presynaptic muscarinic receptors mediating inhibition of sympathetic transmitter release: a study with M2- and M4-receptor-deficient mice. *Br J Pharmacol* **138**(3): 469-480.

Tsai W, Morielli AD, Cachero TG and Peralta EG (1999) Receptor protein tyrosine phosphatase [alpha] participates in the m1 muscarinic acetylcholine receptor-dependent regulation of Kv1.2 channel activity. *EMBO J* **18**(1): 109-118.

Tsai W, Morielli AD and Peralta EG (1997) The m1 muscarinic acetylcholine receptor transactivates the EGF receptor to modulate ion channel activity. *EMBO J* **16**(15): 4597-4605.

Tzavara ET, Bymaster FP, Felder CC, Wade M, Gomeza J, Wess J, McKinzie DL and Nomikos GG (2003) Dysregulated hippocampal acetylcholine neurotransmission and impaired cognition in M2, M4 and M2/M4 muscarinic receptor knockout mice. *Mol Psych* **8**(7): 673-679.

Uchiyama H, Ohara K, Haga K, Haga T and Ichiyama A (1990) Location in muscarinic acetylcholine receptors of sites for [3H]propylbenzilylcholine mustard binding and for phosphorylation with protein kinase C. *J Neurochem* **54**(6): 1870-1881.

Uslaner JM, Eddins D, Puri V, Cannon CE, Sutcliffe J, Chew CS, Pearson M, Vivian JA, Chang RK, Ray WJ, Kuduk SD and Wittmann M (2013) The muscarinic M1 receptor positive allosteric modulator PQCA improves cognitive measures in rat, cynomolgus macaque, and rhesus macaque. *Psychopharmacology* **225**(1): 21-30.

Vaidehi N and Kenakin T (2010) The role of conformational ensembles of seven transmembrane receptors in functional selectivity. *Curr Opin Pharmacol* **10**(6): 775-781.

Valant C, Felder CC, Sexton PM and Christopoulos A (2012a) Probe dependence in the allosteric modulation of a g protein-coupled receptor: implications for detection and validation of allosteric ligand effects. *Mol Pharmacol* **81**(1): 41-52.

Valant C, Gregory KJ, Hall NE, Scammells PJ, Lew MJ, Sexton PM and Christopoulos A (2008) A novel mechanism of G protein-coupled receptor functional selectivity. Muscarinic partial agonist McN-A-343 as a bitopic orthosteric/allosteric ligand. *J Biol Chem* **283**(43): 29312-29321.

Valant C, May LT, Aurelio L, Chuo CH, White PJ, Baltos J-A, Sexton PM, Scammells PJ and Christopoulos A (2014) Separation of on-target efficacy from adverse effects through rational design of a bitopic adenosine receptor agonist. *Proc Natl Acad Sci USA* **111**(12): 4614-4619.

Valant C, Robert Lane J, Sexton PM and Christopoulos A (2012b) The best of both worlds? Bitopic orthosteric/allosteric ligands of g protein-coupled receptors. *Annu Rev Pharmacol Toxicol* **52**: 153-178.

Valant C, Sexton PM and Christopoulos A (2009) Orthosteric/allosteric bitopic ligands: going hybrid at GPCRs. *Mol Interv* **9**(3): 125-135.

van Koppen CJ (2001) Multiple pathways for the dynamin-regulated internalization of muscarinic acetylcholine receptors. *Biochem Soc Trans* **29**(Pt 4): 505-508.

van Koppen CJ and Kaiser B (2003) Regulation of muscarinic acetylcholine receptor signaling. *Pharmacol Ther* **98**(2): 197-220.

van Os J and Kapur S (2009) Schizophrenia. *Lancet* **374**(9690): 635-645.

VanDeMark KL, Guizzetti M, Giordano G and Costa LG (2009) The Activation of M1 Muscarinic Receptor Signaling Induces Neuronal Differentiation in Pyramidal Hippocampal Neurons. *JPET* **329**(2): 532-542.

Vanhauwe JF, Thomas TO, Minshall RD, Tiruppathi C, Li A, Gilchrist A, Yoon EJ, Malik AB and Hamm HE (2002) Thrombin receptors activate G(o) proteins in endothelial cells to regulate intracellular calcium and cell shape changes. *J Biol Chem* **277**(37): 34143-34149.

Venkatakrishnan AJ, Deupi X, Lebon G, Tate CG, Schertler GF and Babu MM (2013) Molecular signatures of G-protein-coupled receptors. *Nature* **494**(7436): 185-194.

Verma V, Mann A, Costain W, Pontoriero G, Castellano JM, Skoblenick K, Gupta SK, Pristupa Z, Niznik HB, Johnson RL, Nair VD and Mishra RK (2005) Modulation of agonist binding to human dopamine receptor subtypes by L-prolyl-L-leucyl-glycinamide and a peptidomimetic analog. *JPET* **315**(3): 1228-1236.

Vilaro MT, Palacios JM and Mengod G (1990) Localization of m5 muscarinic receptor mRNA in rat brain examined by in situ hybridization histochemistry. *Neurosc Letters* **114**(2): 154-159.

Violin JD, Crombie AL, Soergel DG and Lark MW (2014) Biased ligands at G-protein-coupled receptors: promise and progress. *Trends Pharmacol. Sci.* **35**(7): 308-316.

Vogler O, Bogatkewitsch GS, Wriske C, Krummenerl P, Jakobs KH and van Koppen CJ (1998) Receptor subtype-specific regulation of muscarinic acetylcholine receptor sequestration by dynamin. Distinct sequestration of m2 receptors. *J Biol Chem* **273**(20): 12155-12160.

Vogler O, Krummenerl P, Schmidt M, Jakobs KH and Van Koppen CJ (1999a) RhoA-sensitive trafficking of muscarinic acetylcholine receptors. *JPET* **288**(1): 36-42.

Vogler O, Nolte B, Voss M, Schmidt M, Jakobs KH and van Koppen CJ (1999b) Regulation of muscarinic acetylcholine receptor sequestration and function by beta-arrestin. *J Biol Chem* **274**(18): 12333-12338.

Voigtlander U, Johren K, Mohr M, Raasch A, Trankle C, Buller S, Ellis J, Holtje HD and Mohr K (2003) Allosteric site on muscarinic acetylcholine receptors: identification of two amino acids in the muscarinic M2 receptor that account entirely for the M2/M5 subtype selectivities of some structurally diverse allosteric ligands in N-methylscopolamine-occupied receptors. *Mol Pharmacol* **64**(1): 21-31.

Volpicelli LA and Levey AI (2004) Muscarinic acetylcholine receptor subtypes in cerebral cortex and hippocampus. *Progress Brain Res* **145**: 59-66.

Wacker D, Wang C, Katritch V, Han GW, Huang X-P, Vardy E, McCorvy JD, Jiang Y, Chu M, Siu FY, Liu W, Xu HE, Cherezov V, Roth BL and Stevens RC (2013) Structural Features for Functional Selectivity at Serotonin Receptors. *Science* **340**(6132): 615-619.

Wang C, Jiang Y, Ma J, Wu H, Wacker D, Katritch V, Han GW, Liu W, Huang X-P, Vardy E, McCorvy JD, Gao X, Zhou XE, Melcher K, Zhang C, Bai F, Yang H, Yang L, Jiang H, Roth BL, Cherezov V, Stevens RC and Xu HE (2013a) Structural Basis for Molecular Recognition at Serotonin Receptors. *Science* **340**(6132): 610-614.

Wang C, Wu H, Evron T, Vardy E, Han GW, Huang X-P, Hufeisen SJ, Mangano TJ, Urban DJ, Katritch V, Cherezov V, Caron MG, Roth BL and Stevens RC (2014) Structural basis for Smoothened receptor modulation and chemoresistance to anticancer drugs. *Nat Commun* **5**.

Wang C, Wu H, Katritch V, Han GW, Huang X-P, Liu W, Siu FY, Roth BL, Cherezov V and Stevens RC (2013b) Structure of the human smoothened receptor bound to an antitumour agent. *Nature* **497**(7449): 338-343.

Ward SD, Curtis CA and Hulme EC (1999) Alanine-scanning mutagenesis of transmembrane domain 6 of the M(1) muscarinic acetylcholine receptor suggests that Tyr381 plays key roles in receptor function. *Mol Pharmacol* **56**(5): 1031-1041.

Warne T, Serrano-Vega MJ, Baker JG, Moukhametzianov R, Edwards PC, Henderson R, Leslie AG, Tate CG and Schertler GF (2008) Structure of a beta1-adrenergic G-protein-coupled receptor. *Nature* **454**(7203): 486-491.

Watson C, Jenkinson S, Kazmierski W and Kenakin T (2005) The CCR5 receptor-based mechanism of action of 873140, a potent allosteric noncompetitive HIV entry inhibitor. *Mol Pharmacol* **67**(4): 1268-1282.

Waugh MG, Challiss RA, Berstein G, Nahorski SR and Tobin AB (1999) Agonist-induced desensitization and phosphorylation of m1-muscarinic receptors. *Biochem. J.* **338**(1): 175-183.

Wei H, Ahn S, Shenoy SK, Karnik SS, Hunyady L, Luttrell LM and Lefkowitz RJ (2003) Independent beta-arrestin 2 and G protein-mediated pathways for angiotensin II activation of extracellular signal-regulated kinases 1 and 2. *Proc Natl Acad Sci USA* **100**(19): 10782-10787.

Werbonat Y, Kleutges N, Jakobs KH and van Koppen CJ (2000) Essential role of dynamin in internalization of M2 muscarinic acetylcholine and angiotensin AT1A receptors. *J Biol Chem* **275**(29): 21969-21974.

Werry TD, Christopoulos A and Sexton PM (2006) Mechanisms of ERK1/2 regulation by seven-transmembrane-domain receptors. *Curr Pharm Des* **12**(14): 1683-1702.

Werry TD, Sexton PM and Christopoulos A (2005) 'Ins and outs' of seven-transmembrane receptor signalling to ERK. *Trends Endocrin Metabol* **16**(1): 26-33.

Wess J (1996) Molecular biology of muscarinic acetylcholine receptors. *Crit Rev Neurobiol* **10**(1): 69-99.

Wess J (1998) Molecular basis of receptor/G-protein-coupling selectivity. *Pharmacol Ther* **80**(3): 231-264.

Wess J, Eglen RM and Gautam D (2007) Muscarinic acetylcholine receptors: mutant mice provide new insights for drug development. *Nat Rev Drug Discov* **6**(9): 721-733.

Wess J, Gdula D and Brann MR (1991) Site-directed mutagenesis of the m3 muscarinic receptor: identification of a series of threonine and tyrosine residues involved in agonist but not antagonist binding. *EMBO J* **10**(12): 3729-3734.

Wess J, Gdula D and Brann MR (1992a) Structural basis of the subtype selectivity of muscarinic antagonists: a study with chimeric m2/m5 muscarinic receptors. *Mol Pharmacol* **41**(2): 369-374.

Wess J, Maggio R, Palmer JR and Vogel Z (1992b) Role of conserved threonine and tyrosine residues in acetylcholine binding and muscarinic receptor activation. A study with m3 muscarinic receptor point mutants. *J Biol Chem* **267**(27): 19313-19319.

Wess J, Nakajima K and Jain S (2013) Novel designer receptors to probe GPCR signaling and physiology. *Trends Pharmacol. Sci.* **34**(7): 385-392.

Whorton MR and MacKinnon R (2013a) X-ray structure of the mammalian GIRK2-[bgr][ggr] G-protein complex. *Nature* **498**(7453): 190-197.

Whorton MR and MacKinnon R (2013b) X-ray structure of the mammalian GIRK2-betagamma G-protein complex. *Nature* **498**(7453): 190-197.

Wickman K and Clapham DE (1995) Ion channel regulation by G proteins. *Physiol Rev* **75**(4): 865-885.

Willets JM, Nahorski SR and Challiss RAJ (2005) Roles of Phosphorylation-dependent and -independent Mechanisms in the Regulation of M1 Muscarinic Acetylcholine Receptors by G Protein-coupled Receptor Kinase 2 in Hippocampal Neurons. *J Biol Chem* **280**(19): 18950-18958.

Willets JM, Nelson CP, Nahorski SR and Challiss RAJ (2007) The regulation of M1 muscarinic acetylcholine receptor desensitization by synaptic activity in cultured hippocampal neurons1. *J Neurochem* **103**(6): 2268-2280.

Womble MD and Moises HC (1992) Muscarinic inhibition of M-current and a potassium leak conductance in neurones of the rat basolateral amygdala. *J Physiol* **457**: 93-114.

Wootten D, Christopoulos A and Sexton PM (2013) Emerging paradigms in GPCR allostery: implications for drug discovery. *Nat Rev Drug Discov* **12**(8): 630-644.

Wu H, Wang C, Gregory KJ, Han GW, Cho HP, Xia Y, Niswender CM, Katritch V, Meiler J, Cherezov V, Conn PJ and Stevens RC (2014) Structure of a Class C GPCR Metabotropic Glutamate Receptor 1 Bound to an Allosteric Modulator. *Science* **344**(6179): 58-64.

Xiang Z, Thompson AD, Jones CK, Lindsley CW and Conn PJ (2012) Roles of the M1 Muscarinic Acetylcholine Receptor Subtype in the Regulation of Basal Ganglia Function and Implications for the Treatment of Parkinson's Disease. *JPET* **340**(3): 595-603.

Xu M, Yamamoto T and Kato T (1990) In Vivo Striatal Dopamine Release by M1 Muscarinic Receptors Is Induced by Activation of Protein Kinase C. *J Neurochem* **54**(6): 1917-1919.

Yan HD, Villalobos C and Andrade R (2009) TRPC Channels Mediate a Muscarinic Receptor-Induced Afterdepolarization in Cerebral Cortex. *J Neurosci* **29**(32): 10038-10046.

Yeatman HR, Lane JR, Choy KH, Lambert NA, Sexton PM, Christopoulos A and Canals M (2014) Allosteric Modulation of M1 Muscarinic Acetylcholine Receptor Internalization and Subcellular Trafficking. *J Biol Chem* **289**(22): 15856-15866.

Young MB and Thomas SA (2014) M1-Muscarinic Receptors Promote Fear Memory Consolidation via Phospholipase C and the M-Current. *J Neurosci* **34**(5): 1570-1578.

Zhang J-S, Jin D and Higashida H (2005) Acetylcholine stimulates cyclic ADP-ribose formation via M1 muscarinic receptors in rat superior cervical ganglion. *Biochem Biophys Res Comm* **335**(3): 920-924.

Zhang Y, Hamilton SE, Nathanson NM and Yan J (2006) Decreased input-specific plasticity of the auditory cortex in mice lacking M1 muscarinic acetylcholine receptors. *Cereb Cortex* **16**(9): 1258-1265.

Zheng H, Worrall C, Shen H, Issad T, Seregard S, Girnita A and Girnita L (2012) Selective recruitment of G protein-coupled receptor kinases (GRKs) controls signaling of the insulin-like growth factor 1 receptor. *Proc Natl Acad Sci USA* **109**(18): 7055-7060.

Zhu H and Roth Bryan L (2014) Silencing Synapses with DREADDs. *Neuron* **82**(4): 723-725.

Zhuo JM, Prakasam A, Murray ME, Zhang HY, Baxter MG, Sambamurti K and Nicolle MM (2008) An increase in Abeta42 in the prefrontal cortex is associated with a reversal-learning impairment in Alzheimer's disease model Tg2576 APPsw mice. *Curr Alzheimer Res* **5**(4): 385-391.

Zhuo JM, Prescott SL, Murray ME, Zhang HY, Baxter MG and Nicolle MM (2007) Early discrimination reversal learning impairment and preserved spatial learning in a longitudinal study of Tg2576 APPsw mice. *Neurobiol Aging* **28**(8): 1248-1257.

APPENDIX 1

Regulation of G Protein-Coupled Receptors by Allosteric Ligands

J. Robert Lane, Alaa Abdul-Ridha, and Meritxell Canals

ACS Chem. Neurosci **4**: 527-534, February 2013.

ACS Chemical Neuroscience

Review

pubs.acs.org/chemneuro

Regulation of G Protein-Coupled Receptors by Allosteric Ligands

J. Robert Lane,*,† Alaa Abdul-Ridha, and Meritxell Canals*,†

Drug Discovery Biology, Monash Institute of Pharmaceutical Sciences and Department of Pharmacology, Monash University, Parkville, Victoria, 3052, Australia

ABSTRACT: Topographically distinct, druggable, allosteric sites may be present on all G protein-coupled receptors (GPCRs). As such, targeting these sites with synthetic small molecules offers an attractive approach to develop receptor-subtype selective chemical leads for the development of novel therapies. A crucial part of drug development is to understand the acute and chronic effects of such allosteric modulators at their corresponding GPCR target. Key regulatory processes including cell-surface delivery, endocytosis, recycling, and down-regulation tightly control the number of receptors at the surface of the cell. As many GPCR therapeutics will be administered chronically, understanding how such ligands modulate these regulatory pathways forms an essential part of the characterization of novel GPCR ligands. This is true for both orthosteric and allosteric ligands. In this Review, we summarize our current understanding of GPCR regulatory processes with a particular focus on the effects and implications of allosteric targeting of GPCRs.

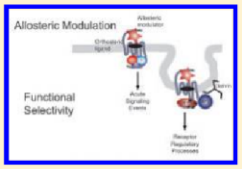

KEYWORDS: *G protein-coupled receptor, allosteric ligand, arrestin, endocytosis, functional selectivity*

G protein-coupled receptors (GPCRs) represent the largest group of cell surface receptors encoded by the human genome (~2%). By binding to a broad variety of ligands (ranging from small ions to amines or large peptides), GPCRs play the essential role of transmitting stimuli from the extracellular milieu and transforming them into specific cellular responses. The diverse physiological roles played by GPCRs, together with evidence for aberrant GPCR expression or signaling in various pathological conditions, emphasize the fundamental biological and clinical importance of this family of membrane proteins, and support their prominent position as targets in drug development programs. As such, GPCRs are currently the therapeutic target of more than 30% of marketed drugs.[1] Classical approaches to GPCR drug discovery have focused upon developing small molecules that target the site at which endogenous hormones or neurotransmitters bind, the so-called "orthosteric" site. Such molecules can either mimic or inhibit the actions of these endogenous ligands. However, the attrition rate of modern drug discovery is higher than ever and the development of selective compounds as potential drug leads represents a significant challenge. One of the key issues in this regard is the fact that many GPCRs share high sequence homology within the orthosteric site across receptor subtypes. As a consequence, targeting this site alone is unlikely to yield highly subtype-selective lead compounds. Indeed, during the past decade, the idea of targeting topographically distinct "allosteric sites" as a novel approach to GPCR drug discovery has become a major topic in receptor pharmacology.[2,3] The phenomenon of functional selectivity (also called "ligand-directed stimulus bias" or biased agonism) refers to the ability of different ligands that, despite acting via the same receptor and in the same cellular background, differentially activate certain subsets of intracellular signaling pathways to the relative exclusion of the others.[4,5] As such, stimulus bias offers a new avenue for attaining "pathway-selective" rather than "receptor-selective" therapeutics. The characterization of the regulatory processes elicited by newly discovered GPCR ligands has often been "secondary" to the main aim of drug discovery and development programs.[6] However, the fact that most of the therapies that target GPCRs are based on chronic exposure of the receptor to its ligand raises the important issue of understanding and investigating the long-term regulatory processes of this family of cell surface receptors. Such mechanisms of GPCR regulation also need to be considered for drugs that target allosteric sites on GPCRs. Furthermore, the concept of stimulus bias suggests that measurements of drug action at multiple signaling end points, including those related to receptor regulation, are required to gain a more complete description of ligand efficacy. In this Review, we summarize studies to date that have investigated the action of allosteric modulators upon receptor regulation. In addition, we discuss the implications that the paradigm of stimulus bias may have upon our interpretation of such studies.

■ GPCR REGULATORY PROCESSES AND THE ROLE OF β-ARRESTINS

The activation mechanism of a GPCR upon ligand binding involves the transmission of a conformational change to the heterotrimeric G protein that promotes the release of GDP, its replacement by GTP and subsequent conformational rearrangements that result in the activation of several effectors (e.g., adenylate cyclases, Phospholipase C), and generation of second messengers (e.g., cAMP, Inositol phosphates). These conformational rearrangements have been confirmed by the recent solution of the high-resolution crystal structure of the ternary complex of the β_2-adrenergic receptor and the stimulatory G

Received: January 7, 2013
Accepted: February 12, 2013
Published: February 12, 2013

dx.doi.org/10.1021/cn400005t | ACS Chem. Neurosci. 2013, 4, 527−534

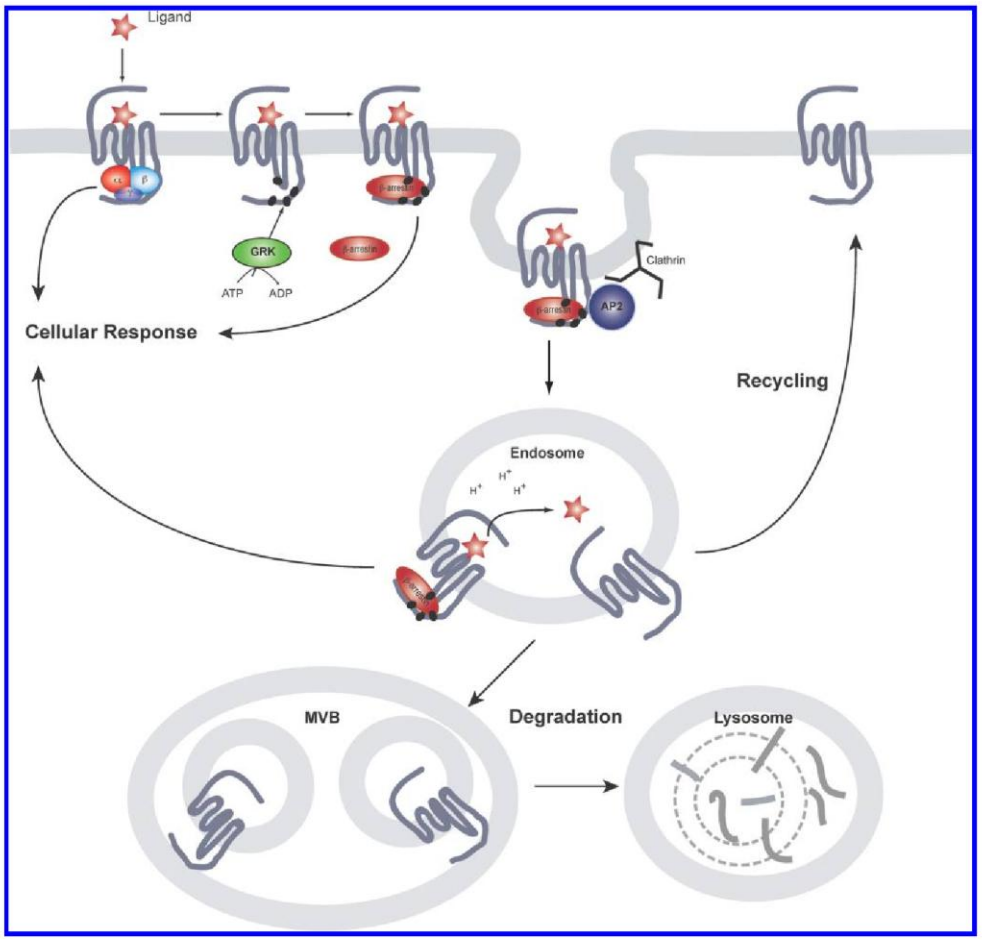

Figure 1. Schematic representation of GPCR regulation by β-arrestin mediated endocytosis. Phosphorylation of the activated receptor by GRKs triggers the recruitment of β-arrestin and the scaffolding of the endocytic machinery that results in receptor internalization. Once in endosomes, GPCRs can be dephosphorylated and recycled to the plasma membrane or, alternatively, be targeted for lysosomal degradation via multivesicular bodies (MVB).

protein, Gs.[7] The intrinsic GTPase activity of Gα leads to hydrolysis of GTP to GDP, the reassociation of Gα-GDP and G$\beta\gamma$ subunits, and the termination of signaling.[8] Upon activation, GPCRs rapidly undergo phosphorylation by GPCR kinases (GRKs) or second messenger activated kinases such as PKA or PKC (Figure 1). Selective phosphorylation of the agonist-activated receptor, and subsequent binding of β-arrestins, prevents the sustained interaction of GPCRs with G proteins, effectively terminating the G protein-mediated signal (receptor desensitization).[9] The classical role proposed for arrestins is to act as scaffolds, binding to the coat structure of clathrin-coated pits (CCPs), thereby promoting endocytosis of arrestin bound receptors (receptor internalization). Eventually, internalized receptors can recycle back to the cell surface (receptor resensitization) or be targeted for lysosomal degradation (receptor down-regulation). However, an alternative role for β-arrestins has recently been demonstrated for a large group of GPCRs; β-arrestins are also able to recruit diverse signaling proteins to activated receptors at plasma and endosomal membranes and thus to be essential signaling mediators. For example, β-arrestins have been shown to scaffold the formation of multiprotein complexes with intracellular kinases such as the MAPKs ERK or JNK, AKT as well as with phosphatases such PP2A.[10,11] It has therefore been proposed that β-arrestins mediate a second wave of GPCR signaling that is distinct from the "classical" G protein-dependent signaling at the plasma membrane (Figure 1).

■ ALLOSTERIC TARGETING OF GPCRs

In recent years it has become apparent that potentially all GPCRs contain topographically distinct, druggable, allosteric binding sites and the targeting of such sites presents an approach to achieve greater subtype selectivity. This fact, together with the increasing use of functional rather than ligand binding approaches in drug discovery programs to screen for small molecule leads, has led to an explosion in the identification of allosteric ligands. Allosteric ligands will bind to a receptor selecting a distinct receptor conformation and modulating both orthosteric ligand affinity and/or efficacy and are thus often referred to as allosteric modulators (Figure 2).[12]

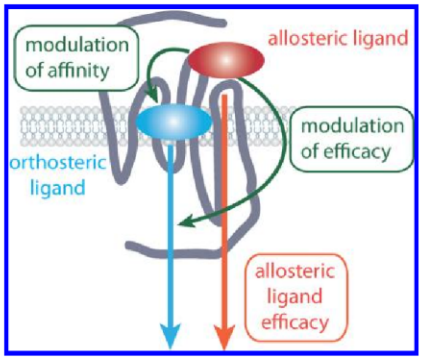

Figure 2. GPCR drug discovery has predominantly focused upon targeting the orthosteric site where the endogenous agonist binds. Allosteric modulators bind to a site on a GPCR that is topographically distinct from this orthosteric binding site. Allosteric modulators will bind to a receptor selecting a distinct receptor conformation but will still allow orthosteric ligands to bind. As such, allosteric ligands can modulate both orthosteric ligand affinity and efficacy. Of particular note, allosteric ligands can also possess their own intrinsic efficacy.

Since allosteric modulators still allow the endogenous agonist to bind to the receptor, allosteric ligands have also been pursued for their ability to "fine tune" the physiological responses linked to a particular receptor, thus accommodating both temporal and spatial rhythms of normal signaling.[12] Furthermore, their modulatory effect is limited, saturable, and therefore less prone to overdose. Currently, two GPCR allosteric modulators have achieved FDA approval; maraviroc that targets the chemokine receptor CCR5 for the treatment of HIV[13] and cinacalcet that targets the calcium sensing receptor (CaSR) for the treatment of hyperthyroidism.[14]

The concept of allosterism was formalized in 1965, by the seminal Monod–Wyman–Changeux (MWC) model, which proposed a conformational selection mechanism to account for ligand actions at bacterial regulatory enzymes.[15] Since then, this model has been extended to other protein families. However, in the field of GPCRs, descriptions of allosteric mechanisms have remained largely theoretical or phenomenological. We have recently described an unprecedented example of a GPCR allosteric modulator whose action is entirely consistent with a two-state, MWC mechanism[16] and proposed a pharmacological framework for the study and classification of allosteric modulators across different GPCR families. Deviations from the predicted MWC behavior may then suggest the existence of more complex (e.g multistate) or mixed (allosteric/orthosteric) modes of action. An important prediction of a two-state mechanism is that all allosteric ligands should display some agonism or inverse agonism in their own right (depending on their ability to select the active or inactive receptor states respectively).[17] In practice, this is not always observed because the bioassay used cannot detect these effects due to signal threshold limitations. However, in an overexpressed receptor system, or an assay monitoring a sensitive or amplified response, low-level allosteric agonism or inverse agonism can be readily unmasked. Indeed, this has been shown to be the case for several GPCR allosteric modulators (Table 1).

■ ALLOSTERIC LIGANDS ARE LIKELY TO MODULATE GPCR REGULATORY PROCESSES

The expectation of all allosteric ligands to display efficacy in their own right means that not all allosteric modulators will conform to one of the suggested advantages of allosteric targeting of GPCRs: The effect of an allosteric modulator will only be observed in the presence of the orthosteric endogenous ligand and therefore will allow for the aforementioned temporal and spatial control of signal modulation. Furthermore, it also emphasizes the fact that, having efficacy on their own, allosteric modulators can not only modulate receptor activation but also potentially elicit receptor regulatory processes (Figure 3). Allosteric modulators could potentially induce receptor desensitization/internalization or conversely increase cell surface expression, act as chaperones of receptor cell surface delivery, or prevent the internalization induced by the endogenous/orthosteric ligand. Indeed, examples of all such scenarios have been described in literature (Table 1).

If we look outside the GPCR family, there is an example where the effect of an allosteric modulator upon receptor regulation may have clinical relevance: the case of the $GABA_A$ receptors ($GABA_ARs$). $GABA_ARs$ are multisubunit ion channels allosterically modulated by benzodiazepines, widely used allosteric modulators in clinical practice for their sedative, anxiolytic, anticonvulsant, and muscle relaxant actions.[18] Benzodiazepines bind to a high affinity binding site located at the α/γ subunit interface but do not open the channel by themselves. Binding to their recognition site leads to a conformational change that that results in an increase of the apparent affinity of the channel for the neurotransmitter GABA.[19]

Use-dependence and tolerance observed after long-term administration of benzodiazepines are commonly linked to the modulation of the expression of $GABA_AR$ binding sites at the cell surface. Such modulation has been shown to be brain-region-specific.[20] Moreover, the prolonged effect of benzodiazepines in receptor regulation has also been shown to be subunit dependent.[21] In vivo studies on long-term benzodiazepine treatments reveal downregulation of $\alpha1$ and $\beta3$ subunits in hippocampal and cortical brain regions and $\gamma2$ subunits in the cerebral cortex. In contrast, benzodiazepine withdrawal causes upregulation of $\alpha4$ and $\gamma4$ subunits.[22] More recently, Jacob and co-workers observed that 24 h treatment of hippocampal neurons with flurazepam dramatically decreased $\alpha2$ subunit-containing $GABA_AR$ surface and total levels without comparable changes in levels of the $\alpha1$ subunit. They suggest that flurazepam exposure enhances degradation of $\alpha2$ subtype $GABA_ARs$ after endocytosis, leading to a reduction in inhibitory synapse size and number along with a decrease in the efficacy of synaptic inhibition.[23]

dx.doi.org/10.1021/cn400005t | ACS Chem. Neurosci. 2013, 4, 527–534

Table 1. Examples to Date in Which the Effect of Allosteric Ligands upon Receptor Regulation (Internalization/β-Arrestin Recruitment) Have Been Studied

GPCR family	GPCR	allosteric ligand	modulator activity[a]	intrinisc activity	effect on regulation	ref
Family A	M_1 mAChR	TBPB	novel M_1 agonist	agonist	slow arrestin recruitment no effect in internalization	28
		AC260584	novel M_1 agonist	agonist	slow arrestin recruitment no effect in internalization	27, 28
		AC-42	novel M_1 agonist	agonist	promotes internalization and downregulation OR no effect in internalization	27 29
		77-LH-28-1	novel M_1 agonist	agonist	promotes internalization but not downregulation	29
	M_2 mAChR	Gallamine	negative		increase in cell surface exp.	25
		Alcuronium	negative		increase in cell surface exp.	25
		C7/3-phth	negative	inverse ago?	increase in cell surface exp.	25
	M_4 mAChR	LY2033298	positive	agonist	promotes internalization	24
	A_1 AdoR	PD81723	positive	agonist	no effect in internalization	60, 61
	LH-R	Org42599	NR	agonist	pharmacological chaperone: cell surface rescue	62
	CXCR3	VUF10661	NR	agonist	promotes internalization	63
	CXCR4	RSVM peptide	NR	agonist	promotes internalization	64
		ASLW peptide	NR	agonist	no effect in internalization	
	CB1	Org27569	positive	agonist	promotes internalization G protein-independent ERK1/2 phosphorylation	31
Family B	GLP-1R	compound 2	positive	agonist	promotes internalization	32
Family C	mGluR7	AMN082	NSA	agonist	promotes internalization	34
	mGluR5	CDPPB	positive	agonist	no effect in internalization in striatum promotes internalization in frontal cortex	35
	CaSR	NPS R-586	positive	agonist	increase of cell surface expression of wt CaR rescue of loss-of-function mutants	36

[a]In interactions with endogenous agonist except in Org27569 in which the orthosteric agonist was CP555940. NR: not reported. NSA: Novel selective agonist.

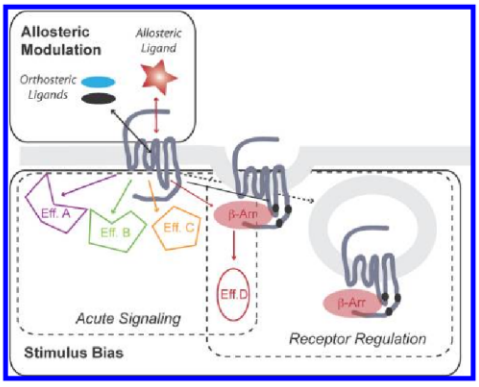

Figure 3. Both orthosteric and allosteric GPCR ligands acting at the same receptor can engage acute signaling and regulatory pathways by interacting with distinct effector proteins (Eff. A-C) and regulatory proteins such as β-arrestin (β-arr). Both orthosteric and allosteric ligands may select different subsets of these signaling and regulatory pathways by stabilizing distinct receptor conformations, a phenomenon termed functional selectivity or stimulus bias. The subset of these pathways and processes engaged by a ligand−receptor complex will underlie the physiological effect of the ligand.

Despite the ever-increasing number of allosteric ligands targeting GPCRs, a surprisingly small number of studies have investigated the effects of such ligands upon receptor regulation. However, examples exist at all three major receptor family classes: Family A (e.g., muscarinic, adenosine, and luteinizing hormone -LH- receptors), Family B (e.g., glucagon-like peptide-1 -GLP-1- receptors), and Family C (e.g., mGluR5, mGluR7, and CaSR). Muscarinic acetylcholine receptors (mAChRs) are perhaps the most studied Family A GPCRs in terms of targeting by small molecule allosteric modulators. Many of the properties of allosteric modulators have been investigated using the mAChR family as a model GPCR system, and several studies have reported the effects of allosteric modulators on mAChR regulation. In agreement with its allosteric agonism, the M_4 mAChR modulator LY2033298 has been shown to induce receptor internalization.[24] In contrast, at the M_2 mAChR, gallamine, alcuronium, and C_7/3-phth, negative allosteric modulators of the endogenous agonist acetylcholine- enhanced cell surface receptor expression.[25,26] More recently, several studies have focused in the regulation of the M_1 mAChR by putative allosteric agonists (AC-42, TBPB) and obtained contradictory results.[27−29] However, it should be noted that it is still unclear if these ligands represent "pure" allosteric modulators or, instead, represent a different and potentially more complex bitopic (i.e., dual allosteric/orthosteric) binding mode, hence their classification as *novel M_1 mAChR agonists*. Interestingly, some studies have also focused on the ability of these ligands to promote β-arrestin recruitment to the receptor. In particular, Ma et al. reported that BQCA (a positive allosteric modulator of M_1 mAChR) is able to induce β-arrestin recruitment with significantly higher potencies than TBPB or AC-42 (novel M_1 mAChR agonists).[30] It is also worth noting that from all these studies, only one of

them investigated the modulatory effect on orthosteric ligand-induced internalization, showing that LY2033298 behaves as an allosteric potentiator when internalization is interrogated in an interaction paradigm as an additional functional end point.[24] More recently, another interesting example of an allosteric ligand of a Family A receptor that mediates receptor internalization is Org27569 at the cannabinoid CB1 receptor. Ahn et al.[31] described the ability of Org27569 not only to mediate receptor internalization but also to engender Gαi/o G protein-independent ERK1/2 phosphorylation.

Receptor regulation by allosteric ligands has also been reported for the prototypical Family B receptor, the GLP-1R. In particular, the small molecule allosteric agonist of GLP-1R, Compound 2, induces receptor internalization in a manner similar to the endogenous peptide, though with slower kinetics.[32] Interestingly, β-arrestin-1 mediates GLP-1R signaling to insulin secretion in cultured pancreatic β cells but does not play a role in GLP-1R desensitization/internalization.[33] However, the ability of Compound 2 to recruit arrestins to the GLP-1R and/or exert modulatory effects upon the physiological outcomes related to this recruitment still remains to be addressed.

Family C receptors present the most striking separation between defined orthosteric and allosteric sites, located in the extracellular Venus Fly Trap domain and the transmembrane bundle, respectively. Multiple allosteric modulators have been described for Family C receptors, with the mGluRs and CaSR being prototypical examples. For instance, AMN082, an allosteric agonist of mGluR7, was shown to internalize the receptor in hippocampal neurons.[34] mGluRs allosteric modulators have also provided interesting examples on differential regulation depending on regions of receptor expression. For example, the effect of prolonged treatment to the mGluR5 positive allosteric modulator, CDPPB, is dependent on the brain region, by which mGluR5 expressed in the cortex is more susceptible to desensitization/internalization than those expressed in the striatum.[35]

It is also worth noting the possibility of allosteric modulators to act as pharmacological chaperones for cell surface delivery of GPCRs. An example of such a scenario is the CaSR. Loss- or gain-of-function mutations identified in different pathological conditions (familial hypocalciuric hypercalcemia (FHH) and neonatal severe hyperparathyroidism (NSHPT) or autosomal dominant hypocalcemia (ADH), respectively) suggest that signaling changes may result from differences in cell surface expression. Allosteric modulators of CaSR such as the calcimimetic NPS R-568 have been shown to differentially regulate the function of plasma membrane-localized CaSR by regulating receptor turnover.[36] NPS R-568, by favoring active conformations, reduces WT CaSR or loss-of-function CaSR mutant ubiquitination, and degradation, hence increasing the levels of functional cell surface CaSR.

The therapeutic relevance of the role of allosteric modulators in GPCR regulation still needs further investigation. One possible research venue is the modulatory effects derived from arrestin recruitment to the receptor and triggering or modulation of arrestin-mediated signals. Concomitantly, an alternative application would rely in the so-called "functional-antagonism", whereby internalization of receptor would inhibit its function by removing it from the cell surface. This latter mechanism has been suggested to be of value in protecting cells from HIV infection in the presence of chemokines and it has been demonstrated that allosteric targeting of CCR5 affecting its internalization properties offers advantageous characteristics as opposed to competitive antagonists.[37]

FUNCTIONAL SELECTIVITY AND RECEPTOR REGULATION: IMPLICATIONS FOR THE CHARACTERIZATION OF ALLOSTERIC LIGANDS

The first unequivocal evidence of functional selectivity was the observation that ligands acting at the same receptor can exhibit reversals in the rank order of potency from one pathway to another.[38] Such inversion in the rank order of potency cannot be explained by differences in the amplification of the signaling pathways or the detection systems used.[5] It follows that these data cannot be easily reconciled with the two-state model classically used to explain agonism, antagonism and inverse agonism, suggesting instead that different ligands can promote distinct receptor active states with preferences toward different signaling pathways. To date, there are numerous examples of receptors for which functionally selective ligands have been described, and it is widely accepted that receptors can exist in multiple conformational states, each eliciting a particular subset of signals. Although many examples of ligand-biased signaling result in relatively modest differences in agonism between individual pathways, some compounds show more extreme pathway bias, characterized by selective agonism toward one pathway and a lack of activity toward another. Many of the best characterized examples of such "extreme" bias refer to drugs with differential activities in G protein-mediated signals versus G protein-independent pathways that often involve the scaffolding protein β-arrestin.[6]

Functional selectivity has also been described at the level of receptor endocytosis (Figure 3). Indeed, the existence of noninternalizing and internalizing ligands has been reported for several GPCRs, and the mechanisms behind such behaviors are starting to be unraveled. As mentioned previously, agonist occupation of GPCRs results in rapid receptor phosphorylation at sites largely within the third intracellular loop and C-terminal tail. This process not only mediates the uncoupling of the receptor from its cognate G protein but also drives G protein-independent receptor signaling. It is now clear that GPCR phosphorylation is a complex regulatory mechanism that involves mainly, but not only, members of the GPCR kinase family (GRKs). The consequence of this phosphorylation is the recruitment of arrestins that mediate both G protein-independent signaling as well as receptor internalization.[9] In line with the idea that GPCRs can adopt multiple conformations that result in differential engagement of signaling proteins, it can be assumed that the phosphorylation patterns adopted by a receptor will be a reflection not only of the complement of kinases and phosphatases expressed in a given cell or tissue but also of the receptor conformation following agonist occupation.[39] Several examples have been recently described that show that biased orthosteric ligands can direct receptor signaling by driving receptor phosphorylation profiles, providing "barcodes" that encode for a particular signaling outcome; for example muscarinic M_3 mAChR, β2-adrenergic receptor, and the chemokine receptors CXCR4 or CCR7.[40−43]

Pioneering work with the β2-adrenergic and angiotensin AT1 receptors demonstrated that recruitment of β-arrestins to phosphorylated receptors can be the initial step for G protein-independent signals as they selectively scaffold intracellular kinases and other signaling effectors.[44,45] Interestingly, β-arrestins also recruit signaling proteins in the endosomal

dx.doi.org/10.1021/cn400005t | ACS Chem. Neurosci. 2013, 4, 527−534

membranes, raising the possibility for receptors that are essentially regarded as cell surface proteins, such as GPCRs, to elicit intracellular signals, although this is just starting to be understood.[11]

In the past decade, numerous ligands that differentially bias receptor signals toward G protein-dependent or -independent pathways have been described, although the physiological relevance of such bias has only been established for a few of them. β-Arrestin-biased signaling has been proposed as a potential therapeutic mechanism for drugs targeting the orthosteric site of β2-adrenergic, AT1, PTH, muscarinic M_3, GLP-1, dopamine D2, or the nicotinic acid receptors[33,46−52] (or ref 6 for review). However, it is worth noting that biased agonism may not always result in a more positive therapeutic profile. It is equally possible that biased agonism may underlie unwanted side effects, although the evidence for this is still very limited.

When receptor internalization is considered as an "end point", stimulus bias can then be extended to ligands that differentially regulate a given GPCR. The most prominent example of this scenario is the opioid receptors. Different from most of the synthetic and endogenous ligands, the widely used analgesic morphine shows compromised ability to internalize the μ-opioid receptor, and this has been proposed to account for the development of tolerance to this drug.[53−55] Recent studies suggest receptor phosphorylation as well as differential recruitment of β-arrestin1 versus β-arrestin2 as a potential mechanism to explain the different regulatory events induced by the different opiates.[56] Stimulus bias for receptor regulation has also recently been shown for the somatostatin SST2A receptor. Two somatostatin analogues currently in clinical investigation (SOM230 and KE108) have been shown to display functional selectivity, not only in terms of acute signaling but also in terms of receptor phosphorylation, endocytosis, and recycling.[57] Functional selectivity in terms of differential receptor internalization has also been demonstrated at the cannabinoid receptor CB2. Despite both orthosteric ligands promoting ERK phosphorylation as well as β-arrestin recruitment, CP55940 was found to internalize the CB2 receptor while the aminoalkylindole WIN55212−2 failed to do so.[58]

Given that the binding of an allosteric modulator to a receptor stabilizes a distinct receptor conformation, it follows that such allosteric modulators may themselves display pathway bias both in terms of their own intrinsic efficacy or their modulation of orthosteric ligand effects.[59] Therefore, it cannot be assumed that if an allosteric modulator is quiescent in the absence of an orthosteric agonist in terms of one signaling pathway it will also be quiescent in terms of receptor regulation (Figure 3). Moreover, it will not necessarily follow that if a modulator is an enhancer of an acute signaling pathway it will display similar potentiation of receptor regulatory events. Thus, it follows that effects upon receptor regulation should be a key focus in studies to characterize novel and existent allosteric modulators in addition to standard readouts of acute receptor signaling events.

■ CONCLUDING REMARKS

Recent research has given us insight into the complexities of GPCR regulation and trafficking. These processes are likely to be both receptor-dependent and in many cases ligand-dependent. Given that many of these GPCR ligands will be administered chronically, an essential part of understanding GPCR ligand efficacy is to understand their ability to modulate these receptor regulatory processes. This in turn will be central to the ability to understand and predict their clinical efficacy. It has now become clear that the development of allosteric modulators offers an attractive approach to achieve selective targeting of GPCRs. These allosteric ligands, in addition to modulating orthosteric ligand effects, may possess efficacy in their own right. As such, it is essential to understand how such ligands modulate GPCR regulatory processes.

■ AUTHOR INFORMATION

Corresponding Author

[redacted] Mailing address: Drug Discovery Biology, Monash Institute of Pharmaceutical Sciences, 399 Royal Parade, Parkville, Victoria, 3052 Australia. [redacted]

Author Contributions

[†]Authors J.R.L. and M.C. contributed equally to this work.

Author Contributions

J.R.L. and M.C. wrote the manuscript. A.A. wrote specific parts of the manuscript.

Funding

Work in the authors' laboratory is supported by the National Health and Medical Research Council (NHMRC) of Australia Project Grants APP1011796 and APP1011920. M.C. is a Monash Fellow, and J.R.L. is a Monash University Larkins Fellow and NHMRC Career Development Awardee. J.R.L. acknowledges the financial support of The Netherlands Organization for Scientific Research [NWO VENI Grant 863.09.018].

Notes

The authors declare no competing financial interest.

■ ABBREVIATIONS

CCP, clathrin-coated pit; GPCR, G protein-coupled receptor; HIV, human immunodeficiency virus

■ REFERENCES

(1) Rask-Andersen, M., Almén, M. S., and Schiöth, H. B. (2011) Trends in the exploitation of novel drug targets. *Nat. Rev. Drug Discovery 10*, 579−590.

(2) Christopoulos, A. (2002) Allosteric binding sites on cell-surface receptors: novel targets for drug discovery. *Nat. Rev. Drug Discovery 1*, 198−210.

(3) Conn, P., Christopoulos, A., and Lindsley, C. (2009) Allosteric modulators of GPCRs: a novel approach for the treatment of CNS disorders. *Nat. Rev. Drug Discovery 8*, 41−54.

(4) Kenakin, T., and Miller, L. J. (2010) Seven transmembrane receptors as shapeshifting proteins: the impact of allosteric modulation and functional selectivity on new drug discovery. *Pharmacol. Rev. 62*, 265−304.

(5) Stallaert, W., Christopoulos, A., and Bouvier, M. (2011) Ligand functional selectivity and quantitative pharmacology at G protein-coupled receptors. *Expert Opin. Drug Discovery 6*, 811−825.

(6) Whalen, E. J., Rajagopal, S., and Lefkowitz, R. J. (2011) Therapeutic potential of β-arrestin- and G protein-biased agonists. *Trends Mol. Med. 17*, 126−139.

(7) Rasmussen, S. G. F., Devree, B. T., Zou, Y., Kruse, A. C., Chung, K. Y., Kobilka, T. S., Thian, F. S., Chae, P. S., Pardon, E., Calinski, D., Mathiesen, J. M., Shah, S. T. A., Lyons, J. A., Caffrey, M., Gellman, S. H., Steyaert, J., Skiniotis, G., Weis, W. I., Sunahara, R. K., and Kobilka, B. K. (2011) Crystal structure of the β2 adrenergic receptor-Gs protein complex. *Nature 477*, 549−555.

(8) Cabrera-Vera, T. M., Vanhauwe, J., Thomas, T. O., Medkova, M., Preininger, A., Mazzoni, M. R., and Hamm, H. E. (2003) Insights into G protein structure, function, and regulation. *Endocr. Rev. 24*, 765−781.
(9) Lefkowitz, R. J., and Whalen, E. J. (2004) beta-arrestins: traffic cops of cell signaling. *Curr. Opin. Cell Biol. 16*, 162−168.
(10) DeWire, S. M., Ahn, S., Lefkowitz, R. J., and Shenoy, S. K. (2007) β-Arrestins and Cell Signaling. *Annu. Rev. Physiol. 69*, 483−510.
(11) Murphy, J. E., Padilla, B. E., Hasdemir, B., Cottrell, G. S., and Bunnett, N. W. (2009) Endosomes: a legitimate platform for the signaling train. *Proc. Natl. Acad. Sci. U.S.A. 106*, 17615−17622.
(12) May, L., Leach, K., Sexton, P., and Christopoulos, A. (2007) Allosteric modulation of G protein-coupled receptors. *Annu. Rev. Pharmacol. Toxicol. 47*, 1−51.
(13) Dorr, P., Westby, M., Dobbs, S., Griffin, P., Irvine, B., Macartney, M., Mori, J., Rickett, G., Smith-Burchnell, C., Napier, C., Webster, R., Armour, D., Price, D., Stammen, B., Wood, A., and Perros, M. (2005) Maraviroc (UK-427,857), a potent, orally bioavailable, and selective small-molecule inhibitor of chemokine receptor CCR5 with broad-spectrum anti-human immunodeficiency virus type 1 activity. *Antimicrob. Agents Chemother. 49*, 4721−4732.
(14) Lindberg, J. S. (2005) Cinacalcet HCl, an Oral Calcimimetic Agent for the Treatment of Secondary Hyperparathyroidism in Hemodialysis and Peritoneal Dialysis: A Randomized, Double-Blind, Multicenter Study. *J. Am. Soc. Nephrol. 16*, 800−807.
(15) Monod, J., Wyman, J., and Changeux, J.-P. (1965) On the nature of allosteric transitions: a plausible model. *J. Mol. Biol.*, 88−118.
(16) Canals, M., Lane, J. R., Wen, A., Scammells, P. J., Sexton, P. M., and Christopoulos, A. (2012) A Monod-Wyman-Changeux Mechanism Can Explain G Protein-coupled Receptor (GPCR) Allosteric Modulation. *J. Biol. Chem. 287*, 650−659.
(17) Canals, M., Sexton, P. M., and Christopoulos, A. (2011) Allostery in GPCRs: "MWC" revisited. *Trends Biochem. Sci. 36*, 663−672.
(18) Tallman, J. F., Thomas, J. W., and Gallager, D. W. (1978) GABAergic modulation of benzodiazepine binding site sensitivity. *Nature 274*, 383−385.
(19) Sigel, E., and Buhr, A. (1997) The benzodiazepine binding site of GABAA receptors. *Trends Pharmacol. Sci. 18*, 425−429.
(20) Jacob, T. C., Moss, S. J., and Jurd, R. (2008) GABA(A) receptor trafficking and its role in the dynamic modulation of neuronal inhibition. *Nat. Rev. Neurosci. 9*, 331−343.
(21) Gassmann, M., and Bettler, B. (2012) Regulation of neuronal GABA(B) receptor functions by subunit composition. *Nat. Rev. Neurosci. 13*, 380−394.
(22) Uusi-Oukari, M., and Korpi, E. R. (2010) Regulation of GABA(A) receptor subunit expression by pharmacological agents. *Pharmacol. Rev. 62*, 97−135.
(23) Jacob, T. C., Michels, G., Silayeva, L., Haydon, J., Succol, F., and Moss, S. J. (2012) Benzodiazepine treatment induces subtype-specific changes in GABAA receptor trafficking and decreases synaptic inhibition. *Proc. Natl. Acad. Sci. U.S.A. 109*, 18595−18600.
(24) Leach, K., Loiacono, R., Felder, C., McKinzie, D., Mogg, A., Shaw, D., Sexton, P., and Christopoulos, A. (2009) Molecular Mechanisms of Action and In Vivo Validation of an M4Muscarinic Acetylcholine Receptor Allosteric Modulator with Potential Antipsychotic Properties. *Neuropsychopharmacology 35*, 855−869.
(25) May, L. T., Lin, Y., Sexton, P. M., and Christopoulos, A. (2005) Regulation of M2 muscarinic acetylcholine receptor expression and signaling by prolonged exposure to allosteric modulators. *J. Pharmacol. Exp. Ther. 312*, 382−390.
(26) Avlani, V. A., Gregory, K. J., Morton, C. J., Parker, M. W., Sexton, P. M., and Christopoulos, A. (2007) Critical role for the second extracellular loop in the binding of both orthosteric and allosteric G protein-coupled receptor ligands. *J. Biol. Chem. 282*, 25677−25686.
(27) Davis, C., Bradley, S., Schiffer, H., Friberg, M., Koch, K., Tolf, B.-R., Bonhaus, D., and Lameh, J. (2009) Differential regulation of muscarinic M1 receptors by orthosteric and allosteric ligands. *BMC Pharmacol. 9*, 9−14.
(28) Davis, A. A., Heilman, C. J., Brady, A. E., Miller, N. R., Fuerstenau-Sharp, M., Hanson, B. J., Lindsley, C. W., Conn, P. J., Lah, J. J., and Levey, A. I. (2010) Differential effects of allosteric M(1) muscarinic acetylcholine receptor agonists on receptor activation, arrestin 3 recruitment, and receptor downregulation. *ACS. Chem. Neurosci. 1*, 542−551.
(29) Thomas, R. L., Langmead, C. J., Wood, M. D., and Challiss, R. A. J. (2009) Contrasting effects of allosteric and orthosteric agonists on m1 muscarinic acetylcholine receptor internalization and down-regulation. *J. Pharmacol. Exp. Ther. 331*, 1086−1095.
(30) Ma, L., Seager, M. A., Seager, M., Wittmann, M., Jacobson, M., Bickel, D., Burno, M., Jones, K., Graufelds, V. K., Xu, G., Pearson, M., McCampbell, A., Gaspar, R., Shughrue, P., Danziger, A., Regan, C., Flick, R., Pascarella, D., Garson, S., Doran, S., Kreatsoulas, C., Veng, L., Lindsley, C. W., Shipe, W., Kuduk, S., Sur, C., Kinney, G., Seabrook, G. R., and Ray, W. J. (2009) Selective activation of the M1 muscarinic acetylcholine receptor achieved by allosteric potentiation. *Proc. Natl. Acad. Sci. U.S.A. 106*, 15950−15955.
(31) Ahn, K. H., Mahmoud, M. M., and Kendall, D. A. (2012) Allosteric modulator ORG27569 induces CB1 Cannabinoid receptor high affinity agonist binding state, receptor internalization, and G_i-independent ERK1/2 kinase activation. *J. Biol. Chem. 287*, 12070−12082.
(32) Coopman, K., Huang, Y., Johnston, N., Bradley, S. J., Wilkinson, G. F., and Willars, G. B. (2010) Comparative effects of the endogenous agonist glucagon-like peptide-1 (GLP-1)-(7−36) amide and the small-molecule ago-allosteric agent "compound 2" at the GLP-1 receptor. *J. Pharmacol. Exp. Ther. 334*, 795−808.
(33) Sonoda, N., Imamura, T., Yoshizaki, T., Babendure, J., Lu, J.-C., and Olefsky, J. (2008) β^2-Arrestin-1 mediates glucagon-like peptide-1 signaling to insulin secretion in cultured pancreatic β^2 cells. *Proc. Natl. Acad. Sci. U.S.A. 105*, 6614−6619.
(34) Pelkey, K. A., Yuan, X., Lavezzari, G., Roche, K. W., and McBain, C. J. (2007) mGluR7 undergoes rapid internalization in response to activation by the allosteric agonist AMN082. *Neuropharmacology 52*, 108−117.
(35) Parmentier-Batteur, S., Obrien, J. A., Doran, S., Nguyen, S. J., Flick, R. B., Uslaner, J. M., Chen, H., Finger, E. N., Williams, T. M., Jacobson, M. A., and Hutson, P. H. (2012) Differential effects of the mGluR5 positive allosteric modulator CDPPB in the cortex and striatum following repeated administration. *Neuropharmacology 62*, 1453−1460.
(36) Huang, Y., and Breitwieser, G. E. (2007) Rescue of calcium-sensing receptor mutants by allosteric modulators reveals a conformational checkpoint in receptor biogenesis. *J. Biol. Chem. 282*, 9517−9525.
(37) Muniz-Medina, V. M., Jones, S., Maglich, J. M., Galardi, C., Hollingsworth, R. E., Kazmierski, W. M., Ferris, R. G., Edelstein, M. P., Chiswell, K. E., and Kenakin, T. P. (2009) The relative activity of "function sparing" HIV-1 entry inhibitors on viral entry and CCR5 internalization: is allosteric functional selectivity a valuable therapeutic property? *Mol. Pharmacol. 75*, 490−501.
(38) Spengler, D., Waeber, C., Pantaloni, C., Holsboer, F., Bockaert, J., Seeburg, P. H., and Journot, L. (1993) Differential signal transduction by five splice variants of the PACAP receptor. *Nature 365*, 170−175.
(39) Tobin, A. B., Butcher, A. J., and Kong, K. C. (2008) Location, location, location...site-specific GPCR phosphorylation offers a mechanism for cell-type-specific signalling. *Trends Pharmacol. Sci. 29*, 413−420.
(40) Butcher, A. J., Prihandoko, R., Kong, K. C., McWilliams, P., Edwards, J. M., Bottrill, A., Mistry, S., and Tobin, A. B. (2011) Differential G-protein-coupled receptor phosphorylation provides evidence for a signaling bar code. *J. Biol. Chem. 286*, 11506−11518.
(41) Nobles, K. N., Xiao, K., Ahn, S., Shukla, A. K., Lam, C. M., Rajagopal, S., Strachan, R. T., Huang, T.-Y., Bressler, E. A., Hara, M. R., Shenoy, S. K., Gygi, S. P., and Lefkowitz, R. J. (2011) Distinct

phosphorylation sites on the β(2)-adrenergic receptor establish a barcode that encodes differential functions of β-arrestin. *Sci. Signaling 4*, ra51.
(42) Busillo, J., Armando, S., Sengupta, R., Meucci, O., Bouvier, M., and Benovic, J. (2010) Site-specific Phosphorylation of CXCR4 Is Dynamically Regulated by Multiple Kinases and Results in Differential Modulation of CXCR4 Signaling. *J. Biol. Chem. 285*, 7805−7817.
(43) Zidar, D. A., Violin, J. D., Whalen, E. J., and Lefkowitz, R. J. (2009) Selective engagement of G protein coupled receptor kinases (GRKs) encodes distinct functions of biased ligands. *Proc. Natl. Acad. Sci. U.S.A. 106*, 9649−9654.
(44) Ahn, S., Maudsley, S., Luttrell, L. M., Lefkowitz, R. J., and Daaka, Y. (1999) Src-mediated tyrosine phosphorylation of dynamin is required for beta2-adrenergic receptor internalization and mitogen-activated protein kinase signaling. *J. Biol. Chem. 274*, 1185−1188.
(45) Tohgo, A., Pierce, K. L., Choy, E. W., Lefkowitz, R. J., and Luttrell, L. M. (2002) beta-Arrestin scaffolding of the ERK cascade enhances cytosolic ERK activity but inhibits ERK-mediated transcription following angiotensin AT1a receptor stimulation. *J. Biol. Chem. 277*, 9429−9436.
(46) Wisler, J. W., DeWire, S. M., Whalen, E. J., Violin, J. D., Drake, M. T., Ahn, S., Shenoy, S. K., and Lefkowitz, R. J. (2007) A unique mechanism of beta-blocker action: carvedilol stimulates beta-arrestin signaling. *Proc. Natl. Acad. Sci. U.S.A. 104*, 16657−16662.
(47) Wei, H., Ahn, S., Shenoy, S. K., Karnik, S. S., Hunyady, L., Luttrell, L. M., and Lefkowitz, R. J. (2003) Independent beta-arrestin 2 and G protein-mediated pathways for angiotensin II activation of extracellular signal-regulated kinases 1 and 2. *Proc. Natl. Acad. Sci. U.S.A. 100*, 10782−10787.
(48) Gesty-Palmer, D., Flannery, P., Yuan, L., Corsino, L., Spurney, R., Lefkowitz, R. J., and Luttrell, L. M. (2009) A beta-arrestin-biased agonist of the parathyroid hormone receptor (PTH1R) promotes bone formation independent of G protein activation. *Sci. Transl. Med. 1*, 1ra1.
(49) Kong, K. C., Butcher, A. J., McWilliams, P., Jones, D., Wess, J., Hamdan, F. F., Werry, T., Rosethorne, E. M., Charlton, S. J., Munson, S. E., Cragg, H. A., Smart, A. D., and Tobin, A. B. (2010) M3-muscarinic receptor promotes insulin release via receptor phosphorylation/arrestin-dependent activation of protein kinase D1. *Proc. Natl. Acad. Sci. U.S.A. 107*, 21181−21186.
(50) Quoyer, J., Longuet, C., Broca, C., Linck, N., Costes, S., Varin, E., Bockaert, J., Bertrand, G., and Dalle, S. (2010) GLP-1 mediates antiapoptotic effect by phosphorylating Bad through a beta-arrestin 1-mediated ERK1/2 activation in pancreatic beta-cells. *J. Biol. Chem. 285*, 1989−2002.
(51) Masri, B., Salahpour, A., Didriksen, M., Ghisi, V., Beaulieu, J.-M., Gainetdinov, R. R., and Caron, M. G. (2008) Antagonism of dopamine D2 receptor/beta-arrestin 2 interaction is a common property of clinically effective antipsychotics. *Proc. Natl. Acad. Sci. U.S.A. 105*, 13656−13661.
(52) Walters, R. W., Shukla, A. K., Kovacs, J. J., Violin, J. D., DeWire, S. M., Lam, C. M., Chen, J. R., Muehlbauer, M. J., Whalen, E. J., and Lefkowitz, R. J. (2009) beta-Arrestin1 mediates nicotinic acid-induced flushing, but not its antilipolytic effect, in mice. *J. Clin. Invest. 119*, 1312−1321.
(53) Bohn, L. M., Lefkowitz, R. J., and Caron, M. G. (2002) Differential mechanisms of morphine antinociceptive tolerance revealed in (beta)arrestin-2 knock-out mice. *J. Neurosci. 22*, 10494−10500.
(54) Dang, V. C., Chieng, B., Azriel, Y., and Christie, M. J. (2011) Cellular Morphine Tolerance Produced by Arrestin-2-Dependent Impairment of -Opioid Receptor Resensitization. *J. Neurosci. 31*, 7122−7130.
(55) Raehal, K. M., Schmid, C. L., Groer, C. E., and Bohn, L. M. (2011) Functional selectivity at the μ-opioid receptor: implications for understanding opioid analgesia and tolerance. *Pharmacol. Rev. 63*, 1001−1019.
(56) Groer, C. E., Schmid, C. L., Jaeger, A. M., and Bohn, L. M. (2011) Agonist-directed interactions with specific arrestins determine μ-opioid receptor trafficking, ubiquitination, and dephosphorylation. *J. Biol. Chem. 286*, 31731−31741.
(57) Kao, Y. J., Ghosh, M., and Schonbrunn, A. (2011) Ligand-dependent mechanisms of sst2A receptor trafficking: role of site-specific phosphorylation and receptor activation in the actions of biased somatostatin agonists. *Mol. Endocrinol. 25*, 1040−1054.
(58) Atwood, B. K., Wager-Miller, J., Haskins, C., Straiker, A., and Mackie, K. (2012) Functional selectivity in CB(2) cannabinoid receptor signaling and regulation: implications for the therapeutic potential of CB(2) ligands. *Mol. Pharmacol. 81*, 250−263.
(59) Leach, K., Sexton, P., and Christopoulos, A. (2007) Allosteric GPCR modulators: taking advantage of permissive receptor pharmacology. *Trends Pharmacol. Sci. 28*, 382−389.
(60) Klaasse, E., den Hout, van, G., Roerink, S., de Grip, W., Ijzerman, A., and Beukers, M. (2005) Allosteric modulators affect the internalization of human adenosine A1 receptors. *Eur. J. Pharmacol. 522*, 1−8.
(61) Bhattacharya, S., and Linden, J. (1996) Effects of long-term treatment with the allosteric enhancer, PD81,723, on Chinese hamster ovary cells expressing recombinant human A1 adenosine receptors. *Mol. Pharmacol. 50*, 104−111.
(62) Newton, C. L., Whay, A. M., McArdle, C. A., Zhang, M., van Koppen, C. J., van de Lagemaat, R., Segaloff, D. L., and Millar, R. P. (2011) Rescue of expression and signaling of human luteinizing hormone G protein-coupled receptor mutants with an allosterically binding small-molecule agonist. *Proc. Natl. Acad. Sci. U.S.A. 108*, 7172−7176.
(63) Scholten, D. J., Canals, M., Wijtmans, M., de Munnik, S., Nguyen, P., Verzijl, D., de Esch, I. J. P., Vischer, H. F., Smit, M. J., and Leurs, R. (2012) Pharmacological characterization of a small-molecule agonist for the chemokine receptor CXCR3. *Br. J. Pharmacol. 166*, 898−911.
(64) Sachpatzidis, A., Benton, B. K., Manfredi, J. P., Wang, H., Hamilton, A., Dohlman, H. G., and Lolis, E. (2003) Identification of allosteric peptide agonists of CXCR4. *J. Biol. Chem. 278*, 896−907.